

**ROLE OF SECOND MESSENGER SIGNALING PATHWAYS IN
THE REGULATION OF SARCOPLASMIC RETICULUM
Ca²⁺-HANDLING PROPERTIES IN THE
LEFT VENTRICLE AND SKELETAL MUSCLES OF
DIFFERENT FIBRE TYPE COMPOSITION**

by

Todd A. D. Duhamel

A thesis
presented to the University of Waterloo
in fulfillment of the
thesis requirement for the degree of
Doctor of Philosophy
in
Kinesiology

Waterloo, Ontario, Canada, 2007

© Todd A.D. Duhamel, 2007

AUTHOR'S DECLARATION

I hereby declare that I am the sole author of this thesis. This is a true copy of the thesis, including any required final revisions, as accepted by my examiners.

I understand that my thesis may be made electronically available to the public.

Todd A.D. Duhamel

ABSTRACT

The overall objective of this thesis was to examine mechanisms involved in the acute regulation of sarcoplasmic reticulum (SR) Ca^{2+} -handling properties by second messenger signaling pathways in skeletal and cardiac muscle. The aim of the first study (Chapter Two) was to characterize changes in the kinetic properties of sarco(endo)-plasmic reticulum Ca^{2+} -ATPase (SERCA) proteins in cardiac and skeletal muscles in response to β -adrenergic, Ca^{2+} -dependent calmodulin kinase II (CaMKII) and protein kinase C (PKC) signaling. The aim of the second study (Chapter Three) was to determine if insulin signaling could acutely regulate SERCA kinetic properties in cardiac and skeletal muscle. The aim of the final study (Chapter Four) was to determine if alterations in plasma glucose, epinephrine and insulin concentrations during exercise are able to influence SR Ca^{2+} -handling properties in contracting human skeletal muscle.

Data collected in Chapter Two and Chapter Three were obtained using tissue prepared from a group of 28 male Sprague-Dawley rats (9 weeks of age; mass = 280 ± 4 g; $X \pm \text{S.E.}$). Crude muscle homogenates (11:1 dilution) were prepared from selected hind limb muscles (soleus, SOL; extensor digitorum longus, EDL; the red portion of gastrocnemius, RG; and the white portion of gastrocnemius, WG) and the left ventricle (LV). Enriched SR membrane fractions, prepared from WG and LV, were also analyzed. A spectrophotometric assay was used to measure kinetic properties of SERCA, namely, maximal SERCA activity (V_{max}), and Ca^{2+} -sensitivity was characterized by both the Ca_{50} , which is defined as the free Ca^{2+} -concentration needed to elicit 50% V_{max} , and the Hill coefficient (n_{H}), which is defined as the relationship between SERCA activity and $\text{Ca}^{2+}_{\text{f}}$ for 10 to 90% V_{max} .

The observations made in Chapter Two indicated that β -adrenergic signaling, activated by epinephrine, increased ($P < 0.05$) Ca^{2+} -sensitivity, as shown by a left-shift in Ca_{50} (i.e. reduced Ca_{50}), without altering V_{\max} in LV and SOL but had no effect ($P < 0.05$) on EDL, RG, or WG. Further analysis using a combination of cAMP, the PKA activator forskolin, and/or the PKA inhibitor KT5270 indicated that the reduced Ca_{50} in LV was activated by cAMP- and PKA-signaling mechanisms. However, although the reduced Ca_{50} in SOL was cAMP-dependent, it was not influenced by a PKA-dependent mechanism. In contrast to the effects of β -adrenergic signaling, CaMKII activation increased SERCA Ca^{2+} -sensitivity, as shown by a left-shift in Ca_{50} and increased n_h , without altering SERCA V_{\max} in LV but was without effect in any of the skeletal muscles examined. The PKC activator PMA significantly reduced SERCA Ca^{2+} -sensitivity, by inducing a right-shift in Ca_{50} and decreased n_H in the LV and all skeletal muscles examined. PKC activation also reduced V_{\max} in the fast-twitch skeletal muscles (i.e. EDL, RG and WG), but did not alter V_{\max} in LV or SOL.

The results of Chapter Three indicated that insulin signaling increased SERCA Ca^{2+} -sensitivity, as shown by a left-shift in Ca_{50} (i.e. reduced Ca_{50}) and an increased n_H , without altering SERCA V_{\max} in crude muscle homogenates prepared from LV, SOL, EDL, RG, and WG. An increase in SERCA Ca^{2+} -sensitivity was also observed in enriched SERCA1a and SERCA2a vesicles when an activated form of the insulin receptor (A-INS-R) was included during biochemical analyses. Co-immunoprecipitation experiments were conducted and indicated that IRS-1 and IRS-2 proteins bind SERCA1a and SERCA2a in an insulin-dependent manner. However, the binding of IRS proteins with SERCA does not appear to alter the structural integrity of the SERCA Ca^{2+} -binding site since no changes in NCD-4 fluorescence were observed in response to insulin or A-INS-R. Moreover, the increase in SERCA Ca^{2+} -

sensitivity due to insulin signaling was not associated with changes in the phosphorylation status of phospholamban (PLN) since Ser16 or Thr17 phosphorylation was not altered by insulin or A-INS-R in LV tissue.

The data described in Chapter Four was collected from 15 untrained human participants (peak O₂ consumption, VO_{2peak} = 3.45 ± 0.17 L/min) who completed a standardized cycle test (~60% VO_{2peak}) on two occasions during which they were provided either an artificially sweetened placebo (PLAC) or a 6% glucose (GLUC) beverage (~1.00 g CHO per kg body mass). Muscle biopsies were collected from the vastus lateralis at rest, after 30 min and 90 min of exercise and at fatigue in both conditions to allow assessment of metabolic and SR data. Glucose supplementation increased exercise ride time by ~19% (137 ± 7 min) compared to PLAC (115 ± 6 min). This performance increase was associated with elevated plasma glucose and insulin concentrations and reduced catecholamine concentrations during GLUC compared to PLAC. Prolonged exercise reduced (p<0.05) SR Ca²⁺-uptake, V_{max}, Phase 1 and Phase 2 Ca²⁺-release rates during both PLAC and GLUC. However, no differences in SR Ca²⁺-handling properties were observed between conditions when direct comparisons were made at matched time points between PLAC and GLUC.

In summary, the results of the first study (Chapter Two) indicate that β-adrenergic and CaMKII signaling increases SERCA Ca²⁺-sensitivity in the LV and SOL; while PKC signaling reduces SERCA Ca²⁺-sensitivity in all tissues. PKC activation also reduces V_{max} in the fast-twitch skeletal muscles (i.e. EDL, RG, and WG) but has no effect on V_{max} in the LV and SOL. The results of the second study (Chapter Three) indicate that insulin signaling acutely increases the Ca²⁺-sensitivity of SERCA1a and SERCA2a in all tissues examined, without altering the V_{max}. Based on our observations, it appears that the increase in SERCA Ca²⁺-sensitivity may be

regulated, in part, through the interaction of IRS proteins with SERCA1a and SERCA2a. The results of the final study (Chapter Four) indicate that alterations in plasma glucose, epinephrine and insulin concentrations associated with glucose supplementation during exercise, do not alter the time course or magnitude of reductions in SERCA or Ca²⁺-release channel (CRC) function in working human skeletal muscle. Although glucose supplementation did increase exercise ride time to fatigue in this study, our data does not reveal an association with SR Ca²⁺-cycling measured *in vitro*. It is possible that the strength of exercise signal overrides the hormonal influences observed in resting muscles. Additionally, these data do not rule out the possibility that glucose supplementation may influence E-C coupling processes or SR Ca²⁺-cycling properties *in vivo*.

ACKNOWLEDGEMENTS

I am honoured by the fact that I have been a member of the University of Waterloo for the past decade. As I move forward in my research career, I will always look fondly upon my time in Waterloo. I will always consider Waterloo my second home (i.e. second only to Atikokan) since I have met many friends and colleagues during my time here.

I must acknowledge that I have been very fortunate to work in a laboratory that was very enjoyable and productive. The people in the Green lab exemplify the highest social and professional qualities. It has been an honour to interact with these people on a daily basis. I wish you all the best in the future.

I would like to specifically acknowledge the contributions of Dr. Howard Green, my graduate supervisor, since he was central to the development of my academic career. Howie has always challenged me to accomplish specific research and academic goals. Although I may have been frustrated by the challenges at times, I appreciate that Howie was willing to devote his time to assist the development of my academic accomplishments. As I look forward to my research career, I look forward to supporting and challenging graduate trainees in a similar fashion.

I would also like to acknowledge my other mentors who have encouraged me to strive to reach academic and research excellence. I have enjoyed the discussions that we have had over the years and value the advice and perspective that you provided me. As I move forward with my research career, I aspire to reach the high professional and academic standards achieved by these mentors.

Finally, I would like to acknowledge my family. I would not have had the strength to complete my education without their encouragement and support. I found that my academic training was challenging at times and required some sacrifices along the way. I appreciate that my family was tolerant of these occasions and that they stood by me without wavering. Your strength, understanding and support are very much appreciated. Thank you.

DEDICATION

I would like to dedicate this work to the people who have supported me through out my life. This thesis is a culmination of hard work, dedication and sacrifice. In fact, it is a testament to the skills and work ethic that were instilled in me by my parents, my friends, and my mentors. I expect that this thesis, in conjunction with the full collection of my research and academic contributions to date, meets the high standards and expectations associated with a Doctoral degree.

I believe that Graduate students should view graduate school as an honor that only a small number of people are able to realize. Graduate students need to be aware that the expectations associated with post-graduate education are significant. Scientific research should be viewed as a profession and graduate training should be regarded as an opportunity to receive advanced training that will contribute to future employment opportunities and financial success. Graduate students should see themselves as apprentices and should seek unique training opportunities that will make their academic careers distinctive. At times these unique training opportunities may require sacrifice; however, it is important that graduate students be committed to advancing their research career through extraordinary means since the academic and research fields are highly competitive. Graduate students need to realize that it is their responsibility to develop a unique curriculum vita that will identify them as an outstanding candidate that should be considered for preferred employment opportunities. Accordingly, I believe that it is vital that successful Graduate students possess four essential characteristics:

- 1) a desire to be extraordinary;
- 2) a commitment to take responsibility for their own career development;
- 3) a willingness to teach less experienced researchers; and,
- 4) a willingness to learn from the success and the mistakes that each of us makes along the way.

I would like to think that I successfully demonstrated these characteristics during my academic training. Nevertheless, I consistently find myself having to put forth great effort to exhibit these characteristics – which is an indication that it takes effort and dedication to be successful.

TABLE OF CONTENTS

AUTHOR'S DECLARATION	ii
ABSTRACT	iii
ACKNOWLEDGEMENTS	vii
DEDICATION	viii
TABLE OF CONTENTS	ix
LIST OF TABLES	xii
LIST OF FIGURES	xv
LIST OF ABBREVIATIONS	xviii
CHAPTER ONE: LITERATURE REVIEW AND STATEMENT OF THE PROBLEM	
▪ The role of the sarcoplasmic reticulum in excitation-contraction coupling and relaxation.	2
▪ Tertiary structure and function of SERCA proteins.	3
▪ Tertiary structure and function of CRC proteins.	8
▪ Experimental models used to characterize sarcoplasmic reticulum function	8
▪ Exercise and the sarcoplasmic reticulum	9
▪ Muscle glycogen content and SR Ca ²⁺ -handling properties in animal models.	12
▪ Effects of muscle glycogen content on SR Ca ²⁺ -handling properties in human skeletal muscle.	14
▪ Effects of second messenger signaling on SR Ca ²⁺ -handling properties	18
▪ Statement of the problem and hypotheses	26
CHAPTER TWO: ACUTE REGULATION OF SERCA KINETIC PROPERTIES BY β-ADRENERGIC, Ca²⁺-DEPENDENT CALMODULIN KINASE II AND PROTEIN KINASE C SIGNALING IN CARDIAC AND SKELETAL MUSCLE.	
▪ Abstract	31
▪ Introduction	33
▪ Research Design & Methods	40
▪ Results	52
▪ Muscle oxidative potential	52
▪ SDS-PAGE and Western blotting	52
▪ β -adrenergic regulation of SERCA kinetics	55
▪ Ca ²⁺ -dependent calmodulin kinase II regulation of SERCA kinetics	62
▪ PKC regulation of SERCA kinetics	65
▪ Discussion	72
▪ Limitations	88
▪ Summary	91

CHAPTER THREE: INSULIN SIGNALING INCREASES THE Ca²⁺-SENSITIVITY OF SERCA PROTEINS IN CARDIAC AND SKELETAL MUSCLE.

▪ Abstract	94
▪ Introduction	96
▪ Research Design & Methods	101
▪ Results	110
▪ SDS-PAGE and Western blotting	110
▪ Insulin regulation of SERCA activity	112
▪ Co-immunoprecipitation of SERCA with IRS proteins	120
▪ FITC binding capacity	120
▪ NCD-4 binding capacity	123
▪ Phospholamban status	123
▪ Discussion	127
▪ Summary	135

CHAPTER FOUR: EFFECTS OF EXERCISE AND ORAL GLUCOSE SUPPLEMENTATION ON SARCOPLASMIC RETICULUM Ca²⁺-CYCLING PROPERTIES IN HUMAN SKELETAL MUSCLE.

▪ Abstract	137
▪ Introduction	139
▪ Research Design & Methods	144
▪ Results	159
▪ Ride time to fatigue	159
▪ Glucose Supplementation	159
▪ Respiratory gas measures	160
▪ Substrate oxidation	160
▪ Blood Hb, Hct and plasma volume changes	161
▪ Blood metabolites	161
▪ Blood hormone concentrations	165
▪ Muscle Metabolites	166
▪ Sarcoplasmic reticulum properties	170
▪ Phospholamban phosphorylation status	175
▪ Discussion	178
▪ Summary	189

CHAPTER FIVE: SUMMARY, CONCLUSIONS AND FUTURE DIRECTIONS

▪ Summary and Conclusions	192
▪ Future directions	197
▪ Limitations	198

REFERENCE LIST	201
-----------------------	------------

APPENDICIES

• APPENDIX ONE: Thesis presentation slides	220
▪ APPENDIX TWO: Data that were not included in Chapter Two	228
▪ APPENDIX THREE: Data that were presented in Figures in Chapter Three	231
▪ APPENDIX FOUR: Example Western blot figures	234
▪ APPENDIX FIVE: Data that were presented in Figures in Chapter Four	239
▪ APPENDIX SIX: Calculation of Substrate Oxidation	248
▪ APPENDIX SEVEN: Detailed procedures for muscle homogenization and isolation of SR vesicles	253
▪ APPENDIX EIGHT: Methods to assess sarcoplasmic reticulum properties	257
▪ APPENDIX NINE: Measurement techniques to assess SR Ca ²⁺ -uptake and release	261
▪ APPENDIX TEN: Co-immuno precipitation assay protocol	265
▪ APPENDIX ELEVEN: NCD-4 assay protocol	273
▪ APPENDIX TWELVE: FITC BINDING assay protocol	276

LIST OF TABLES

CHAPTER TWO

Table 2.1: Experimental conditions used to determine β -adrenergic, CaMKII and PKC signaling effects on SERCA kinetic properties.	44
Table 2.2: Description of primary antibodies and Western blotting protocols in Chapter Two.	46
Table 2.3: Summary of Western blot data characterizing the abundance of selected proteins in the rat left ventricle and skeletal muscle samples assessed in Chapter Two.	53
Table 2.4: Concentration dependent effects of epinephrine on SERCA kinetic properties in homogenates from left ventricle and skeletal muscle of different fibre type composition.	56
Table 2.5: Effects of epinephrine or propranolol + epinephrine on SERCA kinetic properties in homogenates from left ventricle and skeletal muscle of different fibre type composition.	57
Table 2.6: Effects of forskolin or KT5720 + forskolin on SERCA kinetic properties in homogenates from left ventricle and skeletal muscle of different fibre type composition.	58
Table 2.7: Effects of forskolin or Active PKA on SERCA kinetic properties in purified SR vesicles prepared from left ventricle and the white portion of the gastrocnemius.	60
Table 2.8: Effects of cAMP or KT5720 + cAMP on SERCA kinetic properties in homogenates from left ventricle and skeletal muscle of different fibre type composition.	61
Table 2.9: Effects of cAMP or KT5720 + cAMP on SERCA kinetic properties in purified SR vesicles prepared from left ventricle and the white portion of the gastrocnemius.	63
Table 2.10: Effects of CaM or KN62 on SERCA kinetic properties in homogenates from left ventricle and skeletal muscle of different fibre type composition.	64
Table 2.11: Effects of KN62, CaM or KN62 + CaM on SERCA kinetic properties in homogenates from left ventricle and skeletal muscle of different fibre type composition.	66

Table 2.12: Effects of CaM or KN62 on SERCA kinetic properties in purified SR vesicles prepared from left ventricle and the white portion of the gastrocnemius.	67
Table 2.13: Effects of GFX or PMA on SERCA kinetic properties in homogenates from left ventricle and skeletal muscle of different fibre type composition.	68
Table 2.14: Effects of GFX, PMA or GFX + PMA on SERCA kinetic properties in homogenates from left ventricle and skeletal muscle of different fibre type composition.	70
Table 2.15: Effects of GFX or PMA on SERCA kinetic properties in purified SR vesicles prepared from left ventricle and the white portion of the gastrocnemius.	71
 CHAPTER THREE	
Table 3.1: Experimental conditions used to determine insulin signaling effects on SERCA kinetic properties.	103
Table 3.2: Description of primary antibodies and Western blotting protocols in Chapter Three.	105
Table 3.3: Summary of Western blot data characterizing the abundance of selected proteins in the rat left ventricle and skeletal muscle samples assessed in Chapter Three.	111
Table 3.4: Concentration-dependent effects of insulin on SERCA kinetic properties in homogenates from left ventricle and skeletal muscles of different fibre type composition.	113
Table 3.5: Effects of insulin or AGL 2263 on SERCA kinetic properties in homogenates from left ventricle and skeletal muscles of different fibre type composition.	114
Table 3.6: Effects of insulin, AGL 2263 or AGL 2263 + insulin on SERCA kinetic properties in homogenates from left ventricle and skeletal muscle of different fibre type composition.	115
Table 3.7: Effects of active insulin receptor and insulin on SERCA kinetic properties in homogenates and purified SR vesicles prepared from left ventricle and the white portion of the gastrocnemius.	118

CHAPTER FOUR

Table 4.1: Respiratory gas exchange measurements measured at rest and during prolonged exercise in the Placebo and Glucose conditions.	162
Table 4.2: Calculated substrate oxidation rates at rest and during prolonged exercise in the Placebo and Glucose conditions.	163
Table 4.3: Selected muscle metabolite concentrations at rest and during prolonged exercise in the Placebo and Glucose conditions.	167
Table 4.4: Muscle nucleotide concentrations measured at rest and during prolonged exercise in the Placebo and Glucose conditions.	168
Table 4.5: Selected muscle glycolytic intermediate concentrations measured at rest and during prolonged exercise in the Placebo and Glucose conditions.	169
Table 4.6: Sarcoplasmic reticulum Ca ²⁺ -ATPase kinetic parameters measured in muscle homogenates collected at rest and during exercise in the placebo and glucose conditions.	172
Table 4.7: Phospholamban phosphorylation status measured at rest and during prolonged exercise in the Placebo and Glucose conditions.	177

LIST OF FIGURES

CHAPTER ONE

Figure 1.1: Ribbon diagram showing the distribution of elements in the crystal structure of the rabbit skeletal muscle Ca^{2+} -ATPase (SERCA1a) at 2.6 Å resolution.	5
Figure 1.2: Representative curves for sarco(endo)plasmic reticulum Ca^{2+} -ATPase (SERCA) Ca^{2+} -dependent activity and kinetic properties.	11
Figure 1.3: Metabolic indices during prolonged exercise during high and low carbohydrate states.	16
Figure 1.4: SR Ca^{2+} -handling properties measured during prolonged exercise during high and low carbohydrate states.	17
Figure 1.5: Phospholamban (PLN) and sarcolipin (SLN) amino acid sequences and protein structure.	20
Figure 1.6: Phospholamban (PLN) and sarcolipin (SLN) acutely regulate sarco(endo)plasmic reticulum Ca^{2+} -ATPase (SERCA) Ca^{2+} -sensitivity by interacting directly with SERCA in their unphosphorylated states.	21

CHAPTER TWO

Figure 2.1: Potential pathways involved in β -adrenergic signaling in skeletal muscle.	35
Figure 2.2: Potential pathways involved in calcium-dependent calmodulin kinase (CaMKII) signaling in skeletal muscle.	37
Figure 2.3: Potential pathways involved in Protein kinase C (PKC) signaling in skeletal muscle.	38
Figure 2.4: Schematic representation of the general assay steps used to determine Ca^{2+} -dependent SERCA activity.	49
Figure 2.5: Results from representative samples illustrating the relationship between SERCA activity and Ca^{2+} -concentration in left ventricle (LV) and soleus (SOL) homogenates following incubation with selected treatments targeting epinephrine, protein kinase A or cAMP-mediated processes.	
Panel A and B:	73
Panel C and D:	74
Panel E and F:	75

Figure 2.6: Results from representative samples illustrating the relationship between SERCA activity and Ca^{2+} -concentration in left ventricle (LV), soleus (SOL) and white gastrocnemius (WG) homogenates following incubation with 15 μg calmodulin (CaM) or 4 μM KN62.	83
Figure 2.7: Results from representative samples illustrating the relationship between SERCA activity and Ca^{2+} -concentration in left ventricle (LV), soleus (SOL) and white gastrocnemius (WG) homogenates following incubation with 1400 nM GFX or 500 nM PMA.	85
 CHAPTER THREE	
Figure 3.1: Potential pathways involved in insulin signaling in skeletal muscle.	99
Figure 3.2: Results from representative samples illustrating the relationship between SERCA activity and Ca^{2+} -concentration.	119
Figure 3.3: Co-immunoprecipitation of insulin receptor substrate (IRS)-1 and IRS-2 with SERCA1a in white gastrocnemius homogenates.	121
Figure 3.4: Co-immunoprecipitation of insulin-receptor substrate (IRS)-1 and IRS-2 with SERCA2a in left ventricle homogenates.	122
Figure 3.5: Fluorescein isothiocyanate (FITC) binding capacity of enriched SR vesicles in response to 30 ng of active insulin receptor or 100 nM insulin.	124
Figure 3.6: N-cyclohexyl-N'-(dimethylamino- α -naphthyl) carbodiimide (NCD-4) binding capacity of enriched SR vesicles in response to 30 ng active insulin receptor or 100 nM insulin.	125
Figure 3.7: Assessments of phospholamban status in response to activation of insulin signaling in SR vesicles enriched in SERCA2a and prepared from the left ventricle.	126
Figure 3.8: Insulin receptor substrate (IRS)-1 and IRS-2 proteins should be added to the list of endogenous modulator proteins capable of acutely regulating sarco(endo)plasmic reticulum Ca^{2+} -ATPase (SERCA) Ca^{2+} -sensitivity in cardiac and skeletal muscle.	131

CHAPTER FOUR

- Figure 4.1: Experimental design used to characterize the effects of exercise and oral glucose supplementation on sarcoplasmic reticulum Ca^{2+} -cycling properties in human skeletal muscle. 146
- Figure 4.2: Blood metabolite and hormone concentrations measured at rest (0 min) and during prolonged exercise in the placebo (PLAC) and glucose (GLUC) conditions. 164
- Figure 4.3: Muscle glycogen concentrations measured at rest (0 min) and during prolonged exercise in the placebo (PLAC) and glucose (GLUC) conditions. 171
- Figure 4.4: Sarcoplasmic reticulum Ca^{2+} -transport parameters measured at rest (0 min) and during prolonged exercise in the placebo (PLAC) and glucose (GLUC) conditions. 174
- Figure 4.5: Sarcoplasmic reticulum Ca^{2+} -release parameters measured at rest (0 min) and during prolonged exercise in the placebo (PLAC) and glucose (GLUC) conditions. 176

CHAPTER FIVE

- Figure 5.1: Summary of changes in sarco(endoplasmic reticulum Ca^{2+} -ATPase (SERCA) Ca^{2+} -sensitivity obtained from the treatments utilized to characterize β -adrenergic signaling, Ca^{2+} -dependent calmodulin kinase II (CaMKII), Protein Kinase C (PKC) and insulin signaling in muscle homogenates in Chapter Two and Chapter Three. 193

LIST OF ABBREVIATIONS

4-CMC - 4-chloro-m-cresol
ADP - adenosine di-phosphate
ADP_f - free ADP
A-INS-R - an activated form of the insulin receptor
AK - adenylate kinase
AMP - adenosine monophosphate
AMP_f - free AMP
ANOVA - analysis of variance
A-PKA - an activated form of PKA
apparent coupling ratio - calculated as the ratio between Ca²⁺-uptake at 2000 nM/Vmax
Arg - arginine
ATP - adenosine tri-phosphate
BMI - body mass index which is calculated as mass/(height²)
BSA - bovine serum albumin
Ca²⁺ - Calcium
Ca²⁺_f - free cytosolic Ca²⁺ concentration
Ca₅₀ - defined as the Ca²⁺_f required for half maximal activation of the enzyme
CaM - calmodulin
CaMKII - Ca²⁺-dependent calmodulin kinase II
cAMP - adenosine 3',5'-cyclic monophosphate
CHO - carbohydrate
CPA - cyclopiazonic acid
CPK - creatine phosphokinase
Cr - creatine
CRC - Ca²⁺-release channel, also referred to as the ryanodine receptor (RyR)
CS - Citrate synthase
DHPR - the voltage sensitive dihydropyridine receptor
DTT - Dithiothreitol
E₁P - represents a stage in the SERCA Ca²⁺-transport process that requires the formation of a phosphorylated intermediate
E₂P - represents a stage in the SERCA Ca²⁺-transport process during Ca²⁺ translocation where the enzyme reverts back to the low energy state
E-C coupling - Excitation-contraction coupling
EDL - extensor digitorum longus
EPI - epinephrine
F - Emission maxima recorded at 405 nm for Ca²⁺-bound indo-1
F-1-6-P - fructose-1,6-diphosphate
F-6-P - fructose-6-phosphate
FITC - fluorescein isothiocyanate
G - Emission maxima recorded at 485 nm for Ca²⁺-free indo-1
G-1-P - glucose-1-phosphate
G-6-P - glucose-6-phosphate
GFX - GF-109203-XI is a PKC inhibitor and is also called bisindolylmaleimide I
GLUC - the glucose supplementation condition in Chapter Four
Glut-4 - glucose transporter 4

Hb - hemoglobin
Hct - hematocrit
HEPES - N-2-hydroxyethylpiperazine-N'-2-ethanesulfonic acid
Hi CHO - a condition that created a high glycogen status in muscle
HPLC - high performance liquid chromatography
IC₅₀ -the median inhibition concentration
IMP - inosine monophosphate
INS - insulin
INS-TK - insulin tyrosine kinase
Ionophore - Ca²⁺-ionophore A23187
Ionophore ratio - calculated as the ratio of V_{max}/V_{max}(-)
IRS - insulin receptor substrate
K_{AK} - equilibrium constants used for the AK
K_{CPK} - equilibrium constants used for the CPK
K_d - is the equilibrium constant for the interaction between Ca²⁺ and Indo-1
kDa - kiloDaltons
KN62 - is a CaMKII inhibitor with the chemical name (S)-5-Isoquinolinesulfonic acid 4-[2-[(5-isoquinolinylylsulfonyl) methylamino]-3-oxo-3-(4-phenyl-1-piperazinyl)propyl]phenylester)1-[N,O-bis (5-Isoquinolinesulfonyl) -N-methyl-L-tyrosyl]-4-phenylpiperazine
KT5720 - is PKA inhibitor with the chemical name (9S,10S,12R)-2,3,9,10,11,12-Hexahydro-10-hydroxy-9-methyl-1-oxo-9,12-epoxy-1H-diindolo[1,2,3-fg:3',2',1'-kl] pyrrolo[3,4-i][1,6]benzodiazocine-10-carboxylic acid hexyl ester
Lac - lactate
LDH - lactate dehydrogenase
Lo CHO - a condition that created a low glycogen status in muscle
LV - left ventricle
M - molar concentration
Mg²⁺ - Magnesium
M10 - the transmembrane region 10 of SERCA
NaN₃ - sodium azide
NCD-4 - N-cyclohexyl-N'- (dimethylamino-alpha-naphthyl) carbodiimide
NE -norepinephrine
n_H - Hill coefficient - defined as the relationship between SERCA activity and Ca²⁺_f for 10 to 90% V_{max}
NO - nitric oxide
PA - phosphatidic acid
PCA - perchloric acid
pCa -the negative logarithm of the Ca²⁺_f
PCr - Phosphocreatine
pH - the negative log of the H⁺ concentration
Phase 1 Ca²⁺-release - the initial rapid phase of Ca²⁺-release that lasts from 0-3 s
Phase 2 Ca²⁺-release - the slower, more prolonged rate of Ca²⁺-release that lasts from 4-10 s
Pi - inorganic phosphate
PI3K - phosphatidyl inositol 3 kinase
PK - pyruvate kinase

PKA - cAMP-dependent protein kinase A
PKC - protein kinase C
PLAC - the placebo condition in Chapter Four
PLD - phospholipase D
PLN - phospholamban
PMA - is a phorbol ester with the chemical name phorbol-12-myristate-13-acetate
PP1 - protein phosphatase 1
PP-1G - a glycogen bound form of protein phosphatase-1
PP2a - protein phosphatase 2a
Pyr - pyruvate
R - the ratio (R) of F to G
RER - respiratory exchange ratio
RG - red gastrocnemius
ROS - reactive oxygen species
RyR - ryanodine receptor, also referred to as the CRC
SDS-PAGE - Sodium dodecyl sulfate polyacrylamide gel electrophoresis
Ser - serine
SERCA - sarco(endo)-plasmic reticulum Ca^{2+} -ATPase
SH2 - src homology 2 domain
SLN - sarcolipin
SOL - soleus
SR - sarcoplasmic reticulum
Std - standard
STK16 - serine/threonine kinase 16
TCr - total creatine
Thr - threonine
T-tubule - transverse-tubule
VCO₂ – minute carbon dioxide output
V_e – minute expiratory ventilation
V_{max} - maximal enzyme activity
V_{max(-)} - maximal enzyme activity in the absence of the Ca^{2+} -ionophore A23187
VO₂ – minute oxygen consumption
VO_{2peak} - peak aerobic power
WG - white gastrocnemius

CHAPTER ONE

LITERATURE REVIEW AND STATEMENT OF THE PROBLEM

Literature Review

The role of the sarcoplasmic reticulum in excitation-contraction coupling and relaxation.

Excitation-contraction coupling in skeletal muscle involves a series of processes that are initiated by the propagation of an action potential along the sarcolemma and the transverse-tubule (T-tubule) that culminates with an increase in the free cytosolic Ca^{2+} concentration (Ca^{2+}_f) and activation of the contractile apparatus (Berchtold *et al.*, 2000).

The sarcoplasmic reticulum (SR) is a membrane system that extends throughout the myofibril and is primarily responsible for the regulation of Ca^{2+}_f within the sarcomere of skeletal muscle. Calcium transients in skeletal muscle fibres are controlled by the function of several SR-associated proteins and by the SR membrane itself. The Ca^{2+} -release channel (CRC) is the protein that regulates Ca^{2+} -release rates within the sarcomere. The CRC is activated when an action potential activates the voltage sensitive dihydropyridine receptor (DHPR) in the T-tubule, which is located adjacent to and physically interacts with the CRC in the SR membrane. Activation of the DHPR triggers the release of Ca^{2+} from the SR, through the CRC. The rapid release of Ca^{2+} from the SR increases the cellular Ca^{2+}_f thereby activating the contractile apparatus to produce force. In addition to being influenced by SR Ca^{2+} -release rates, cytosolic Ca^{2+}_f is also influenced by cytosolic Ca^{2+} -binding proteins (e.g. calmodulin and parvalbumin) and also the rate of Ca^{2+} -uptake back into the SR by the sarco(endo)plasmic reticulum Ca^{2+} -ATPase (SERCA).

Relaxation, which involves the dissociation of actin and myosin, is dependent on the restoration of cytosolic Ca^{2+}_f to nM levels. SERCA is the primary protein responsible for the sequestration (Ca^{2+} uptake) of cytosolic Ca^{2+}_f following contractile activation. Fast-twitch fibres predominately express the SERCA1 isoform, while slow twitch and cardiac fibres

predominately express the SERCA2a isoform. Calcium-uptake rates are determined by the net movement of Ca^{2+} -ions across the SR membrane as determined by the kinetic properties of SERCA and can be influenced by alterations to SR membrane integrity and composition.

The rapid contraction and relaxation cycles that make up repetitive activity requires that intracellular Ca^{2+} -cycling rates be increased during physical activity. However, it appears that repetitive activity of prolonged duration (Duhamel *et al.*, 2004a; Duhamel *et al.*, 2004b; Duhamel *et al.*, 2005; Duhamel *et al.*, 2006c; Duhamel *et al.*, 2006b; Duhamel *et al.*, 2006a; Booth *et al.*, 1997; Chin, 2005) can lead to a progressive loss of Ca^{2+} -cycling properties assessed *in vitro*. Exercise-induced reductions in Ca^{2+} -cycling would be expected to have profound effects on muscle contractile performance since disturbances in Ca^{2+} -release and/or Ca^{2+} -uptake kinetics would disrupt the integrity of the cytosolic Ca^{2+} -transient and would depress contractile activation and relaxation. Therefore, it would be of value to characterize the mechanisms governing the acute regulatory behaviour of SR Ca^{2+} -transport properties in muscle since this knowledge would advance our understanding of the mechanisms regulating performance in both health and disease.

Tertiary structure and function of SERCA proteins.

Three genes, located on different chromosomes in the human, code for the three major SERCA protein isoforms, namely SERCA1, SERCA2 and SERCA3 (Lytton *et al.*, 1992). The three major SERCA isoforms are developmentally regulated or alternatively spliced to create various sub isoforms. Although several sub isoforms for each major SERCA protein exists, the primary amino acid structure is highly conserved. For this reason, all SERCA proteins act as Ca^{2+} -pumps and have similar transmembrane and tertiary structures (Lytton *et al.*, 1992).

Although the SERCA isoforms are similar in structure and function, they are expressed in a tissue specific manner. Specifically, two sub isoforms of SERCA1 are expressed in mammalian adult (SERCA1a) and neonatal (SERCA1b) fast-twitch muscle and are not expressed to any significant extent in any other tissue (MacLennan *et al.*, 1985). In contrast to SERCA1, SERCA2 is not developmentally regulated but is alternatively spliced depending on the tissue. Cardiac and slow-twitch skeletal muscle primarily expresses the SERCA2a isoform; whereas SERCA2b is primarily expressed in non-muscle tissues as well as smooth muscle (Lytton *et al.*, 1992). The SERCA3 protein isoforms (SERCA3a-c) are ubiquitously expressed at low levels in many different tissues (Lytton *et al.*, 1992).

In general, SERCA proteins weigh approximately 95-110-kDa and have cytoplasmic, transmembrane and luminal regions. The isolation and cloning of the full-length cDNA encoding for the rabbit SERCA2a enzyme (MacLennan *et al.*, 1985) allowed for the assessment of the complete primary (Brandl *et al.*, 1986), secondary and tertiary structural features of the enzyme (MacLennan & Lytton, 1992), which has since been supported by the determination of the crystal structure of SERCA1a by electron microscopy (Toyoshima *et al.*, 2000). Based on these studies, a large cytosolic globular headpiece was identified which is made up 3 globular domains (Figure 1.1), consisting of an actuator domain, the phosphorylation-domain and the nucleotide-binding domain (Arg₅₀₅) (MacLennan *et al.*, 2002; MacLennan & Lytton, 1992). The transmembrane domain is made up from ten, largely helical transmembrane segments, four of which are juxtaposed in the E1 conformation to form the sites for binding of Ca²⁺, seen as spheres. The β -strand, which is a narrow stalk region, links the large cytoplasmic head to the much smaller transmembrane region. The β -strand contains an abundance of negatively charged glutamate residues, which are thought to attract positively charged Ca²⁺ ions and are

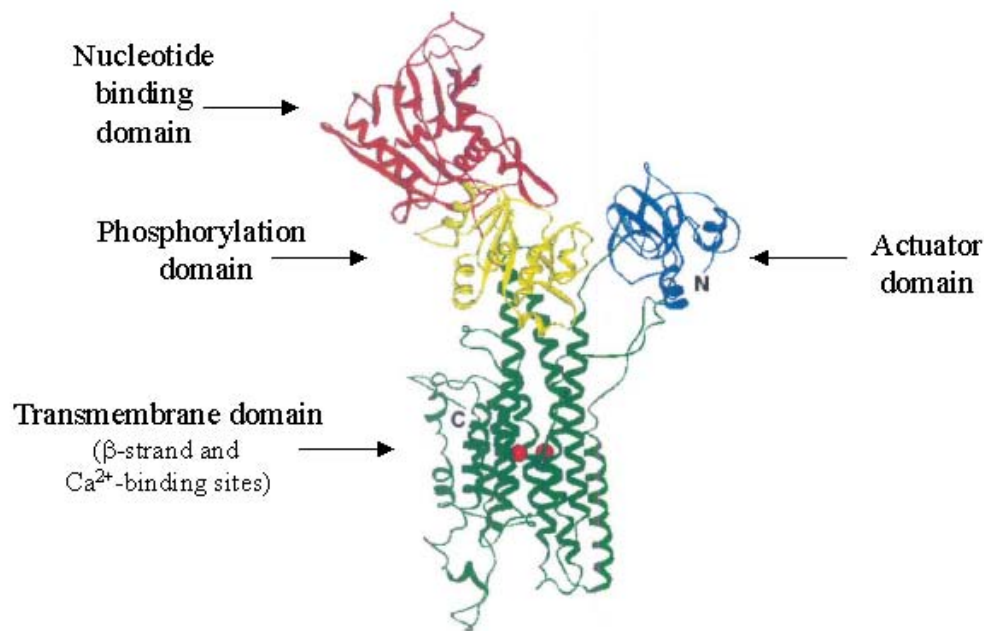


Figure 1.1: Ribbon diagram showing the distribution of elements in the crystal structure of the rabbit skeletal muscle Ca^{2+} -ATPase (SERCA1a) at 2.6Å resolution. The cytoplasmic segment, accounting for 75% of the total protein mass, is organized into three interacting domains: the nucleotide-binding (N) domain; the phosphorylation (P) domain; and the actuator (A) domain in blue. The transmembrane domain is made up from ten, largely helical transmembrane segments, four of which are juxtaposed in the E1 conformation to form the sites for binding of Ca^{2+} , seen as spheres. Major conformational changes that can be predicted to occur during ATP-energized Ca^{2+} transport are the closing of the "jaws" formed by the P and N domains to permit phosphorylation of Asp351 in the P domain, closing of the gap between the A domain and the P+N domains and transmission of these conformational changes to the Ca^{2+} -binding and translocation domain to disrupt the Ca^{2+} -binding sites and alter their accessibility from cytosolic and luminal spaces. This figure was prepared using Molscript and Raster-3D.141. Adapted from MacLennana *et al.*, 2002, which was originally published by Toyoshima *et al.*, 2000.

necessary for normal Ca^{2+} transport, as demonstrated by site-directed mutagenesis studies (MacLennan, 1990). The stalk sector is made up of 5 alpha helices. Because of its strong negative charge, the stalk region is thought to be a possible location for aiding in the sequestration of Ca^{2+} . However, the stalk region does not contain Ca^{2+} -binding sites; rather it appears that the stalk region channels Ca^{2+} to high affinity Ca^{2+} -binding sites located in the center region of the base piece (Clarke *et al.*, 1989a; Clarke *et al.*, 1989b). The base piece is made of 10 transmembrane helices, located adjacent to the stalk sector. Residues located in the center of the base piece, which includes transmembrane sequences M4, M5, M6, and M8, are thought to include Ca^{2+} -binding sites. Site-directed mutagenesis studies has been used to identify many of the residues that are required for the normal functioning of the nucleotide and Ca^{2+} -binding domains of SERCA (MacLennan, 1990). All known SERCA2 proteins from different species show 100% homology in the β -strand, transmembrane and stalk domains, and high amino acid conservation in the phosphorylation (97.8%), ATP-binding (97.7%) and hinge (98.3%) domains (Sakuntabhai *et al.*, 1999). The deduced amino acid sequence of human SERCA2 is also highly conserved among the other human SERCA proteins, showing 82% and 76% identity with SERCA1 and SERCA3, respectively. Differences in the 3' end are primarily responsible for the differences in amino acid sequences observed.

Proteins of the SERCA family are classified as a P-Type ion motive-ATPases. This family of ATPases requires the formation of a phosphorylated intermediate (E_1P) to induce conformational changes to SERCA structure in order to transport Ca^{2+} ions into the lumen of the SR. The binding of ATP at the nucleotide binding site (Arg₅₀₅) and its hydrolysis forms a phosphorylated intermediate (E_1P), which induces a transformational change within SERCA to promote the translocation of Ca^{2+} from the cytosol into the SR lumen. During Ca^{2+} ion

translocation, the enzyme reverts back to the low energy (E₂P) state (Taylor & Green, 1989). Cytoplasmic Ca²⁺ binds to the Ca²⁺-binding domain of the enzyme with high affinity in a cooperative manner but as the translocation proceeds, the affinity of these binding sites for Ca²⁺ decreases, allowing release of Ca²⁺ ions into the lumen of the SR (Berchtold *et al.*, 2000; MacLennan, 1990).

The binding affinity for ATP is similar between all SERCA isoforms (Lytton *et al.*, 1992); however, differences in maximal enzyme activity (V_{max}) and Ca²⁺-sensitivity do exist between the different isoforms (Lytton *et al.*, 1992). Specifically, it was found that the non-muscle SERCA isoforms (SERCA2b, SERCA3a, SERCA3b, and SERCA 3c) have lower maximal activities compared to the muscle specific SERCA isoforms (SERCA1a, SERCA1b and SERCA2a) (Lytton *et al.*, 1992). These results suggest that the muscle specific isoforms of SERCA have the ability to pump Ca²⁺_f from the cytosol into the SR at a faster rate compared to non-muscle SERCA isoforms. A second functional property that differs between SERCA proteins is their affinity for Ca²⁺_f. Observations made by Lytton *et al.*, (Lytton *et al.*, 1992) indicate that SERCA3a has a lower affinity for Ca²⁺_f compared to SERCA1a; while SERCA3b and SERCA3c have even lower affinities for Ca²⁺_f compared to SERCA3a (Dode *et al.*, 1998). The higher V_{max} and Ca²⁺-sensitivity of SERCA1a and SERCA2a, compared to SERCA2b and SERCA3a-c, are most probably associated with the frequent requirements of the muscle specific isoforms to sequester cytosolic Ca²⁺_f in response to repetitive contraction in muscle. Since our laboratory is primarily interested in studying the acute and chronic regulatory factors that influence SERCA in cardiac and skeletal muscle, SERCA1a and SERCA2a remains the primary interest of this thesis.

Tertiary structure and function of CRC proteins.

The CRC is composed of 4-identical subunits and weighs ~565-kDa (Takeshima *et al.*, 1989). The CRC has a high affinity for the plant alkaloid ryanodine and is commonly referred to as the ryanodine receptor (RyR). Three isoforms of RyR have been identified in skeletal muscle, liver and brain tissues. The primary isoform in mammalian skeletal muscle is RyR1 [for review see (Franzini-Armstrong & Protasi, 1997)]. The activity of the CRC can be regulated by endogenous modulators such as Ca^{2+} , Mg^{2+} , ATP, ADP, IMP, NO, superoxide, H_2O_2 and by the interaction with calmodulin (CaM). Calmodulin is a Ca^{2+} -binding protein that has binding sites on the CRC and has been shown to increase Ca^{2+} -release at low concentrations (nM) of Ca^{2+} and inhibit Ca^{2+} -release when Ca^{2+}_f is elevated (μM) (Favero, 1999).

Experimental models used to characterize sarcoplasmic reticulum function

Researchers have employed many different models to investigate the acute and chronic regulation of SR proteins. These various models have strengths and weaknesses, and need to be selected appropriately to properly address specific research questions. For example, the single fibre technique has proven to be a very powerful tool when examining the regulation of Ca^{2+}_f *ex vivo*. The strength of the single fibre technique can be stimulated to contract using various chemical or electric stimuli (Barnes *et al.*, 2001; Chin & Allen, 1997; Helander *et al.*, 2002; Lunde *et al.*, 2001). Observations made using the single fibre technique have demonstrated that repetitive activation of skeletal muscle fibres until they fatigue results in the progressive loss of Ca^{2+} -homeostasis (Barnes *et al.*, 2001; Chin & Allen, 1997; Helander *et al.*, 2002; Lunde *et al.*, 2001). However, since Ca^{2+}_f is influenced by Ca^{2+} -release, Ca^{2+} -uptake, and Ca^{2+} -binding

protein capacities, it is difficult to identify the underlying mechanisms for any observed reductions in Ca^{2+}_f . Several methods exist to directly assess the effects of an experimental perturbation on SERCA or CRC functional characteristics. For example, *in vitro* biochemical assays have been developed to assess the specific activities of SERCA (Simonides & van Hardeveld, 1990) and CRC (Ruell *et al.*, 1995). Since these assays are performed using supposedly optimal conditions *in vitro*, alterations in SR Ca^{2+} -handling properties between experimental conditions are thought to reflect intrinsic structural and/or compositional modifications to SR proteins or the SR membrane. However, the limitation of *in vitro* techniques is the issue of physiological relevance. Since our laboratory is interested in studying the acute and chronic regulatory factors that influence SERCA and the CRC, many of our experiments utilize *in vitro* techniques.

Exercise and the sarcoplasmic reticulum

The effects of exercise on SR Ca^{2+} -handling properties in muscle have been studied both *in situ* (Barnes *et al.*, 2001; Helander *et al.*, 2002; Lunde *et al.*, 2001) and *in vitro* (Booth *et al.*, 1997; Duhamel *et al.*, 2006c; Duhamel *et al.*, 2004b; Green *et al.*, 1998; Chin & Green, 1996). Generally, the literature supports a reduction in V_{\max} , Ca^{2+} -uptake and Ca^{2+} -release rates following repetitive activity in humans (Booth *et al.*, 1997; Duhamel *et al.*, 2006c; Duhamel *et al.*, 2004b; Chin & Green, 1996) and animals (Chin & Allen, 1997; Barnes *et al.*, 2001; Stephenson *et al.*, 1999). However, discrepancies do exist as some studies do not support exercise-induced reductions in V_{\max} , particularly in rat skeletal muscle (Chin & Green, 1996; Ferrington *et al.*, 1996; Schertzer *et al.*, 2004). The differences appear to be related to factors such as exercise protocols, tissue sampling schedule, tissue preparation, species and fibre type

composition of the muscle examined. In studies that have demonstrated an exercise-induced reduction in SR Ca^{2+} -handling properties, the reductions in these properties have been linked to structural changes within the CRC and SERCA proteins (Booth *et al.*, 1997; Luckin *et al.*, 1991; Dux *et al.*, 1990; Favero *et al.*, 1993; Duhamel *et al.*, 2006c; Duhamel *et al.*, 2004b; Green *et al.*, 1998). Contraction-induced intracellular changes in oxidative and/or thermal stress (Schertzer *et al.*, 2002), in addition to the accumulation of intracellular metabolites such as inorganic phosphate (Chin & Allen, 1997; Fitts, 1994), nitric oxide (NO) or reactive oxygen species (Fitts, 1994; Tupling *et al.*, 2001c; Tupling *et al.*, 2001a) are known to induce structural alterations to SERCA and the CRC (Luckin *et al.*, 1991; Dux *et al.*, 1990; Favero *et al.*, 1993), thereby reducing SR Ca^{2+} -transport properties assessed *in vitro*. For example, high concentrations of NO have been associated with increased nitrosylation of Cys364, Cys360 and Cys471 within SERCA, leading to a down-regulation of V_{\max} in rat skeletal muscle (Viner *et al.*, 2000). Recent literature has also provided evidence linking the depletion of muscle glycogen with reduced SR Ca^{2+} -transport properties in human (Duhamel *et al.*, 2006c; Duhamel *et al.*, 2006b; Duhamel *et al.*, 2006a), rat (Lees *et al.*, 2001), mouse (Chin & Allen, 1997), and toad (Stephenson *et al.*, 1999).

Additional insight into the effects of exercise on SERCA properties can be provided by the assessment of Ca^{2+} dependent SERCA activity (Figure 1.2). In addition to determining V_{\max} , this technique allows for the assessment of the Ca^{2+} -sensitivity of the enzyme, which can be measured by the calculation of the Hill coefficient (n_H ; defined as the relationship between SERCA activity and Ca^{2+}_f) and Ca_{50} (defined as the Ca^{2+}_f required for half maximal activation of the enzyme). Interestingly, at least in humans, prolonged exercise does not alter the Ca^{2+} -sensitivity of SERCA (i.e. n_H or Ca_{50}), assessed *in vitro* (Duhamel *et al.*, 2004a; Duhamel *et al.*,

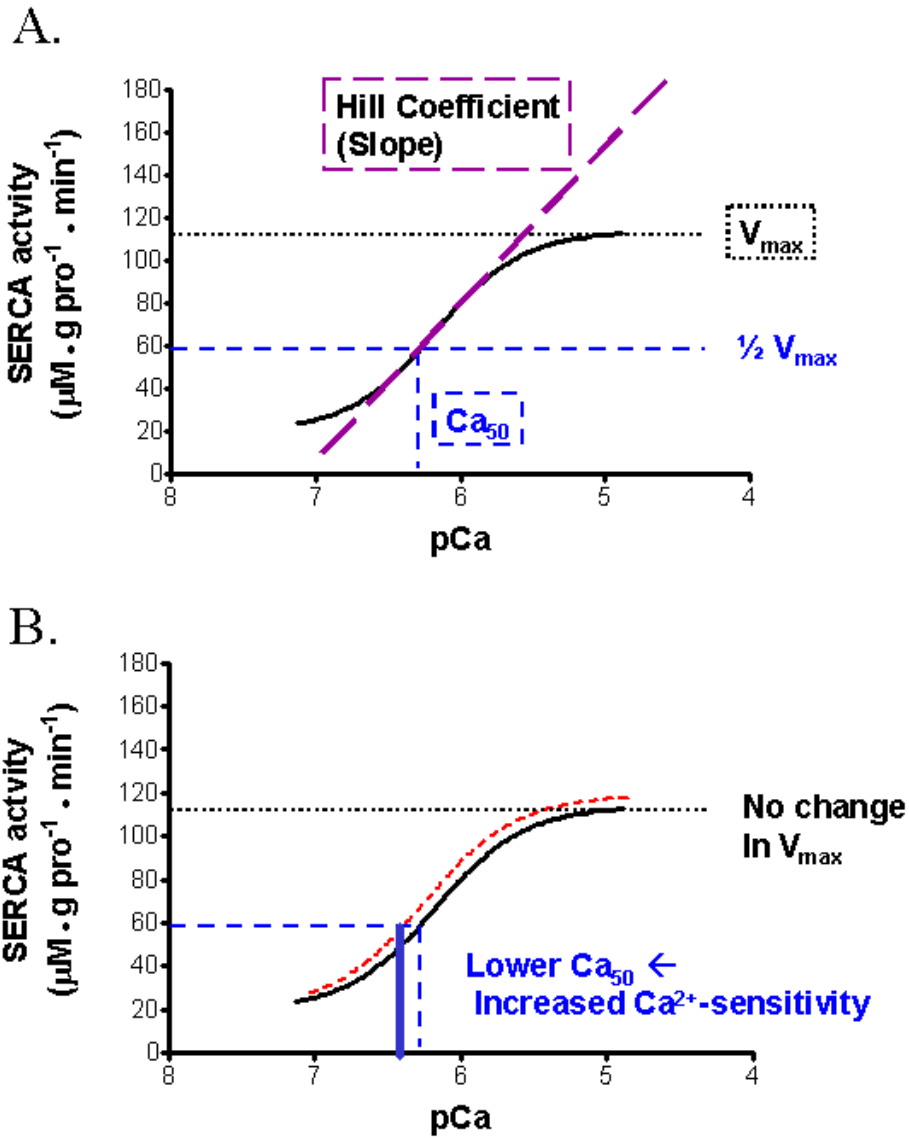


Figure 1.2: Representative curves for sarco(endo)plasmic reticulum Ca^{2+} -ATPase (SERCA) Ca^{2+} -dependent activity and kinetic properties. Panel A: The three kinetic properties assessed in this thesis have been indicated. V_{max} , maximal SERCA activity. n_{H} , hill slope defined as the relationship between SERCA activity and $\text{Ca}^{2+}_{\text{f}}$ for 10 to 90% V_{max} . Ca_{50} , the Ca^{2+} -concentration at $\frac{1}{2} V_{\text{max}}$. Panel B: Representative curve illustrating the effect of reducing Ca_{50} and how this kinetic properties represents an increased SERCA Ca^{2+} -sensitivity. Reductions in Ca_{50} occur as a result of a reduced inhibitory interaction of phospholamban and sarcolipin with SERCA at sub-maximal $\text{Ca}^{2+}_{\text{f}}$.

2004b; Duhamel *et al.*, 2006c). The lack of change in SERCA Ca²⁺-sensitivity is notable since a variety of environmental factors are known to influence SERCA Ca²⁺-sensitivity measured *in vitro* in both cardiac and skeletal muscle (Saucerman & McCulloch, 2004). This observation serves to emphasize that the mechanisms regulating SERCA Ca²⁺-sensitivity are not yet fully understood.

Muscle glycogen content and SR Ca²⁺-handling properties in animal models.

Evidence, obtained from examination of the ultrastructural composition of muscle, has demonstrated that glycogen particles, glycogen phosphorylase, glycogen debranching enzyme, all the enzymes involved in the glycolytic pathway and creatine phosphokinase (CPK), are located in close proximity to the SR (Entman *et al.*, 1977a; Entman *et al.*, 1977b; Entman *et al.*, 1980; Xu *et al.*, 1995; Xu & Becker, 1998). The characterization of this SR-glycogenolytic complex raises several interesting questions with respect to its functional role within muscle. For example, glycogen particles in close proximity with the SR are more heavily depleted (~95% depletion of SR-bound glycogen) relative to glycogen particles assessed in the whole muscle (~77% depletion) in rat skeletal muscle following a 15 min electrical stimulation protocol (Lees *et al.*, 2001). However, since pre-exercise muscle glycogen content was not manipulated, it is unclear if the depletion of glycogen in close proximity to the SR or some other exercise-induced mechanism was responsible for reductions in SR Ca²⁺-transport properties observed (Lees *et al.*, 2001). It is possible that glycogen particles in close proximity to the SR may link ATP utilization processes with ATP production pathways. In fact, evidence has been provided to link ATP produced from glycolysis and CPK to Ca²⁺-transport properties in skeletal muscle (Korge & Campbell, 1994; Korge *et al.*, 1993; Xu *et al.*, 1995). However, in

addition to being a metabolic substrate, it appears that glycogen may also influence SR Ca^{2+} -handling properties as a result of structural alterations induced by direct effects of substrate loss (Cuenda *et al.*, 1991; Lees *et al.*, 2001) or by interrupting second messenger signaling pathways (Liu & Brautigan, 2000).

A non-energy related mechanism by which glycogen can be involved has been proposed. It has been suggested that the physical interactions between glycogen and SR-associated proteins may be interrupted when glycogen particles associated with the SR are reduced below a threshold level (Barnes *et al.*, 2001). As an example, glycogen phosphorylase and glycogen debranching enzymes dissociate from the SR-glycogen complex during muscle stimulation (Lees *et al.*, 2001; Lees *et al.*, 2004). Recent experiments using the isolated single fibre technique has offered support to the hypothesis that glycogen has a structural role in muscle E-C coupling, independent of energy metabolism (Barnes *et al.*, 2001; Chin & Allen, 1997; Stephenson *et al.*, 1999). According to this hypothesis, it is possible that an increase in pre-exercise muscle glycogen content, also known to increase the average glycogen particle size in humans (Marchand *et al.*, 2002), may prolong the duration of exercise required before this critical limit is passed, thereby delaying the onset of exercise-induced reductions in SR Ca^{2+} -transport properties during exercise. In fact, a highly significant correlation ($P < 0.0001$) between reductions in single fibre Ca^{2+}_f and initial glycogen content has been reported in electrically stimulated single fibres collected from cane toads (Stephenson *et al.*, 1999). Another study (Barnes *et al.*, 2001) has confirmed that reductions in Ca^{2+}_f occur much later in electrically stimulated skinned fibres from muscles with elevated glycogen content compared to fibres from muscles with low glycogen content (Barnes *et al.*, 2001). Since the observations made by these groups (Barnes *et al.*, 2001; Chin & Allen, 1997; Stephenson *et al.*, 1999) were

based on the single fibre technique, the specific process within E-C coupling responsible for the reductions in Ca^{2+}_f during low glycogen states can not be identified. It is possible that glycogen depletion may cause one or more of the signaling processes within the T-tubule, the DHPR or the CRC channel to be interrupted. Additionally, it is also possible that second messenger signaling processes involved in E-C coupling may be interrupted during low glycogen states.

The provision of glucose during a recovery period can influence the regulation of muscle glycogen, cytosolic Ca^{2+}_f and contractile function in mammalian single fibres (Chin & Allen, 1997; Helander *et al.*, 2002). In fact, the beneficial effects of glucose were attributed to the resynthesis of muscle glycogen during the recovery period between tests (Chin & Allen, 1997; Helander *et al.*, 2002). In contrast, no resynthesis of glycogen occurred, and only minimal improvements in the regulation of cytosolic Ca^{2+}_f and contractile function were observed, when glucose was not provided during the recovery period in these studies (Chin & Allen, 1997; Helander *et al.*, 2002). Based on the observations, it appears that Ca^{2+} -transport properties and muscle contractile properties are influenced by the availability of muscle glycogen during exercise and recovery.

Effects of muscle glycogen content on SR Ca^{2+} -handling properties in human skeletal muscle.

We have reported that muscle glycogen content may modify the exercise-induced reductions in SR Ca^{2+} -handling properties during prolonged exercise in humans (Duhamel *et al.*, 2005; Duhamel *et al.*, 2006b). In these studies, untrained males performed submaximal cycling trials on two occasions following a standardized glycogen depletion protocol, namely after a 4-day low CHO diet (Lo CHO) and after a 4-day high CHO diet (Hi CHO). SR Ca^{2+} -handling properties were assessed *in vitro* using homogenates prepared from tissue extracted

from the vastus lateralis at rest, after 30 min of exercise and at a time corresponding to fatigue during Lo CHO (66 ± 6 min) in both Lo CHO and Hi CHO, and at fatigue in Hi CHO (103 ± 9 min). Pre-exercise muscle glycogen content (Figure 1.3a) was lower by 37% in the Lo CHO group compared to the Hi CHO group. Muscle glycogen content was also lower after 30 min and at fatigue in Lo CHO, compared to the matching time points in Hi CHO. Glycogen content was not different at fatigue in Lo CHO compared to fatigue in Hi CHO.

No differences in V_{\max} were observed at rest between diets (Figure 1.4a). However, when the two conditions were compared, reductions in V_{\max} were observed after 30 min of exercise and at fatigue in Lo CHO, but not for matched time points in Hi CHO. When a comparison was made at fatigue in Lo CHO and fatigue in Hi CHO, it was observed that V_{\max} was not different between Lo CHO and Hi CHO. No differences in Ca^{2+} -uptake (Figure 1.4b) or Ca^{2+} -release rates (Figure 1.4c) were observed at rest between conditions. However, when the different conditions were compared at matched time points during exercise, reductions in SR Ca^{2+} -uptake and Ca^{2+} -release rates were observed at 30 min of exercise in Lo CHO but not in Hi CHO. No differences in Ca^{2+} -uptake and Ca^{2+} -release rates were observed at fatigue in Lo CHO compared to the matched Lo CHO fatigue time point during Hi CHO.

Although, these data suggested that muscle glycogen content might directly influence the time course of exercise-induced structural alterations to SERCA and the CRC, other mechanisms involved in the regulation of whole-body CHO metabolism may be involved. One possibility to explain the reduced time-course for exercise-induced reductions in SR Ca^{2+} -handling properties may be the loss of plasma glucose homeostasis that occurred during the Lo CHO condition, but not the Hi CHO condition (Figure 1.3b). Increased blood glucose availability could increase SR Ca^{2+} -cycling properties via improved energy homeostasis and/or

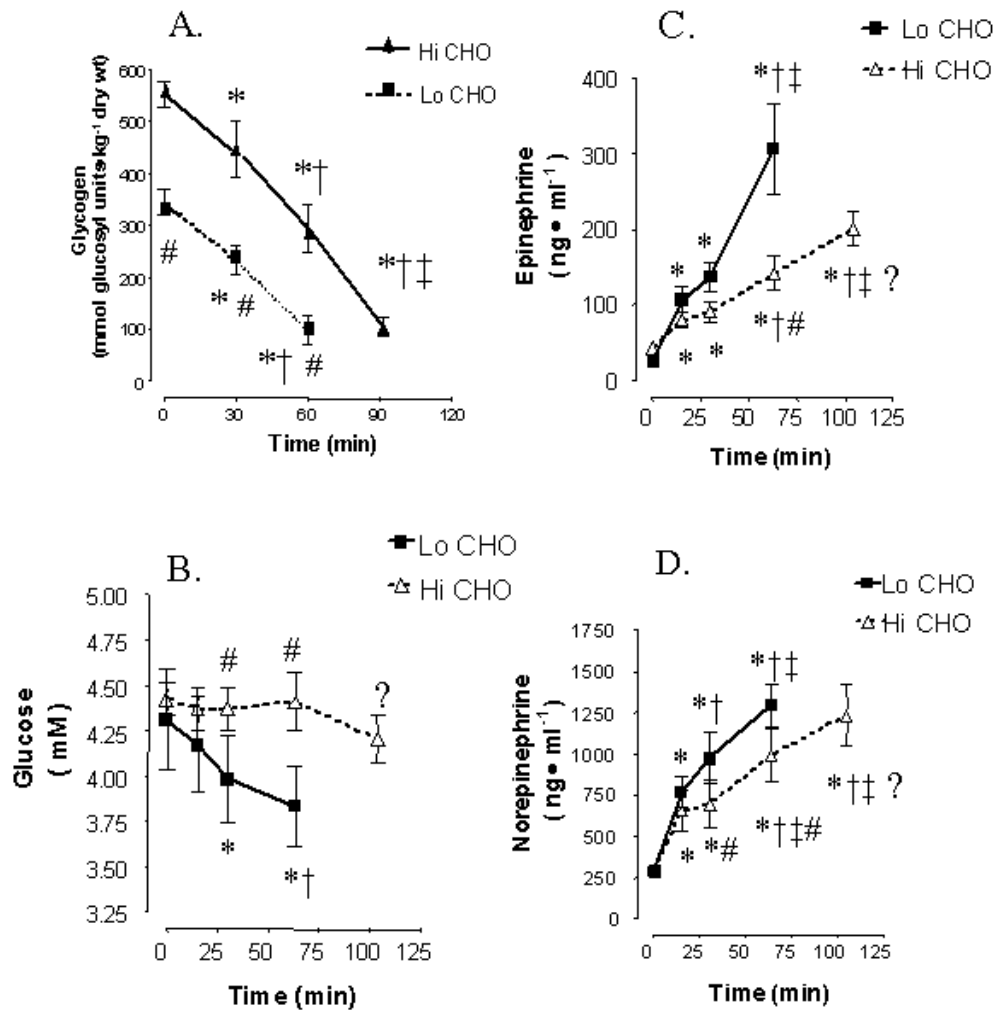


Figure 1.3: Metabolic indices during prolonged exercise during high and low carbohydrate states. A. Muscle glycogen content. B. Plasma glucose. C. Plasma epinephrine. D. Norepinephrine. * Significantly different from Rest ($P < 0.05$). † Significantly different from 15 min ($P < 0.05$). ‡ Significantly different from 30 min ($P < 0.05$). ? Significantly different from LCHO Fatigue ($P < 0.05$). # Significantly different from LCHO ($P < 0.05$). Adapted from Duhamel et al., 2006c.

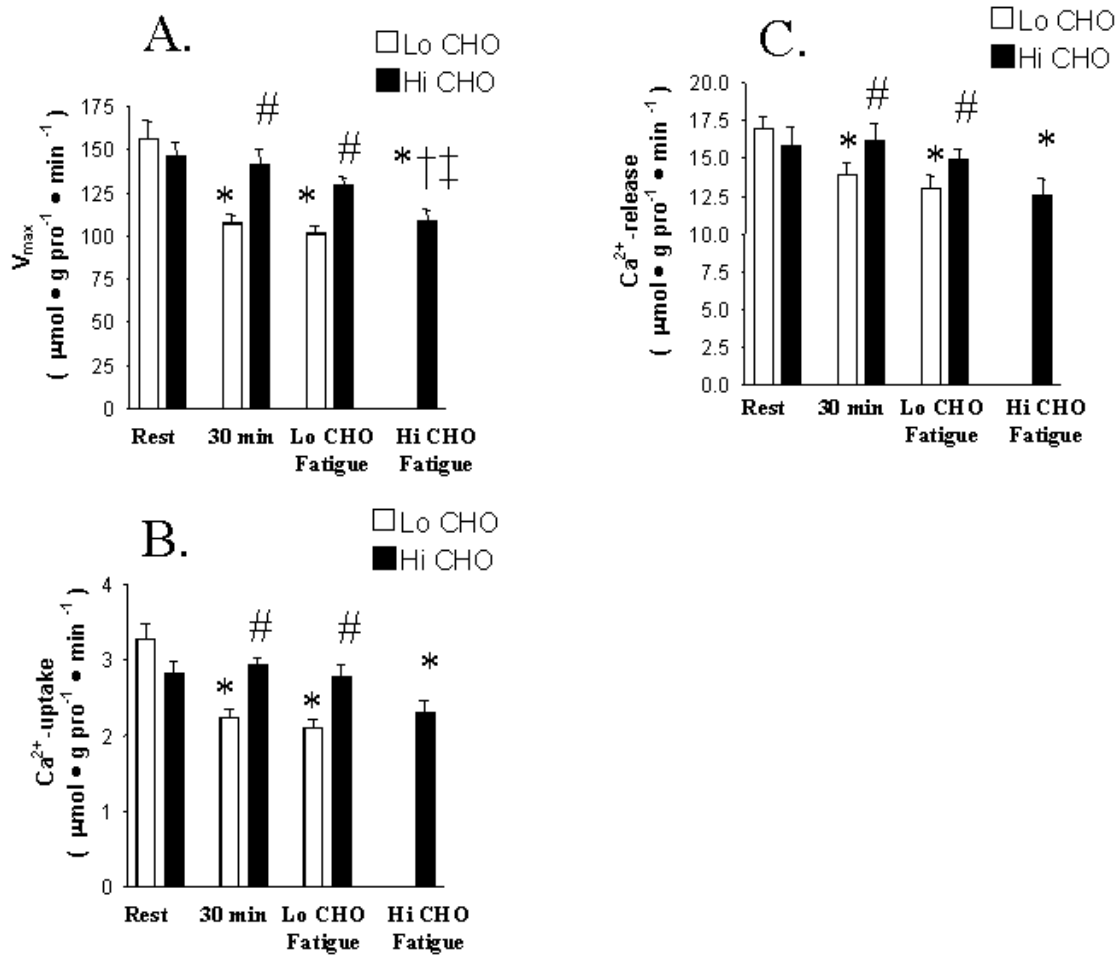


Figure 1.4: SR Ca^{2+} -handling properties measured during prolonged exercise during high and low carbohydrate states. A. Maximal Ca^{2+} -ATPase activity (V_{max}) B. Ca^{2+} -uptake rates. C. Ca^{2+} release rates. * Significantly different from Rest ($P < 0.05$). † Significantly different from 15 min ($P < 0.05$). ‡ Significantly different from 30 min ($P < 0.05$). # Significantly different from LCHO ($P < 0.05$). Adapted from Duhamel et al., 2006c.

protection of muscle glycogen reserves (Xu *et al.*, 1995; Lees & Williams, 2004). Interestingly, as with experiments designed to manipulate muscle glycogen levels by exercise and diet (Bergstrom *et al.*, 1967), oral glucose supplementation during exercise also has an ergogenic effect (Coyle, 1992a; Hargreaves, 1999).

A second possible mechanism to explain the reductions in SR Ca^{2+} -handling properties observed during exercise with Lo CHO, compared to Hi CHO, is based on the effect of altered blood glucose concentrations on the glucoregulatory hormone insulin (INS) and the catecholamines epinephrine (EPI) and norepinephrine (NE). In our previous work, alterations in the dietary intake of CHO resulted in differences in blood glucose concentrations during prolonged exercise that were also accompanied by differences between conditions in plasma NE and EPI (Figure 1.4c and 1.4d) (Duhamel *et al.*, 2006c) and most probably INS as well (Galbo, 1999). Differences in the hormonal responses could affect intrinsic behaviour of SERCA or the CRC through second messenger regulation (MacLennan *et al.*, 2003; Wuytack *et al.*, 2002). In general, the role of blood hormone changes in modifying the intrinsic regulation of SERCA and the CRC remain largely unexplored.

Effects of second messenger signaling on SR Ca^{2+} -handling properties

Signaling pathways translate a variety of environmental cues, such as hormones, neurotransmitters and local metabolites, into physiological responses within the cell (Saucerman & McCulloch, 2004). In this regard, the balance of many different signaling pathways must be coordinated within the cell to ensure an appropriate response is completed. Evidence implicates catecholamine (Bers, 2004; Tada & Inui, 1983; Simmerman *et al.*, 1996; Kimura *et al.*, 1998; Loukianov *et al.*, 1998) and insulin (Algenstaedt *et al.*, 1997; Ragolia &

Begum, 1997; Liu & Brautigan, 2000) pathways with the binding of second messenger proteins to SR-associated proteins in cardiac and skeletal muscles.

The regulation of intracellular Ca^{2+} -transients during contractile activity by SERCA is accomplished through the intrinsic control of functional parameters by intracellular signaling pathways and endogenous modulators. Phospholamban (PLN; Figure 1.5), as an example, directly interacts with SERCA2a in cardiac tissue and reduces the specific activity of SERCA at submaximal concentrations of Ca^{2+} (MacLennan *et al.*, 1997). Site-specific phosphorylation of PLN by cAMP-dependent protein kinase A (PKA) and Ca^{2+} -dependent calmodulin kinase II (CaMKII) pathways promotes the dissociation of PLN from SERCA, thereby alleviating the inhibitory effects of PLN on SERCA and restoring SERCA Ca^{2+} -sensitivity (Figure 1.6, Panel A). Sarcoplipin (SLN; Figure 1.5) is another endogenous protein known to modulate SERCA Ca^{2+} -sensitivity by directly binding with SERCA1a or SERCA2a by a mechanism similar to that of PLN (Asahi *et al.*, 2003). The phosphorylation of SLN is regulated by serine/threonine kinase 16 (STK16), which promotes the dissociation of SLN from SERCA and increases Ca^{2+} -sensitivity (Figure 1.6, Panel A) (Gramolini *et al.*, 2006). The interaction of SLN with PLN promotes the transformation of PLN pentamers to monomers (Figure 1.6, Panel B), which increases the inhibition of SERCA by PLN since monomers are more effective SERCA inhibitors (Toyofuku *et al.*, 1992; Asahi *et al.*, 2002). In tissues of species where SLN is co-expressed, SLN directly interacts with PLN to form super-inhibitory complexes (Figure 1.6, Panel C) that reduce SERCA Ca^{2+} -sensitivity to a greater extent than SLN or PLN alone (Asahi *et al.*, 2002; MacLennan & Kranias, 2003). In the rat, PLN is predominately expressed in cardiac but not skeletal muscle (Damiani *et al.*, 2000), whereas SLN is primarily expressed in high quantities in atria and in lower quantities in slow-twitch skeletal muscle in the rat

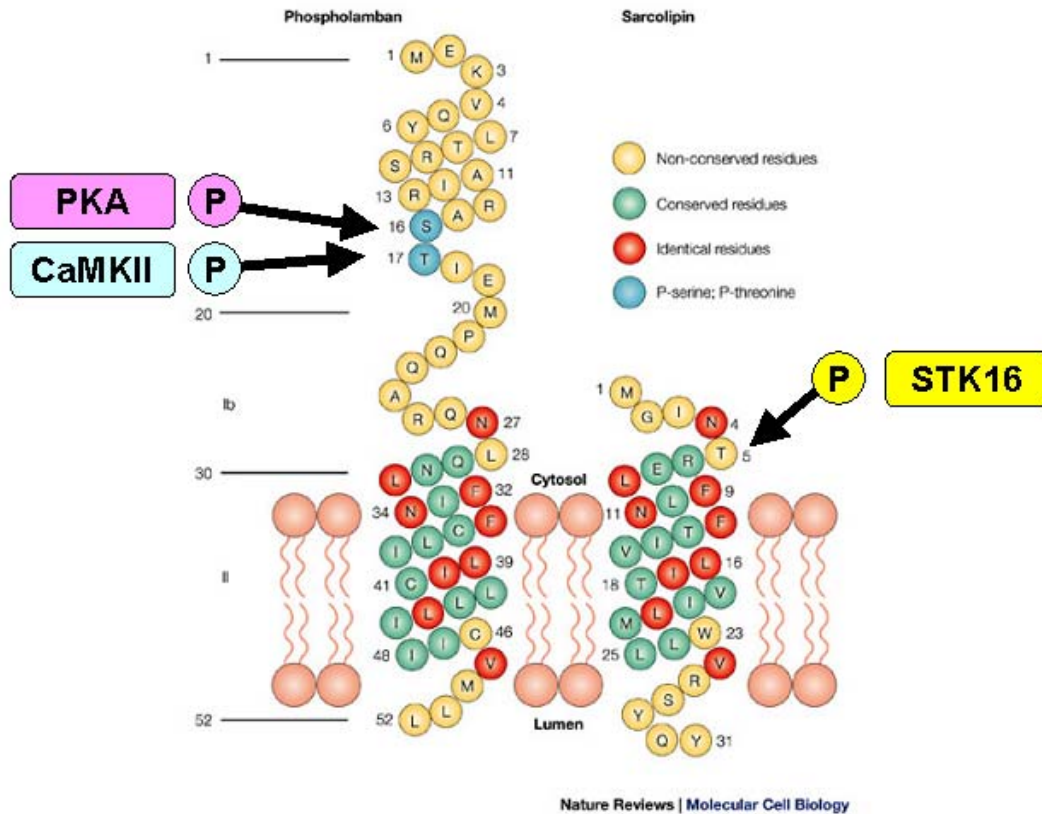


Figure 1.5: Phospholamban (PLN) and sarcoplipin (SLN) amino acid sequences and protein structure. Sarco(endo)plasmic reticulum Ca^{2+} -ATPase (SERCA) Ca^{2+} -sensitivity by interacting directly with SERCA in their unphosphorylated states. The homology of the two proteins is most clearly seen in their transmembrane helices. In humans, SLN expression is high in fast-twitch skeletal muscle and low in the heart. In the rat, PLN is predominately expressed in cardiac but not skeletal muscle; whereas in the rat, SLN is primarily expressed in the soleus and in the atria but not in the left ventricle. Site-specific phosphorylation of PLN by cAMP-dependent protein kinase A (PKA; Serine 16) and Ca^{2+} -dependent calmodulin kinase II (CaMKII; Threonine 17) pathways promotes the dissociation of PLN from SERCA, thereby alleviating the inhibitory affects of PLN on SERCA and restoring SERCA Ca^{2+} -sensitivity. Site-specific phosphorylation of SLN (Threonine 5) by STK16 also increases SERCA Ca^{2+} -sensitivity by promoting the dissociation of SLN from SERCA. (Adapted from MacLennan and Kranias, 2003)

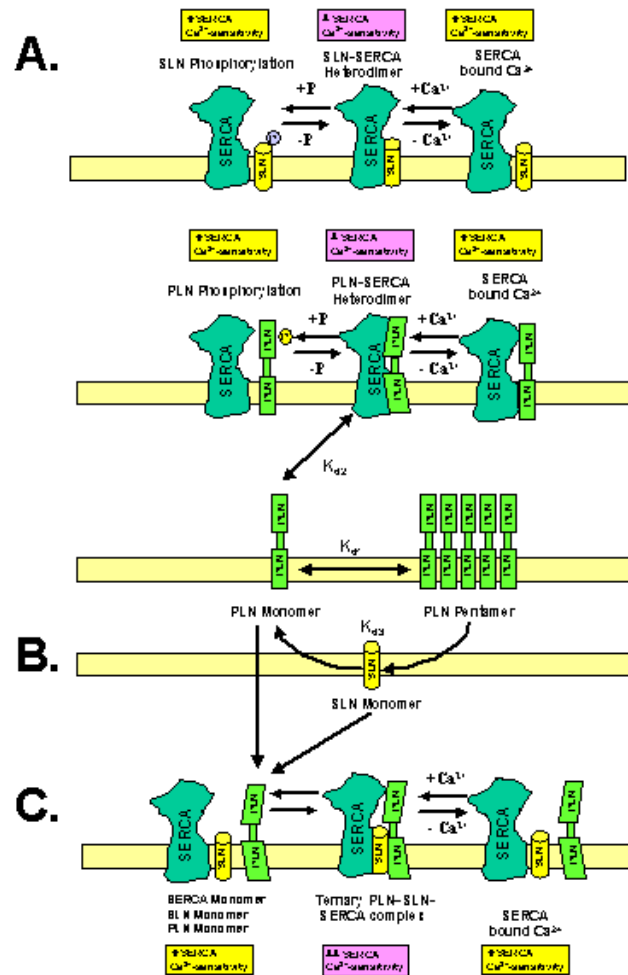


Figure 1.6: Phospholamban (PLN) and sarcoplipin (SLN) acutely regulate sarco(endo)plasmic reticulum Ca^{2+} -ATPase (SERCA) Ca^{2+} -sensitivity by interacting directly with SERCA in their unphosphorylated states. Panel A: The phosphorylation of SLN and Ca^{2+} binding to SERCA are driving forces for the dissociation of the SLN-SERCA complex, thereby activating SERCA. Two steps can be dissected in the reversible inhibition of SERCA activity by PLN: first, the association/ dissociation of pentameric PLN (K_d) and the association/dissociation of monomeric PLN and SERCA (K_p). The phosphorylation of PLN and Ca^{2+} binding to SERCA are driving forces for the dissociation of the PLN-SERCA complex, thereby activating SERCA. Phosphorylation of PLN dissociates functional interactions, but is less effective than Ca^{2+} binding to SERCA in breaking up physical interactions. Panel B: SLN has a higher affinity for PLN than PLN itself, so that it can depolymerize PLN pentamers. Panel C: When all three proteins are expressed together, SERCA, PLN and SLN form a ternary complex that is superinhibitory. Calcium binding to SERCA promotes the dissociation of the SERCA-PLN-SLN complex, restoring SERCA Ca^{2+} -sensitivity. In the rat, PLN is predominately expressed in cardiac but not skeletal muscle; whereas SLN is primarily expressed in high quantities in atria and in the soleus in the rat. Adapted from MacLennan and Kranias, 2003.

(Damiani *et al.*, 2000). In contrast to the rabbit, which expresses high amounts of SLN in fast-twitch skeletal muscles, it appears as though the SLN is not expressed in the rat EDL, which is a fast twitch skeletal muscle (Damiani *et al.*, 2000).

In addition to PKA, two other cellular kinases, namely CaMKII (Kranias, 1985; Berchtold *et al.*, 2000; Hawkins *et al.*, 1994) and Ca²⁺-activated-phospholipid-dependent protein kinase (PKC) (Rogers *et al.*, 1990; Nicolas *et al.*, 1998) also regulate intracellular Ca²⁺_i-transients by targeting a number of cellular proteins involved in the excitation and contraction (E-C) processes, including SR Ca²⁺-cycling proteins (Berchtold *et al.*, 2000; Tupling, 2004). Ca²⁺/calmodulin-dependent protein kinase II influences SERCA Ca²⁺-sensitivity by influencing the site-specific phosphorylation of PLN Threonine 17 (Thr17) (Hawkins *et al.*, 1994; Odermatt *et al.*, 1996). In addition, CaMKII also directly phosphorylates SERCA2a in cardiac and slow-twitch skeletal muscle in the rabbit, which increases the maximal enzyme activity (V_{max}) of the Ca²⁺-pump (Hawkins *et al.*, 1994). However, the physiological capacity of CaMKII to directly phosphorylate SERCA2a is still controversial since this observation could not be confirmed using a HEK-293 cell line expressing SERCA2a (Odermatt *et al.*, 1996). In contrast to SERCA2a, CaMKII does not directly phosphorylate SERCA1a in the fast-twitch skeletal muscle in the rabbit (Hawkins *et al.*, 1994).

Protein kinase C signaling is also capable of influencing intracellular Ca²⁺_i-transients and SERCA activity. However, in contrast to the positive inotropic effects of β -adrenergic and CaMKII activation, it is generally accepted that PKC signaling reduces muscle contractility (Capogrossi *et al.*, 1990; Nicolas *et al.*, 1998; Rogers *et al.*, 1990) by reducing SERCA V_{max} , without altering the Ca²⁺-sensitivity of the enzyme in cardiomyocytes (Rogers *et al.*, 1990). *In vitro* studies using enriched SR membranes prepared from cardiac tissue have demonstrated

that PLN can be phosphorylated on Serine 10 (Ser10) by PKC (Tada *et al.*, 1983; Iwasa & Hosey, 1984; Movsesian *et al.*, 1984). However, the role of PKC-mediated PLN phosphorylation of Ser10 is still controversial since this amino acid does not appear to be phosphorylated in response to PKC activation *in vivo* (Wegener *et al.*, 1989). In contrast to a PKC-mediated increase in PLN-phosphorylation, there is evidence to indicate that PKC signaling may actually reduce PLN-phosphorylation through the activation of protein phosphatase 1 (PP1) and 2a (PP2a) (Liu & Brautigan, 2000; Ragolia & Begum, 1997), which would increase the interaction of PLN with SERCA and would reduce enzyme activity at submaximal levels of Ca^{2+}_f (Braz *et al.*, 2004). It is also possible that the activation of phospholipase D (PLD) by PKC signaling may influence SERCA kinetic properties since phosphatidic acid (PA) promotes the transformation of PLN pentamers to monomers, thereby increasing the interaction of PLN with SERCA to reduce enzyme activity (Toyofuku *et al.*, 1992; Asahi *et al.*, 2002). However, the specific mechanisms responsible for the PKC-dependent reduction in SERCA activity in cardiomyocytes have not been identified. Additionally, given that PLN is not expressed in rat skeletal muscle, it is not clear if PKC signaling would influence Ca^{2+} -handling properties in this tissue.

Hormone stimulated signaling pathways are also known to interact with the CRC and to modulate CRC function in skeletal and cardiac muscle (Bers, 2004). For example, PKA is located in close proximity with the CRC in cardiac tissue. It is generally believed that PKA activation leads to the phosphorylation of the CRC and is thought to increase the open probability of the CRC. The reversal of this phosphorylation step is catalyzed by protein phosphatase 1 (PP1) and 2a (PP2A) (Marx *et al.*, 2001; Marx *et al.*, 2000). The increase in CRC open probability, coupled with increased SR Ca^{2+} -loading (due to PLN phosphorylation),

could greatly enhance the amount of SR Ca-release during E-C coupling in response to adrenergic stimulation (Bers, 2004) and may alter contractile performance in response to β -adrenergic stimulation. The activity of the CRC can be also be influenced by CaM binding and CaMKII mediated phosphorylation processes. In cardiac and skeletal muscle, the phosphorylation of the CRC by CaMKII acts to increase the open probability of the CRC at low Ca^{2+} concentrations (<100 nM) while inhibiting CRC opening at high Ca^{2+} concentrations (> 1 μM) (Berchtold *et al.*, 2000).

Insulin binding to the insulin receptor leads to the phosphorylation of several second messenger pathways. Insulin signaling in skeletal muscle is complex and will not be reviewed here. For a thorough review of the topic, refer to Zierath (Zierath, 2002). The insulin signaling cascades includes several intracellular proteins, such as the insulin receptor substrates (IRS) 1 and 2 (Algenstaedt *et al.*, 1997). These signaling proteins are known to activate various downstream pathways involved in the regulation of cellular protein function through the interaction of tyrosine phosphorylation motifs and specific domains within target proteins termed SH2 (*src* homology 2) domains (Algenstaedt *et al.*, 1997). Binding of IRS proteins to phosphatidylinositol 3 kinase (PI3K), as an example, is known to result in the translocation of Glut-4 to the sarcolemmal membrane and to acutely regulate glycogen synthase activity within the sarcomere. Screening of the human skeletal muscle cDNA expression library, conducted in an attempt to identify novel IRS binding proteins in skeletal muscle, indicated that IRS-1 and IRS-2 can directly bind with SERCA proteins (SERCA1a and SERCA2a) in an insulin-stimulated, time and concentration-dependent manner (Algenstaedt *et al.*, 1997). These observations were supported by further experiments in which the interaction of IRS proteins with SERCA was reduced in diabetic rats (Algenstaedt *et al.*, 1997). The binding of IRS to SERCA appears to be

accomplished through IRS-binding to the C terminus of SERCA through an amino acid sequence similar to the traditional SH2 domain. However, the effect that IRS binding may exert on SERCA activity was not investigated and has not been established (Algenstaedt *et al.*, 1997). Given that the interaction of IRS and proteins containing the traditional SH2 domain leads to alterations in the specific activity of the target protein, it is likely that the interaction of IRS with SERCA would result in the acute regulation of SERCA kinetic parameters (i.e. V_{\max} , n_H , or Ca_{50}).

Insulin signaling may also exert effects on SR Ca^{2+} -handling properties through a glycogen bound form of protein phosphatase-1 (PP-1G) (Liu & Brautigan, 2000). Protein phosphatase-1G exists as a heterodimer composed of a phosphatase catalytic subunit and a glycogen targeting subunit, G_m . The localization of PP-1G is accomplished through the interaction of G_m with an amino acid sequence within C-terminus of SERCA (Liu & Brautigan, 2000). When activated through insulin signaling pathways, PP-1G can reduce the specific activities of glycogen-metabolizing enzymes and may also influence SERCA by influencing dephosphorylation events of regulatory proteins involved in the acute regulation of these enzymes. For example, PP-1G has been shown to influence the dephosphorylation state of glycogen synthase and PLN (Liu & Brautigan, 2000; Ragolia & Begum, 1997). In contrast, cAMP mediated pathways, stimulated by epinephrine, act to decrease the activity of the G_m subunit, thereby removing the inhibition of G_m on the various proteins that it exerts an effect (Liu & Brautigan, 2000; Ragolia & Begum, 1997).

Statement of the Problem

The purpose of this thesis was to investigate the acute regulation of the SR Ca^{2+} -handling proteins, namely SERCA and CRC, in heart and skeletal muscle of different fiber type composition. Emphasis has been given to both non-physiologic and physiologic models. In the non-physiologic model, crude homogenates and enriched SR vesicles prepared from rat LV and various skeletal muscles have been used to characterize the influence that β -adrenergic, CaMKII, PKC, and insulin signaling pathways on SERCA kinetic properties. In the physiologic model, SERCA and CRC behaviour in crude muscle homogenates has been examined in samples taken from humans during exercise and glucose supplementation. To examine acute regulatory behaviour, three studies were completed. The details of these studies are presented in Chapters Two, Three and Four.

The purpose of the first study (Chapter Two) was to investigate the role of β -adrenergic, CaMKII and PKC signaling in the intrinsic regulation of SERCA kinetic properties in the LV and skeletal muscles of different fibre type composition in the rat. To address the role of these signaling proteins, crude muscle homogenates and enriched SR vesicles were incubated with various pathway activators and inhibitors. The specific SERCA kinetic properties assessed included V_{\max} , n_H , and Ca_{50} . This study also characterized the tissue-specific expression pattern for SERCA isoforms, PLN, and STK16, and CaMKII isoforms.

We have hypothesized that

- 1) β -adrenergic signaling does not alter V_{\max} but increases SERCA Ca^{2+} -sensitivity, as indicated by an increased n_H and reduced Ca_{50} , in both crude muscle homogenates and enriched SR vesicles. Based on the tissue-specific protein expression pattern for SERCA, PLN and SLN, we hypothesized that the changes in SERCA kinetic

properties associated with β -adrenergic signaling are mediated by cAMP-dependent PKA activation in LV tissue; whereas, an alternative cAMP-dependent mechanism that is not PKA-dependent influences SERCA kinetic properties in skeletal muscle.

- 2) CaMKII signaling increases V_{\max} in the tissues that predominately express SERCA2a; whereas CaMKII does not alter V_{\max} in tissues that predominately express SERCA1a. Based on the tissue-specific protein expression pattern for PLN, it is proposed that CaMKII activation will increase SERCA Ca^{2+} -sensitivity (n_H and Ca_{50}) in crude muscle homogenates and enriched SR vesicles prepared from rat LV; while CaMKII signaling does not alter SERCA Ca^{2+} -sensitivity in the skeletal muscles studied.
- 3) PKC signaling reduces V_{\max} and SERCA Ca^{2+} -sensitivity (n_H and Ca_{50}) in crude muscle homogenates and enriched SR vesicles prepared from rat LV and skeletal muscles.

The purpose of the second study (Chapter Three) was to investigate the role of insulin signaling on the intrinsic regulation of SERCA kinetic properties in the left ventricle and skeletal muscles of different fibre type composition. To determine the role of signaling crude muscle homogenates and enriched SR vesicles were incubated with INS, an activated form of the insulin receptor (A-INS-R) or inhibitors of the insulin signaling pathway. The specific SERCA kinetic properties assessed included V_{\max} , n_H , and Ca_{50} . In addition, tissue-specific expression pattern for IRS-1 and IRS-2 and their interaction with SERCA1a and SERCA2a and the changes to the PLN pentamer: monomer ratio and PLN Ser16 or Thr17 phosphorylation in response to insulin signaling were also studied.

We have hypothesized that

- 1) insulin signaling acutely alters V_{\max} and Ca^{2+} -sensitivity (n_H and Ca_{50}) in crude muscle homogenates and enriched SR vesicles prepared from rat cardiac and skeletal muscles.
- 2) insulin signaling results in the interaction of IRS proteins (i.e. IRS-1 and IRS-2) with SERCA1a and SERCA2a regardless of tissue type.
- 3) the insulin-induced changes in SERCA2a Ca^{2+} -sensitivity in LV muscle is associated with changes in the PLN pentamer: monomer ratio and changes in the PLN Ser16 or Thr17 phosphorylation.
- 4) the insulin-induced changes in SERCA kinetic properties would be greater for slow-twitch cardiac and skeletal muscles, compared to fast-twitch skeletal muscle, given the intrinsic differences in SERCA isoform expression and insulin-sensitivity between tissues.

The purpose of the third study (Chapter Four) was to examine the collective effects of exercise and alterations in plasma glucose, catecholamine and insulin concentrations on SR Ca^{2+} -handling properties in human skeletal muscle by directly manipulating these properties through the administration of oral glucose supplements during exercise. The specific properties assessed included V_{\max} , n_H , Ca_{50} , SR Ca^{2+} -uptake and Ca^{2+} -release kinetics, Ca^{2+} -transport efficiency (i.e. apparent coupling ratio), membrane permeability for Ca^{2+} (i.e. ionophore ratio) and PLN Ser16 or Thr17 phosphorylation. In addition, the muscle metabolic responses to prolonged exercise and prolonged exercise with glucose supplementation are examined. The specific metabolic properties assessed include respiratory exchange ratios,

carbohydrate and lipid oxidation rates, as well as muscle glycogen, metabolite and nucleotide concentrations.

We have hypothesized that:

- 1) prolonged exercise progressively reduces V_{\max} , Ca^{2+} -uptake, and Ca^{2+} -release kinetics and that the reductions in SR Ca^{2+} -handling properties occurs in the absence of changes in Ca^{2+} -sensitivity (i.e. n_{H} and Ca_{50}), Ca^{2+} -transport efficiency (i.e. apparent coupling ratio) and membrane permeability for Ca^{2+} (i.e. ionophore ratio).
- 2) when the same absolute exercise is performed with glucose supplementation, the disturbances in the V_{\max} , Ca^{2+} -uptake, and Ca^{2+} -release kinetics will be attenuated. The reduced disturbance in these properties will be associated with improved blood glucose homeostasis and will occur in the absence of differences in energy metabolism and glycogen content.
- 3) Based on data from our laboratory (Duhamel *et al.*, 2006c) indicating that Ca_{50} and n_{H} are not different when plasma glucose concentrations are decreased and catecholamine concentrations are increased during exercise in Lo CHO states, we have hypothesized that glucose supplementation will not alter n_{H} , Ca_{50} or PLN phosphorylation during exercise in the current study.

CHAPTER TWO

ACUTE REGULATION OF SERCA KINETIC PROPERTIES BY β -ADRENERGIC, Ca^{2+} -DEPENDENT CALMODULIN KINASE II AND PROTEIN KINASE C SIGNALING IN CARDIAC AND SKELETAL MUSCLE

TA DUHAMEL, HJ GREEN, AR TUPLING and J OUYANG.

Department of Kinesiology, University of Waterloo,

Waterloo, Ontario, Canada, N2L 3G1

Short Title: Acute regulation of SERCA function.

Abstract

This study investigated the hypothesis that β -adrenergic, Ca^{2+} -dependent calmodulin (CaMKII) and protein kinase C (PKC) signaling would alter the kinetic properties of SERCA proteins in left ventricular and skeletal muscles of different fibre type composition. Crude muscle homogenates were prepared from soleus (SOL), extensor digitorum longus (EDL), the red portion of gastrocnemius (RG), the white portion of gastrocnemius (WG) and the left ventricle (LV) from a group of male Sprague-Dawley rats ($n=28$, 9 weeks of age; mass = 280 ± 4 g). SR vesicles were prepared using crude muscle homogenates from WG and LV, respectively. Samples were incubated for 10 min in the presence or absence of various pathway activators or inhibitors and the Ca^{2+} -dependent SERCA activity was assessed *in vitro* using a spectrophotometric assay. Three SERCA kinetic properties were assessed, namely, the maximal SERCA activity (V_{\max}), the Hill Coefficient (n_H) and the Ca_{50} .

It was found that V_{\max} was not altered by epinephrine (EPI) in any tissue. However, EPI (15 nM) reduced ($P<0.05$) Ca_{50} by 24 and 25% in LV and SOL, respectively, but had no effect for EDL, WG or RG. Similar changes in LV and SOL were observed following treatment with 150 nM EPI. The effects of EPI on Ca_{50} were blocked by propranolol (i.e. 4 μM propranolol + 150 nM EPI). Treatment of samples with cAMP (10 μM) reduced Ca_{50} by 12 and 14% in LV and SOL, respectively, but was without effect in the fast-twitch skeletal muscles. In addition, forskolin (25 μM) reduced Ca_{50} by 16% in LV but had no effect in SOL. As expected, KT5720 (100 nM) prevented the forskolin-induced change in Ca_{50} for LV. The incubation of samples with 100 nM KT5720 + 10 μM cAMP prevented the cAMP-induced reductions in Ca_{50} in LV but did not prevent the cAMP-induced reductions in Ca_{50} in SOL.

To determine the effects of CaMKII signaling on SERCA kinetic properties, crude muscle homogenates were incubated in the presence of the CaMKII substrate calmodulin (CaM; 15 μ g), and/or the CaMKII inhibitor KN62 (4 μ M). Incubation of samples with CaM did not alter V_{\max} in any tissue. Activation of CaMKII did not alter SERCA kinetic properties in SOL, EDL, RG, or WG. However, CaM increased n_H by 12% and Ca_{50} by 13% in the LV. The effects of CaM on n_H and Ca_{50} were blocked by KN62 (i.e. KN62 + CaM).

To determine the effects of PKC signaling on SERCA kinetic properties, crude muscle homogenates were incubated in the presence of the PKC activator PMA (500 nM) or the PKC inhibitor GFX (1400 nM). Incubation of muscle samples with PMA did not alter V_{\max} in LV or SOL but reduced V_{\max} by \sim 15% in EDL, WG and RG. Treatment of samples with PMA, also reduced n_H by 13, 28, 22, and 14% in LV, EDL, WG and RG, respectively and increased Ca_{50} by \sim 34, 52, 196, 166 and 65% in LV, SOL, EDL, WG and RG, respectively. Unexpectedly, GFX did not prevent the PMA-induced changes in V_{\max} in EDL, WG and RG or the changes in n_H and Ca_{50} in any tissue.

These results indicate that β -adrenergic signaling influences Ca_{50} in LV and SOL are regulated by PKA signaling in LV while an alternative mechanism that is not PKA-dependent regulates Ca_{50} in SOL; whereas β -adrenergic signaling is without effect in the fast-twitch skeletal muscle. Our data also indicate that CaMKII signaling influences SERCA Ca^{2+} -sensitivity in LV samples but does not alter SERCA kinetic properties in skeletal muscle. These data indicate that PMA reduces the V_{\max} in skeletal muscles that predominately express SERCA1a, but not SERCA2a, and also reduces SERCA Ca^{2+} -sensitivity (n_H and Ca_{50}) in all tissues studied.

Introduction

Signaling pathways translate a variety of environmental cues, such as hormones, neurotransmitters and local metabolites, into physiological responses within the cell (Saucerman & McCulloch, 2004). As a result, the balance of various signaling pathways must be coordinated within the cell to ensure that an appropriate response is completed. Cardiac and skeletal muscle contractility, as an example, can be influenced by at least three different cellular kinases, namely, cAMP-dependent protein kinase (PKA) (Gramolini *et al.*, 2006; Reading *et al.*, 2003), Ca²⁺/calmodulin-dependent protein kinase II (CaMKII) (Kranias, 1985; Berchtold *et al.*, 2000; Hawkins *et al.*, 1994), and Ca²⁺-activated-phospholipid-dependent protein kinase (PKC) (Rogers *et al.*, 1990; Nicolas *et al.*, 1998). These protein kinases phosphorylate a number of cellular targets that are involved in the excitation and contraction (E-C) processes, such as the regulation of sarcoplasmic reticulum (SR) Ca²⁺-cycling proteins (Berchtold *et al.*, 2000; Tupling, 2004).

The SR influences muscle contractility via several integral proteins that contribute to the regulation of intracellular free Ca²⁺-concentration (Ca²⁺_f). For example, rates of muscle force development are influenced by the kinetic properties of the Ca²⁺-release channel (CRC or the ryanodine receptor), which regulates the frequency and magnitude of Ca²⁺-release during E-C coupling (Berchtold *et al.*, 2000); whereas, rates of relaxation are influenced by sarco(endo)plasmic reticulum Ca²⁺-ATPase (SERCA) proteins, which actively sequester cytosolic Ca²⁺ and restore Ca²⁺_f to basal levels (Berchtold *et al.*, 2000) and also influence the SR Ca²⁺ load available for the next E-C cycle and repetitive activity (Berchtold *et al.*, 2000). In fact, differences in SERCA isoform expression (Wu & Lytton, 1993) and SR membrane density (Damiani *et al.*, 2000) contribute to the different rates of relaxation for cardiac and slow

twitch skeletal muscle compared to fast-twitch skeletal muscle fibres. Regulation of SR Ca^{2+} -handling properties can be directly influenced by SERCA isoform composition or by the expression of specific SR-associated proteins that can modulate SERCA function in the different fibre-types (MacLennan *et al.*, 2002; Tupling, 2004). Moreover, the regulation of SR Ca^{2+} -cycling during exercise appears to be influenced by the oxidative potential of the muscle as well as the major fibre-type composition as indicated by myosin heavy chain composition and contractile speed (Holloway *et al.*, 2006).

There is evidence to indicate that β -adrenergic signaling can increase muscle contractility in cardiac (Slack *et al.*, 1997) and skeletal muscle (Kadambi *et al.*, 1996; Tupling *et al.*, 2002) by elevating the intracellular content of cAMP (Reading *et al.*, 2003) to increase SERCA activity at submaximal Ca^{2+}_f (Figure 2.1) (Gramolini *et al.*, 2006). These inotropic effects appear to be mediated, at least in part, through the regulation of the endogenous SR-modulator proteins, phospholamban (PLN) and sarcolipin (SLN). During states where cAMP concentrations are low, PLN and SLN exist in their unphosphorylated forms and are bound directly to SERCA proteins. The binding of PLN or SLN with SERCA is inhibitory and reduces the Ca^{2+} -sensitivity of SERCA at submaximal Ca^{2+}_f . β -adrenergic signaling reduces the interaction of PLN and SLN with SERCA by increasing cellular cAMP concentrations to activate PKA (Gramolini *et al.*, 2006) and serine/threonine kinase 16 (STK16)-mediated phosphorylation processes that promote the dissociation of PLN and SLN from SERCA, respectively (Gramolini *et al.*, 2006). In the rat, PLN is predominately expressed in cardiac (i.e. atria and ventricular tissue) but not in skeletal muscle (Damiani *et al.*, 2000; Vangheluwe *et al.*, 2005), whereas, SLN is primarily expressed in the atria but not the left ventricle (LV) and in lower quantities in the skeletal muscles of the rat (Damiani *et al.*, 2000; Vangheluwe *et al.*,

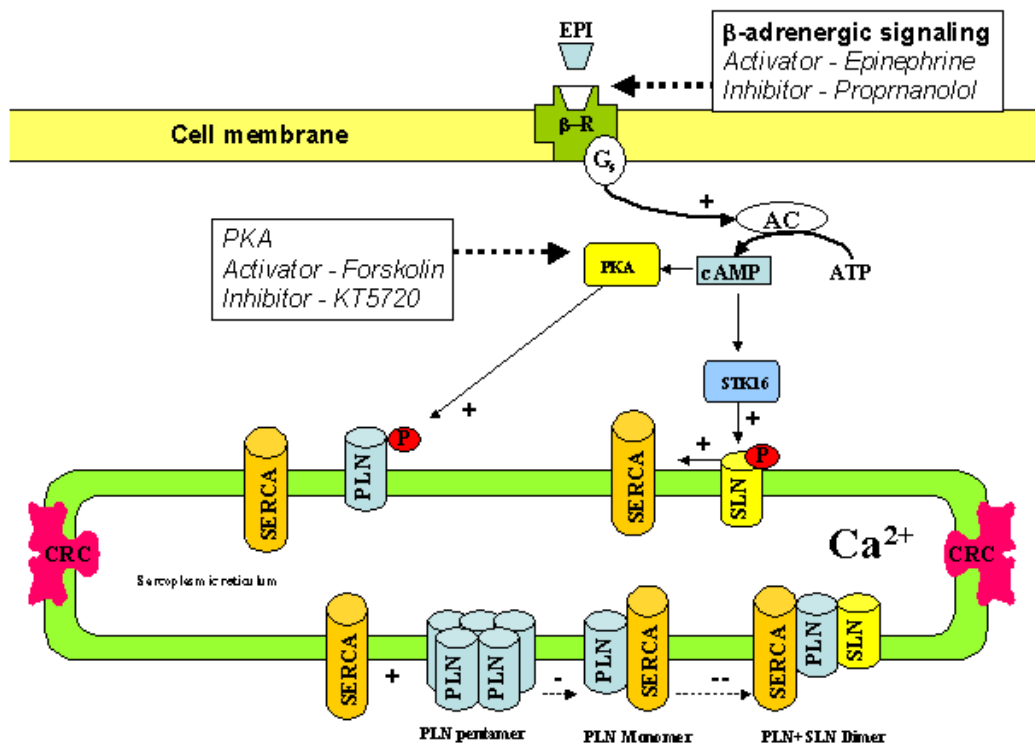


Figure 2.1: Potential pathways involved in β -adrenergic signaling in skeletal muscle. Epinephrine signaling acutely regulates sarco(endo)plasmic reticulum Ca^{2+} -ATPase (SERCA) function by influencing the phosphorylation status of phospholamban (PLN) via cAMP-dependent protein kinase A (PKA) activation and also by influencing the phosphorylation status of sarcolipin (SLN) through the activation of cAMP-dependent serine/threonine kinase 16 (STK16). Phosphorylation of PLN and SLN causes these proteins to disassociate from SERCA, which alters SERCA Ca^{2+} -sensitivity by increasing the specific activity of SERCA at submaximal concentrations of Ca^{2+} . Sarcolipin can also influence SERCA function by directly interacting with PLN-SERCA to form SLN-PLN-SERCA trimers that are super-inhibitory or by preventing the formation of PLN pentamers from PLN monomers. Phospholamban pentamers are known to inhibit SERCA Ca^{2+} -sensitivity to a much lower extent than do PLN monomers. Epinephrine (EPI) is a β -adrenergic activator. β -r, β -receptor. G_s , a subunit of the β -receptor involved in epinephrine signaling. AC, adenylyl cyclase. ATP, adenosine triphosphate, cAMP, cyclic-AMP. Propranolol is a β -adrenergic inhibitor. Forskolin is a PKA activator. KT5720 is a PKA inhibitor. cAMP, adenosine 3',5'-cyclic monophosphate. CRC, Ca^{2+} -release channel. P, indicates a phosphorylation process regulates protein function. +, indicates that process increases protein activity. -, indicates that process reduces protein activity.

2005). This tissue-specific expression pattern for PLN and SLN suggests that specific signaling pathways may influence SERCA kinetic properties to a greater extent in tissues that express specific cellular or molecular characteristics unique to one tissue compared to another and is not based solely on the SERCA isoform expressed by a specific fibre-type population.

The increase in Ca^{2+}_f associated with β -adrenergic signaling is also known to stimulate CaMKII-mediated phosphorylation of PLN (Figure 2.2) (Hawkins *et al.*, 1995; Wegener *et al.*, 1989). In contrast to PKA, CaMKII regulates the site-specific phosphorylation of PLN Threonine 17 (Thr17) (Hawkins *et al.*, 1994; Odermatt *et al.*, 1996). In addition, CaMKII also directly phosphorylates SERCA2a in cardiac and slow-twitch skeletal muscle in the rabbit, which increases the maximal enzyme activity (V_{\max}) of the Ca^{2+} -pump (Hawkins *et al.*, 1994). However, the physiological capacity of CaMKII to directly phosphorylate SERCA2a is still controversial since this observation could not be confirmed in another model system that used a HEK-293 cell line (Odermatt *et al.*, 1996). In contrast to SERCA2a, CaMKII does not directly phosphorylate SERCA1a in the fast-twitch skeletal muscle in the rabbit (Hawkins *et al.*, 1994).

Protein kinase C signaling is also capable of influencing muscle contractility and SERCA activity (Figure 2.3). However, in contrast to the positive inotropic effects of β -adrenergic and CaMKII activation, it is generally accepted that PKC signaling reduces muscle contractility (Capogrossi *et al.*, 1990; Nicolas *et al.*, 1998; Rogers *et al.*, 1990) by reducing SERCA V_{\max} , without altering the Ca^{2+} -sensitivity of the enzyme in cardiomyocytes (Rogers *et al.*, 1990). *In vitro* studies using enriched SR membranes prepared from cardiac tissue have demonstrated that PLN can be phosphorylated on Serine 10 (Ser10) by PKC (Tada *et al.*, 1983; Iwasa & Hosey, 1984; Movsesian *et al.*, 1984). However, the role of PKC-mediated PLN phosphorylation of Ser10 is still controversial since this amino acid does not appear to be

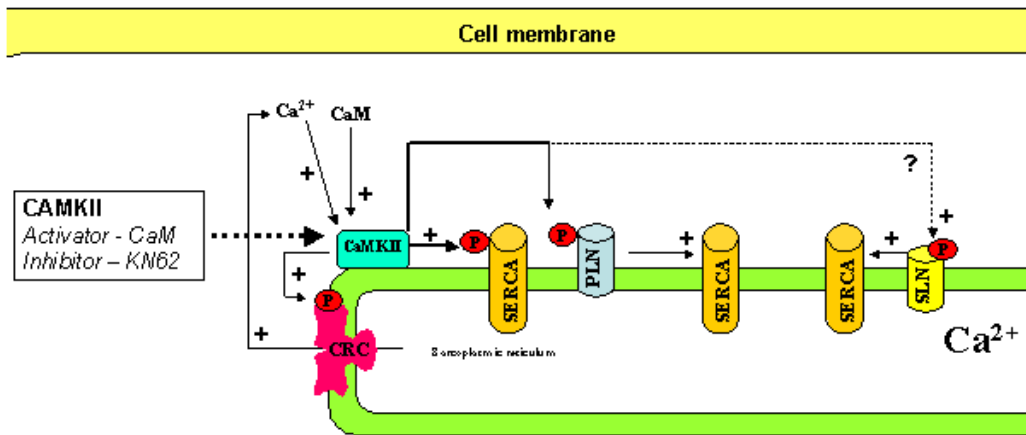


Figure 2.2: Potential pathways involved in Calcium-dependent calmodulin kinase (CaMKII) signaling in skeletal muscle. CaMKII signaling acutely regulates sarco(endo)plasmic reticulum Ca^{2+} -ATPase (SERCA) function by influencing phosphorylation-mediated processes through two mechanisms: 1) CaMKII phosphorylation of phospholamban (PLN) Thr17 promotes the dissociation of PLN from SERCA, thereby increasing SERCA Ca^{2+} -sensitivity by increasing the specific activity of SERCA at submaximal concentrations of Ca^{2+} . 2) Direct phosphorylation of SERCA2a, but not SERCA1a, at Ser38 reportedly increases maximal SERCA2a activity. It is currently not known if CaMKII activity can regulated sarcolipin (SLN) phosphorylation. CaM, bovine brain calmodulin. KN62 is a CaMKII inhibitor. CRC, Ca^{2+} -release channel. P, indicates a phosphorylation process regulates protein function. +, indicates that process increases protein activity. -, indicates that process reduces protein activity. ?, indicates that this process has not yet been characterized.

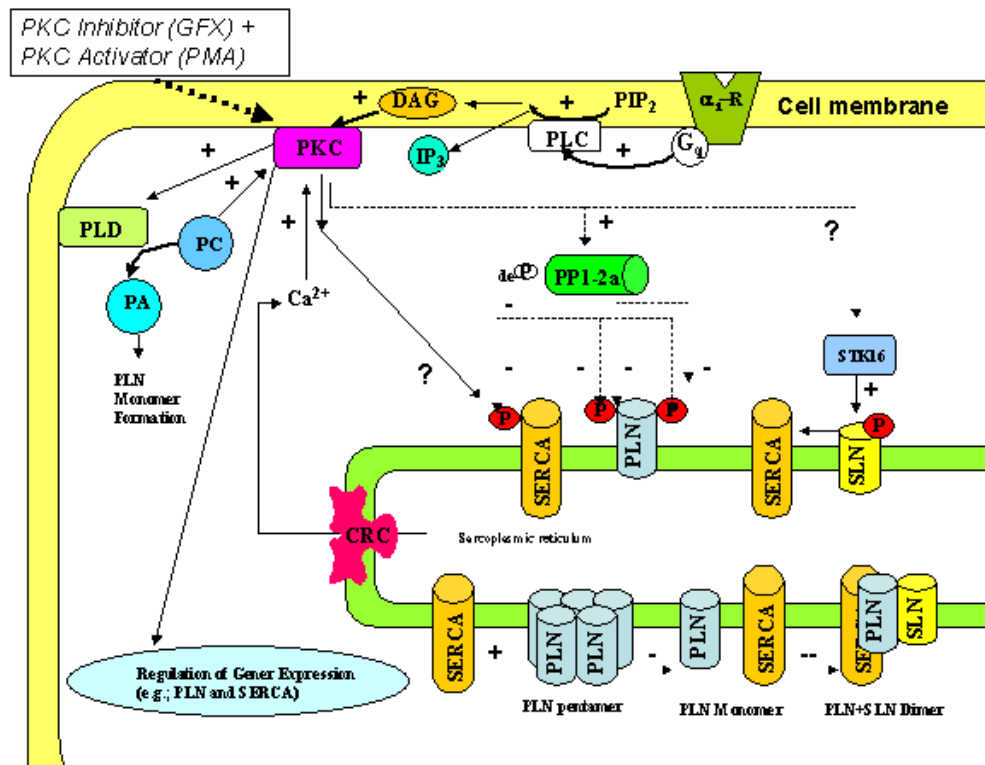


Figure 2.3: Potential pathways involved in Protein kinase C (PKC) signaling in skeletal muscle. PKC signaling has the ability to acutely regulate sarco(endo)plasmic reticulum Ca^{2+} -ATPase (SERCA) function through one of several different mechanisms. Protein kinase C signaling is activated by Ca^{2+} and phospholipids in response to hormone regulation. *In vitro* studies have demonstrated that PKC can phosphorylate PLN at Ser10, thereby increasing SERCA Ca^{2+} -sensitivity by increasing the specific activity of SERCA at submaximal concentrations of Ca^{2+} . However, the *in vivo* significance of PLN Ser10 phosphorylation has been questioned. It has also been proposed that PKC-stimulated activation of protein phosphatase 1+2a (PP1+2a) reduces the phosphorylation level of PLN, thereby reducing SERCA Ca^{2+} -sensitivity by promoting the interaction of PLN with SERCA. Protein kinase C activation of phospholipase D (PLD) may also influence PLN:SERCA interactions since phosphatidic acid (PA) promotes the transformation of PLN pentamers to monomers. Phospholamban pentamers are known to inhibit SERCA Ca^{2+} -sensitivity to a much lower extent than do PLN monomers. Sarcoplipin (SLN) is a known regulator of SERCA kinetic properties in cardiac and skeletal muscle. It is currently not known if PKC activity can regulated sarcoplipin (SLN). CRC, Ca^{2+} -release channel. STK16, serine/threonine 16. α_1 -r, α_1 -adrenergic receptor. PIP_2 , phosphatidylinositol-4,5-bisphosphate. PLC, phospholipase C. DAG, diacylglycerol. IP_3 , inositol trisphosphate. PC, phosphatidyl choline. PLD, phospholipase D. P, indicates a phosphorylation process regulates protein function. +, indicates that process increases protein activity. -, indicates that process reduces protein activity. ?, indicates that this process has not yet been characterized.

phosphorylated in response to PKC activation *in vivo* (Wegener *et al.*, 1989). In contrast to a PKC-mediated increase in PLN-phosphorylation, there is evidence to indicate that PKC signaling may actually reduce PLN-phosphorylation through the activation of protein phosphatase 1 (PP1) and 2a (PP2a) (Liu & Brautigan, 2000; Ragolia & Begum, 1997), which would increase the interaction of PLN with SERCA and would reduce enzyme activity at submaximal levels of Ca^{2+}_f (Braz *et al.*, 2004). It is also possible that the activation of phospholipase D (PLD) by PKC signaling may influence SERCA kinetic properties since phosphatidic acid (PA) promotes the transformation of PLN pentamers to monomers, thereby increasing the interaction of PLN with SERCA to reduce enzyme activity (Toyofuku *et al.*, 1992; Asahi *et al.*, 2002). However, the specific mechanisms responsible for the PKC-dependent reduction in SERCA activity in cardiomyocytes have not been identified. Additionally, given that PLN is not expressed in rat skeletal muscle, it is not clear if PKC signaling would influence Ca^{2+} -handling properties in this tissue.

The purpose of this study was to investigate the role of β -adrenergic, CaMKII and PKC signaling in the intrinsic regulation of SERCA kinetic properties in the LV and skeletal muscles of different fibre type composition and oxidative potential in the rat. We have hypothesized that β -adrenergic signaling would not alter V_{max} but would increase SERCA Ca^{2+} -sensitivity, as indicated by an increased Hill Coefficient (n_H) and reduced Ca_{50} in crude muscle homogenates and enriched SR vesicles prepared from rat LV and skeletal muscles. Based on the tissue-specific protein expression pattern for SERCA, PLN and SLN, we have hypothesized that the changes in SERCA kinetic properties associated with β -adrenergic signaling would be mediated by cAMP-dependent PKA activation in LV tissue; whereas, an alternative cAMP-dependent mechanism that is not PKA-dependent would influence SERCA kinetic properties in

skeletal muscle. We have also hypothesized that CaMKII signaling would increase V_{\max} in the tissues that predominately express SERCA2a; whereas CaMKII would not alter V_{\max} in tissues that predominately express SERCA1a. Based on the tissue-specific protein expression pattern for PLN, it is possible that CaMKII activation will increase SERCA Ca^{2+} -sensitivity (n_H and Ca_{50}) in crude muscle homogenates and enriched SR vesicles prepared from rat LV; while, CaMKII signaling would not alter SERCA Ca^{2+} -sensitivity in the skeletal muscles studied. In contrast to the effects of β -adrenergic and CaMKII signaling, we have hypothesized that PKC signaling would reduce V_{\max} and SERCA Ca^{2+} -sensitivity (n_H and Ca_{50}) in crude muscle homogenates and enriched SR vesicles prepared from rat LV and skeletal muscles.

Research Design & Methods

Materials

Epinephrine (EPI), bovine brain calmodulin (CaM), adenosine 3',5'-cyclic monophosphate (cAMP), an activated form of PKA (A-PKA), forskolin and KT5720 [i.e. (9S,10S,12R)-2,3,9,10,11,12-Hexahydro-10-hydroxy-9-methyl-1-oxo-9,12-epoxy-1H-diindolo[1,2,3-fg:3',2',1'-kl] pyrrolo[3,4-i][1,6]benzodiazocine-10-carboxylic acid hexyl ester] were purchased from Sigma (Oakville, ON, Canada). GF-109203-XI (GFX; also called bisindolylmaleimide I), phorbol-12-myristate-13-acetate (PMA), propranolol, and KN-62 (i.e. (S)-5-Isoquinolinesulfonic acid 4-[2-[(5-isoquinoliny)sulfonyl] methylamino]-3-oxo-3-(4-phenyl-1-piperaziny)propyl]phenylester)1-[N,O-bis (5-Isoquinolinesulfonyl) -N-methyl-L-tyrosyl]-4-phenylpiperazine) were purchased from Calbiochem (San Diego, CA, USA). Dimethylsulfoxide and water were used as solvents. Epinephrine is a β -adrenergic activator. Propranolol is a β -adrenergic inhibitor. forskolin is a PKA activator. KT5720 is a PKA

inhibitor. cAMP is a PKA and STK16 activator. CaM is a substrate required for CaMKII activity. KN62 is a CaMKII inhibitor. PMA, is a PKC activator. GFX is a PKC inhibitor.

Mouse anti-CaMKII monoclonal (sc-5306) and goat anti-phospholamban polyclonal (sc-21923) antibodies were purchased from Santa Cruz Biotechnology (Santa Cruz, CA, USA). Rabbit anti-STK16 polyclonal (AP7241c) antibody was purchased from Abgent (San Diego, CA, USA). Mouse anti-SERCA1a monoclonal (A52) antibody was a gift from D. MacLennan (Clarke *et al.*, 1990). Mouse-anti SERCA2a monoclonal (MA3-919) antibody was purchased from Affinity Bioreagents (Golden, CO, USA).

Animals

Male Sprague-Dawley rats (9 weeks of age; n=28, mass = 280 ± 4 g; Harlan Animal Supplier, Wisconsin; USA) were used to collect tissue for analysis in this study. Animals were fed water and laboratory chow ad libitum, and housed in an environmentally controlled room on a reverse 12:12-h light/dark cycle until sacrificed. Tissue collection was conducted at approximately the same time over a three-day period, between 8 am and 12 pm, in order to limit diurnal variations in muscle glycogen (Conlee *et al.*, 1976). On a given day, 8-10 animals were anesthetized for tissue sampling. The Animal Care Committee of the University of Waterloo approved the experimental protocols prior to starting the study. Rats were anesthetized with pentobarbital sodium (6 mg/100 g body wt) prior to muscle sampling.

Sample preparation

Rats were anesthetized with pentobarbital sodium (6 mg/100 g body wt) and prepared for muscle sampling. Following anesthetization, tissue from the soleus (SOL), extensor digitorum longus (EDL), the red portion of gastrocnemius (RG), and the white portion of gastrocnemius

(WG) were sampled from both hind limbs from each animal prior to excision of the left ventricle (LV). Each sample was immediately placed in ice-cold homogenization buffer. An additional small piece of tissue was rapidly sampled from each muscle from 5 animals and frozen in liquid nitrogen for later analysis of muscle oxidative potential. Crude muscle homogenates were prepared 11:1 (wt/vol) in ice-cold homogenizing buffer containing 250 mM sucrose, 5 mM HEPES, 0.2 mM phenylmethylsulfonyl fluoride (PMSF), and 0.2% sodium azide (NaN₃), pH 7.5. Dithiothreitol (DTT) was not used in the preparation of crude muscle homogenates since DTT can influence sulfhydryl oxidation. Tissue samples were kept on ice and homogenized mechanically with a Polytron homogenizer (PT 3100) at 16500 rpm for two 30 s bursts, separated by a 30 s break. Tissue homogenates were aliquoted into 30-115 μ L volumes, frozen in liquid N₂ and stored at -80°C for later analysis of Ca²⁺-dependent SERCA activity and Western blotting.

Enrichment of SR vesicles was completed using tissue homogenates pooled from 4 animals on the same day of tissue extraction and was accomplished using differential centrifugation protocols previously explained by our laboratory (Tupling *et al.*, 2001b). The final pellet, which contained enriched SERCA1a vesicles (prepared using WG tissue) or SERCA2a vesicles (prepared using LV tissue), was suspended in homogenizing buffer to a final protein concentration of ~ 2-4 mg/mL, frozen and stored at -80°C for later analysis.

Protein determination of homogenates and enriched SR vesicles were made by the method of Lowry (Lowry & Passonneau, 1972) as modified by Schacterle and Pollock (Schacterle & Pollack, 1973). Samples were analyzed in triplicate and the average was used to determine protein concentrations.

Experimental design

The general strategy used in this study was to incubate samples for 10 min in the presence or absence of various β -adrenergic, CaMKII, or PKC pathway activators or inhibitors and then to assess Ca^{2+} -dependent SERCA activity *in vitro* using a spectrophotometric assay adapted for a plate reader. For each tissue sample, 3 treatments were assayed simultaneously during the same analytical session to limit variability between treatments during assay procedures as indicated within Table 2.1. In most cases, control samples, which were incubated in the absence of any activators or inhibitors, were measured concurrently with two other treatments. Once added, activators and/or inhibitors remained present until the measurements had been completed. Treatment concentrations for EPI were selected based on the maximal expected concentration of this hormone during exercise (15 nM) and a 10x higher (150 nM) concentration (Jansson *et al.*, 1982). Treatment concentrations for propranolol, forskolin, KT5720, cAMP, KN62, GFX and PMA were selected to be ~2x higher than the listed effective concentrations of these chemicals, as indicated on the material data sheets provided by the suppliers. The concentrations of A-PKA and CaM protein utilized in this experiment were selected based on the materials information sheet provided by the supplier.

Muscle oxidative potential

Citrate synthase (CS) activity, used as a measure of oxidative potential, was determined fluorometrically as described by Henriksson *et al.* (Henriksson *et al.*, 1986) using frozen muscle homogenized in a phosphate buffer (pH 7.4) containing 0.02% bovine serum albumin

Table 2.1: Experimental conditions used to determine β -adrenergic, CaMKII and PKC signaling effects on SERCA kinetic properties.

Sample	Treatment 1	Treatment 2	Treatment 3
β -adrenergic signaling			
Crude muscle homogenates	Control	15 nM Epinephrine	150 nM Epinephrine
Crude muscle homogenates	Control	150 nM Epinephrine	4 μ M Propranolol + 150 nM Epinephrine
Crude muscle homogenates	4 μ M Propranolol	150 nM Epinephrine	4 μ M Propranolol + 150 nM Epinephrine
PKA signaling			
Crude muscle homogenates	Control	25 μ M Forskolin	100 nM KTS720 + 25 μ M Forskolin
Crude muscle homogenates	100 nM KTS720	25 μ M Forskolin	100 nM KTS720 + 25 μ M Forskolin
Enriched SR vesicles	Control	1 μ g Active PKA	25 μ M Forskolin
cAMP-dependent signaling			
Crude muscle homogenates	Control	10 μ M cAMP	100 nM KTS720 + 10 μ M cAMP
Enriched SR vesicles	Control	10 μ M cAMP	100 nM KTS720 + 10 μ M cAMP
CaMKII signaling			
Crude muscle homogenates	Control	15 μ g CaM	4 μ M KN62
Crude muscle homogenates	4 μ M KN62	15 μ g CaM	15 μ g CaM + 4 μ M KN62
Enriched SR vesicles	Control	15 μ g CaM	15 μ g CaM + 4 μ M KN62
PKC signaling			
Crude muscle homogenates	Control	1400 nM GFX	500 nM PMA
Crude muscle homogenates	1400 nM GFX	500 nM PMA	1400 nM GFX + 500 nM PMA
Enriched SR vesicles	Control	1400 nM GFX	500 nM PMA

Crude muscle homogenates were prepared from tissues collected from the left ventricle (LV), the soleus (SOL), the extensor digitorum longus (EDL), the red portion of gastrocnemius (RG), and the white portion of gastrocnemius (WG) from each animal. SR vesicles enriched in SERCA1a and SERCA2a were prepared using crude muscle homogenates from WG and LV, respectively. Control, control samples that were incubated in the absence of any activators or inhibitors. Epinephrine is a β -adrenergic activator. Propranolol is a β -adrenergic inhibitor. Forskolin is a PKA activator. KTS720 is a PKA inhibitor. Active PKA is an activated form of the PKA protein. cAMP, adenosine 3',5'-cyclic monophosphate. CaM, bovine brain calmodulin. KN62 is a CaMKII inhibitor. GFX, GF-109203-XI is a PKC inhibitor. PMA, phorbol-12-myristate-13-acetate is a PKC activator.

(BSA), 5 mM β -mercaptoethanol, and 0.5 mM EDTA and diluted (1:100) in 20 mM imidazole buffer with 0.2% BSA.

SDS-PAGE and Western blotting

Sodium dodecyl sulfate (SDS) polyacrylamide gel electrophoresis (PAGE) was performed to separate and isolate proteins by size. Specific parameters for antibody concentrations, transfer voltages and durations used for Western blotting protocols are described in Table 2.2. Crude muscle homogenates and enriched SR vesicles (final protein concentration of 2 mg/mL) were prepared in homogenizing buffer and sample buffer (1.25 M sucrose, 0.25 M Tris · HCl, pH 6.8, 5% SDS, and 0.01% bromphenol). Five to 50 μ g of protein was loaded for SDS-PAGE, with the quantity dependent on the protein concentration required for each specific antibody. All samples were analyzed in duplicate. A 7% polyacrylamide SDS gel (Mini-PROTEAN II; Bio-Rad), with a 3.75% stacking gel, was used to assess SERCA1a, SERCA2a, STK16 and CaMKII contents. Phospholamban samples were analyzed using a 15% polyacrylamide SDS gel with a 3.75% stacking gel.

After SDS-PAGE and a 5 min equilibration with cold transfer buffer (25 mM Tris, 192 mM glycine and 20% vol/vol methanol), proteins were transferred to a polyvinylidene difluoride membrane (PVDF membrane, Bio-Rad) by placing the gel in transfer buffer and applying a low voltage (21-22 mV) for 45-50 min (Trans-Blot Cell, Bio-Rad). Non-specific binding sites were blocked with 5% non-fat skim milk powder in Tris-buffered saline (pH 7.5), applied for 1 h at room temperature. Incubation of the PVDF membrane with primary antibodies was performed as described in Table 2.2. After incubation with primary antibodies, the membrane was washed three times before application of the secondary antibody. Secondary

Table 2.2: Description of primary antibodies and Western blotting protocols in Chapter 2.

Antibody	Supplier	Product #	Species	Primary Antibody Class	Transfer Time (min)	Transfer Voltage (mV)	Primary Dilution (ng/μL)	Incubation Time (h)	Secondary Dilution (ng/μL)
anti-SERCA1a	gift from D. McLennan	A62	Mouse	Monoclonal	46	21	1:20000	1	1:5000
anti-SERCA2a	Affinity Bioreagents	MA3-919	Mouse	Monoclonal	46	21	1:4000	1	1:5000
anti-PLN	Santa Cruz	sc-21923	Goat	Polyclonal	46	21	1:400	16	1:4000
anti-SLN	Antibody is not commercially available.								
anti-STK16	Abgent	AP7241c	Rabbit	Polyclonal	46	21	1:200	16	1:1000
anti-CaMKII	Santa Cruz	sc-6306	Mouse	Monoclonal	50	22	1:400	16	1:4000

SERCA1a, *sarco(endo)plasmic reticulum Ca²⁺-ATPase 1a*. *SERCA2a*, *sarco(endo)plasmic reticulum Ca²⁺-ATPase 2a*. *PLN*, *phospholamban*. *SLN*, *sarcoplipin*. *STK16*, *Serine Threonine kinase 16*. *CaMKII*, *Ca²⁺- dependent calmodulin kinase II*. *CaMKII isoforms* (α , β , δ and γ) were detected using a single anti-*CaMKII* monoclonal antibody. *Specific CaMKII isoforms were identified by molecular weights following sodium dodecyl sulfate (SDS) polyacrylamide gel electrophoresis (PAGE)*. *Transfer Time*, represents the duration of time used to transfer proteins from the SDS polyacrylamide gel to a polyvinylidene difluoride membrane. *Transfer Voltage*, the voltage used to transfer proteins from the SDS polyacrylamide gel to a polyvinylidene difluoride membrane. *Primary Dilution*, represents the dilution factor for primary antibodies used to probe proteins on the polyvinylidene difluoride membrane. *Incubation Time*, represents the time that the primary antibody was in contact with the polyvinylidene difluoride membrane.

antibodies were specific to the species required for each primary antibody, as indicated on the material data sheets provided by the antibody suppliers, and were conjugated to horseradish peroxidase. After application of the appropriate secondary antibody for 1 h, protein quantification was performed using an enhanced chemiluminescence immunodetection procedure (Amersham ECL-RPN2106P1) using a bio-imaging system and GeneSnap software (Syngene). For each antibody, the linearity of progressive increases in protein content was established before experiments were conducted (data not shown). Relative protein levels were determined by scanning densitometry and values were expressed as a % of standard (Std). When direct comparisons were made between pharmaceutical conditions, values were normalized to control samples and expressed as % of control. All samples were analyzed in duplicate and on different gels.

Quantification of CaMKII isoforms (i.e. α , β , δ and γ) was completed using a single anti-CaMKII monoclonal antibody. This approach was utilized since α , β , δ and γ CaMKII isoforms are known to migrate at relative mobilities of ~55, 77, 60 and 60 kDa, respectively. CaMKII δ and γ appear as a common band since both isoforms have relative mobilities of ~60 kDa. Quantification of all CaMKII isoforms has been normalized to CaMKII β from the LV since expression of this isoform was highest in all tissues, with LV containing the highest CaMKII β content.

Ca²⁺-dependent SERCA activity assay

Measurement of Ca²⁺-dependent SERCA activity was made using crude muscle homogenates (~15-90 μ L per 15 mL reaction cocktail), enriched SERCA1a vesicles (~6 μ L per 15 mL reaction cocktail) and enriched SERCA2a vesicles (~45 μ L per 15 mL reaction

cocktail). SERCA kinetic properties were measured by use of a spectrophotometric assay (Simonides & van Hardeveld, 1990) modified by TA Duhamel (unpublished) for use on a plate reader (SPECTRAMax Plus; Molecular Devices). Three SERCA kinetic properties have been assessed, namely, V_{max} , Hill Coefficient (n_H), which is defined as the relationship between SERCA activity and Ca^{2+}_f for 10 to 90% of V_{max} , and Ca_{50} , which is defined as the Ca^{2+}_f required to activate the enzyme to 50% V_{max} . A schematic representation of the general assay steps used to determine Ca^{2+} -dependent kinetic properties in this chapter is illustrated on Figure 2.4.

The SERCA reaction buffer for homogenates (SR in parentheses) contained (in mM) 200 (100) KCl, 20 HEPES, 15 (10) $MgCl_2$, 10 NaN_3 , 10 phosphoenolpyruvate (PEP), 5 ATP, 1 ethylene glycol-bis(β -aminoethyl ether)-N,N,N',N' -tetraacetic acid (EGTA). The pH of the reaction buffer was adjusted to 7.0 at 37 °C. For each set of conditions (i.e. 3 treatments assessed simultaneously), a single aliquot of sample (i.e. homogenates or enriched SR vesicles) was added to 15.3 mL of reaction cocktail, which contained 18 U/mL of lactate dehydrogenase (LDH), 18 U/mL pyruvate kinase (PK), 0.3 mM NADH, 5 mM ATP, and 1 μM Ca^{2+} ionophore A23187.

The 15 mL homogenate cocktail was then aliquoted into 3 test tubes each containing 5 mL. Pathway activators or inhibitors were then added to each test tube as outlined in Table 2.1. This approach ensured that the only difference between treatments was the addition of selected activator/inhibitors to each sample. The contents of each test tube were mixed and aliquoted (300 μL) into 16 Eppendorf tubes containing 15 different Ca^{2+}_f ranging between 7.6 and 4.7 pCa units. The Eppendorf tubes containing the 15 different Ca^{2+}_f were used to generate a substrate-activity curve in which a plateau and subsequent decline in SERCA activity was

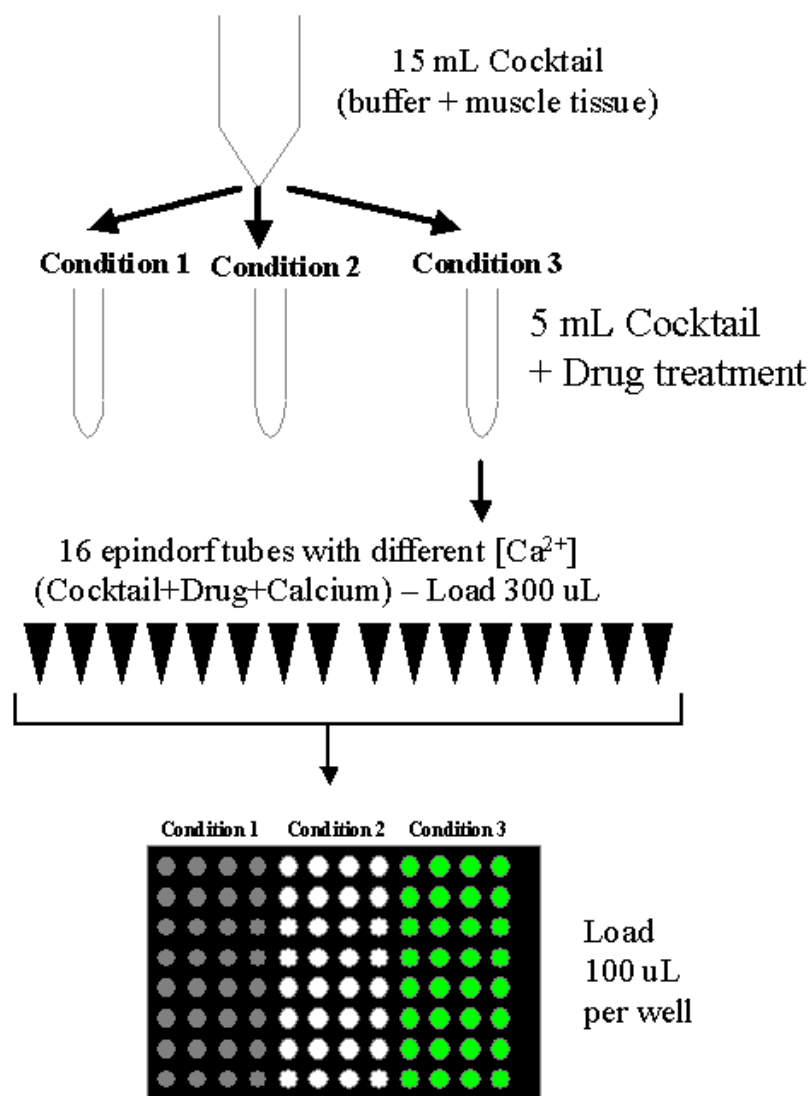


Figure 2.4: Schematic representation of the general assay steps used to determine Ca^{2+} -dependent SERCA activity. This procedure was based on the original assay that was developed by Simonides and van Hardeveld (1990) and was modified by TA Duhamel (unpublished) for use on a spectrophotometric plate reader. Specific assay protocols and concentrations have been described within the Methods section of Chapter 2.

observed with increasing Ca^{2+} . The content of the 16th Eppendorf tube was used to determine basal ATPase activity. This was accomplished by adding 40 μM cyclopiazonic acid (CPA), which is a specific inhibitor of SERCA (Seidler *et al.*, 1989), to one aliquot of the reaction cocktail at a pCa of 4.7.

After mixing, the contents from all Eppendorf tubes were loaded in duplicate (100 μL per well) onto a 96 well round-bottom clear plate. Activity measurements were then completed at 37°C and 340 nm using a spectrophotometric plate reader (SPECTRAMax Plus; Molecular Devices). A correction factor was used to adjust absorbance readings to a 1 cm path length since activity measurements were made using 100 μL volumes. On a given day, 14 tissue samples were analyzed.

SERCA activity was calculated as the difference between Ca^{2+} -stimulated and basal ATPase rates. Kinetic parameters describing the pCa-activity relationship were determined using Computer Software (GraphPad PrismTM Version 4.0) and an IBM computer. Hill coefficient (n_H) and Ca_{50} values for these data were calculated by use of a non-linear regression curve fit using the dose-response relationship that is characterized by *Equation 2.1*.

$$Y = Y_{\text{bot}} + (Y_{\text{top}} - Y_{\text{bot}}) / (1 + 10^{(10(\text{LogCa}_{50} - x) * n_H)}) \quad \text{Equation 2.1}$$

Kinetic data obtained using this plate reader technique were similar to results previously published from our group (Duhamel *et al.*, 2005; Duhamel *et al.*, 2004a; Schertzer *et al.*, 2002; Tupling *et al.*, 2001a). The coefficient of variation for V_{max} during this assay is 8.6% when the same sample was analyzed on different days and was 7.4% when analysis is repeated on the same day.

The accurate assessment of Ca^{2+}_f in the homogenate cocktail is important in the assay procedure. To measure Ca^{2+}_f a fluorescence measurement technique was adapted for use on a plate reader. Fluorescence measurements were made using Indo-1, which is a Ca^{2+} -sensitive dye, and a spectrofluorometric plate reader (SPECTRAMax Gemini XS; Molecular Devices) using the same assay conditions, volumes and mechanics used to determine SERCA activity. Indo-1 was added to the homogenate cocktail immediately before the sample was aliquoted (300 μL) into 16 Eppendorf tubes containing 15 different Ca^{2+}_f ranging between 7.6 and 4.7 pCa units. NADH was not included in the assay buffer during the assessment of Ca^{2+}_f since NADH also has fluorescent properties. The measurement of Ca^{2+}_f using this procedure is based on the difference in maximal emission wavelengths between the Ca^{2+} bound-Indo-1 complex and the Ca^{2+} free-Indo-1 complex. An excitation wavelength of 355 nm was used to excite Indo-1. Emission maxima were recorded at 405 nm for Ca^{2+} -bound (F) and at 485 nm for Ca^{2+} -free (G) Indo-1. The ratio (R) of F to G is directly affected by small changes in Ca^{2+} concentrations and was used to calculate Ca^{2+}_f according to *Equation 2.2* (Grynkiewicz *et al.*, 1985).

$$\text{Ca}^{2+}_f = K_d * (G_{\text{max}} / G_{\text{min}}) * (R - R_{\text{min}}) / (R_{\text{max}} - R) \quad \text{Equation 2.2}$$

Where K_d is the equilibrium constant for the interaction between Ca^{2+} and Indo-1, R_{min} is the minimum value of R with the addition of 250 μM EGTA, G_{max} is the maximum value of G with the addition of 1 mM CaCl_2 . The K_d value used for the interaction of Ca^{2+} and Indo-1 for muscle homogenates and enriched SERCA vesicles was 250 and 135, respectively (Grynkiewicz *et al.*, 1985). Samples were analyzed in triplicate to determine Ca^{2+}_f . By utilizing

this measurement protocol, Ca^{2+}_f was assessed in the sample buffer and the concentration used to generate pCa-activity curves for SERCA.

Statistical Analyses

Data are presented as means \pm S.E. A one-way analysis of variance (ANOVA; one repeated measure) was utilized to compare differences between the different treatments. Where significant differences were found, Neuman-Kuels post hoc procedures were used to compare specific means. Significance was accepted at $P < 0.05$.

Results

Muscle oxidative potential

Maximal CS activity, used as a measure of oxidative potential, was graded (LV > RG > SOL > EDL > WG) according to muscle type. The highest CS values ($\text{mols.kg}^{-1} \text{ protein.hr}^{-1}$) was observed in LV (10.4 ± 0.3), followed by RG (5.7 ± 0.4), SOL (4.5 ± 0.2), EDL (3.5 ± 0.4) and was lowest in WG (1.7 ± 0.2).

SDS-PAGE and Western blotting

Since this study was designed to investigate the regulation of SERCA kinetic properties in LV and skeletal muscle of different fibre type and oxidative capacity, it was important to characterize the tissue specific expression of SERCA1a and SERCA2a. Western blot data (Table 2.3) indicated that LV expressed exclusively the SERCA2a isoform and the SOL was the only skeletal muscle that expressed SERCA2a. In contrast, SERCA1a was detected in all skeletal muscles sampled. SERCA1a protein content was highest in EDL, followed by RG and

Table 2.3: Summary of Western blot data characterizing the abundance of selected proteins in the rat left ventricle and skeletal muscle samples assessed in Chapter 2.

	Homogenates			Vesicles			
	LV	SOL	EDL	RG	WG	LV	WG
SERCA1a (normalized to SOL)	N.D.	100	208 ± 29	162 ± 23	179 ± 28	N.D.	376 ± 21
SERCA2a (normalized to SOL)	127 ± 5	100	N.D.	N.D.	N.D.	478 ± 14	N.D.
PLN (normalized to LV)	100	N.D.	N.D.	N.D.	N.D.	343 ± 12	N.D.
SLN	No antibody.						
STK16 (normalized to liver)	39 ± 7	28 ± 1	26 ± 1	37 ± 11	27 ± 9	25 ± 7	37 ± 5
CaMKII α (normalized to LV Ca β)	12 ± 5	9 ± 6	54 ± 9	32 ± 1	99 ± 13	8 ± 4	8 ± 1
CaMKII β (normalized to LV Ca β)	100	70 ± 1	68 ± 5	64 ± 4	70 ± 8	12 ± 2	65 ± 5
CaMKII $\delta + \gamma$ (normalized to LV Ca β)	17 ± 7	24 ± 7	18 ± 5	15 ± 1	16 ± 5	N.D.	N.D.

Values are Means ± S.E. n=4. Homogenates were prepared from tissues collected from the left ventricle (LV), soleus (SOL), extensor digitorum longus (EDL), the red portion of gastrocnemius (RG), and the white portion of gastrocnemius (WG) from each animal. Purified SR vesicles enriched in sarco(endo)plasmic reticulum Ca^{2+} -ATPase (SERCA) 2a and SERCA1a were prepared using crude muscle homogenates from LV and WG, respectively. PLN, phospholamban. SLN, sarcolipin. STK16, Serine Threonine kinase 16. CaMKII, Ca^{2+} -dependent calmodulin kinase II. Soleus was used as a reference for SERCA1a and SERCA2a values since this tissue expressed both SERCA isoforms. PLN was detected in LV homogenates and in purified SERCA2a vesicles isolated from LV but not in any other tissue. N.D., not detected. No Antibody, indicates that a commercially available antibody was not available for SLN. CaMKII isoforms (α , β , δ and γ) were detected using a single anti-CaMKII monoclonal antibody. Specific CaMKII isoforms were identified by molecular weights following sodium dodecyl sulfate (SDS) polyacrylamide gel electrophoresis (PAGE). CaMKII isoforms were normalized to LV CaMKII β since expression was highest in this tissue. ^a, Significantly different from LV homogenate (P<0.05). ^b, Significantly different from SOL homogenate (P<0.05). ^c, Significantly different from EDL homogenate (P<0.05). ^d, Significantly different from RG homogenate (P<0.05). ^e, Significantly different from WG homogenate (P<0.05). ^f, Significantly different from SR vesicles enriched in SERCA2a prepared from LV (P<0.05).

WG, and lowest in SOL (EDL > RG and WG > SOL). After correcting for total protein loading, SERCA1a and SERCA2a protein contents were enriched by ~10 fold in SR vesicles, compared to WG and LV homogenates. This enrichment resulted in 20 and 5 fold increases in V_{\max} for SERCA1a and SERCA2a vesicles, respectively, compared to WG and LV homogenates (data not shown).

Our Western blot data supports previous literature in the rat (Damiani *et al.*, 2000) demonstrating that PLN protein is expressed in rat LV tissue but not in any of the skeletal muscles examined (Table 2.3). Phospholamban content was increased by ~3-fold in SR vesicles enriched in SERCA2a. We also planned to assess SLN protein content. Unfortunately, an antibody specific for SLN was not commercial available. As a substitute, we searched for an antibody capable of detecting a protein known to influence SLN protein function. The protein that we selected was STK16 since this kinase mediates the phosphorylation of SLN and thereby increases SERCA Ca^{2+} -sensitivity (Gramolini *et al.*, 2006). Serine/threonine kinase 16 protein was found in high quantities in the liver (data not shown) and in lower quantities in the LV and skeletal muscle tissues of the rat (Table 2.3). Compared to the liver, the content of STK16 protein in the LV and the skeletal muscles of the rat was ~27-40%. Enrichment of SR vesicles did not alter STK16 protein content from that observed in WG or LV crude muscle homogenates.

Quantification of CaMKII isoforms (i.e. α , β , $\delta+\gamma$) was performed using a single anti-CaMKII monoclonal antibody. Values have been normalized to CaMKII β content in LV since this tissue expressed the highest quantity of CaMKII β (Table 2.3). The expression pattern of CaMKII α was different between the various tissues sampled. For CaMKII α , LV and SOL < RG < EDL < WG; whereas CaMKII β protein content was highest in LV, compared to all

other tissues, with no additional differences between tissues noted. Compared to CaMKII β , only low amounts of CaMKII δ and γ were detected in all tissues analyzed, with no differences being observed between muscles.

β -adrenergic regulation of SERCA kinetics

To determine the effects of EPI signaling on SERCA function, homogenates were incubated for 10 min in the presence of 15 nM EPI or 150 nM EPI (Table 2.4). Epinephrine has no effect on V_{\max} in any tissue. In contrast, the n_H and Ca_{50} were altered by EPI in a tissue specific manner. Specifically, EPI increased n_H by ~17% in the EDL and reduced Ca_{50} by ~25% in the LV and SOL, with no effects for any other tissue.

Based on these observations, another series of conditions were designed to determine if the effects of EPI could be reversed by the β -blocker propranolol (Table 2.5). As expected, the EPI-induced reduction in Ca_{50} in both the LV and the SOL was prevented by propranolol. Our results for V_{\max} support our initial observations, namely that 150 nM EPI did not influence V_{\max} in LV and SOL, or any other tissue studied. The n_H was increased by 22% in LV in response to EPI treatment, compared to control. Propranolol + EPI (i.e. 4 μ M propranolol + 150 nM EPI) prevented the EPI-induced increases to n_H in LV tissue. Interestingly, for the SOL, n_H was not changed with EPI, compared to control, but was 12% lower during the combined propranolol + EPI treatment, compared to the EPI treatment. Hill coefficients were not altered by the EPI treatment or the combined propranolol + EPI treatment in any other tissue studied.

To determine if the reduction in Ca_{50} observed in LV and SOL during EPI treatment was mediated by a PKA-dependent process, samples were incubated in the presence of 25 μ M forskolin or 100 nM KT5720 + 25 μ M forskolin (Table 2.6). The only effect of forskolin was a

Table 2.4: Concentration dependent effects of epinephrine on SERCA kinetic properties in homogenates from left ventricle and skeletal muscle of different fibre type composition.

	Control	15 nM Epinephrine	150 nM Epinephrine
LV			
V_{max}	156 ± 5	159 ± 7	157 ± 6
n_H	1.85 ± 0.09	1.88 ± 0.11	1.95 ± 0.11
Ca_{50}	1764 ± 189	1340 ± 135 †	1284 ± 100 †
SOL			
V_{max}	122 ± 3	119 ± 4	122 ± 4
n_H	1.21 ± 0.08	1.27 ± 0.13	1.15 ± 0.07
Ca_{50}	995 ± 101	751 ± 63 †	726 ± 77 †
EDL			
V_{max}	671 ± 32	668 ± 34	676 ± 34
n_H	1.27 ± 0.07	1.49 ± 0.14 †	1.45 ± 0.12 †
Ca_{50}	818 ± 85	779 ± 74	876 ± 118
WG			
V_{max}	717 ± 30	716 ± 28	723 ± 31
n_H	1.53 ± 0.08	1.52 ± 0.09	1.55 ± 0.09
Ca_{50}	976 ± 53	961 ± 66	1014 ± 58
RG			
V_{max}	529 ± 9	528 ± 8	518 ± 11
n_H	1.60 ± 0.05	1.68 ± 0.04	1.68 ± 0.06
Ca_{50}	939 ± 37	973 ± 75	917 ± 54

Values are Means ± S.E. n=7. LV, left ventricle. SOL, soleus. EDL, extensor digitorum longus. WG, the white portion of the gastrocnemius. RG, the red portion of the gastrocnemius. Epinephrine is a β -adrenergic activator. V_{max} , maximal SERCA activity. n_H , hill slope defined as the relationship between SERCA activity and $[Ca^{2+}]_i$ for 10 to 90% V_{max} . Ca_{50} , the Ca^{2+} -concentration at $\frac{1}{2} V_{max}$. Units for V_{max} are $nmol.mg^{-1}.min^{-1}$. Units for n_H are arbitrary units. Units for Ca_{50} are nM. † - Significantly different from Control (P<0.05).

Table 2.5: Effects of epinephrine or propranolol + epinephrine on SERCA kinetic properties in homogenates from left ventricle and skeletal muscle of different fibre type composition.

	Control	150 nM Epinephrine	4 μ M Propranolol + 150 nM Epinephrine
LV			
V_{max}	152 \pm 7	154 \pm 3	147 \pm 2
n_H	1.43 \pm 0.16	1.74 \pm 0.15 †	1.46 \pm 0.18 ‡
Ca_{50}	1404 \pm 122	1030 \pm 71 †	1424 \pm 189 ‡
SOL			
V_{max}	119 \pm 2	114 \pm 10	123 \pm 6
n_H	1.39 \pm 0.07	1.44 \pm 0.11	1.27 \pm 0.05 ‡
Ca_{50}	882 \pm 45	675 \pm 131 †	938 \pm 123 ‡
EDL			
V_{max}	708 \pm 6	700 \pm 10	706 \pm 7
n_H	1.47 \pm 0.03	1.47 \pm 0.08	1.43 \pm 0.08
Ca_{50}	1038 \pm 51	1036 \pm 29	1066 \pm 50
WG			
V_{max}	680 \pm 15	677 \pm 8	672 \pm 10
n_H	1.42 \pm 0.01	1.44 \pm 0.15	1.40 \pm 0.11
Ca_{50}	783 \pm 24	758 \pm 80	746 \pm 63
RG			
V_{max}	430 \pm 9	429 \pm 17	429 \pm 11
n_H	1.38 \pm 0.10	1.32 \pm 0.02	1.24 \pm 0.03
Ca_{50}	990 \pm 82	926 \pm 54	908 \pm 71

Values are Means \pm S.E. n=7. LV, left ventricle. SOL, soleus. EDL, extensor digitorum longus. WG, the white portion of the gastrocnemius. RG, the red portion of the gastrocnemius. Epinephrine is a β -adrenergic activator. Propranolol is a β -adrenergic inhibitor. V_{max} , maximal SERCA activity. n_H , hill slope defined as the relationship between SERCA activity and $[Ca^{2+}]_f$ for 10 to 90% V_{max} . Ca_{50} , the Ca^{2+} -concentration at $\frac{1}{2} V_{max}$. Units for V_{max} are $nmol \cdot mg^{-1} \cdot min^{-1}$. Units for n_H are arbitrary units. Units for Ca_{50} are nM. † - Significantly different from Control ($P < 0.05$). ‡ - Significantly different from 150 nM epinephrine ($P < 0.05$).

Table 2.6: Effects of forskolin or KT5720 + forskolin on SERCA kinetic properties in homogenates from left ventricle and skeletal muscle of different fibre type composition.

	Control	25 μ M Forskolin		100 nM KT5720 + 25 μ M Forskolin	
LV					
V_{max}	169 \pm 1	172 \pm 5		176 \pm 4	
n_H	1.33 \pm 0.04	1.33 \pm 0.05		1.35 \pm 0.03	
Ca_{50}	1178 \pm 51	989 \pm 68	†	1218 \pm 74	‡
SOL					
V_{max}	108 \pm 8	109 \pm 7		112 \pm 7	
n_H	1.20 \pm 0.05	1.17 \pm 0.08		1.15 \pm 0.08	
Ca_{50}	848 \pm 68	842 \pm 54		820 \pm 76	
EDL					
V_{max}	667 \pm 10	672 \pm 2		671 \pm 8	
n_H	1.25 \pm 0.04	1.23 \pm 0.05		1.26 \pm 0.04	
Ca_{50}	1015 \pm 38	1087 \pm 29		1019 \pm 25	
WG					
V_{max}	730 \pm 8	722 \pm 11		733 \pm 16	
n_H	1.25 \pm 0.08	1.27 \pm 0.04		1.31 \pm 0.04	
Ca_{50}	1086 \pm 29	1000 \pm 43		1041 \pm 48	
RG					
V_{max}	398 \pm 8	399 \pm 10		402 \pm 6	
n_H	1.21 \pm 0.02	1.22 \pm 0.03		1.25 \pm 0.05	
Ca_{50}	1024 \pm 57	1069 \pm 56		1024 \pm 24	

Values are Means \pm S.E. n=7. LV, left ventricle. SOL, soleus. EDL, extensor digitorum longus. WG, the white portion of the gastrocnemius. RG, the red portion of the gastrocnemius. Forskolin is a protein kinase A (PKA) activator. KT5720 is a PKA inhibitor. V_{max} , maximal SERCA activity. n_H , hill slope defined as the relationship between SERCA activity and $[Ca^{2+}]_f$ for 10 to 90% V_{max} . Ca_{50} , the Ca^{2+} -concentration at $\frac{1}{2} V_{max}$. Units for V_{max} are nmol.mg⁻¹.min⁻¹. Units for n_H are arbitrary units. Units for Ca_{50} are nM. † - Significantly different from control (P<0.05). ‡ - Significantly different from 25 μ M forskolin (P<0.05).

16% reduction in Ca_{50} in the LV. This reduction was prevented by the combined KT5720 + forskolin treatment.

To determine if PKA-mediated signaling was influencing the Ca^{2+} -sensitivity of a particular SERCA isoform, another series of conditions were designed to compare the effects of forskolin or an activated form of PKA (A-PKA) on SERCA kinetic properties using enriched SR vesicles. Enriched SERCA1a and SERCA2a vesicles, prepared from the WG and LV, respectively, were incubated with either 25 μ M forskolin or 1 mg A-PKA. Incubation of enriched SERCA2a vesicles with forskolin and A-PKA increased n_H by 7 and 9%, respectively; while Ca_{50} was reduced by 12 and 9%, respectively (Table 2.7). Incubation of enriched SERCA1a vesicles with forskolin and A-PKA did not alter any SERCA kinetic property.

Since our data indicated that EPI decreases Ca_{50} in both the LV and SOL, while forskolin reduced Ca_{50} in LV but not the SOL, we designed another set of conditions to gain further insight into the mechanisms responsible for influencing the tissue-specific regulation of Ca_{50} . Specifically, we were interested in determining if tissue-specific regulation of Ca_{50} in LV and SOL was influenced by cAMP-dependent PKA signaling or an alternative cAMP-dependent mechanism that is not regulated by PKA signaling (Table 2.8). In these experiments, samples were incubated in the presence of 10 μ M cAMP or 10 μ M cAMP + 100 nM KT5720. Neither the cAMP treatment nor the combined cAMP + KT5720 treatment altered V_{max} or n_H in any tissue studied. Interestingly, Ca_{50} was reduced by ~12 and 14% in LV and SOL, respectively, during the cAMP treatment, compared to control. Incubation of LV samples with the combined cAMP + KT5720 treatment restored Ca_{50} to control levels, suggesting that Ca_{50} is regulated by PKA-mediated events in this tissue. In contrast, incubation of SOL samples with the combined treatment failed to restore Ca_{50} to control levels, suggesting that a non-PKA-dependent, cAMP-

Table 2.7: Effects of forskolin or Active PKA on SERCA kinetic properties in purified SR vesicles prepared from left ventricle and the white portion of the gastrocnemius.

	Control	25 μ M Forskolin	1 mg Active PKA
SERCA2a vesicles			
V_{\max}	809 \pm 26	796 \pm 16	803 \pm 11
n_H	1.62 \pm 0.05	1.77 \pm 0.05 †	1.73 \pm 0.03 †
Ca_{50}	2114 \pm 110	1855 \pm 55 †	1915 \pm 27 †
SERCA1a vesicles			
V_{\max}	11340 \pm 584	11085 \pm 499	11011 \pm 474
n_H	1.47 \pm 0.05	1.45 \pm 0.07	1.41 \pm 0.03
Ca_{50}	974 \pm 40	938 \pm 48	965 \pm 52

Values are Means \pm S.E. n=7. SERCA2a vesicles, purified SR vesicles enriched in SERCA2a were prepared using LV. SERCA1a vesicles, purified SR vesicles enriched in SERCA1a were prepared using WG. Active PKA is an activated form of the protein kinase A (PKA) catalytic subunit. Forskolin is a PKA activator. V_{\max} , maximal SERCA activity. n_H , hill slope defined as the relationship between SERCA activity and $[Ca^{2+}]_i$ for 10 to 90% V_{\max} . Ca_{50} , the Ca^{2+} -concentration at $\frac{1}{2} V_{\max}$. Units for V_{\max} are $nmol.mg^{-1}.min^{-1}$. Units for n_H are arbitrary units. Units for Ca_{50} are nM. † - Significantly different from control ($P < 0.05$). ‡ - Significantly different from Active PKA ($P < 0.05$).

Table 2.8: Effects of cAMP or KT5720 + cAMP on SERCA kinetic properties in homogenates from left ventricle and skeletal muscle of different fibre type composition.

	Control	10 μ M cAMP	100 nM KT5720 + 10 μ M cAMP
LV			
V_{max}	127 \pm 29	129 \pm 28	123 \pm 27
n_H	1.99 \pm 0.04	1.93 \pm 0.12	1.90 \pm 0.09
Ca_{50}	1873 \pm 169	1461 \pm 95	1712 \pm 142 ‡
SOL			
V_{max}	128 \pm 8	129 \pm 4	128 \pm 7
n_H	1.42 \pm 0.03	1.46 \pm 0.06	1.39 \pm 0.04
Ca_{50}	1414 \pm 95	1075 \pm 76 †	1017 \pm 69 †
EDL			
V_{max}	683 \pm 33	681 \pm 25	679 \pm 31
n_H	1.51 \pm 0.04	1.55 \pm 0.07	1.52 \pm 0.06
Ca_{50}	1270 \pm 43	1211 \pm 21	1292 \pm 39
WG			
V_{max}	583 \pm 14	587 \pm 18	587 \pm 18
n_H	1.63 \pm 0.07	1.61 \pm 0.09	1.64 \pm 0.13
Ca_{50}	1203 \pm 45	1263 \pm 75	1264 \pm 36
RG			
V_{max}	457 \pm 26	454 \pm 18	453 \pm 20
n_H	1.48 \pm 0.09	1.42 \pm 0.04	1.34 \pm 0.06
Ca_{50}	1227 \pm 128	1254 \pm 115	1228 \pm 115

Values are Means \pm S.E. n=7. LV, left ventricle. SOL, soleus. EDL, extensor digitorum longus. WG, the white portion of the gastrocnemius. RG, the red portion of the gastrocnemius. cAMP, adenosine 3',5'-cyclic monophosphate is a protein kinase A (PKA) and Serine/Threonine kinase 16 (STK16) activator. KT5720 is a PKA inhibitor. V_{max} , maximal SERCA activity. n_H , hill slope defined as the relationship between SERCA activity and $[Ca^{2+}]_f$ for 10 to 90% V_{max} . Ca_{50} , the Ca^{2+} -concentration at $\frac{1}{2} V_{max}$. Units for V_{max} are nmol.mg⁻¹.min⁻¹. Units for n_H are arbitrary units. Units for Ca_{50} are nM. † - Significantly different from control (P<0.05). ‡ - Significantly different from 10 μ M cAMP(P<0.05).

activated process may regulate Ca_{50} in this tissue. Neither the cAMP treatment nor the combined cAMP + KT5720 treatment altered the Ca_{50} for any of the other skeletal muscles studied.

To determine if cAMP-mediated signaling was influencing the Ca^{2+} -sensitivity of a particular SERCA isoform, SR vesicles enriched in SERCA2a and SERCA1a were incubated with cAMP or cAMP + KT5720 (Table 2.9). As expected, the V_{max} of enriched SERCA2a vesicles, prepared from the LV, was not altered by these treatments. However, n_H was increased by 20% and Ca_{50} was reduced by 15% following incubation of SERCA2a vesicles with cAMP. Incubation of enriched SERCA2a vesicles with the combined agents restored n_H and Ca_{50} to control levels, suggesting that n_H and Ca_{50} is regulated by PKA mediated signaling in enriched SERCA2a vesicles. Maximal SERCA activity, n_H , and Ca_{50} were not altered by the cAMP treatment or the combined cAMP + KT5720 treatment in enriched SERCA1a vesicles prepared from the WG.

Ca^{2+} -dependent calmodulin kinase II regulation of SERCA kinetics

To determine the effects that CaMKII signaling has on SERCA kinetic properties, homogenates were incubated in the presence of 15 μ g CaM or 4 μ M KN62 (Table 2.10). Maximal activity and n_H were not altered by CaM treatment in any tissue. Compared to control, incubation of samples with CaM reduced Ca_{50} in the LV by 13%, but did not alter Ca_{50} in any skeletal muscle. Incubation of SOL, EDL or WG with CaM did not alter V_{max} , n_H , or Ca_{50} . Incubation of samples with KN62 compared to control and CaM treated samples, reduced n_H by 14 and 19% in LV and by 10 and 11% in RG, respectively, without altering kinetic properties in any other tissue.

Table 2.9: Effects of cAMP or KT5720 + cAMP on SERCA kinetic properties in purified SR vesicles prepared from left ventricle and the white portion of the gastrocnemius.

	Control	10 μ M cAMP	100 nM KT5720 + 10 μ M cAMP
SERCA2a vesicles			
V_{max}	984 \pm 24	973 \pm 24	977 \pm 30
n_H	1.46 \pm 0.04	1.75 \pm 0.08 †	1.53 \pm 0.04 ‡
Ca_{50}	2310 \pm 65	1970 \pm 87 †	2217 \pm 38 ‡
SERCA1a vesicles			
V_{max}	12185 \pm 200	12131 \pm 207	12102 \pm 302
n_H	1.59 \pm 0.02	1.62 \pm 0.04	1.62 \pm 0.06
Ca_{50}	945 \pm 21	941 \pm 28	924 \pm 12

Values are Means \pm S.E. n=7. SERCA2a vesicles, purified SR vesicles enriched in SERCA2a were prepared using LV. SERCA1a vesicles, purified SR vesicles enriched in SERCA1a were prepared using WG. cAMP, adenosine 3',5'-cyclic monophosphate is a protein kinase A (PKA) and Serine/Threonine kinase 16 (STK16) activator. KT5720 is a PKA inhibitor. V_{max} , maximal SERCA activity. n_H , hill slope defined as the relationship between SERCA activity and $[Ca^{2+}]_f$ for 10 to 90% V_{max} . Ca_{50} , the Ca^{2+} -concentration at $\frac{1}{2} V_{max}$. Units for V_{max} are nmol.mg⁻¹.min⁻¹. Units for n_H are arbitrary units. Units for Ca_{50} are nM. † - Significantly different from control (P<0.05). ‡ - Significantly different from 10 μ M cAMP (P<0.05).

Table 2.10: Effects of CaM or KN62 on SERCA kinetic properties in homogenates from left ventricle and skeletal muscle of different fibre type composition.

	Control	15 μ g CaM	4 μ M KN62	
LV				
V_{max}	165 \pm 10	169 \pm 5	163 \pm 5	
n_H	1.54 \pm 0.09	1.63 \pm 0.09	1.32 \pm 0.10	‡‡
Ca_{50}	1442 \pm 97	1250 \pm 86	1434 \pm 76	† ‡
SOL				
V_{max}	128 \pm 1	130 \pm 5	128 \pm 4	
n_H	1.36 \pm 0.05	1.38 \pm 0.09	1.40 \pm 0.05	
Ca_{50}	747 \pm 29	706 \pm 51	720 \pm 32	
EDL				
V_{max}	721 \pm 17	709 \pm 9	714 \pm 22	
n_H	1.22 \pm 0.11	1.27 \pm 0.08	1.21 \pm 0.03	
Ca_{50}	1057 \pm 120	1126 \pm 86	1059 \pm 11	
WG				
V_{max}	654 \pm 11	652 \pm 15	648 \pm 6	
n_H	1.31 \pm 0.05	1.31 \pm 0.06	1.32 \pm 0.10	
Ca_{50}	1198 \pm 192	1158 \pm 250	1134 \pm 220	
RG				
V_{max}	421 \pm 13	429 \pm 14	425 \pm 8	
n_H	1.35 \pm 0.05	1.33 \pm 0.10	1.20 \pm 0.05	‡‡
Ca_{50}	1092 \pm 17	1087 \pm 88	1139 \pm 32	

Values are Means \pm S.E. n=7. LV, left ventricle. SOL, soleus. EDL, extensor digitorum longus. WG, the white portion of the gastrocnemius. RG, the red portion of the gastrocnemius. CaM, bovine brain calmodulin is a substrate for Ca^{2+} -dependent calmodulin kinase II (CaMKII). KN62 is a CaMKII inhibitor. V_{max} , maximal SERCA activity. n_H , hill slope defined as the relationship between SERCA activity and $[Ca^{2+}]_f$ for 10 to 90% V_{max} . Ca_{50} , the Ca^{2+} -concentration at $\frac{1}{2} V_{max}$. Units for V_{max} are $nmol.mg^{-1}.min^{-1}$. Units for n_H are arbitrary units. Units for Ca_{50} are nM. † - Significantly different from control ($P < 0.05$). ‡ - Significantly different from 600 units CaM ($P < 0.05$).

In order to determine if KN62 was able to inhibit the CaM-dependent changes in Ca_{50} observed in LV tissue, homogenates were incubated in the presence of 4 μ M KN62, 15 μ g CaM or 4 μ M KN62 + 15 μ g CaM (Table 2.11). As expected, these treatments did not alter V_{max} . However, CaM treatment, compared to KN62 treatment, increased n_H by 12% and reduced Ca_{50} by 17% in LV. The effects of the CaM treatment on n_H and Ca_{50} were prevented when LV samples were incubated with the combined KN62 + CaM treatment. Interestingly, CaM also increased n_H by 13% in the SOL. This effect of CaM on SOL n_H was not observed in the previous set of conditions (Table 2.10). Additionally, the CaM-dependent increase in n_H was not inhibited when SOL was incubated in the presence of the combined KN62 + CaM treatment. As in our previous experiment, n_H and Ca_{50} were not altered by CaM or the combined KN62 + CaM treatment in EDL, WG or RG.

To determine if CaMKII-mediated signaling was influencing the Ca^{2+} -sensitivity of a particular SERCA isoform, SR vesicles enriched in SERCA1a and SERCA2a were treated with 15 μ g CaM or 4 μ M KN62 + 15 μ g CaM (Table 2.12). These treatments did not alter V_{max} in SR vesicles enriched in SERCA2a prepared from LV. Compared to control, incubation of enriched SERCA2a vesicles with the CaM treatment increased n_H by 20% and reduced Ca_{50} by 13%. These changes in n_H and Ca_{50} were prevented when enriched SERCA2a vesicles were incubated with KN62 + CaM in combination. Incubation of SR vesicles enriched in SERCA1a with these same treatments did not alter V_{max} , n_H , or Ca_{50} .

PKC regulation of SERCA kinetics

To determine the effects of PKC signaling on SERCA kinetic properties, homogenates were incubated in the presence of 500 nM PMA or 1400 nM GFX (Table 2.13). Incubation of

Table 2.11: Effects of KN62, CaM or KN62 + CaM on SERCA kinetic properties in homogenates from left ventricle and skeletal muscle of different fibre type composition.

	4 μ M KN62	15 μ g CaM		4 μ M KN62 + 15 μ g CaM	
LV					
V_{max}	148 \pm 5	147 \pm 3		149 \pm 5	
n_H	2.08 \pm 0.09	2.34 \pm 0.02	†	2.15 \pm 0.04	‡
Ca_{50}	1467 \pm 56	1214 \pm 24	†	1475 \pm 38	‡
SOL					
V_{max}	137 \pm 5	135 \pm 6		128 \pm 6	
n_H	1.77 \pm 0.05	2.00 \pm 0.06	†	1.93 \pm 0.08	†
Ca_{50}	1356 \pm 45	1296 \pm 35		1304 \pm 41	
EDL					
V_{max}	790 \pm 23	793 \pm 29		762 \pm 27	
n_H	1.82 \pm 0.05	1.89 \pm 0.04		1.89 \pm 0.06	
Ca_{50}	765 \pm 33	745 \pm 28		766 \pm 33	
WG					
V_{max}	675 \pm 47	682 \pm 49		680 \pm 50	
n_H	1.59 \pm 0.08	1.71 \pm 0.08		1.64 \pm 0.09	
Ca_{50}	670 \pm 82	659 \pm 68		675 \pm 71	
RG					
V_{max}	430 \pm 13	428 \pm 15		430 \pm 11	
n_H	1.72 \pm 0.08	1.79 \pm 0.07		1.73 \pm 0.07	
Ca_{50}	878 \pm 92	875 \pm 98		866 \pm 69	

Values are Means \pm S.E. n=7. LV, left ventricle. SOL, soleus. EDL, extensor digitorum longus. WG, the white portion of the gastrocnemius. RG, the red portion of the gastrocnemius. CaM, bovine brain calmodulin is a substrate for Ca^{2+} -dependent calmodulin kinase II (CaMKII). KN62 is a CaMKII inhibitor. V_{max} , maximal SERCA activity. n_H , hill slope defined as the relationship between SERCA activity and $[Ca^{2+}]_f$ for 10 to 90% V_{max} . Ca_{50} , the Ca^{2+} -concentration at $\frac{1}{2} V_{max}$. Units for V_{max} are nmol.mg⁻¹.min⁻¹. Units for n_H are arbitrary units. Units for Ca_{50} are nM. † - Significantly different from control (P<0.05). ‡ - Significantly different from 600 units CaM (P<0.05).

Table 2.12: Effects of CaM or KN62 on SERCA kinetic properties in purified SR vesicles prepared from left ventricle and the white portion of the gastrocnemius.

	Control	15 μ g CaM	4 μ M KN62 + 15 μ g CaM
SERCA2a vesicles			
V_{\max}	986 \pm 26	980 \pm 27	975 \pm 35
n_H	1.45 \pm 0.04	1.74 \pm 0.07 †	1.47 \pm 0.06 ‡
Ca_{50}	2308 \pm 64	2014 \pm 81 †	2259 \pm 74 ‡
SERCA1a vesicles			
V_{\max}	12301 \pm 167	12214 \pm 182	12191 \pm 258
n_H	1.59 \pm 0.02	1.60 \pm 0.03	1.59 \pm 0.03
Ca_{50}	939 \pm 20	950 \pm 21	945 \pm 28

Values are Means \pm S.E. n=7. SERCA2a vesicles, purified SR vesicles enriched in SERCA2a were prepared using LV. SERCA1a vesicles, purified SR vesicles enriched in SERCA1a were prepared using WG. CaM, bovine brain calmodulin is a substrate for Ca^{2+} -dependent calmodulin kinase II (CaMKII). KN62 is a CaMKII inhibitor. V_{\max} , maximal SERCA activity. n_H , hill slope defined as the relationship between SERCA activity and $[Ca^{2+}]_i$ for 10 to 90% V_{\max} . Ca_{50} , the Ca^{2+} -concentration at $\frac{1}{2} V_{\max}$. Units for V_{\max} are $nmol \cdot mg^{-1} \cdot min^{-1}$. Units for n_H are arbitrary units. Units for Ca_{50} are nM. † - Significantly different from control ($P < 0.05$). ‡ - Significantly different from 600 units CaM ($P < 0.05$).

Table 2.13: Effects of GFX or PMA on SERCA kinetic properties in homogenates from left ventricle and skeletal muscle of different fibre type composition.

	Control	1400 nM GFX	500 nM PMA	
LV				
V_{max}	173 ± 4	172 ± 7	171 ± 4	
n_H	1.45 ± 0.08	1.43 ± 0.09	1.25 ± 0.02	††
Ca_{50}	1536 ± 70	1404 ± 59	1877 ± 210	††
SOL				
V_{max}	132 ± 6	138 ± 6	135 ± 4	
n_H	1.30 ± 0.05	1.32 ± 0.09	1.32 ± 0.08	
Ca_{50}	1001 ± 25	1030 ± 39	1566 ± 214	††
EDL				
V_{max}	636 ± 2	643 ± 5	536 ± 8	††
n_H	1.41 ± 0.03	1.34 ± 0.07	1.01 ± 0.12	††
Ca_{50}	1176 ± 150	1058 ± 108	3135 ± 446	††
WG				
V_{max}	650 ± 3	643 ± 15	552 ± 9	††
n_H	1.29 ± 0.08	1.34 ± 0.11	1.00 ± 0.09	††
Ca_{50}	1007 ± 113	932 ± 68	2478 ± 46	††
RG				
V_{max}	455 ± 34	439 ± 39	374 ± 22	††
n_H	1.27 ± 0.03	1.28 ± 0.05	1.08 ± 0.10	††
Ca_{50}	1159 ± 155	1103 ± 243	1815 ± 284	††

Values are Means ± S.E. n=7. LV, left ventricle. SOL, soleus. EDL, extensor digitorum longus. WG, the white portion of the gastrocnemius. RG, the red portion of the gastrocnemius. GFX, GF-109203-XI is a protein kinase C (PKC) activator. PMA, phorbol-12-myristate-13-acetate is a PKC activator. V_{max} , maximal SERCA activity. n_H , hill slope defined as the relationship between SERCA activity and $[Ca^{2+}]_i$ for 10 to 90% V_{max} . Ca_{50} , the Ca^{2+} -concentration at $\frac{1}{2} V_{max}$. Units for V_{max} are $nmol \cdot mg^{-1} \cdot min^{-1}$. Units for n_H are arbitrary units. Units for Ca_{50} are nM. † - Significantly different from control ($P < 0.05$). †† - Significantly different from 1400 nM GFX ($P < 0.05$).

muscle homogenates with GFX had no effect on V_{\max} , n_H , or Ca_{50} in any tissue. In contrast, incubation of muscle homogenates with PMA altered kinetic properties in all tissues. Although the PMA treatment, compared to control, did not alter V_{\max} in LV or SOL, it did reduce V_{\max} by ~15% in EDL, WG and RG. Additionally, PMA treatment also reduced n_H by 13, 28, 22, and 14% in LV, EDL, WG and RG, respectively, but not in SOL. The PMA treatment also increased Ca_{50} in all tissues. Compared to control, PMA increased Ca_{50} by ~34, 52, 196, 166 and 65% in LV, SOL, EDL, WG and RG, respectively.

In order to determine if GFX was able to inhibit the PMA-dependent changes in SERCA kinetic properties, another set of treatment conditions was designed to incubate samples with 1400 nM GFX + 500 nM PMA (Table 2.14). Although we expected that GFX would prevent the PMA-induced changes in SERCA kinetic properties, our data indicates that V_{\max} was reduced by 11-13% in EDL, WG and RG during the combined GFX + PMA treatment compared to GFX. Additionally, n_H was decreased and Ca_{50} was increased during the combined GFX + PMA treatment, compared to GFX alone, regardless of the tissue studied. GFX did not prevent the PMA-induced changes in V_{\max} in EDL, WG and RG and did not prevent the PMA-induced changes in n_H or Ca_{50} in any tissue.

To determine if PKC-mediated signaling was influencing the Ca^{2+} -sensitivity of a particular SERCA isoform, SR vesicles enriched in SERCA1a and SERCA2a were treated with 1400 nM GFX or 500 nM PMA (Table 2.15). As expected, GFX treatment had no effect on V_{\max} , n_H , or Ca_{50} for SR vesicles enriched in SERCA2a and SR vesicles enriched in SERCA1a. In contrast to GFX, PMA altered kinetic properties in SR vesicles enriched in SERCA2a and SERCA1a. For enriched SERCA2a vesicles, V_{\max} was not altered by the PMA treatment. However, n_H was reduced by 14% and Ca_{50} was increased by 21% in enriched SERCA2a

Table 2.14: Effects of GFX, PMA or GFX + PMA on SERCA kinetic properties in homogenates from left ventricle and skeletal muscle of different fibre type composition.

	1400 nM GFX	500 nM PMA		1400 nM GFX + 500 nM PMA	
LV					
V_{max}	130 ± 7	128 ± 6		124 ± 7	
n_H	2.06 ± 0.09	1.81 ± 0.07	†	1.77 ± 0.05	†
Ca_{50}	1333 ± 42	1514 ± 57	†	1546 ± 39	†
SOL					
V_{max}	108 ± 10	111 ± 5		107 ± 7	
n_H	1.57 ± 0.07	1.30 ± 0.06	†	1.30 ± 0.07	†
Ca_{50}	682 ± 29	905 ± 45	†	890 ± 68	†
EDL					
V_{max}	755 ± 40	664 ± 35	†	660 ± 44	†
n_H	1.70 ± 0.06	1.12 ± 0.05	†	1.06 ± 0.03	†
Ca_{50}	870 ± 43	1895 ± 74	†	2099 ± 62	‡
WG					
V_{max}	591 ± 18	526 ± 23	†	525 ± 19	†
n_H	2.06 ± 0.06	1.73 ± 0.06	†	1.68 ± 0.09	†
Ca_{50}	636 ± 12	1197 ± 61	†	1172 ± 46	†
RG					
V_{max}	426 ± 13	391 ± 15	†	374 ± 14	†
n_H	2.10 ± 0.07	1.73 ± 0.08	†	1.73 ± 0.11	†
Ca_{50}	662 ± 34	1013 ± 62	†	1063 ± 82	†

Values are Means ± S.E. n=7. LV, left ventricle. SOL, soleus. EDL, extensor digitorum longus. WG, the white portion of the gastrocnemius. RG, the red portion of the gastrocnemius. GFX, GF-109203-XI is a protein kinase C (PKC) activator. PMA, phorbol-12-myristate-13-acetate is a PKC activator. V_{max} , maximal SERCA activity. n_H , hill slope defined as the relationship between SERCA activity and $[Ca^{2+}]_i$ for 10 to 90% V_{max} . Ca_{50} , the Ca^{2+} -concentration at ½ V_{max} . Units for V_{max} are nmol.mg⁻¹.min⁻¹. Units for n_H are arbitrary units. Units for Ca_{50} are nM. † - Significantly different from 1400 nM GFX (P<0.05). ‡ - Significantly different from 500 nM PMA (P<0.05).

Table 2.15: Effects of GFX or PMA on SERCA kinetic properties in purified SR vesicles prepared from left ventricle and the white portion of the gastrocnemius.

	Control	1400 nM GFX	500 nM PMA	
SERCA2a vesicles				
V_{\max}	915 ± 34	912 ± 29	896 ± 32	
n_H	1.49 ± 0.05	1.48 ± 0.09	1.28 ± 0.08	††
Ca_{50}	2216 ± 83	2286 ± 75	2679 ± 189	††
SERCA1a vesicles				
V_{\max}	11794 ± 313	11964 ± 293	9554 ± 340	††
n_H	1.53 ± 0.03	1.56 ± 0.05	1.06 ± 0.04	††
Ca_{50}	941 ± 54	1003 ± 79	1934 ± 30	††

Values are Means ± S.E. n=7. SERCA2a vesicles, purified SR vesicles enriched in SERCA2a were prepared using LV. SERCA1a vesicles, purified SR vesicles enriched in SERCA1a were prepared using WG. GFX, GF-109203-XI is a protein kinase C (PKC) activator. PMA, phorbol-12-myristate-13-acetate is a PKC activator. V_{\max} , maximal SERCA activity. n_H , hill slope defined as the relationship between SERCA activity and $[Ca^{2+}]_f$ for 10 to 90% V_{\max} . Ca_{50} , the Ca^{2+} -concentration at $\frac{1}{2} V_{\max}$. Units for V_{\max} are $nmol \cdot mg^{-1} \cdot min^{-1}$. Units for n_H are arbitrary units. Units for Ca_{50} are nM. † - Significantly different from control ($P < 0.05$). †† - Significantly different from 1400 nM GFX ($P < 0.05$).

vesicles when samples were treated with PMA. In contrast to enriched SERCA2a vesicles, PMA reduced V_{\max} by 19%, n_H by 30% and increased Ca_{50} by 106% in enriched SERCA1a vesicles.

Discussion

The present study characterized the effects of β -adrenergic, CaMKII and PKC signaling on SERCA kinetic properties in the LV and skeletal muscles of different fibre type composition in the rat. The results indicate that β -adrenergic, CaMKII and PKC signaling influence SERCA kinetic properties in a tissue-specific manner that is generally unique to each pathway. Our observations indicate that β -adrenergic signaling increases SERCA Ca^{2+} -sensitivity in the LV by a cAMP-dependent PKA-mediated mechanism and in the SOL by a cAMP-dependent mechanism that is not mediated by PKA. In contrast, β -adrenergic signaling did not alter kinetic properties in fast-twitch skeletal muscle. The activation of CaMKII signaling by a CaM-dependent mechanism reduced Ca_{50} , without altering V_{\max} , in the LV and did not alter SERCA kinetic properties in any other tissue. In contrast to β -adrenergic and CaMKII signaling, the activation of PKC by PMA reduced the V_{\max} of SERCA1a in EDL, WG and RG by ~15%, without altering V_{\max} in the LV or the SOL, and reduced SERCA Ca^{2+} -sensitivity in all tissues examined.

β -adrenergic regulation of SERCA kinetics

The observations made in this paper contribute to the growing body of evidence demonstrating that β -adrenergic signaling increases SERCA Ca^{2+} -sensitivity, without altering V_{\max} , in the LV and the SOL (Figure 2.5, Panel A and B). In contrast, β -adrenergic signaling

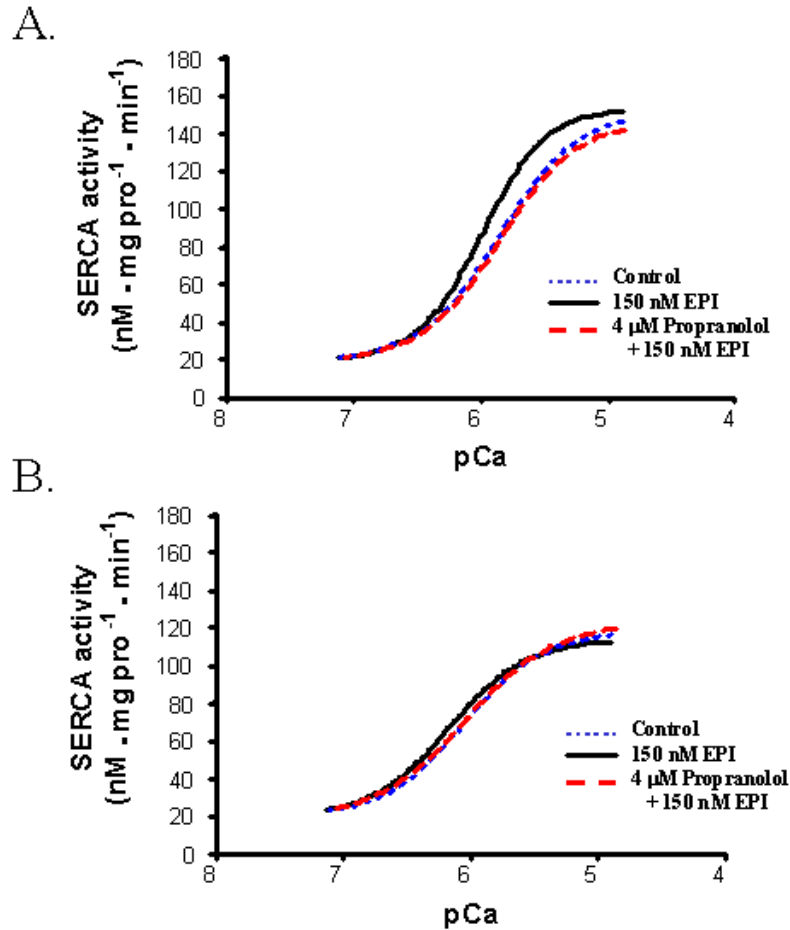


Figure 2.5: Panel A and B: Results from representative samples illustrating the relationship between SERCA activity and Ca^{2+} -concentration in left ventricle (LV) and soleus (SOL) homogenates following incubation with selected treatments targeting epinephrine, protein kinase A or cAMP-mediated processes. Effects of 150 nM epinephrine or 80 μM propranolol + 150 nM epinephrine on SERCA kinetics in LV (Panel A) and SOL (Panel B). Control, control samples that were incubated in the absence of any activators or inhibitors. Epinephrine is a β -adrenergic activator. Propranolol is a β -adrenergic inhibitor. Forskolin is a PKA activator. KT5720 is a PKA inhibitor. cAMP, adenosine 3',5'-cyclic monophosphate. pCa, is the negative logarithm of the Ca^{2+} concentration. V_{\max} , maximal SERCA activity. n_H , hill slope defined as the relationship between SERCA activity and Ca^{2+} for 10 to 90% V_{\max} . Ca_{50} , the Ca^{2+} -concentration at $\frac{1}{2} V_{\max}$. Refer to Table 2.5, Table 2.6 and Table 2.7 to view data represented by these curves.

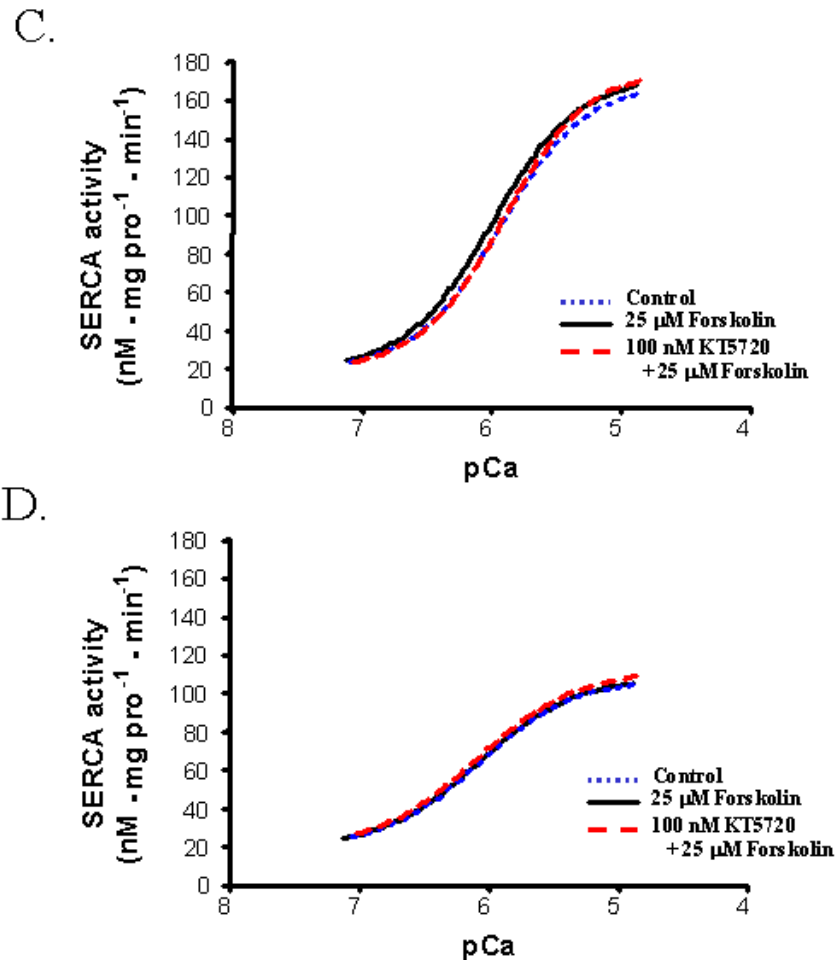
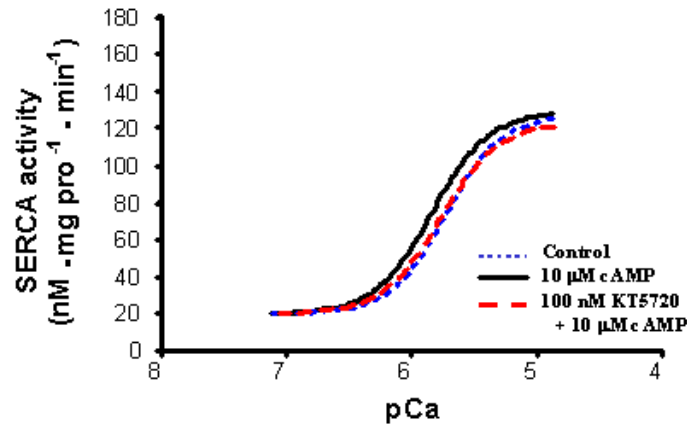


Figure 2.5: Panel C and D: Results from representative samples illustrating the relationship between SERCA activity and Ca^{2+} -concentration in left ventricle (LV) and soleus (SOL) homogenates following incubation with selected treatments targeting epinephrine, protein kinase A or cAMP-mediated processes. Effects of 25 μM Forskolin or 100 nM KT5720 + 25 μM Forskolin on SERCA kinetics in LV (Panel C) and SOL (Panel D). Control, control samples that were incubated in the absence of any activators or inhibitors. Epinephrine is a β -adrenergic activator. Propranolol is a β -adrenergic inhibitor. Forskolin is a PKA activator. KT5720 is a PKA inhibitor. cAMP, adenosine 3',5'-cyclic monophosphate. pCa, is the negative logarithm of the Ca^{2+} concentration. V_{max} , maximal SERCA activity. n_{H} , hill slope defined as the relationship between SERCA activity and $\text{Ca}^{2+}_{\text{f}}$ for 10 to 90% V_{max} . Ca_{50} , the Ca^{2+} -concentration at $\frac{1}{2} V_{\text{max}}$. Refer to Table 2.5, Table 2.6 and Table 2.7 to view data represented by these curves.

E.



F.

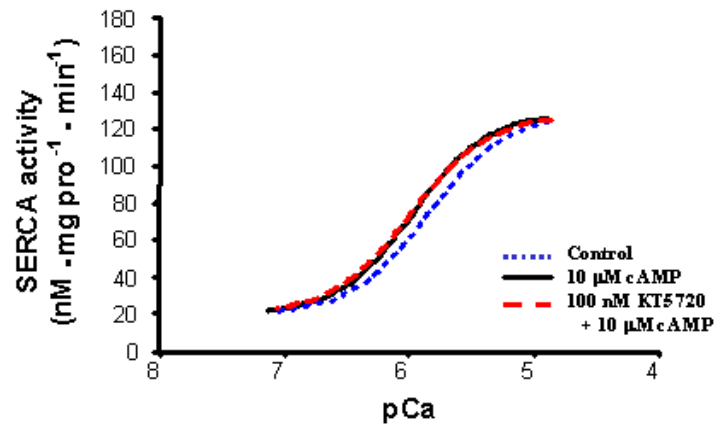


Figure 2.5: Panel E and F: Results from representative samples illustrating the relationship between SERCA activity and Ca^{2+} -concentration in left ventricle (LV) and soleus (SOL) homogenates following incubation with selected treatments targeting epinephrine, protein kinase A or cAMP-mediated processes. Effects of $10 \mu\text{M}$ cAMP or 100 nM KT5720 + $10 \mu\text{M}$ cAMP or 100 nM KT5720 + $10 \mu\text{M}$ cAMP on SERCA kinetics in LV (Panel E) and SOL (Panel F). Control, control samples that were incubated in the absence of any activators or inhibitors. Epinephrine is a β -adrenergic activator. Propranolol is a β -adrenergic inhibitor. Forskolin is a PKA activator. KT5720 is a PKA inhibitor. cAMP, adenosine 3',5'-cyclic monophosphate. pCa, is the negative logarithm of the Ca^{2+} concentration. V_{max} , maximal SERCA activity. n_H , hill slope defined as the relationship between SERCA activity and Ca^{2+} for 10 to 90% V_{max} . Ca_{50} , the Ca^{2+} -concentration at $\frac{1}{2} V_{\text{max}}$. Refer to Table 2.5, Table 2.6 and Table 2.7 to view data represented by these curves.

did not alter any of the SERCA kinetic properties assessed in EDL, RG or WG, which are all classified as fast-twitch skeletal muscles based on contractile speed and myosin heavy chain composition (Delp & Duan, 1996). It is possible that this tissue-specific effect may be attributed to the SERCA2a isoform expression in the LV and SOL, compared to the fast-twitch skeletal muscles that predominately express the SERCA1a isoform. On the other hand, the tissue-specific effect may not be fully explained by SERCA isoform expression in different tissues since the SOL expresses both SERCA2a and SERCA1a protein isoforms; whereas, the LV expresses only SERCA2a. Therefore, based on the mixed SERCA isoform composition of the SOL, it is difficult to determine if the EPI-induced changes in this tissue occur as a result of changes in the Ca^{2+} -sensitivity of the SERCA2a or SERCA1a isoform specifically, or if they occur as a result of changes in the Ca^{2+} -sensitivity of both isoforms in the SOL.

Epinephrine activates a series of intracellular signaling pathways known to influence protein function through phosphorylation-mediated processes. Phospholamban is one target protein that is regulated by β -adrenergic signaling via cAMP-dependent PKA phosphorylation (MacLennan *et al.*, 2003). Phosphorylation of PLN reduces the interaction of SERCA with PLN, thereby reducing Ca_{50} (Asahi *et al.*, 2002). This regulatory mechanism is actively involved in the regulation of SERCA Ca^{2+} -sensitivity in the LV (Asahi *et al.*, 2002) and is the most likely mechanism underlying the EPI-induced Ca^{2+} -sensitivity changes observed in the current study. In contrast, this mechanism cannot explain the EPI-induced changes in SERCA Ca^{2+} -sensitivity in the SOL since PLN protein was not detected by Western blot techniques in this tissue or any of the other skeletal muscles examined, which is consistent with previous results (Damiani *et al.*, 2000; Vangheluwe *et al.*, 2005). Therefore, it is apparent that another pathway that is activated by EPI is involved in the regulation of Ca_{50} in SOL.

Sarcolipin, which is similar to PLN in structure and function (Asahi *et al.*, 2002; Odermatt *et al.*, 1998), is expressed in the atria and skeletal muscle (Vangheluwe *et al.*, 2005). The regulation of SERCA Ca^{2+} -sensitivity by SLN in response to β -adrenergic signaling is analogous to that of PLN. However, in contrast to the PKA-mediated phosphorylation of PLN, an STK16-mediated phosphorylation-process regulates the inhibitory effects of SLN on SERCA activity at submaximal Ca^{2+}_f (Gramolini *et al.*, 2006). Based on the known regulatory role that SLN has on SERCA kinetic properties in isolated NF-SLN/PLN KO cardiomyocytes (Gramolini *et al.*, 2006) and in cardiac (Asahi *et al.*, 2002) and skeletal muscle (Odermatt *et al.*, 1998; Tupling *et al.*, 2002), it is likely that this protein may be contributing to the EPI-induced changes in Ca_{50} observed in the SOL. Although we would have liked to assess SLN protein content in the tissues examined in this study, it was not possible since an antibody for SLN was not commercially available. Therefore, a limitation of this study was our inability to directly determine if SLN was responsible for the observed EPI-induced changes in SERCA Ca^{2+} -sensitivity observed. However, the literature (Vangheluwe *et al.*, 2005) does indicate that SLN mRNA and protein is expressed at low levels in the SOL but is absent in the LV or the EDL of the rat (Vangheluwe *et al.*, 2005). If correct, such a SLN protein expression pattern would be consistent with the observations made in the current study.

Since we could not secure an antibody to detect SLN, we attempted to characterize the tissue-specific expression of STK16, which is a signaling protein that lies upstream of SLN and is known to increase SLN phosphorylation in response to β -adrenergic stimulation (Gramolini *et al.*, 2006). Our Western blot data indicated that STK16 protein was expressed in the LV and also in all of the skeletal muscles analyzed. These data support previous research indicating that STK16 mRNA is expressed in cardiac and skeletal muscle (Ligos *et al.*, 1998; Ohta *et al.*,

2000). Although STK16 influences SLN-phosphorylation *in vitro* (Gramolini *et al.*, 2006), the physiological function of STK16 and its effectiveness to influence SLN-phosphorylation has not yet been evaluated in cardiac or skeletal muscle.

Since β -adrenergic stimulation increases phosphorylation of PLN and SLN by activating the cAMP-dependent PKA and the cAMP-dependent STK16 pathways, respectively, several different treatment conditions were necessary to isolate the PKA-dependent from the PKA-independent signaling processes involved in the acute regulation of SERCA. To identify the PKA-dependent changes in Ca_{50} for the LV and SOL, samples were incubated in the presence of the PKA activator forskolin and also with a combination of the PKA inhibitor KT5720 plus forskolin. Our data indicated that forskolin reduced Ca_{50} , without altering V_{max} or n_H , in the LV (Figure 2.5, Panel C). In contrast, forskolin was without an effect in the SOL (Figure 2.5, Panel D). These data support the hypothesis that PKA signaling contributes to the regulation of SERCA kinetic properties in the LV but not the SOL. This tissue-specific effect may be explained, at least in part, by the expression of PLN protein, which is present in the LV but not in the SOL or fast-twitch skeletal muscles of the rat (Damiani *et al.*, 2000; Vangheluwe *et al.*, 2005). The results using isolated SR vesicles, enriched in SERCA2a, reinforces the hypothesis that PKA-mediated signaling is acting to influence SERCA Ca^{2+} -sensitivity since Ca_{50} was increased in the presence of forskolin and also in the presence of an activated form of the PKA catalytic subunit (i.e. A-PKA). Since our Western blot data indicated that enriched SERCA2a vesicles prepared from LV tissue contained PLN, it is likely that PKA-mediated PLN phosphorylation was responsible for the observed reduction in Ca_{50} in response to forskolin and A-PKA. In contrast to enriched SERCA2a vesicles, enriched SERCA1a vesicles prepared from WG, which did not contain PLN, did not respond to PKA activation by forskolin or A-PKA.

Since PKA-dependent signaling did not alter Ca_{50} in the SOL, a series of treatments were designed to determine if the tissue-specific regulation of Ca_{50} in the SOL was influenced by a cAMP-dependent mechanism. To achieve this objective, samples were incubated in the presence of cAMP. Samples were also incubated with a combination of cAMP + PKA inhibitor KT5720 to determine if the response to cAMP would be modified by the inhibition of PKA, which would indicate that a non-PKA dependent-mechanism was involved. The rationale for these treatments was based on the knowledge of the tissue-specific protein expression patterns for PLN and SLN in the LV and SOL, respectively. Additionally, cAMP acutely influences SERCA kinetic properties by activating PKA and STK16-mediated phosphorylation processes for PLN and SLN, respectively (Gramolini *et al.*, 2006). Therefore, by isolating the PKA-dependent and the PKA-independent effects of cAMP, it may be possible to isolate the contribution of PKA and STK16 to the regulation of SERCA Ca^{2+} -sensitivity in the LV and SOL, respectively.

As expected, cAMP reduced Ca_{50} in both the LV and the SOL (Figure 2.5, Panel E and F). Although the combined cAMP + KT5720 treatment did not alter SERCA kinetic properties in the LV or any of the fast-twitch skeletal muscles, it did reduce Ca_{50} in the SOL. Collectively, these data suggest that SERCA Ca^{2+} -sensitivity in the LV is regulated by a cAMP-dependent PKA-mediated mechanism; whereas in the SOL a cAMP-dependent mechanism that is not mediated by PKA signaling is influencing SERCA Ca^{2+} -sensitivity. These data support the notion that SLN may regulate SERCA kinetic properties in skeletal muscle (Odermatt *et al.*, 1998), which would be consistent with the known SLN mRNA and protein expression for the LV and SOL in the rat (Vangheluwe *et al.*, 2005). Nonetheless, the interpretation of these data should be put into perspective given our inability to assess the tissue-specific expression of

SLN protein. Additionally, our data does not rule out the possibility that protein kinases that do not include PKA or STK16, or proteins other than SLN, influenced the observed changes in SERCA Ca^{2+} -sensitivity that occurred in response to cAMP-activation in the SOL. Even so, based on our observations demonstrating the effectiveness of EPI and cAMP, but not forskolin, to increase SERCA Ca^{2+} -sensitivity in the SOL, in combination with the reported expression of SLN (Vangheluwe *et al.*, 2005) and STK16 protein in this tissue, it is likely that STK16-mediated SLN-phosphorylation processes are contributing, at least in part, to the regulation of SERCA Ca^{2+} -sensitivity observed in the SOL.

Sarcoplipin was originally proposed to be a regulator of SERCA1a function in fast-twitch skeletal muscle of the human and the rabbit (Odermatt *et al.*, 1998). Therefore, it was unexpected that the EPI- and cAMP-treatments did not alter SERCA kinetic properties in the fast-twitch skeletal muscles. However, in contrast to other species, the expression of SLN protein in the rat appears to be limited to the atria and the slow-twitch skeletal muscles and is not expressed in the LV or the fast-twitch skeletal muscles (Vangheluwe *et al.*, 2005). Phospholamban is also not expressed in the skeletal muscles of the rat. Therefore, of the two proteins known to regulate SERCA Ca^{2+} -sensitivity in response to β -adrenergic signaling, it appears that neither PLN nor SLN are expressed in the EDL, WG or RG muscles of the rat, which could account for absence of an effect of EPI and cAMP on SERCA kinetic properties in the fast-twitch skeletal muscles.

Ca²⁺-dependent calmodulin kinase II regulation of SERCA kinetics

The main findings of the CaMKII signaling experiments conducted in this study indicate that a CaM-dependent mechanism reduced Ca_{50} , without altering V_{max} or n_{H} in the LV (Figure

2.6). In contrast, CaM-treatment did not alter SERCA kinetic properties in the SOL or the fast-twitch skeletal muscles. In general, our data are consistent with previous research demonstrating that CaMKII increases the Ca^{2+} -sensitivity of SERCA2a, which most likely occurs as a result of CaMKII-mediated PLN phosphorylation in the LV (Hawkins *et al.*, 1994; Hawkins *et al.*, 1995; Odermatt *et al.*, 1996; Xu & Narayanan, 2000) and that CaMKII does not alter SERCA kinetic properties in fast-twitch skeletal muscle (Hawkins *et al.*, 1994; Xu & Narayanan, 2000). Our data do not support previous reports that have indicated that: 1) CaMKII-activation increases the Ca^{2+} -sensitivity of SERCA in the SOL (Hawkins *et al.*, 1995); and 2) CaMKII-activation increases the V_{\max} of SERCA2a in cardiac and slow-twitch skeletal muscles (Hawkins *et al.*, 1994; Hawkins *et al.*, 1995; Xu & Narayanan, 2000).

Species differences between the current study, in which used rats, and the studies completed by the Narayanan laboratory (Hawkins *et al.*, 1994; Hawkins *et al.*, 1995; Xu & Narayanan, 2000), which used rabbits, most likely account for the different results obtained with respect to Ca_{50} since PLN protein is not expressed in rat SOL, but is expressed in this tissue in the rabbit (Damiani *et al.*, 2000; Vangheluwe *et al.*, 2005). The tissue specific changes in SERCA Ca^{2+} -sensitivity observed in the current study are also most likely explained by the tissue expression of PLN in the rat since this protein is expressed in the LV, but not the SOL or the fast-twitch skeletal muscles of the rat.

It is still controversial (Odermatt *et al.*, 1996; Xu & Narayanan, 2000) whether CaMKII can increase the V_{\max} of SERCA2a by directly phosphorylating Ser38 within the enzyme (Hawkins *et al.*, 1994). However, this possibility appears to be strongly supported by evidence that indicates that a CaM binding peptide can reduce the V_{\max} and relative level of SERCA2a Ser38 phosphorylation in rabbit cardiac tissue (Xu & Narayanan, 2000). Nonetheless, our data

does not support this possibility since CaMKII did not alter V_{\max} in crude muscle homogenates or enriched SERCA2a vesicles prepared from the LV. Our data does support the findings of Odermatt *et al.* (Odermatt *et al.*, 1996) showing no effect of CaM on the V_{\max} of SERCA2a. It is possible that methodological differences between studies can account for the contradictory observations made regarding the effects of CaM on V_{\max} . Odermatt *et al.* (Odermatt *et al.*, 1996) used a HEK-293 cell line that expressed the rabbit SERCA2a clone; whereas, the Narayanan laboratory (Hawkins *et al.*, 1994; Hawkins *et al.*, 1995; Xu & Narayanan, 2000) used isolated SR vesicles enriched in SERCA2a, prepared from the rabbit heart. Based on the known differences in SR protein expression and regulation between the rat and the rabbit (Damiani *et al.*, 2000; Vangheluwe *et al.*, 2005), it is likely that species differences contributed to the observed lack of CaM-dependent changes in SERCA2a V_{\max} .

In order to determine if the tissue-specific changes in SERCA Ca^{2+} -sensitivity were influenced by the expression of different CaMKII isoforms (i.e. α , β , δ and γ) between the LV and the skeletal muscles, we characterized the subunit composition pattern of CaMKII by Western blot techniques. As expected, the expression pattern of the various CaMKII isoforms was different between the LV and the skeletal muscles sampled. Specifically, our data indicated that CaMKII β was the major isoform expressed in both the LV and the skeletal muscles, with the expression of this subunit being higher in the LV compared to the skeletal muscles. This expression pattern is consistent with the proposed coordinated expression of CaMKII β with SERCA2a in cardiac and slow-twitch muscle (Sacchetto *et al.*, 2000). Our data also indicated that CaMKII α protein expression is low in the LV and the SOL but is significantly higher in the fast-twitch skeletal muscles. Given these differences in CaMKII isoform expression between tissues, it is possible that our results can be explained by differences in CaMKII α and

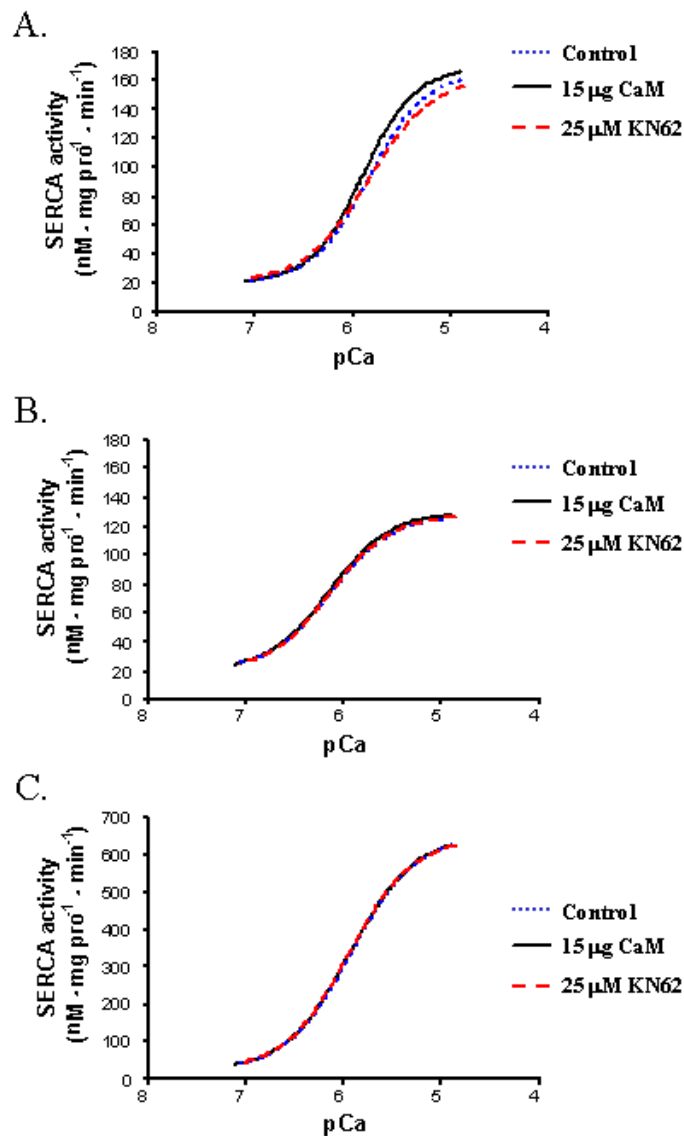


Figure 2.6: Results from representative samples illustrating the relationship between SERCA activity and Ca²⁺-concentration in left ventricle (LV), soleus (SOL) and white gastrocnemius (WG) homogenates following incubation with 15 μg calmodulin (CaM) or 4 μM KN62. Panel A. LV. Panel B. SOL. Panel C. WG. Control, control samples that were incubated in the absence of any activators or inhibitors. KN62 is a CaMKII inhibitor. pCa, is the negative logarithm of the Ca²⁺ concentration. V_{max} , maximal SERCA activity. n_H , hill slope defined as the relationship between SERCA activity and Ca²⁺ for 10 to 90% V_{max} . Ca_{50} , the Ca²⁺-concentration at $\frac{1}{2} V_{max}$. Refer to Table 2.10 to view data represented by these curves.

β subunits. Further research is needed to identify if the various CaMKII isoforms differentially influence SERCA kinetic properties in the LV and skeletal muscles.

PKC regulation of SERCA kinetics

The main findings of the PKC signaling experiments indicate that the synthetic phorbol ester PMA negatively influenced SERCA kinetic properties in all tissues examined. Although PMA did not alter V_{\max} in the LV or SOL, it did reduce V_{\max} in the EDL, WG, and RG (Figure 2.7). In addition, PMA depressed SERCA Ca^{2+} -sensitivity, as indicated by a lower n_H and higher Ca_{50} , in all tissues examined.

Protein kinase C is expressed in many tissues (Nishizuka, 1986) and it is generally accepted that PKC signaling activates several intracellular processes that activate negative inotropic pathways in the heart and reduce contractility in skeletal muscle (Capogrossi *et al.*, 1990; Nicolas *et al.*, 1998; Rogers *et al.*, 1990). Our data supports the data of Rogers *et al.* (Rogers *et al.*, 1990) and indicate that phorbol esters reduce SR Ca^{2+} -transport kinetics in cardiac tissue. In contrast to Rogers *et al.* (Rogers *et al.*, 1990), who found that phorbol esters were without effect on Ca_{50} , our data demonstrate that PMA increased Ca_{50} in all tissues examined. Methodological differences between studies most likely account for the contradictory observations made in the previous study (Rogers *et al.*, 1990) and the current study. For example, our data were collected using crude muscle homogenates and enriched SR vesicles prepared from the adult rat LV and skeletal muscles; whereas Rogers *et al.* (Rogers *et al.*, 1990) utilized rat neonatal cardiomyocytes. This distinction is significant because neonatal cardiomyocytes contain significantly lower quantities of SR protein compared to adult cardiomyocytes. In addition, SERCA proteins are developmentally regulated, which may

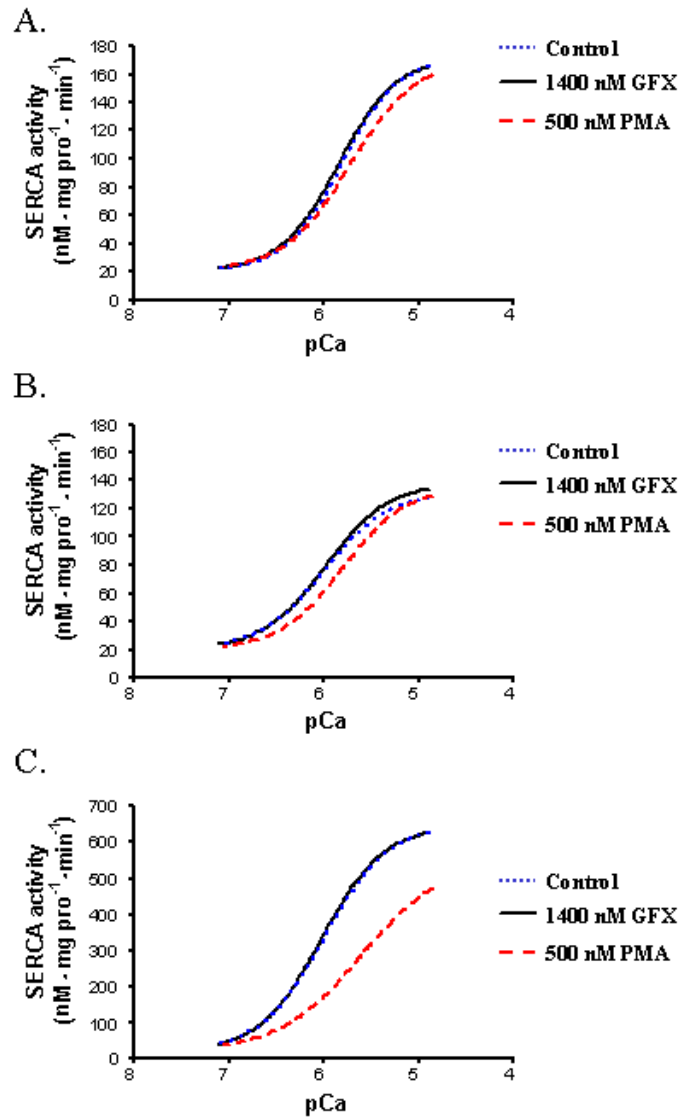


Figure 2.7: Results from representative samples illustrating the relationship between SERCA activity and Ca^{2+} -concentration in left ventricle (LV), soleus (SOL) and white gastrocnemius (WG) homogenates following incubation with 1400 nM GFX or 500 nM PMA. Panel A. LV. Panel B. SOL. Panel C. WG. Control, control samples that were incubated in the absence of any activators or inhibitors. GFX, GF-109203-XI is a PKC inhibitor. PMA, phorbol-12-myristate-13-acetate is a PKC activator. pCa, is the negative logarithm of the Ca^{2+} concentration. V_{\max} , maximal SERCA activity. n_H , hill slope defined as the relationship between SERCA activity and Ca^{2+}_f for 10 to 90% V_{\max} . Ca_{50} , the Ca^{2+} -concentration at $\frac{1}{2} V_{\max}$. Refer to Table 2.13 to view data represented by these curves.

account for the different responses observed between studies since the Ca_{50} of SERCA isoforms are different (Lytton *et al.*, 1992). Differences in the analytical techniques used to characterize Ca^{2+} -transport kinetics also may have contributed to the differences between studies. We have used a spectrophotometric assay to determine the hydrolytic activity of SERCA at 15 different Ca^{2+}_f ; whereas, Rogers *et al.* (Rogers *et al.*, 1990) used a $^{45}Ca^{2+}$ -transport assay to assess Ca^{2+} -transport kinetics into cardiomyocytes at 7 different Ca^{2+}_f . In addition, we have calculated Ca_{50} based on the relationship between Ca^{2+}_f and SERCA activity over a range of 0 to 100% V_{max} ; whereas it was unclear how Rogers *et al.* (Rogers *et al.*, 1990) calculated this parameter. Based on these methodical differences, it is likely that our assessment techniques may be better suited to detect changes in Ca^{2+} -sensitivity.

Rogers *et al.* (Rogers *et al.*, 1990) have reported that two different phorbol esters (i.e. PDBu and TPA) effectively reduce SR Ca^{2+} -uptake rates into cardiomyocytes, as assessed by $^{45}Ca^{2+}$ -transport assay; whereas, the biologically inactivated forms of these phorbol esters (i.e. α -PDBu, and α -TPA) did not alter SR Ca^{2+} -uptake rates. Moreover, the inhibition of PKC signaling prior to addition of the phorbol esters to the cardiomyocytes prevented the phorbol-induced reductions in SR Ca^{2+} -transport. Collectively, these data indicate that SR Ca^{2+} -transport rates are reduced by phorbol esters and that the effects are mediated through PKC-dependent signaling pathways.

A limitation of the current study was the inability to determine if the PMA-dependent changes in n_H and Ca_{50} were mediated through a PKC dependent mechanism. We attempted to establish that the PMA-induced changes in SERCA kinetic properties occurred as a result of PKC-dependent signaling by incubating samples in the presence of the PKC inhibitor GFX. However, GFX did not prevent the PMA-dependent effects. In addition, we did not characterize

SERCA kinetic properties in the presence of a different PKC inhibitor or in the presence of the biologically inactivated form of PMA, which would have been beneficial since it would have established that the PMA was not directly responsible for the observed effects. Therefore, since GFX did not block the PMA-induced changes in SERCA kinetic properties in the current study, we cannot discount the possibility that the PMA-induced effects occurred independent of PKC signaling.

Although our data clearly indicated that PMA negatively influenced SERCA kinetic properties in all tissues examined, it is not yet clear what mechanism(s) are mediating this effect. Moreover, it is not clear why V_{\max} was not reduced by PMA in the LV and SOL, but was reduced in the fast twitch skeletal muscles examined. It is possible that differences in SERCA isoform expression may have contributed to the tissue-specific responses. This possibility is supported by our observations indicating that PMA did not alter the V_{\max} of enriched SR vesicles containing SERCA2a prepared from LV, but that it did reduce the V_{\max} of enriched SR vesicles containing SERCA1a prepared from WG. However, our data does not rule out the possibility that proteins other than SERCA may have contributed to the tissue-specific responses observed. As an example, it has been demonstrated phorbol esters also influence the regulation of skeletal muscle glucose transport in a fibre-type specific manner (Wright *et al.*, 2004).

The regulation of SERCA Ca^{2+} -sensitivity in the LV is usually attributed to the regulation of PLN phosphorylation mechanisms or to changes in phospholamban pentamer: monomer ratio. Given that SERCA Ca^{2+} -sensitivity was adversely affected in the LV, it is likely that PLN phosphorylation was attenuated in response to PMA-treatment. Indeed, this possibility does exist since PKC signaling is known to activate PP1 and PP2a (Liu & Brautigan, 2000; Ragolia

& Begum, 1997). Activation of PP1 and PP2 would reduce PLN-phosphorylation and would decrease SERCA Ca^{2+} -sensitivity in the LV. Since PKC increases the phosphorylation of PLN on Ser10 (Tada *et al.*, 1983; Iwasa & Hosey, 1984; Movsesian *et al.*, 1984) *in vitro*, it is also possible that this site-specific phosphorylation process may have contributed to the observed reduction in SERCA Ca^{2+} -sensitivity. However, the physiological significance of PLN-Ser10 phosphorylation is still controversial since it is known that this process may not occur in response to acute stimuli *in vivo* (Wegener *et al.*, 1989). The changes in Ca_{50} in the LV might also be associated with changes in PLN pentamer: monomer ratio since an increase in PKC signaling may contribute to the formation of PLN monomers by altering phospholipid metabolism in membrane structures (Zhang *et al.*, 2005). Although it would have been of value to characterize the proposed PLN mechanisms described here in LV tissue, it is important to note that PMA also adversely affected SERCA kinetic properties in tissues that do not express PLN (i.e. SOL, EDL, WG and RG). Based on this observation, we did not assess PLN phosphorylation or PLN pentamer:monomer ratio in this study. Nonetheless, it is apparent that further research is needed to identify the PKC-dependent mechanisms that regulate SERCA kinetic properties in the LV and skeletal muscles.

Limitations

The results of this paper need to be put into perspective given the limitations of the experimental design. To assess the role of β -adrenergic, CaMKII and PKC signaling on the regulation of SERCA kinetic properties, samples were incubated *in vitro* in the presence and absence of various signaling pathway activators and/or inhibitors. This experimental approach assumed that the treatment conditions and concentrations selected would effectively activate

the targeted pathway through the *in vivo* signaling cascade. For example, by incubating tissue samples in the presence of EPI, it was assumed that the β -receptor signaling cascade was intact. As it turned out, this approach appears to have been successful since propranolol prevented the EPI-induced changes in Ca_{50} in the LV and SOL. In addition, the observation that Ca_{50} was altered in a similar manner by the cAMP-, forskolin-, A-PKA- and EPI-treatments supports the notion that the β -receptor signaling cascade was viable since these treatments influenced different aspects within the β -receptor signaling cascade. The utilization of a combination of pathway inhibitors and activators also supports the notion that our treatments were specific to the targeted pathways since propranolol, KT5720 and KN52 prevented the EPI-, forskolin-, and CaM-induced changes in Ca_{50} observed in the LV. In contrast, the inability of GFX to block the PMA-dependent changes in V_{max} , n_H and Ca_{50} limits the interpretation of our data since we cannot conclude that the effects of PMA were mediated through a PKC-dependent mechanism.

Another important issue that needs to be addressed is the amount of variability between similar treatments that were repeated and reported in different tables within this study. The major factor contributing to the variability between similar treatments was caused by the assessment of different samples (i.e. between sample variability) for each table plus analytical variability. The values presented on each table represent samples that were assayed using repeated measurements to determine treatment effects from a total of 7 different samples. In fact, a different group of 7 samples was used to generate the data for each data table (e.g. Table 2.4 used samples #1 to #7; whereas, Table 2.5 used samples #8 to #14). Although it would have been beneficial to analyze the same samples with each treatment, tissue limitations restricted the number of repeated measures that could be assessed. As a result of these tissue

limitations, a decision was made to characterize treatment effects by repeated measures to limit the amount of variability for this comparison in our experimental design.

Although our data indicate that treatments effects are generally consistent for V_{\max} and Ca_{50} between days, several discrepancies do exist for n_H . For example, it is not clear why Table 2.4 indicates that EPI increased n_H by ~17% in the EDL when this effect was not observed in Table 2.5. Moreover, it is not clear why EPI did not influence n_H in the LV on Table 2.4 but increased n_H by 22% on Table 2.5. In general, n_H in the LV were higher in the presence of CaM compared to KN62. However, it is not clear why n_H was not altered by the CaM treatment, compared to Control, in the LV (Table 2.10). Moreover, it was unexpected that n_H were ~10% lower in the presence of KN62 compared to both the Control and CaM treatment for the RG on Table 2.10. This effect of KN62 for the RG was not observed on Table 2.11. The ~10% higher n_H in the SOL on Table 2.11 was also unexpected since CaM was without effect on this property on Table 2.10. The lack of an effect of PMA on n_H in the SOL on Table 2.13 was unexpected since PMA reduced this property in all other muscles and reduced n_H by ~17% in this tissue on Table 2.14. Our data also indicate that the forskolin, cAMP and CaM treatments also created some discrepancies with respect to n_H since this treatment was without effect in the LV homogenates but increased n_H by 9, 20 and 20%, respectively, in SR vesicles enriched in SERCA2a. It is possible that the discrepancies could be explained by the different muscle homogenate samples used to generate the data for each table and by the protocol used to isolate SR vesicles from tissue homogenates. For example, differences in the level of stress (i.e. increased β -adrenergic signaling) between animals existed at the time of tissue sampling, which theoretically could alter the background activation of the various pathways examined and would alter the response of the tissue to treatment *in vitro*.

The majority of discrepancies in our data involve the n_H . It is possible that the analytical methods used to measure n_H and Ca_{50} contributed to tendencies for this property to respond variably. For example, although n_H and Ca_{50} values have been calculated using a non-linear regression curve fit and the dose-response relationship that is characterized by *Equation 2.1*, these properties are calculated using different segments of the substrate-activity curve. Specifically, n_H is calculated using the data representing 10 to 90% V_{max} ; whereas Ca_{50} is calculated for 0 to 100% V_{max} . This measurement difference is utilized to minimize the amount of error when calculating n_H since the extreme ends of the activity curve tend to contain a large amount of variability that may influence the slope describing the pCa-activity relationship representing the co-operative binding properties of the SERCA (Simonides & van Hardeveld, 1990). As a result, it is possible that calculation differences contributed to the sensitivity of each property to change in response to small differences in the pCa-activity relationship. However, it is unlikely that this analytical difference could account for the discrepancies in n_H observed in our data between repeated treatments.

Summary

In summary, this is the first comprehensive study that has attempted to characterize the influence that β -adrenergic, CaMKII, and PKC signaling pathways have on the regulation of SERCA kinetic properties in the LV and in skeletal muscle of different oxidative potential and fibre type composition in the rat. Our results demonstrate that β -adrenergic, CaMKII and PKC signaling alter the kinetic properties of SERCA proteins in cardiac and skeletal muscles. In addition, the effects that each pathway exerts on regulation of SERCA kinetic properties appear to be tissue specific and unique to each pathway. As such, this study should serve as a catalyst

for future research designed to systematically isolate the potential mechanisms and proteins that might be involved in the regulation of SERCA kinetic properties in the various tissues.

CHAPTER THREE

INSULIN SIGNALING INCREASES THE Ca²⁺-SENSITIVITY OF SERCA PROTEINS IN CARDIAC AND SKELETAL MUSCLE

TA DUHAMEL, HJ GREEN and J OUYANG.

Department of Kinesiology, University of Waterloo,

Waterloo, Ontario, Canada, N2L 3G1

Short Title: Insulin regulation of SERCA.

Abstract

This study investigated the hypothesis that insulin (INS) signaling acutely regulates SERCA kinetic properties in cardiac and skeletal muscle. Crude muscle homogenates were prepared from soleus (SOL), extensor digitorum longus (EDL), the red portion of gastrocnemius (RG), the white portion of gastrocnemius (WG) and the left ventricle (LV) from a group of 28 male Sprague-Dawley rats (9 weeks of age; mass = 280 ± 4 g). Purified SR vesicles enriched in sarco(endo)plasmic reticulum Ca^{2+} -ATPase (SERCA) 1a and SERCA2a were prepared using crude muscle homogenates from WG and LV, respectively. Samples were incubated *in vitro* for 10 min with 100 nM insulin (INS), 80 μM AGL 2263, 100 nM INS + 80 μM AGL 2263, or 30 ng of a commercially available activated form of the insulin receptor (A-INS-R). After incubation, samples were assayed spectrophotometrically to characterize three kinetic properties, namely, maximal activity (V_{max}), Hill coefficient (n_{H}), which is defined as the relationship between SERCA activity and $\text{Ca}^{2+}_{\text{f}}$ for 10 to 90% V_{max} and is an indication of the co-operative binding behaviour of SERCA for Ca^{2+} , and Ca_{50} , which is defined as the $\text{Ca}^{2+}_{\text{f}}$ required to activate the enzyme to 50% V_{max} . Compared to controls, 100 nM INS and A-INS-R did not alter V_{max} but increased ($P < 0.05$) SERCA Ca^{2+} -sensitivity, as indicated by an increased n_{H} and reduced Ca_{50} in both crude muscle homogenates and enriched SR vesicles. Co-immunoprecipitation experiments indicated that both 100 nM INS and 30 ng A-INS-R signaling promoted the physical interaction of insulin receptor substrates (IRS)-1 and 2 with SERCA in crude muscle homogenates from WG and LV tissues. Changes in Ca_{50} and n_{H} cannot be explained by alterations to the SERCA nucleotide or Ca^{2+} -binding domain since fluorescein isothiocyanate (FITC) and N-cyclohexyl-N'-(dimethylamino- α -naphthyl) carbodiimide (NCD-4) binding capacity were not altered when samples were incubated with

100 nM INS or 30 ng A-INS-R. Changes in SERCA Ca^{2+} -sensitivity also cannot be explained by changes in phospholamban pentamer: monomer ratio, or by changes to Ser16 or Thr17 phosphorylation within phospholamban since these properties were not altered by INS or by A-INS-R. Collectively, these results indicate that insulin signaling promotes the binding of IRS with SERCA proteins in cardiac and skeletal muscle, which may contribute, at least in part, to the observed increases in SERCA Ca^{2+} -sensitivity in this study.

Introduction

Sarco(endoplasmic reticulum Ca^{2+} -ATPase (SERCA) proteins are involved in the regulation of intracellular free Ca^{2+} -concentrations (Ca^{2+}_f) by sequestering cytosolic Ca^{2+} into lumen of the sarcoplasmic reticulum (SR) (MacLennan *et al.*, 1997). Although SERCA proteins are ubiquitously expressed in all tissues, the abundance and isoform type depend on the type of tissue. In skeletal muscle, SERCA1a is primarily expressed in fast-twitch skeletal muscle; whereas cardiac and slow-twitch skeletal muscles are known to express large amounts of SERCA2a (Wu & Lytton, 1993). This muscle specific expression pattern suggests that these isoforms are specialized for demands related to the contractile properties of the cell. The regulation of intracellular Ca^{2+}_f -transients during contractile activity by SERCA is accomplished by intracellular signaling pathways and endogenous modulators that regulate the functional parameters of the enzyme, such as maximal enzyme activity (V_{\max}) or the sensitivity of the enzyme for Ca^{2+} , which can be characterized by the Hill coefficient (n_H), defined as the relationship between SERCA activity and Ca^{2+}_f for 10 to 90% V_{\max} , and the Ca_{50} , defined as the Ca^{2+}_f required to activate the enzyme to 50% V_{\max} .

Phospholamban (PLN) and sarcolipin (SLN) are recognized as key regulators of SERCA function and muscle contractility (Gramolini *et al.*, 2006). In the rat, PLN is predominately expressed in cardiac but not skeletal muscle (Damiani *et al.*, 2000), whereas SLN is primarily expressed in the atria and in skeletal muscle (Damiani *et al.*, 2000). These proteins inhibit SERCA Ca^{2+} -sensitivity by directly interacting with SERCA in their unphosphorylated forms. Phosphorylation of PLN and SLN by protein kinases promotes the dissociation of PLN and SLN from SERCA and enhances muscle relaxation and contractility by restoring SERCA Ca^{2+} -

sensitivity and increasing the rate of Ca^{2+} -sequestration into the SR at submaximal Ca^{2+}_f (Kranias, 1985; Wegener *et al.*, 1989).

Increasing evidence (James *et al.*, 1989; Hartell *et al.*, 2005) indicates that insulin signaling regulates a variety of cellular process associated with energy metabolism, substrate utilization and storage, muscle contractility, protein expression and nitric oxide production. Binding of insulin (INS) to the insulin receptor results in an up-regulation of insulin tyrosine kinase (INS-TK) activity, which initiates the insulin signaling cascade by phosphorylating various insulin receptor substrate (IRS) proteins (Cheatham & Kahn, 1995; Sun *et al.*, 1991; Sun *et al.*, 1995). Proteins in the IRS family (e.g. IRS-1 and IRS-2) play critical roles in insulin signaling since they are known to regulate the functional properties of target proteins by directly binding to regions that contain SH2 (src homology 2) domains (White & Kahn, 1994; Korn *et al.*, 1987; Yamauchi *et al.*, 1995). For example, binding of IRS proteins to phosphatidyl inositol 3 kinase (PI3K) is known to result in the translocation of glucose transporters (i.e. Glut-4) to the sarcolemmal membrane and to acutely regulate glycogen synthase activity within muscle (Cheatham & Kahn, 1995; White & Kahn, 1994).

Insulin receptor substrate proteins can also bind with SERCA proteins in cardiac and skeletal muscle (Algenstaedt *et al.*, 1997) and also in pancreatic β -cells (Borge & Wolf, 2003; Xu *et al.*, 2000). Although SERCA proteins do not contain the traditional SH2 domain, the binding of IRS proteins to SERCA appears to be accomplished through IRS-binding to an amino acid sequence that is similar to the traditional SH2 domain (Algenstaedt *et al.*, 1997). Since the interaction of IRS proteins with proteins that contain the traditional SH2 domain are known to acutely modify the functional properties of the target protein, it is likely that the interaction of IRS with SERCA would result in the altered regulation of SERCA functional

properties as well. However, to our knowledge, the influence that IRS binding exerts on the functional properties of SERCA1a and SERCA2a in skeletal and cardiac muscle remains unknown.

It is possible that insulin signaling may acutely regulate SERCA function through several different intracellular processes (Figure 3.1). One likely process is via the direct interaction of IRS proteins with SERCA, which could alter the V_{\max} or the sensitivity of the enzyme for Ca^{2+} (n_H or Ca_{50}). Insulin signaling may also alter SERCA Ca^{2+} -sensitivity by influencing PLN-Thr17 phosphorylation since insulin is known to increase CaMKII activity in slow-twitch cardiac and skeletal muscle (Brozinick, Jr. *et al.*, 1999). Insulin signaling may also influence SERCA function through the regulation of SLN phosphorylation processes. However, this possibility has not yet been examined. Insulin signaling may also reduce SERCA function by reducing PLN or SLN phosphorylation by activating protein phosphatase-1 (PP-1) and protein phosphatase-2 (PP-2) in skeletal muscle (Liu & Brautigan, 2000; Ragolia & Begum, 1997), thereby promoting the interaction of PLN, SLN and SERCA proteins, which would increase Ca_{50} . Based on a recent report (Yu *et al.*, 2006), it also appears possible that acute AKT signaling may influence SERCA kinetics through a mechanism that is not yet identified.

Skeletal muscle fibres from rats are generally classified into four major categories based on myosin heavy chain composition: Type I (i.e. slow twitch oxidative), Type IIA (i.e. fast twitch, oxidative), Type IIB and Type IIX (i.e. fast twitch, glycolytic) (Bottinelli *et al.*, 1994). Although the general organization of the various fibre types is similar, the tissue specific expression of protein isoforms contributes to the unique metabolic and biochemical characteristics of the different skeletal muscle fibre types. As an example, differences in SERCA1a and SERCA2a isoform expression between fast-twitch and slow-twitch skeletal and

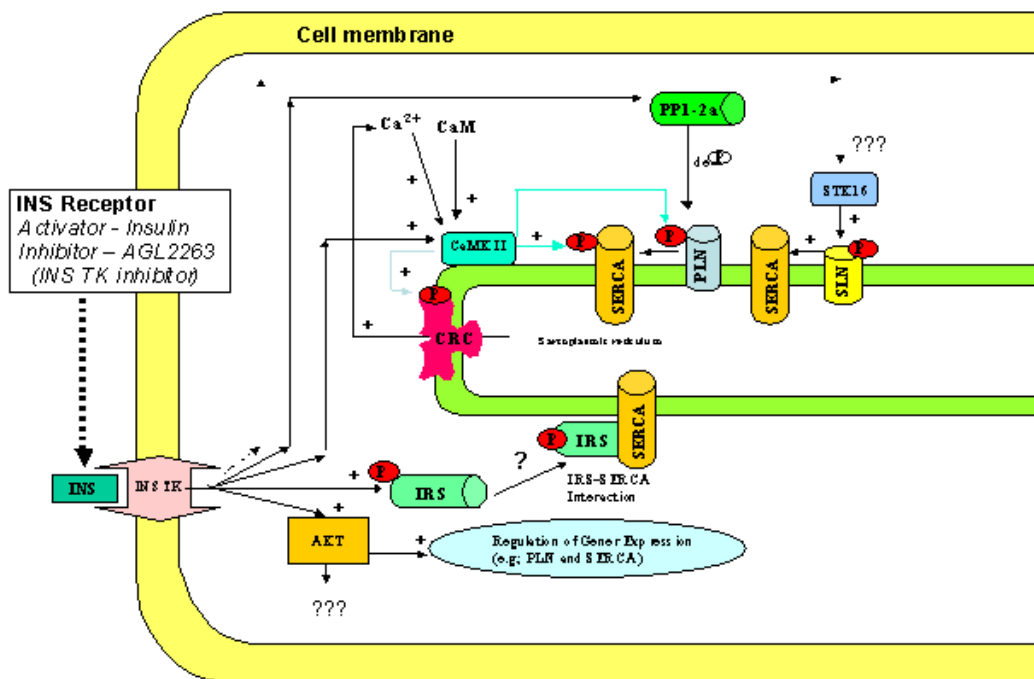


Figure 3.1: Potential pathways involved in insulin signaling in skeletal muscle. Insulin signaling has the potential to acutely regulate sarco(endo)plasmic reticulum Ca^{2+} -ATPase (SERCA) function through several pathways. For example, insulin has the ability to activate protein phosphatase 1 and 2a (PP1-2a), which may alter the phosphorylation status of phospholamban (PLN), thereby altering the interaction of SERCA with PLN and shifting SERCA activity at submaximal Ca^{2+} concentrations. Insulin signaling can also activate Ca^{2+} /calmodulin-dependent kinase II (CaMKII), which is a known regulator of SERCA2a function. Specifically, CaMKII activation can phosphorylate SERCA2a, which causes an increase in maximal SERCA activity. CaMKII can also phosphorylate phospholamban, which alters SERCA sensitivity for Ca^{2+} and increases the specific activity of SERCA at submaximal concentrations of Ca^{2+} . Insulin receptor substrates (IRS) 1 and 2 can directly bind with SERCA proteins (SERCA1 and SERCA2a) in an insulin-stimulated manner. The effect that IRS binding may exert on SERCA activity has not yet been established. It is also likely that acute AKT signaling can also influence SERCA protein kinetics. It is also not clear if insulin signaling can influence SERCA through the regulation of sarcolipin (SLN) phosphorylation by altering serine/threonine kinase 16 (STK16) activity. AGL 2263 is an insulin tyrosine kinase inhibitor. CaM, calmodulin. INS, insulin. INS TK, insulin tyrosine kinase. P, indicates a phosphorylation process regulates protein function. +, indicates that process increases protein activity. -, indicates that process reduces protein activity. ?, indicates that this process has not yet been characterized.

cardiac muscle fibres (Wu & Lytton, 1993) as well as differences in the regulatory control of SERCA kinetic properties are known to exist (Tupling, 2004). Additionally, fibre type-specific differences exist for insulin signaling (Song *et al.*, 1999; Bonen *et al.*, 1981; James *et al.*, 1985). Specifically, Type 1 fibres exhibit a higher sensitivity to insulin (Song *et al.*, 1999) as a result of greater insulin receptor binding capacity (Bonen *et al.*, 1981) and increased INS-TK activity, compared to Type II fibres (James *et al.*, 1986). However, the fibre type-specific differences in insulin-sensitivity are not related to differences in insulin-receptor, IRS-1 or IRS-2 protein content since the expression of these proteins appears to be similar in Type I and Type II muscle fibres (Song *et al.*, 1999).

The purpose of this study was to investigate the role of insulin signaling on the intrinsic regulation of SERCA kinetic properties in the left ventricle and skeletal muscles of different fibre type composition and oxidative potential. We have hypothesized that insulin signaling will acutely alter V_{\max} and Ca^{2+} -sensitivity (n_H and Ca_{50}) in crude muscle homogenates and enriched SR vesicles prepared from rat cardiac and skeletal muscles. Moreover, we have also hypothesized that insulin signaling will promote the interaction of IRS proteins (i.e. IRS-1 and IRS-2) with SERCA1a and SERCA2a in an insulin-dependent manner regardless of tissue type (i.e. left ventricle and skeletal muscle). Furthermore, we have hypothesized that the insulin-induced changes in SERCA2a Ca^{2+} -sensitivity in LV muscle would be associated with changes in the PLN pentamer: monomer ratio and changes in the PLN Ser16 or Thr17 phosphorylation. Given the intrinsic differences in SERCA isoform expression and insulin-sensitivity between tissues, it is possible that the insulin-induced changes in SERCA kinetic properties would be greater for slow-twitch cardiac and skeletal muscles, compared to fast-twitch skeletal muscle.

Research Design & Methods

Materials

Insulin (INS), an activated form of protein kinase A (A-PKA), and bovine brain calmodulin (CaM) were purchased from Sigma (Oakville, ON, Canada). The INS-TK inhibitors AGL 2263 and genistein were purchased from Calbiochem (San Diego, CA, USA). An activated form of the insulin receptor (A-INS-R) was purchased from Upstate Biotechnology (Charlottesville, VA, USA). The fluorescent indicators N-cyclohexyl-N'-(dimethylamino-alpha-naphthyl) carbodiimide (NCD-4) and fluorescein isothiocyanate (FITC), along with anti-fluorescein/Oregon Green monoclonal antibody (A-6421) were purchased from Molecular Probes (Burlington, ON, Canada). Dimethyl-sulfoxide, 0.001 M HCl and ethanol were used as solvents for these chemicals as required. Mouse-anti SERCA2a monoclonal (MA3-919) antibody was purchased from Affinity Bioreagents (Golden, CO, USA). Mouse anti-SERCA1a monoclonal (A52) antibody was a gift from D. MacLennan (Clarke *et al.*, 1990). Rabbit anti-IRS-1 (I7153) and anti-IRS-2 (I7278) polyclonal antibodies were purchased from Sigma (Oakville, ON, Canada). Co-immunoprecipitation assays were completed using a Seize-X Protein G immunoprecipitation kit purchased from Pierce (Rockford, IL, USA). Goat anti-PLN polyclonal (sc-21923), goat anti-Ser16 phosphorylated PLN polyclonal (sc-12963), and goat anti-Thr17 phosphorylated PLN polyclonal (sc-21923) antibodies were purchased from Santa Cruz Biotechnology (Santa Cruz, CA, USA).

Animals and sample preparation

Untrained male Sprague-Dawley rats (9 weeks of age; n=28; mass = 280 ± 4 g) were used to collect tissue for analysis. Specific details of the tissue collection procedures have been

described earlier (Chapter 2, Methods). In general, prior to muscle sampling, rats were anesthetized with pentobarbital sodium (6 mg/100 g body wt). Crude muscle homogenates were prepared from soleus (SOL), extensor digitorum longus (EDL), the red portion of gastrocnemius (RG), the white portion of gastrocnemius (WG) and the left ventricle (LV) from each animal. Purified SR vesicles enriched in SERCA1a and SERCA2a were prepared using crude muscle homogenates from WG and LV, respectively, according to procedures previously described (Chapter 2, Methods). The Animal Care Committee of the University of Waterloo approved all protocols prior to the start the experiment.

Experimental design

To assess the role of insulin signaling in the regulation of Ca^{2+} -dependent SERCA kinetics, crude muscle homogenates and purified SR vesicles were incubated *in vitro* in the presence and absence of various insulin signaling pathway activators and/or inhibitors. Three SERCA kinetic properties have been assessed, namely, the maximal SERCA activity (V_{\max}), the Hill coefficient (n_H), which is defined as the relationship between SERCA activity and Ca^{2+}_f for 10 to 90% V_{\max} and is an indication of the co-operative binding behaviour of SERCA for Ca^{2+} , and the Ca_{50} , which is defined as the Ca^{2+}_f at 50% V_{\max} . For crude muscle homogenates and enriched SR vesicles, three conditions were assayed simultaneously for each sample as indicated in Table 3.1. Control samples were incubated in the absence of any activators or inhibitors and were measured concurrently with two other conditions. Once added, activators and/or inhibitors remained present for the duration of the experiment. Specific conditions tested using crude muscle homogenates included 100 nM INS, 1000 nM INS, 80 μM AGL 2263, and 100 nM INS+80 μM AGL 2263. Homogenates and enriched SR vesicles from LV and WG tissue were also analyzed following incubation of samples with 30 ng (~ 1.2 IU) of A-INS-R or 100 nM

Table 3.1: Experimental conditions used to determine insulin signaling effects on SERCA kinetic properties.

Sample	Treatment 1	Treatment 2	Treatment 3
Crude muscle homogenates	Control	100 nM INS	1000 nM INS
Crude muscle homogenates	Control	80 μ M AGL 2263	100 nM INS
Crude muscle homogenates	80 μ M AGL 2263	100 nM INS	80 μ M AGL 2263 + 100 nM INS
LV and WG crude muscle homogenates	Control	30 ng (~1.2IU) A-INS-R	100 nM INS
Purified SR vesicles	Control	30 ng (~1.2IU) A-INS-R	100 nM INS

Crude muscle homogenates were prepared from tissues collected from soleus (SOL), extensor digitorum longus (EDL), the red portion of gastrocnemius (RG), the white portion of gastrocnemius (WG) and the left ventricle (LV) from each animal. Purified SR vesicles enriched in SERCA1a and SERCA2a were prepared using crude muscle homogenates from WG and LV, respectively. Treatments represent a block of conditions that were assayed simultaneously for each sample as indicated. Control, control samples were incubated in the absence of any activators or inhibitors. INS, insulin. AGL 2263, an insulin-tyrosine kinase inhibitor. A-INS-R, an activated form of the insulin receptor.

INS. Insulin concentrations were selected based on previous publications that have demonstrated that a 10 min incubation period with 100 nM INS does activate the insulin signaling pathway in skeletal muscle (Wegener & Jones, 1984). The 1000 nM INS treatment was used to establish that the lower dose was sufficient. The concentration of AGL 2263 was selected based on the median inhibition concentration (IC_{50}) of 40 μ M for the insulin-receptor as indicated by the information data provided by Calbiochem. The total amount of A-INS-R protein loaded was selected based on the information provided by Upstate Biotechnology.

SDS-PAGE and Western blotting

Sodium dodecyl sulfate (SDS) polyacrylamide gel electrophoresis (PAGE) was performed to separate and isolate proteins by molecular weight. Details describing the specific properties for Western blotting protocols in this study have been described in Table 3.2. In brief, 5 to 50 μ g of protein was loaded for SDS-PAGE, with the quantity being dependent on the protein concentration required for each specific antibody. All samples were analyzed in duplicate. A 7% polyacrylamide SDS gel (Mini-PROTEAN II; Bio-Rad), with a 3.75% stacking gel was used to assess SERCA1a, SERCA2a and FITC-binding content. Insulin receptor substrate-1 and IRS-2 samples were analyzed in duplicate on 5% polyacrylamide SDS gels with a 3.75% stacking gel.

To assess PLN pentamer: monomer ratios, purified SERCA2a vesicles were prepared and assessed using a PLN antibody (L15) by comparing the 25 kDa band in non-boiled samples (which represent PLN pentamers) to the 5 kDa band in samples that were boiled for 10 min (which represents total PLN monomers). Samples were boiled to disrupt PLN pentamer interactions, thereby causing PLN to exist in the monomeric form (Wegener & Jones, 1984).

Table 3.2: Description of primary antibodies and Western blotting protocols in Chapter 3.

Antibody	Supplier	Product #	Species	Primary Antibody Class	Transfer Time (min)	Transfer Voltage (mV)	Primary Dilution (ng uL)	Incubation Time (h)
anti-PLN	Santa Cruz	sc-21923	Goat	Polyclonal	45	21	1:400	16
anti-PLN-Ser16	Santa Cruz	sc-12963	Goat	Polyclonal	45	21	1:400	16
anti-PLN-Thr17	Santa Cruz	sc-17024	Goat	Polyclonal	45	21	1:400	16
anti-IRS1	Sigma	I7153	Rabbit	Polyclonal	120	23	1:1000	16
anti-IRS2	Sigma	I7278	Rabbit	Polyclonal	120	23	1:500	16
anti-SERCA1a	gift from D. MacLennan	A52	Mouse	Monoclonal	45	21	1:20000	1
anti-SERCA2a	Abtrity Bioreagents	MA3-919	Mouse	Monoclonal	45	21	1:4000	1
anti-FITC	Molecular Probes	A-6421	Mouse	Monoclonal	45	21	1:5000	1

PLN, phospholamban. PLN-Ser16, PLN phosphorylated at Ser16, PLN-Thr17, PLN phosphorylated at Thr17, IRS-1, insulin receptor substrate 1. IRS-2, insulin receptor substrate 2. SERCA1a, sarco(endo)plasmic reticulum Ca²⁺-ATPase 1a. SERCA2a, sarco(endo)plasmic reticulum Ca²⁺-ATPase 2a. FITC, Fluorescein isothiocyanate. Transfer Time, represents the duration of time used to transfer proteins from the sodium dodecyl sulfate (SDS) polyacrylamide gel to a polyvinylidene difluoride membrane. Transfer Voltage, the voltage used to transfer proteins from the SDS polyacrylamide gel to a polyvinylidene difluoride membrane. Primary Dilution, represents the dilution factor for primary antibodies used to probe proteins on the polyvinylidene difluoride membrane. Incubation Time, represents the time that the primary antibody was in contact with the polyvinylidene difluoride membrane.

Site specific PLN phosphorylation was assessed using the PLN phosphorylation specific antibodies sc-12963 and sc-17024 for the Ser16 and Thr17 phosphorylated forms of PLN, respectively. Phospholamban (sc-21923) and the phosphorylated forms of PLN (i.e. PLN-Ser16 and PLN-Thr17) were analyzed using non-boiled samples loaded onto a 15% polyacrylamide SDS gel with a 3.75% stacking gel.

To confirm that the site-specific PLN antibodies were able to detect changes in Ser16 and Thr17 phosphorylation, two additional conditions were assessed. The first condition incubated enriched SERCA2a vesicles prepared from LV homogenates for 10 min in 1 mg A-PKA and confirmed that PKA-dependent phosphorylation processes mediated Ser16 phosphorylation. The second condition incubated SERCA2a vesicles for 10 min with 15 μ g CaM and 3.5 μ M Ca^{2+} and confirmed that Thr17 phosphorylation is mediated through CaMKII pathways. Phosphorylation levels were determined by quantifying the optical density of bands at 25 kDa, since PKA and CaMKII can phosphorylate PLN pentamers (Damiani *et al.*, 2000). Quantification of the \sim 10 kDa band was also completed, but has not been reported since no changes in the phosphorylation level of the \sim 10 kDa band was observed during any experimental condition in this study.

For each antibody, the linearity of progressive increases in protein content was established before any experiments were conducted (data not shown). Secondary antibodies were specific to the species required for each primary antibody, as indicated on the information sheet provided by the suppliers and was conjugated to horseradish peroxidase. Relative protein levels were determined by using a bio imaging system and the GeneSnap software (Syngene). Values were normalized to an internal standard and expressed as % of standard. When direct comparisons were made between treatment conditions, values were normalized to control

samples and expressed as % of control. All samples were analyzed in duplicate and on different gels.

SERCA activity assay

Measurement of SERCA activity was made using crude muscle homogenates (~5-30 μ L per 5 mL cocktail buffer) and enriched SERCA1a (~2 μ L per 5 mL cocktail buffer) and SERCA2a (~15 μ L per 5 mL cocktail buffer) vesicles. Calcium-dependent SERCA activity was measured using a spectrophotometric assay originally developed by Simonides and van Hardeveld (Simonides & van Hardeveld, 1990), which has been modified for use on a spectrophotometric plate reader (SPECTRAmax Plus; Molecular Devices) by TA Duhamel (unpublished). Specific assay protocols for determination of Ca^{2+} -dependent SERCA activity have been described earlier (Chapter 2, Methods). No alterations to the assay protocol were made. Three SERCA kinetic properties have been characterized, namely the V_{max} , n_{H} , and Ca_{50} .

Co-immunoprecipitation of SERCA with IRS proteins

To determine if IRS proteins bind to SERCA proteins in an insulin-stimulated manner, co-immunoprecipitation assays were conducted using WG and LV crude muscle homogenates (~5 mg protein/mL) according to the procedures detailed in the Pierce Seize-X Protein G co-immunoprecipitation kit. Prior to co-immunoprecipitation, samples were incubated in ATPase cocktail buffer for 10 min in the presence of 100 nM INS or 30 ng of A-INS-R. An additional aliquot of each sample, which contained no INS or A-INS-R served as a control. The incubation medium contained 200 mM KCl, 20 mM HEPES, 15 mM MgCl_2 , 10 mM NaN_3 , 10 mM PEP, 5 mM ATP, 1 mM EGTA and 3.5 μ M Ca^{2+} . Following incubation, samples were

diluted (1:1) in Tween 20 buffer, which contained 40 mM HEPES-NaOH, 300 mM NaCl, 2 mM EDTA, 4 mM phenylmethylsulfonyl fluoride (PMSF), 1% Tween 20, pH 7.5. Samples were then vortexed for 60 s and centrifuged in a Beckman GS-15R centrifuge with a F2402 rotor for 30 min at 16000 g (~14900 rpm). The supernatants were extracted, diluted (1:1) with Pierce binding/wash buffer and loaded (400 μ L) into Pierce spin-cups that contained Protein G cross-linked with SERCA specific antibodies. Samples were then mixed by rotation and incubated in ATPase cocktail buffer for 6 h at 25 °C. For WG samples, the co-immunoprecipitation antibody cross-linked to Protein G was anti-SERCA1a (100 μ g A52), the predominant SERCA isoform expressed in rat WG. For LV samples, anti-SERCA2a (85 μ g MA3-919) was utilized as the co-immunoprecipitation antibody since SERCA2a is the principal isoform expressed in rat cardiac tissue. Following the elution of antigens from the cross-linked co-immunoprecipitation antibody, samples were loaded onto 5% polyacrylamide gels, and proteins were separated using SDS-PAGE. Detection of IRS-1 and IRS-2 proteins was completed using 50 μ L of sample eluted from the cross-linked antibody by Western blot procedures using anti-IRS-1 (I7153) and anti-IRS-2 (I7278) antibodies according to the protocols described earlier.

FITC binding capacity

The fluorescent probe FITC was used to determine if IRS-binding with SERCA occurs in the region of the SERCA nucleotide-binding domain (Champeil *et al.*, 1988). Samples (250 μ g of enriched SERCA1a and SERCA2a vesicles) were incubated in ATPase cocktail buffer for 10 min with 100 nM INS or 30 ng A-INS-R, and prepared for FITC labeling by adding 7.5 mL of wash buffer to each sample. Wash buffer contained (pH 7.5) 5 mM HEPES, 0.2 mM PMSF,

and 0.2% NaN₃. Each sample was then centrifuged at 23400 rpm for 15 min at 4°C. Following centrifugation, the pellets for each sample were resuspended in wash buffer plus 2.5 μM FITC (pH 8.8) and mixed by inversion in darkness for 20 min at 25°C. To quantify the amount of FITC binding, Western blot techniques were completed according to the methods described by Tupling *et al.* (Tupling *et al.*, 2004). All samples were analyzed in duplicate and on different gels.

NCD-4 binding capacity

The fluorescent probe NCD-4 was used to determine if IRS-binding with SERCA occurs in the region of the SERCA Ca²⁺-binding domain (Lalonde *et al.*, 1991). NCD-4 labeling was measured using a similar protocol as that described for FITC, with several minor alterations. Specifically, NCD-4 labeling was achieved by mixing enriched SERCA1a and SERCA2a vesicles with wash buffer plus 150 μM NCD-4 (pH 6.2) in darkness for 3 h at 25°C (Lalonde *et al.*, 1991). To quantify the amount of NCD-4 binding, 200 μL aliquots from each sample were loaded in triplicate onto a black plate and read using a spectrofluorometric plate reader (SPECTRAMax Gemini XS; Molecular Devices). To assess NCD-4 fluorescence, an excitation wavelength of 340 nm was utilized and NCD-4 emission spectra were recorded using 1 nm increments with a wavelength range between 400 to 430 nm.

Statistical Analyses

Data are presented as means ± S.E. A one-way analysis of variance (ANOVA; one repeated measure) was utilized to compare differences between the different treatments. Where

significant differences were found, Neuman-Kuels post hoc procedures were used to compare specific means. Significance was accepted at $P < 0.05$.

Results

SDS-PAGE and Western blotting

The characterization of the tissue specific expression patterns of SERCA1a, SERCA2a and PLN were described in earlier (Chapter 2, Results). Our findings, support previous literature showing SERCA1a is expressed in skeletal muscle (i.e. SOL, EDL, RG, and WG) tissues, but is not expressed in cardiac (i.e. LV) tissue; while SERCA2a is expressed in LV and SOL tissues, but not EDL, RG, or WG (Table 3.3). Our observations also support previous literature (Damiani *et al.*, 2000) demonstrating that PLN protein is expressed in rat cardiac tissue (i.e. LV) but not skeletal muscle (i.e. SOL, EDL, RG and WG). The tissue-specific expression of SERCA isoforms and PLN were not reassessed since the tissue was obtained from the same group of animals (n=28) for both studies. As indicated previously (Chapter 2), the quantification of SLN protein content was not attempted since an anti-SLN antibody was not available.

It was important to characterize the tissue specific expression of IRS proteins in this study since it has been reported that IRS proteins can interact with SERCA in response to insulin-stimulation (Algenstaedt *et al.*, 1997). Western blot data collected using cardiac and skeletal muscle homogenates indicated that IRS-1 protein contents were similar in LV, SOL, EDL, RG and WG tissues (Table 3.3). Additionally, it appears that all tissues also expressed IRS-2; however, the expression of IRS-2 was ~5-6 fold higher in LV compared to SOL, EDL, RG and WG. Enrichment of SERCA1a vesicles from the WG caused a ~3 fold increase in IRS-1

Table 3.3: Summary of Western blot data characterizing the abundance of selected proteins in the rat left ventricle and skeletal muscle samples assessed in Chapter 3.

	Homogenates			Vesicles			
	LV	SOL	EDL	RG	WG	LV	WG
SERCA1a (normalized to SOL)	N.D.	100	a 208 ± 17	ab 162 ± 13	abc 179 ± 28	ab 376 ± 21	abdef
SERCA2a (normalized to SOL)	127 ± 5	100	a N.D.	a N.D.	a N.D.	ab 478 ± 15	abdef N.D.
IRS-1 (normalized to LV)	100	129 ± 19	103 ± 1	105 ± 15	120 ± 4	17 ± 2	abdef 392 ± 36
IRS-2 (normalized to LV)	100	16 ± 1	a 12 ± 0.5	ab 15 ± 1	ac 18 ± 0.3	abdef N.D.	abdef N.D.
PLN (normalized to LV)	100	N.D.	a N.D.	a N.D.	a N.D.	343 ± 12	abdef N.D.

Values are Means ± S.E; n=4. Homogenates were prepared from tissues collected from the left ventricle (LV), soleus (SOL), extensor digitorum longus (EDL), the red portion of gastrocnemius (RG), and the white portion of gastrocnemius (WG) from each animal. Purified SR vesicles enriched in sarco(endo)plasmic reticulum Ca^{2+} -ATPase (SERCA) 2a and SERCA1a were prepared using crude muscle homogenates from LV and WG, respectively. IRS-1, insulin receptor substrate 1. IRS-2, insulin receptor substrate 2. PLN, phospholamban. N.D., not detected. Soleus was used as a reference for SERCA1a and SERCA2a values since this tissue expressed both SERCA isoforms. IRS-1 and IRS-2 were normalized to LV since IRS-2 expression was highest in this tissue. PLN was detected in LV homogenates and in enriched SERCA2a vesicles isolated from LV but not in any other tissue. ^a, Significantly different from LV homogenate (P<0.05). ^b, Significantly different from SOL homogenate (P<0.05). ^c, Significantly different from EDL homogenate (P<0.05). ^d, Significantly different from RG homogenate (P<0.05). ^e, Significantly different from WG homogenate (P<0.05). ^f, Significantly different from SR vesicles enriched in SERCA2a prepared from LV (P<0.05).

content compared to WG homogenates. In contrast, enrichment of SERCA2a vesicles from the LV was associated with only low amounts (~17%) of IRS-1 protein, compared to the IRS-1 content in homogenates. Western blot analysis could not detect IRS-2 proteins in purified SERCA1a or SERCA2a vesicles.

Insulin regulation of SERCA activity

To determine the effects of insulin signaling on SERCA function, Ca^{2+} -dependent SERCA activity was measured using crude muscle homogenates that were incubated in the presence of 100 or 1000 nM INS for 10 min (Table 3.4). Insulin treatment did not alter V_{\max} in any tissue. However, 100 nM INS increased n_H and reduced Ca_{50} in LV, SOL, EDL, WG and RG. Compared to control samples, 100 nM INS increased n_H by 13, 15, 25, 16, and 15% and reduced Ca_{50} by 12, 11, 15, 10 and 8% in LV, SOL, EDL, WG, and RG, respectively. Even greater increases in n_H and reductions in Ca_{50} were observed when samples were incubated with 1000 nM INS in LV, SOL, EDL, and WG, but not RG.

To determine if the changes in SERCA function were mediated by activation of INS-TK dependent mechanisms, experiments were performed using several combinations of insulin or the INS-TK inhibitor AGL 2263 (Table 3.5 and Table 3.6). Kinetic data from this series of experiments confirmed that 100 nM INS, compared to control values, increased n_H and reduced Ca_{50} without altering V_{\max} in all muscles studied. The magnitude of change observed following the incubation of samples with 100 nM INS, compared to control samples, ranged between 7-19% for n_H and between 29-45% for Ca_{50} . Maximal SERCA activity was not altered by 80 μM AGL 2263. However, incubation of crude muscle homogenates with AGL 2263, compared to Control, reduced n_H by 11, 13, and 9% in LV, SOL, and EDL, respectively. Additionally, the

Table 3.4: Concentration-dependent effects of insulin on SERCA kinetic properties in homogenates from left ventricle and skeletal muscles of different fibre type composition.

	Control	100 nM Insulin	1000 nM Insulin
LV			
V_{\max}	172 ± 6	169 ± 6	172 ± 5
n_H	1.56 ± 0.08	1.77 ± 0.08 †	1.91 ± 0.05 ††
Ca_{50}	1597 ± 54	1244 ± 78 †	924 ± 43 ††
SOL			
V_{\max}	141 ± 6	136 ± 5	133 ± 7
n_H	1.05 ± 0.04	1.21 ± 0.05 †	1.52 ± 0.04 ††
Ca_{50}	756 ± 31	670 ± 53 †	579 ± 26 ††
EDL			
V_{\max}	769 ± 43	767 ± 43	762 ± 45
n_H	1.28 ± 0.05	1.60 ± 0.07 †	1.75 ± 0.04 ††
Ca_{50}	818 ± 34	697 ± 20 †	588 ± 22 ††
WG			
V_{\max}	694 ± 36	703 ± 34	709 ± 34
n_H	1.64 ± 0.05	1.90 ± 0.09 †	2.18 ± 0.10 ††
Ca_{50}	853 ± 26	766 ± 10 †	700 ± 16 ††
RG			
V_{\max}	502 ± 9	505 ± 8	517 ± 14
n_H	1.21 ± 0.05	1.39 ± 0.06 †	1.50 ± 0.08 †
Ca_{50}	1118 ± 81	913 ± 29 †	846 ± 29 †

Values are Means ± S.E; n=7. LV, left ventricle. SOL, soleus. EDL, extensor digitorum longus. WG, the white portion of the gastrocnemius. RG, the red portion of the gastrocnemius. V_{\max} , maximal SERCA activity, n_H , Hill coefficient, defined as the relationship between SERCA activity and $[Ca^{2+}]_f$ for 10 to 90% V_{\max} . Ca_{50} , the Ca^{2+} -concentration at $\frac{1}{2}V_{\max}$. Units for V_{\max} are $nmol.mg^{-1}.min^{-1}$. Units for n_H are arbitrary units. Units for Ca_{50} are nM. † - Significantly different from Control ($P < 0.05$). †† - Significantly different from 100 nM Insulin ($P < 0.05$).

Table 3.5: Effects of insulin or AGL 2263 on SERCA kinetic properties in homogenates from left ventricle and skeletal muscles of different fibre type composition.

	Control	100 nM Insulin	80 μ M AGL 2263
LV			
V_{\max}	170 \pm 3	175 \pm 5	173 \pm 1
n_H	1.58 \pm 0.04	1.84 \pm 0.03 †	1.41 \pm 0.06 †‡
Ca_{50}	1543 \pm 75	969 \pm 65 †	1035 \pm 86 †
SOL			
V_{\max}	138 \pm 3	138 \pm 1	141 \pm 4
n_H	1.43 \pm 0.09	1.53 \pm 0.06 †	1.24 \pm 0.04 †‡
Ca_{50}	944 \pm 52	517 \pm 20 †	582 \pm 55 †
EDL			
V_{\max}	675 \pm 7	671 \pm 5	679 \pm 3
n_H	1.31 \pm 0.03	1.50 \pm 0.05 †	1.20 \pm 0.02 †‡
Ca_{50}	858 \pm 23	613 \pm 18 †	686 \pm 14 †‡
WG			
V_{\max}	665 \pm 13	665 \pm 6	666 \pm 9
n_H	1.31 \pm 0.06	1.47 \pm 0.06 †	1.33 \pm 0.08 ‡
Ca_{50}	1228 \pm 73	759 \pm 41 †	821 \pm 85 †
RG			
V_{\max}	433 \pm 5	446 \pm 2	439 \pm 8
n_H	1.20 \pm 0.06	1.44 \pm 0.07 †	1.16 \pm 0.05 ‡
Ca_{50}	1190 \pm 58	717 \pm 58 †	781 \pm 35 †

Values are Means \pm S.E; n=7. AGL 2263 is an insulin tyrosine kinase inhibitor. LV, left ventricle. SOL, soleus. EDL, extensor digitorum longus. WG, the white portion of the gastrocnemius. RG, the red portion of the gastrocnemius. V_{\max} , maximal SERCA activity. n_H , Hill coefficient defined as the relationship between SERCA activity and $[Ca^{2+}]_f$ for 10 to 90% V_{\max} . Ca_{50} , the Ca^{2+} -concentration at $\frac{1}{2} V_{\max}$. Units for V_{\max} are $nmol \cdot mg^{-1} \cdot min^{-1}$. Units for n_H are arbitrary units. Units for Ca_{50} are nM. † - Significantly different from Control ($P < 0.05$). ‡ Significantly different from 100 nM insulin ($P < 0.05$).

Table 3.6: Effects of insulin, AGL 2263 or AGL 2263 + insulin on SERCA kinetic properties in homogenates from left ventricle and skeletal muscle of different fibre type composition.

	100 nM Insulin	80 μ M AGL 2263	80 μ M AGL 2263 + 100 nM Insulin
LV			
V_{max}	139 \pm 4	135 \pm 5	135 \pm 4
n_H	2.63 \pm 0.10	2.15 \pm 0.10 †	2.54 \pm 0.13 ‡
Ca_{50}	1024 \pm 45	943 \pm 51	809 \pm 44 †‡
SOL			
V_{max}	108 \pm 8	101 \pm 6	108 \pm 5
n_H	2.61 \pm 0.14	1.85 \pm 0.10 †	2.32 \pm 0.13 †‡
Ca_{50}	550 \pm 32	482 \pm 50	537 \pm 31
EDL			
V_{max}	721 \pm 28	710 \pm 33	716 \pm 31
n_H	2.83 \pm 0.14	2.02 \pm 0.07 †	2.52 \pm 0.16 †‡
Ca_{50}	655 \pm 14	559 \pm 13 †	586 \pm 23 †
WG			
V_{max}	692 \pm 37	682 \pm 37	692 \pm 36
n_H	2.52 \pm 0.12	1.67 \pm 0.08 †	2.34 \pm 0.13 ‡
Ca_{50}	733 \pm 27	632 \pm 30 †	631 \pm 25 †
RG			
V_{max}	486 \pm 13	469 \pm 10	488 \pm 17
n_H	1.70 \pm 0.07	1.22 \pm 0.09 †	1.71 \pm 0.12 ‡
Ca_{50}	784 \pm 40	706 \pm 35 †	635 \pm 29 †

Values are Means \pm S.E; n=7. AGL 2263 is an insulin tyrosine kinase inhibitor. LV, left ventricle. SOL, soleus. EDL, extensor digitorum longus. WG, the white portion of the gastrocnemius. RG, the red portion of the gastrocnemius. V_{max} , maximal SERCA activity. n_H , Hill coefficient defined as the relationship between SERCA activity and $[Ca^{2+}]_f$ for 10 to 90% V_{max} . Ca_{50} , the Ca^{2+} -concentration at $\frac{1}{2} V_{max}$. Units for V_{max} are nmol.mg⁻¹.min⁻¹. Units for n_H are arbitrary units. Units for Ca_{50} are nM. † Significantly different from 100 nM Insulin (P<0.05). ‡ Significantly different from 80 μ M AGL 2263 (P<0.05).

AGL 2263 also reduced Ca_{50} by 33, 38, 20, 33 and 34% in LV, SOL, EDL, WG and RG, respectively. Insulin treatment increased n_H in all muscles, compared to AGL 2263. The elevations amounted to 31, 24, 26, 11 and 29% in LV, SOL, EDL, WG and RG, respectively. In contrast to n_H , Ca_{50} was altered by INS, compared to AGL 2263, only in EDL tissue. In this tissue, Ca_{50} was 11% lower during INS treatment compared with AGL 2263.

The next series of conditions were designed to determine if 80 μ M AGL 2263 was able to offset the insulin-stimulated changes in SERCA function. In this series of conditions, samples were incubated with 100 nM INS, 80 μ M AGL 2263 or 80 μ M AGL 2263 + 100 nM INS (Table 3.6). A control sample was not included in this series of experiments. Maximal SERCA activity was not different between any of these conditions, which supports our earlier observation that 100 nM INS and 80 μ M AGL do not alter this property. As expected, the AGL 2263 treatment reduced n_H by 22, 41, 40, 51, and 40% in LV, SOL, EDL, WG, and RG, respectively, compared to the INS treatment. Our data also indicates that AGL 2263 treatment, compared to INS treatment, did not result in differences in Ca_{50} in LV or SOL, but decreased Ca_{50} by 15, 14, and 10% in EDL, WG and RG tissues, respectively. This effect was not observed in our previous experiment when comparisons were made between 100 nM INS and 80 μ M AGL 2263.

Hill coefficients were higher (~30%) in all tissues during the combined AGL 2263 + INS treatment, compared to the AGL 2263 treatment (Table 3.6). In contrast, Ca_{50} was reduced by 15% in LV during the combined AGL 2263 + INS treatment, compared to the AGL 2263 treatment, but was not different between these conditions in any other tissue. These data suggest that AGL 2263 did not completely block the insulin-induced alterations in Ca^{2+} -sensitivity. However it does appear that AGL 2263 is partially inhibiting the insulin-induced

changes in Ca^{2+} -sensitivity since n_{H} were $\sim 11\%$ lower during the combined AGL 2263 + INS treatment, compared to the INS treatment, in SOL and EDL. Unexpectedly, Ca_{50} values in all muscles except the SOL were lower during the combined AGL 2263 + INS treatment, compared to the INS treatment.

Since our insulin treatment data indicated that SERCA Ca^{2+} -sensitivity is modified in the presence of insulin, another series of conditions were completed to determine if insulin or if activation of the insulin signaling pathway was responsible for the increased SERCA Ca^{2+} -sensitivity observed. In this series of conditions, crude muscle homogenates and SR vesicles enriched in SERCA1a and SERCA2a from the WG and LV, respectively, were incubated with 30 ng of an activated form of the insulin-receptor (A-INS-R) or 100 nM INS for 10 min (Table 3.7, Figure 3.2). Incubation of samples with 30 ng A-INS-R increased n_{H} by 12 and 17% in LV and WG homogenates, but had no effect on n_{H} in enriched SERCA2a or SERCA1a vesicles prepared from the LV and WG, respectively. In contrast, 100 nM INS increased n_{H} in all tissues. The percent increase amounted to 17, 19, 35 and 25% in LV homogenates, enriched SERCA2a vesicles prepared from LV, WG homogenates, and enriched SERCA1a vesicles prepared from WG, respectively. In contrast to the tissue-specific effect of the A-INS-R and INS treatments on n_{H} , both treatments reduced Ca_{50} in all tissues studied. When comparisons were made between Control samples and A-INS-R for Ca_{50} , reductions of 23, 24, 8 and 21% were observed in LV homogenate, enriched SERCA2a vesicles prepared from the LV, WG homogenates, and enriched SERCA1a vesicles prepared from the WG, respectively. Reductions in Ca_{50} were greater with the INS treatment compared to A-INS-R.

Table 3.7: Effects of active insulin receptor and insulin on SERCA kinetic properties in homogenates and purified SR vesicles prepared from left ventricle and the white portion of the gastrocnemius.

	Control	30 ng A-INS-R	100 nM Insulin
LV			
Homogenate			
V_{\max}	177 ± 8	173 ± 9	177 ± 7
n_H	1.61 ± 0.09	1.80 ± 0.08 †	1.88 ± 0.06 †
Ca_{50}	1649 ± 62	1268 ± 64 †	976 ± 35 ‡
Vesicles			
V_{\max}	872 ± 25	873 ± 26	853 ± 18
n_H	1.74 ± 0.09	1.72 ± 0.11	2.07 ± 0.13 ‡
Ca_{50}	2060 ± 131	1563 ± 96 †	1091 ± 50 ‡
WG			
Homogenate			
V_{\max}	669 ± 39	676 ± 35	679 ± 33
n_H	1.67 ± 0.05	1.96 ± 0.06 †	2.25 ± 0.10 ‡
Ca_{50}	842 ± 30	773 ± 29 †	686 ± 41 ‡
Vesicles			
V_{\max}	11183 ± 147	10743 ± 247	10803 ± 207
n_H	1.57 ± 0.07	1.58 ± 0.05	1.96 ± 0.07 ‡
Ca_{50}	918 ± 25	730 ± 10 †	628 ± 14 ‡

Values are Means ± S.E; n=7. A-INS-R is an activated form of the insulin receptor. LV, left ventricle. WG, the white portion of the gastrocnemius. Homogenate, crude muscle homogenate. Vesicles, purified SR vesicles enriched in SERCA2a and SERCA1a were prepared using crude muscle homogenates from LV and WG, respectively. V_{\max} , maximal SERCA activity. n_H , Hill coefficient defined as the relationship between SERCA activity and $[Ca^{2+}]_i$ for 10 to 90% V_{\max} . Ca_{50} , the Ca^{2+} -concentration at $\frac{1}{2} V_{\max}$. Units for V_{\max} are $nmol \cdot mg^{-1} \cdot min^{-1}$. Units for n_H are arbitrary units. Units for Ca_{50} are nM. † Significantly different from Control ($P < 0.05$). ‡ Significantly different from 30 ng AINS-R ($P < 0.05$).

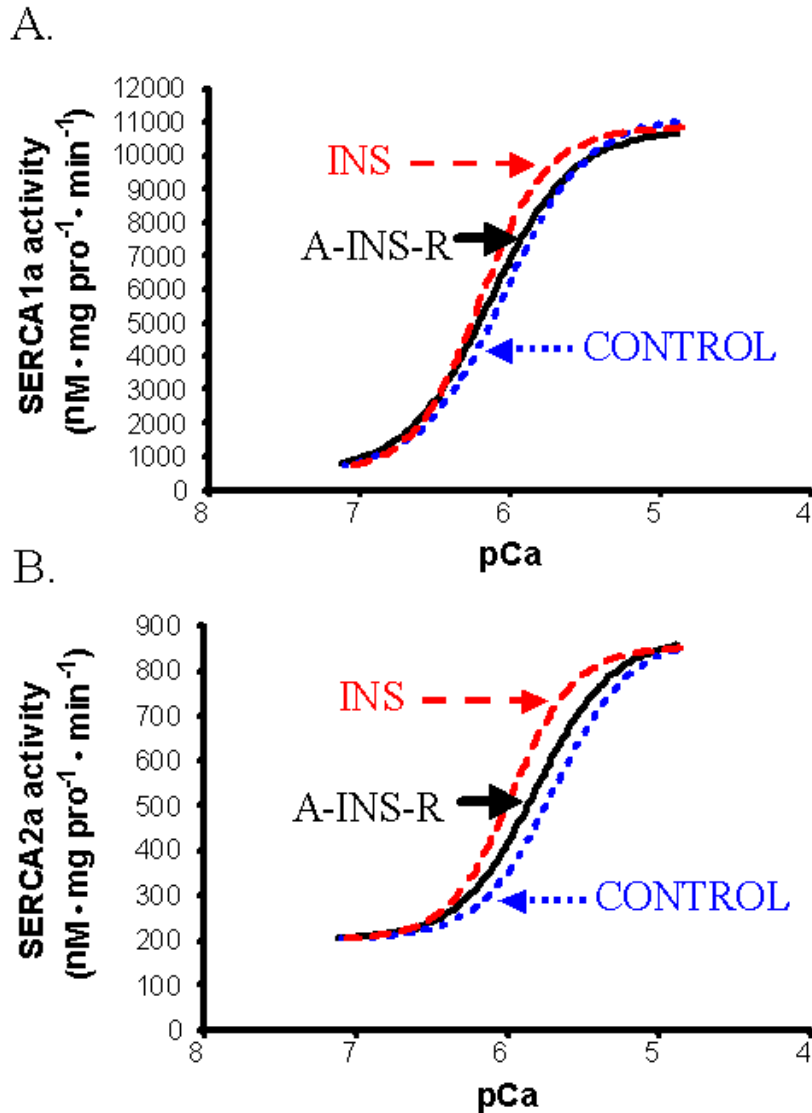


Figure 3.2: Results from representative samples illustrating the relationship between SERCA activity and Ca^{2+} -concentration. Panel A, Kinetic properties assessed in purified SR vesicles prepared from the white portion of the white gastrocnemius and enriched in SERCA1a. Panel B, Kinetic properties assessed in purified SR vesicles prepared from the left ventricle and enriched in SERCA2a. Control, control sample. A-INS-R, 30 ng of an activated form of the insulin receptor. INS, 100 nM insulin. V_{\max} , maximal SERCA activity. n_H , Hill coefficient defined as the relationship between SERCA activity and Ca^{2+}_f for 10 to 90% V_{\max} . Ca_{50} , the Ca^{2+} -concentration at $\frac{1}{2} V_{\max}$. Refer to Table 3.7 to view data represented by these curves.

Co-immunoprecipitation of SERCA with IRS proteins

To determine if insulin signaling promoted the co-localization of IRS proteins with SERCA proteins, co-immunoprecipitation assays were conducted using crude muscle homogenates prepared from WG and LV. Western blot data indicated that both IRS-1 and IRS-2 physically interacted with SERCA1a in WG homogenates during both the 30 ng A-INS-R treatment and the 100 nM INS treatment (Figure 3.3). Compared to control, A-INS-R increased the binding of SERCA1a with IRS-1 and IRS-2 by ~ 25 and 400%, respectively in WG homogenates; whereas, INS treatment increased the binding of SERCA1a with IRS-1 and IRS-2 by ~75 and 1000%, respectively, in WG homogenates. Co-immunoprecipitation assays also confirmed that both the A-INS-R and INS treatments did increase the interaction of IRS-1 and IRS-2 with SERCA2a in LV homogenates (Figure 3.4). Compared to control, A-INS-R increased the binding of SERCA2a with IRS-1 and IRS-2 by ~300%; whereas, the INS treatment increased the binding of SERCA2a with IRS-1 and IRS-2 by ~400 and 450%, respectively, in LV homogenates.

FITC binding capacity

To determine if the binding of IRS proteins occurs in the region of the SERCA nucleotide-binding domain, FITC binding capacity was assessed in SR vesicles enriched with SERCA1a prepared from the WG and SERCA2a prepared from the LV following incubation of vesicles with 30 ng A-INS-R or 100 nM INS. Western blot data indicate that FITC binding was not altered by incubation of SERCA1a or SERCA2a vesicles with 30 ng A-INS-R or 100 nM INS

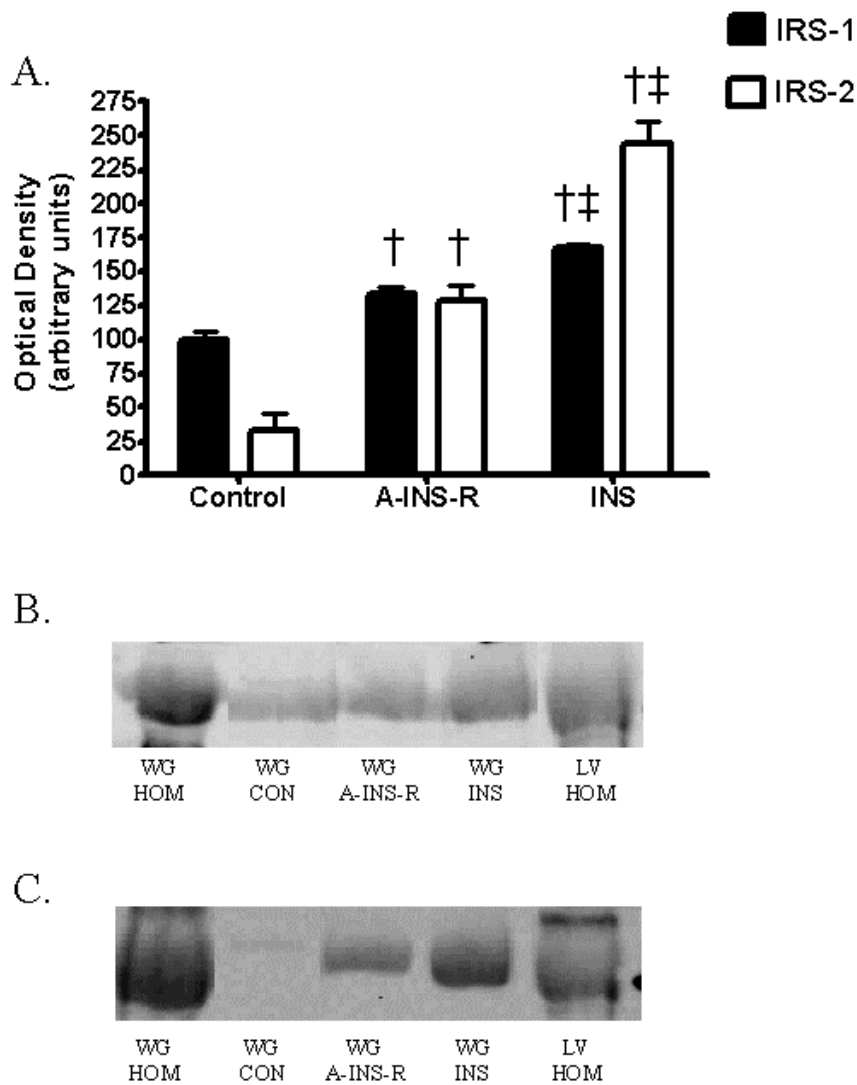


Figure 3.3: Co-immunoprecipitation of insulin receptor substrate (IRS)-1 and IRS-2 with SERCA1a in white gastrocnemius homogenates. Panel A, Optical density of IRS-1 and IRS-2 proteins assessed by Western blot techniques using the 1st elution of sample from the co-immunoprecipitation antibody A52. Panel B, Representative Western blot for IRS-1. Panel C, Representative Western blot for IRS-2. CON, control sample. A-INS-R, 30 ng of an activated form of the insulin receptor. INS, 100 nM insulin. WG HOM, white gastrocnemius homogenate sample that was not co-immunoprecipitated. LV HOM, left ventricle homogenate sample that was not co-immunoprecipitated. Values are Means \pm S.E; n=4. † Significantly different from Control ($P < 0.05$). ‡ Significantly different from A-INS-R ($P < 0.05$).

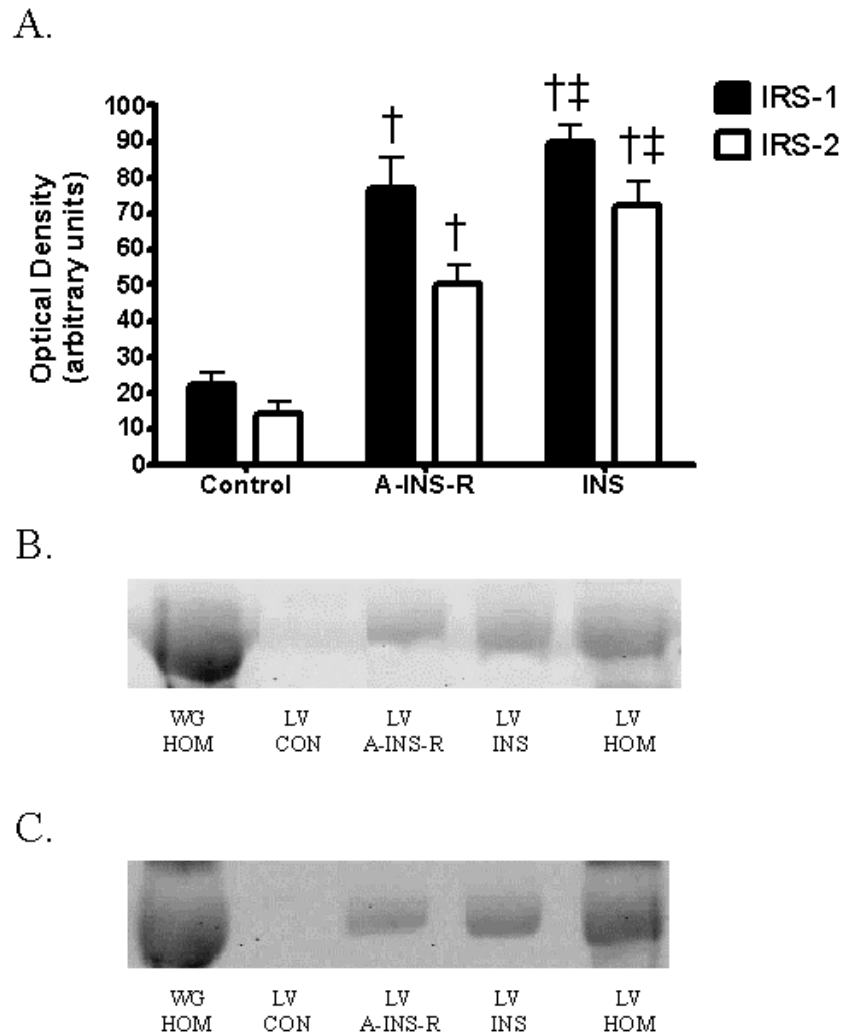


Figure 3.4: Co-immunoprecipitation of insulin-receptor substrate (IRS)-1 and IRS-2 with SERCA2a in left ventricle homogenates. Panel A, Optical density of IRS-1 and IRS-2 proteins assessed by Western blot techniques using the 1st elution of sample from the co-immunoprecipitation antibody MA3-919. Panel B, Representative Western blot for IRS-1. Panel C, Representative Western blot for IRS-2. CON, control sample. A-INS-R, 30 ng of an activated form of the insulin receptor. INS, 100 nM insulin. WG HOM, white gastrocnemius homogenate sample that was not co-immunoprecipitated. LV HOM, left ventricle homogenate sample that was not co-immunoprecipitated. Values are Means \pm S.E; n=4. [†] Significantly different from Control ($P < 0.05$). [‡] Significantly different from A-INS-R ($P < 0.05$).

(Figure 3.5). These data suggest that the interaction between IRS and SERCA proteins does not occur in the region of the SERCA nucleotide-binding site.

NCD-4 binding capacity

To determine if the binding of IRS proteins occurs in the region of the SERCA Ca²⁺-binding domain, NCD-4 binding capacity was assessed in SR vesicles enriched with SERCA1a and SERCA2a following incubation of vesicles with 30 ng A-INS-R or 100 nM INS. The data indicate that NCD-4 binding is not altered by 30 ng A-INS-R or 100 nM INS (Figure 3.6).

Phospholamban status

Phospholamban is an endogenous SERCA2a modulator that is known to influence Ca²⁺-sensitivity. In rats, PLN is expressed in the LV but not in skeletal muscle (Damiani *et al.*, 2000). To determine if PLN is contributing to the insulin-dependent increases in SR Ca²⁺-sensitivity (i.e. n_H and Ca₅₀), we assessed the ratio of PLN pentamer: PLN monomer in enriched SERCA2a vesicles that were incubated in the presence of 30 ng A-INS-R or 100 nM INS. Our data indicate that activation of insulin signaling by 30 ng A-INS-R or 100 nM INS did not alter the PLN pentamer: monomer ratio in SERCA2a vesicles (Figure 3.7, Panel A).

The phosphorylation status of PLN is known to alter SERCA Ca²⁺-sensitivity and can be assessed using site-specific antibodies for the Ser16 and Thr17 phosphorylated forms of PLN. Our data indicates that treatment of enriched SERCA2a vesicles with 30 ng A-INS-R or 100 nM INS did not alter phosphorylation at either site, compared to control (Figure 3.7, Panels B and C). Collectively, these data indicate that PLN does not contribute to the insulin-dependent mechanisms influencing SERCA Ca²⁺-sensitivity in this study.

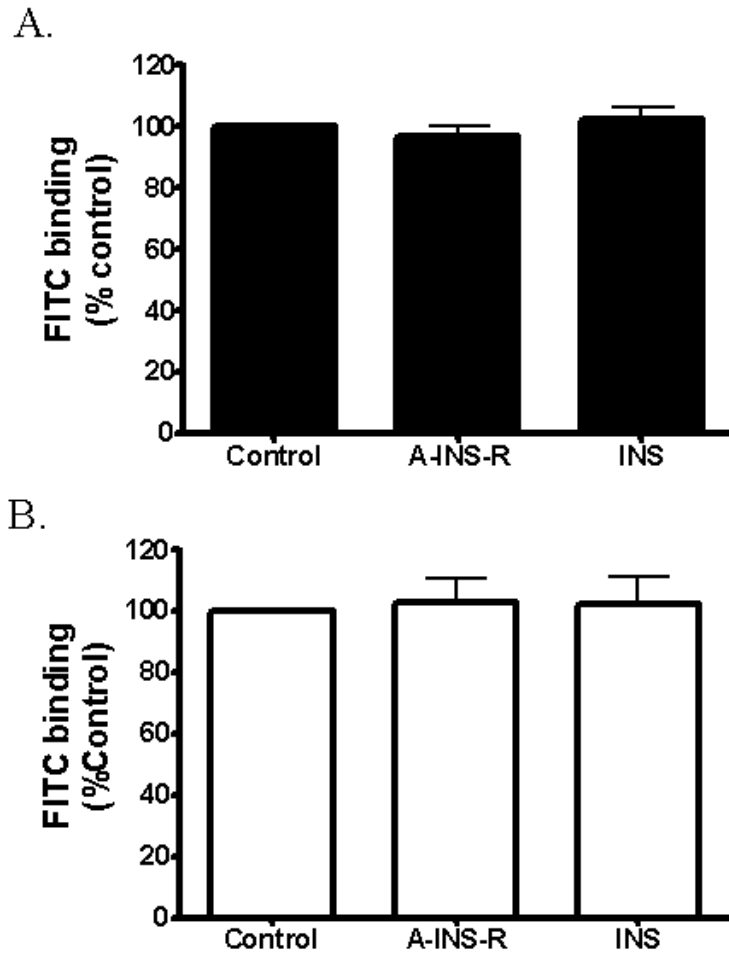


Figure 3.5: Fluorescein isothiocyanate (FITC) binding capacity of enriched SR vesicles in response to 30 ng active insulin receptor or 100 nM insulin. Panel A, Purified SR vesicles enriched in SERCA1a prepared from the white gastrocnemius. Panel B, Purified SR vesicles enriched in SERCA2a prepared from the left ventricle. Control, a control sample. A-INS-R, 30 ng of an activated form of the insulin receptor. INS, 100 nM insulin. Values are Means \pm S.E; n=8.

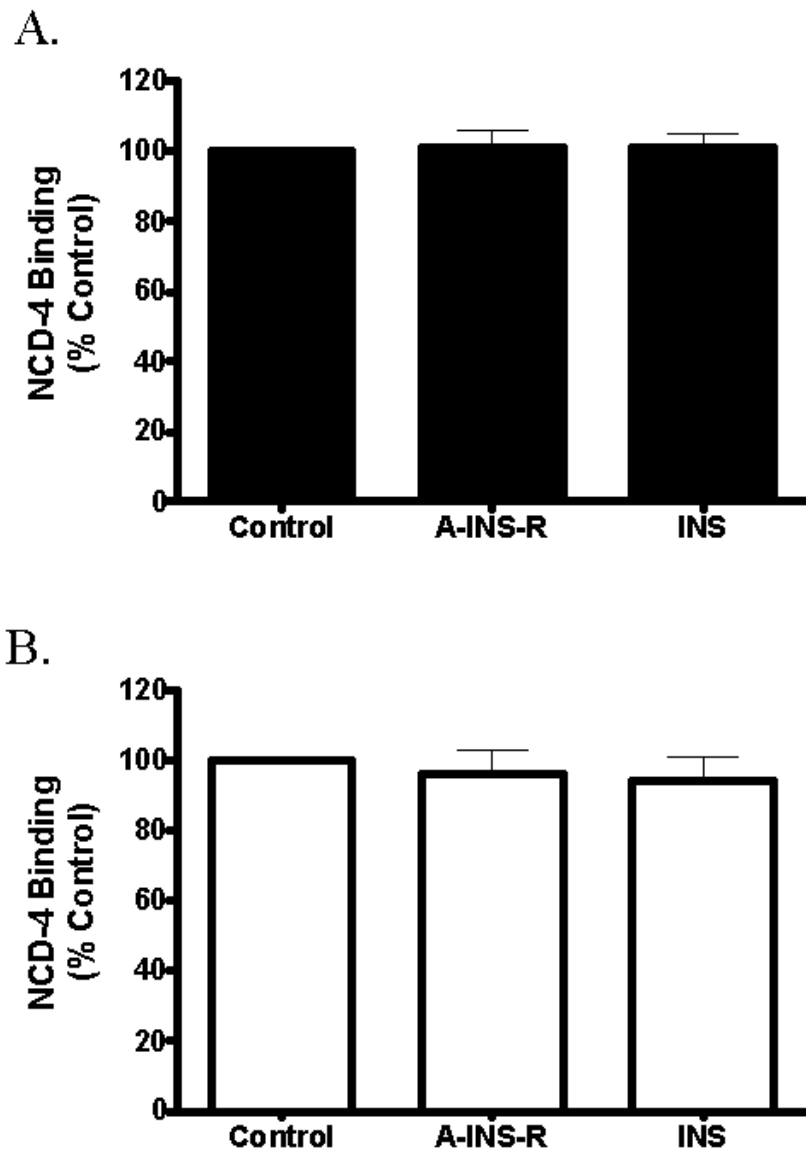


Figure 3.6: N-cyclohexyl-N'- (dimethylamino-alpha-naphthyl) carbodiimide (NCD-4) binding capacity of enriched SR vesicles in response to 30 ng active insulin receptor or 100 nM insulin. Panel A, Purified SR vesicles enriched in SERCA1a prepared from the white gastrocnemius. Panel B, Purified SR vesicles enriched in SERCA2a prepared from the left ventricle. Control, a control sample. A-INS-R, 30 ng of an activated form of the insulin receptor. INS, 100 nM insulin. Values are Means \pm S.E; n=8.

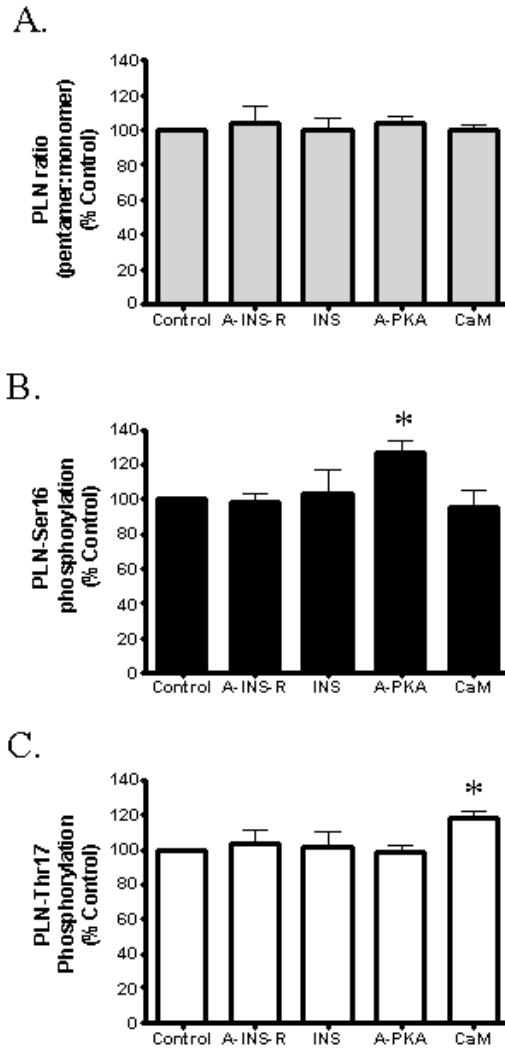


Figure 3.7: Assessments of phospholamban status in response to activation of insulin signaling in SR vesicles enriched in SERCA2a and prepared from the left ventricle. Panel A, phospholamban pentamer:monomer ratio. Panel B, phospholamban Ser16 phosphorylation. Panel C, phospholamban Thr17 phosphorylation. Control, a control sample. A-INS-R, 30 ng of an activated form of the insulin receptor. INS, 100 nM insulin. A-PKA, an activated form of PKA. CaM, bovine brain calmodulin. A 1 way-ANOVA indicated no differences between control, A-INS-R or INS. Therefore, A-PKA and CaM samples were tested to confirm the validity of the Ser16 and Thr17 antibodies. Student T-tests were utilized to make comparisons between control samples with A-PKA and control samples with CaM since these conditions were assessed on independent gels and not concurrently with A-INS-R or 100 nM INS. * Significantly different from control. Values are Means \pm S.E; n=8.

To confirm that the site-specific PLN- antibodies were able to detect changes in Ser16 and Thr17 phosphorylation, SERCA2a vesicles were incubated for 10 min in 1 mg A-PKA or 15 μ g CaM + 3.5 μ M Ca^{2+} to characterize PKA and CaMKII mediated phosphorylation of PLN Ser16 and Thr17, respectively. Incubation of enriched SERCA2a vesicles with 1 mg A-PKA increased PLN Ser16 phosphorylation by ~27%, while incubation with 15 μ g CaM + 3.5 μ M Ca^{2+} increased PLN Thr17 phosphorylation by ~18%, compared to control (Figure 3.7).

Sarcolipin is another endogenous protein that is known to influence SERCA Ca^{2+} -sensitivity through a direct interaction between SLN and SERCA. Phosphorylation of SLN by STK16 is known to reduce the binding of SLN with SERCA, thereby increasing the Ca^{2+} -sensitivity of SERCA. Although it would have been beneficial to examine the effect that insulin signaling has on SLN-phosphorylation, the quantification of SLN phosphorylation was not performed since a site-specific SLN-phosphorylation antibody was not available.

Discussion

There is a growing body of evidence linking insulin signaling pathways with intracellular Ca^{2+} -regulatory pathways in cardiac and skeletal muscle (Algenstaedt *et al.*, 1997) and also in pancreatic β -cells (Borge & Wolf, 2003; Xu *et al.*, 2000). The binding of IRS-1 and IRS-2 with SERCA proteins creates a link between insulin signaling and intracellular Ca^{2+} -regulation and would suggest that insulin signaling can acutely modify SERCA functional properties (Algenstaedt *et al.*, 1997). To our knowledge, no published study has examined the role of insulin signaling on the regulation SERCA kinetic properties in cardiac and skeletal muscle. Therefore, this study was designed to investigate the hypothesis that insulin signaling acutely regulates the kinetic properties of SERCA isoforms in cardiac and skeletal muscles. Since fibre

type differences in SERCA expression and insulin action exist, we studied the left ventricle and a variety of skeletal muscles of different fibre type composition and oxidative potential. The muscles selected included LV, SOL, EDL, WG and RG tissues.

The novel findings of this study indicate that insulin signaling increases the Ca^{2+} -sensitivity (i.e. n_H and Ca_{50}) of SERCA proteins expressed in both cardiac and skeletal muscle. Contrary to our hypothesis, V_{\max} was not altered by insulin signaling. However, the insulin-induced changes in Ca_{50} and n_H indicate that insulin treatment did increase SERCA activity at submaximal Ca^{2+}_f in both homogenates and enriched SR vesicles. Since these effects were observed for all muscles sampled, which included tissue that predominately expressed SERCA1a and SERCA2a, it can be concluded that insulin signaling influences SERCA Ca^{2+} -sensitivity in all fibre type populations of the rat sampled in this study. The changes in SERCA Ca^{2+} -sensitivity that were observed are consistent with the reported inotropic effect of insulin on myocardial contractility (Netticadan *et al.*, 2001; Yu *et al.*, 2006) and the vasodilatory effect of insulin in smooth muscle (Baron, 1994). The observed reductions in Ca_{50} occur as a result of changes in SERCA activity at submaximal Ca^{2+}_f and are consistent with the recent observations of Yu *et al.* (Yu *et al.*, 2006), who found that insulin acutely increases SERCA2a activity in cardiomyocytes using different assay conditions.

Our co-immunoprecipitation data supports previous literature (Algenstaedt *et al.*, 1997; Borge & Wolf, 2003; Xu *et al.*, 2000) showing that insulin signaling promotes the physical interaction of IRS proteins with SERCA *in vitro*. The binding of IRS-1 and IRS-2 with SERCA proteins occurs through the binding of IRS proteins with a 10 amino acid sequence located within transmembrane region 10 (M10) of SERCA (Algenstaedt *et al.*, 1997). This amino acid sequence is not a part of the SERCA nucleotide binding domain, which is located in close

proximity to Lysine 515, or the Ca²⁺-binding domain, which is predicted to be composed of the transmembrane sequences M4, M5, M6 and M8 (Clarke *et al.*, 1989a).

To determine if IRS-SERCA interactions occur in close proximity to the SERCA nucleotide-binding domain (Champeil *et al.*, 1988) or Ca²⁺-binding domain (Lalonde *et al.*, 1991) the fluorescent probes, FITC and NCD-4 were used. These parameters were of interest since structural alterations in the region of the SERCA nucleotide-binding or Ca²⁺-binding domains could influence V_{\max} by reducing the catalytic turnover of the enzyme (Dux *et al.*, 1990; Matsushita & Pette, 1992; Schertzer *et al.*, 2003); whereas, structural changes to the SERCA Ca²⁺-binding domain could alter Ca²⁺-sensitivity by influencing the co-operative binding properties (i.e. n_H) or the affinity of the enzyme for Ca²⁺ (i.e. Ca_{50}) (Dux *et al.*, 1990; Matsushita & Pette, 1992; Schertzer *et al.*, 2003). However, our data indicates that insulin signaling did not influence FITC and NCD-4 binding. These observations suggest that the interaction between IRS and SERCA proteins does not alter the structural integrity of the SERCA nucleotide-binding domain or Ca²⁺-binding domain. As a result, it would appear that the alterations in SERCA Ca²⁺-sensitivity that were observed are influenced by a different mechanism. For example, it is possible that insulin could alter SERCA Ca²⁺-sensitivity by influencing PLN or SLN.

To our knowledge, no published study has examined the role of insulin signaling on the regulation of PLN pentamer:monomer ratio or PLN phosphorylation status. Phospholamban pentamers are known to be less effective inhibitors of SERCA Ca²⁺-sensitivity compared to PLN monomers (Toyofuku *et al.*, 1992; Asahi *et al.*, 2002). Our data indicated that the insulin-induced increases in SERCA2a Ca²⁺-sensitivity observed were not associated with changes in the PLN pentamer: monomer ratio or PLN phosphorylation status. In addition, insulin signaling

increased SERCA Ca^{2+} -sensitivity in rat skeletal muscle fibres that do not contain PLN. Based on this observation, it appears as though another endogenous protein, different from PLN, may be influencing the insulin-induced increase in SERCA Ca^{2+} -sensitivity in the current study.

Sarcoplipin is another endogenous protein known to influence SERCA Ca^{2+} -sensitivity by inhibiting SERCA activity at sub-maximal Ca^{2+}_f by directly binding to SERCA in cardiac and skeletal muscle (Damiani *et al.*, 2000). The interaction of SLN with SERCA is reduced by STK16-mediated phosphorylation of SLN Thr5 (Gramolini *et al.*, 2006). To our knowledge, no published study has examined the role of insulin signaling on the regulation of SLN phosphorylation status. The quantification of SLN phosphorylation was not performed in this study since a site-specific SLN-phosphorylation antibody was not available. Therefore, the possibility that insulin signaling altered SLN phosphorylation remains.

Our data, in conjunction with the observations made by others (Algenstaedt *et al.*, 1997; Borge & Wolf, 2003; Xu *et al.*, 2000), demonstrate that IRS-1 and IRS-2 proteins should be added to the list of endogenous modulator proteins capable of acutely regulating SERCA kinetic properties in cardiac and skeletal muscle at submaximal Ca^{2+}_f . In this study, the amount of IRS-SERCA interaction was smallest during control conditions and was increased in response to insulin signaling. This finding is consistent with the observations of others (Algenstaedt *et al.*, 1997) who demonstrated that IRS proteins bind to SERCA proteins in the presence, but not in the absence, of insulin. Moreover, these investigators (Algenstaedt *et al.*, 1997) were able to establish that INS-TK activity was required to promote the interaction of IRS proteins with SERCA since IRS proteins bind with SERCA in their phosphorylated, but not unphosphorylated, form. For that reason, it appears that the binding of IRS proteins with SERCA is regulated by a phosphorylation-mediated mechanism (Figure 3.8). This mechanism

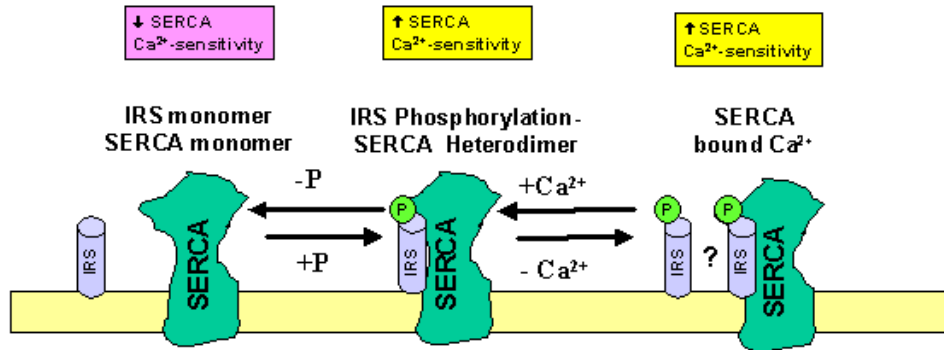


Figure 3.8: Insulin receptor substrate (IRS)-1 and IRS-2 proteins should be added to the list of endogenous modulator proteins capable of acutely regulating sarco(endo)plasmic reticulum Ca^{2+} -ATPase (SERCA) Ca^{2+} -sensitivity in cardiac and skeletal muscle. IRS proteins interact directly with SERCA in their phosphorylated forms and increase SERCA Ca^{2+} -sensitivity.

may be analogous to the phosphorylation-mediated regulation of SERCA Ca^{2+} -sensitivity by PLN (James *et al.*, 1989) and SLN (Gramolini *et al.*, 2006).

Yet to be determined is the effect of AKT signaling on SERCA functional properties. Although our data generally supports the importance of IRS-SERCA interactions on the insulin-dependent increase in SERCA Ca^{2+} -sensitivity, there is a possibility that insulin signaling may also be activating alternative pathways. For example, Yu *et al.* (Yu *et al.*, 2006) provided evidence that the insulin-PI3K-AKT pathway can increase SERCA activity in cardiomyocytes. In fact, the insulin-stimulated increase in SERCA activity was prevented by the inhibition of AKT signaling in that study. However, caution needs to be used when interpreting the data of Yu *et al.* (Yu *et al.*, 2006) since they characterized the effects of AKT-inhibition in cells that were exposed to ischemia/reperfusion but not in control cells. This limitation is notable because ischemia/reperfusion is associated with an increase in oxidative stress (Rubin *et al.*, 1996), which is known to reduce SERCA activity (Morris & Sulakhe, 1997) due to oxidative damage. Moreover, insulin is known to increase nitric oxide synthase activity, which can also alter the redox status of the cardiomyocytes (Hartell *et al.*, 2005). As a result, it is likely that the inhibition of AKT during ischemia/reperfusion influences SERCA activity by altering the redox potential of cardiomyocytes in response to insulin treatment.

This study did not examine the role of AKT signaling on SERCA kinetic properties since there was little information linking acute AKT signaling and SERCA functional properties at the time of our study. It is noteworthy that the literature reports a 6 fold higher expression of AKT protein in soleus (i.e. which is predominately Type I fibres), compared to EDL (i.e. which is predominately Type II fibres) (Song *et al.*, 1999). This large difference in AKT protein content contributes to the fibre type-specific differences in insulin-sensitivity in skeletal muscle

(Song *et al.*, 1999). Since our data indicate that SERCA Ca^{2+} -sensitivity is altered in cardiac and skeletal muscles of different fibre type composition and oxidative potential, it is unclear if the differences in AKT protein content contribute to observed changes in Ca_{50} and n_{H} observed in this study. Since our data has shown that IRS-1 and IRS-2 directly interact with SERCA proteins *in vitro* and given that AKT is situated down-stream of IRS-1 and PI3K, it appears that insulin signaling acts through mechanisms other than AKT signaling alone.

A limitation of this study was the inability to determine if the insulin-dependent changes in n_{H} and Ca_{50} were mediated through an INS-TK dependent mechanism. A common observation made in this study was that n_{H} were consistently higher when samples were incubated in the presence of 100 nM INS (i.e. 100 nM INS and also 80 μM AGL 2263 + 100 nM INS), compared to samples that were not incubated with 100 nM INS (i.e. control and 80 μM AGL 2263). Collectively, these observations could be interpreted to indicate that insulin signaling regulates SERCA Ca^{2+} -sensitivity through an INS-TK dependent mechanism. However, caution must be used when interpreting the results obtained with AGL 2263 since this treatment presented several confounding observations with regard to Ca_{50} . Based on the changes in n_{H} and Ca_{50} with AGL 2263, compared to control and also the combined INS + AGL 2263 treatment, we attempted another series of experiments using a different INS-TK inhibitor, namely genistein (data not shown), to determine if the changes in the properties were mediated through an INS-TK dependent mechanism. However, these experiments were terminated after several trials since the hydrophobic nature of genistein caused a precipitate to form, which prevented accurate assessment of Ca^{2+} -dependent SERCA activity by spectrophotometric analysis.

An important issue is the contradictory effects of A-INS-R for crude muscle homogenates compared to enriched SR vesicles for n_H . Specifically, our data indicated that A-INS-R increased n_H by ~12% in LV homogenates but had no effect on n_H in enriched SERCA2a vesicles prepared from LV. Similarly, A-INS-R increased n_H by ~17% in WG homogenates but did not influence n_H in enriched SERCA1a vesicles prepared from WG. This observation was unexpected since A-INS-R did reduce Ca_{50} in both the homogenate and also enriched SR vesicle samples prepared from the LV and WG, respectively. Additionally, INS treatment did alter n_H and Ca_{50} in both the homogenate and also enriched SR vesicle samples prepared from the LV and WG, respectively. Nonetheless, it is apparent that A-INS-R influenced n_H differently in homogenates versus enriched SR vesicles. The possibility exists that the enrichment protocol used to prepare SR vesicles may have altered the content of one or more proteins that was responsible for increasing n_H in response to A-INS-R treatment. In addition, it is also possible that the analytical methods used to measure n_H and Ca_{50} contributed to the differences between homogenates and vesicles for A-INS-R. Specifically, n_H is determined based on the slope of the relationship between SERCA activity and Ca_f^{2+} for 10 to 90% V_{max} ; whereas, Ca_{50} is defined as the Ca_f^{2+} required to activate the enzyme to 50% V_{max} and is determined based on the relationship between SERCA activity and Ca_f^{2+} for 0 to 100% V_{max} .

The results of this paper also need to be put into perspective given the limitations of the experimental design. To assess the role of insulin signaling in the regulation of Ca^{2+} -dependent SERCA kinetics, samples were incubated *in vitro* in the presence and absence of various insulin signaling pathway activators and/or inhibitors. This experimental approach assumes that the insulin signaling pathway is intact and is able to be influenced by the various insulin signaling pathway activators and/or inhibitors in muscle homogenates and enriched SR

vesicles. *In vivo*, insulin signaling occurs when insulin binds to insulin-receptors located on the cell surface, which is followed by signal transduction into the cell via INS-TK-mediated signaling. It is not known if the protocol used to prepare muscle homogenates disrupted the insulin signaling pathway. However, based on co-immunoprecipitation data, which indicated that both INS and A-INS-R were able to increase the physical binding of IRS with SERCA, it appears that the insulin signaling cascade was, at least in part, functioning as expected. It is noteworthy that INS treatment, compared to A-INS-R treatment, was most effective at promoting the physical interaction of IRS proteins with SERCA. This observation provides indirect support to indicate that the insulin signaling cascade was functioning *in vitro* in this model system.

Summary

The current study indicates that insulin signaling acutely regulates the kinetic properties of SERCA1a and SERCA2a in the LV and skeletal muscles of different fibre type composition and oxidative potential by increasing SERCA Ca^{2+} -sensitivity (i.e. n_H and Ca_{50}), without altering V_{\max} . Furthermore, we have shown that insulin signaling promotes the physical interaction of IRS proteins with SERCA1a and SERCA2a *in vitro*. Finally, it appears that the insulin-dependent increase in SERCA Ca^{2+} -sensitivity observed in this study cannot be explained by IRS binding in close proximity to the SERCA nucleotide binding domain or Ca^{2+} -binding domain and cannot be explained by changes in PLN pentamer: monomer ratio or PLN Ser16 or Thr17 phosphorylation. Collectively, these data suggest that IRS-SERCA interaction may contribute, at least in part, to the insulin-induced changes in SERCA Ca^{2+} -sensitivity observed in this study by mechanisms that are as yet unclear.

CHAPTER FOUR

EFFECTS OF EXERCISE AND ORAL GLUCOSE SUPPLEMENTATION ON SARCOPLASMIC RETICULUM Ca²⁺-CYCLING PROPERTIES IN HUMAN SKELETAL MUSCLE

TA DUHAMEL, HJ GREEN, RD STEWART, KP FOLEY, IC SMITH, and J OUYANG.

Department of Kinesiology, University of Waterloo,

Waterloo, Ontario, Canada, N2L 3G1

Short Title: Glucose Supplementation, Exercise and SR Ca²⁺-cycling

Abstract

This study investigated the effects of prolonged exercise with and without glucose supplementation on muscle sarcoplasmic reticulum (SR) Ca^{2+} -handling properties. Fifteen untrained volunteers (peak O_2 consumption, $\text{VO}_{2\text{peak}} = 3.45 \pm 0.17$ L/min; Mean \pm SE) performed a standardized cycle test ($\sim 60\% \text{VO}_{2\text{peak}}$) on two randomized occasions during which they were provided with either an artificially sweetened placebo (PLAC) or a 6% glucose (GLUC) beverage (~ 1.00 g CHO per kg body mass). Beverages were provided starting after 30 min of exercise and every 15 min thereafter. Muscle SR Ca^{2+} -handling and metabolic properties were assessed in tissue extracted from the vastus lateralis at rest, after 30 min and 90 min of exercise and at fatigue in both conditions. Blood samples were collected at rest, during exercise (15, 30, 45, 60, and 90 min) and at fatigue in both conditions from a catheter inserted in the pre-warmed dorsal region of the hand and were analyzed for blood metabolites and hormones. Cycle ride time to fatigue was increased ($P < 0.05$) by $\sim 19\%$ during GLUC (137 ± 7 min) compared to PLAC (115 ± 6 min). Plasma glucose and insulin concentrations during GLUC were 15-23% higher ($P < 0.05$) than those observed during PLAC following 60 min of exercise until fatigue. Additionally, greater increases ($P < 0.05$) in epinephrine (EPI) and norepinephrine (NE) concentrations were observed during PLAC following 90 min and 115 ± 6 min of exercise compared to GLUC. Prolonged exercise reduced ($P < 0.05$) maximal SERCA activity (V_{max} ; 174 ± 7 vs. 142 ± 5 $\mu\text{mol.g protein}^{-1}.\text{min}^{-1}$), SR Ca^{2+} -uptake (rest vs. fatigue; 6.41 ± 0.31 vs. 4.68 ± 0.33 $\mu\text{mol.g protein}^{-1}.\text{min}^{-1}$), and both Phase 1 (23.4 ± 1.3 vs. 18.2 ± 0.8 $\mu\text{mol.g protein}^{-1}.\text{min}^{-1}$) and Phase 2 (7.3 ± 0.4 vs. 4.8 ± 0.4 $\mu\text{mol.g protein}^{-1}.\text{min}^{-1}$) Ca^{2+} -release rates during PLAC. The reductions in SR Ca^{2+} -handling properties occurred in the absence of changes in Ca^{2+} -sensitivity (i.e. n_{H} and Ca_{50}), Ca^{2+} -transport efficiency (i.e. apparent coupling

ratio), and membrane permeability for Ca^{2+} (i.e. ionophore ratio). No differences for any SR property assessed were observed between conditions at any sampling point. The metabolic response to exercise also appeared to be unaltered by GLUC since no differences in respiratory exchange ratios, carbohydrate and lipid oxidation rates, muscle metabolite and glycogen concentrations, or nucleotide concentrations were observed between conditions. Collectively, these results indicate that the increase in exercise cycle time during GLUC cannot be explained by differences in the muscle metabolic, endogenous glycogen or SR Ca^{2+} -handling responses to exercise. Moreover, the reductions in SR Ca^{2+} -handling properties that occur in response to exercise are not modified by the differences in plasma glucose concentrations and glucoregulatory hormone concentrations that occur with glucose supplementation.

Key words: Ca^{2+} -regulation, glucose supplementation, exercise, human skeletal muscle, and metabolism.

Introduction

Excitation-contraction (E-C) coupling in skeletal muscle involves a series of events that are initiated by sarcolemmal depolarization which culminate in an increase in the cytosolic free Ca^{2+} concentration (Ca^{2+}_f). The rise in Ca^{2+}_f following excitation occurs when the voltage sensitive dihydropyridine receptor (DHPR) interacts with the sarcoplasmic reticulum (SR) Ca^{2+} -release channel (CRC, or ryanodine receptor), triggering the release of Ca^{2+} from the SR, through the CRC. The rapid release of Ca^{2+} from the SR increases the Ca^{2+}_f , where it acts as a second messenger to activate not only the contractile apparatus (Winegrad, 1965) but a variety of other functions including carbohydrate (CHO) metabolism (Hargreaves & Richter, 1988) and protein expression (Chin, 2005). The restoration of Ca^{2+}_f to resting levels (i.e. ~ 100 nM) (Berchtold *et al.*, 2000) occurs through the activation of the sarco(endo)plasmic reticulum Ca^{2+} -ATPase (SERCA) protein, which actively pumps Ca^{2+} from the cytosol back into the SR through an ATP-dependent process. The reduction in Ca^{2+}_f promotes the dissociation of actin and myosin, leading to relaxation of muscle fibres. Achievement of a desired force during repetitive muscle contractions requires regulation of intracellular Ca^{2+}_f -transients, which are directly dependent on the SR Ca^{2+} -release and Ca^{2+} -uptake properties. Accordingly, alterations to the functional characteristics of the CRC and/or SERCA could adversely affect the Ca^{2+}_f , resulting in inadequate myofibrillar activation, reduced force production and impaired relaxation. Depending on the characteristics of the task, disturbances in one or more of the processes involved in E-C coupling could result in impaired performance and the failure to produce a desired level of force (i.e. fatigue).

Sarcoplasmic reticulum Ca^{2+} -cycling properties are influenced by a complex of factors, including protein and isoform abundance (Wu & Lytton, 1993), intrinsic regulatory factors (e.g.

phospholamban, PLN; sarcolipin, SLN) (Gramolini *et al.*, 2006) and the intracellular milieu (Meyer & Terjung, 1980). Repetitive contractile activity presents a unique opportunity to study the intrinsic regulation of SR Ca^{2+} -handling properties since Ca^{2+} -cycling must be greatly accelerated to meet contractile demands. As might be expected, both the CRC and SERCA are under complex intrinsic regulatory control (MacLennan *et al.*, 2003). As an example, exercise-induced increases in plasma epinephrine (EPI) and increases in intracellular Ca^{2+}_f are known to activate cAMP-dependent protein kinase A (PKA) and Ca^{2+} -dependent calmodulin kinase II (CaMKII) phosphorylation-mediated processes, respectively, which can influence CRC (Reiken *et al.*, 2003; Berchtold *et al.*, 2000) and SERCA (Gramolini *et al.*, 2006; Kranias, 1985; Berchtold *et al.*, 2000) kinetic properties.

Prolonged, moderate intensity exercise (i.e. 50-65%) is known to cause progressive reductions in SR Ca^{2+} -handling properties (i.e. Ca^{2+} -release, Ca^{2+} -uptake, maximal SERCA activity, V_{\max}) in human skeletal muscle (Booth *et al.*, 1997; Duhamel *et al.*, 2004a; Duhamel *et al.*, 2004b). These reductions in SR Ca^{2+} -handling properties are thought to occur due to structural modifications to the CRC and/or SERCA proteins (Booth *et al.*, 1997; Duhamel *et al.*, 2006c; Duhamel *et al.*, 2004a; Duhamel *et al.*, 2004b) as a result of oxidative stress (Fitts, 1994; Tupling *et al.*, 2003), thermal stress (Schertzer *et al.*, 2002), or the accumulation of intracellular metabolites (e.g. inorganic phosphate) (Chin & Allen, 1997; Fitts, 1994) during exercise. Interestingly, at least in humans, prolonged exercise does not alter the Ca^{2+} -sensitivity of SERCA activity (Duhamel *et al.*, 2004a; Duhamel *et al.*, 2004b; Duhamel *et al.*, 2006c), as assessed by Ca_{50} (defined as the Ca^{2+}_f needed to elicit 50% of V_{\max}) and the Hill coefficient (n_H ; defined as the relationship between SERCA activity and Ca^{2+}_f for 10 to 90% V_{\max}). The lack of change in SERCA Ca^{2+} -sensitivity during exercise is notable since it has been reported

that PKA and CaMKII increase PLN phosphorylation by ~5 fold soon after the onset of moderate intensity exercise (Rose *et al.*, 2006). Since PLN phosphorylation is known to increase SERCA Ca²⁺-sensitivity (MacLennan *et al.*, 1997), it remains unclear why n_H and Ca₅₀ are not altered by prolonged exercise. This observation, in combination with others (Duhamel *et al.*, 2004a; Duhamel *et al.*, 2004b; Duhamel *et al.*, 2006c), serves to emphasize that the mechanisms regulating SERCA Ca²⁺-sensitivity during exercise are not yet fully understood.

Several laboratories have also linked the depletion of muscle glycogen with reduced Ca²⁺-transients in contracting rat (Lees *et al.*, 2001), mouse (Chin & Allen, 1997), and toad (Stephenson *et al.*, 1999) skeletal muscle; while our laboratory (Duhamel *et al.*, 2006c) has demonstrated that exercise-induced reductions in SR Ca²⁺-handling properties, measured *in vitro*, occur earlier during low glycogen (Lo CHO) compared to high glycogen (Hi CHO) states in human skeletal muscle. The proposed link between muscle glycogen content and SR Ca²⁺-handling properties is based on the existence of a SR-glycogenolytic complex containing glycogen phosphorylase, glycogen debranching enzyme, many of the enzymes involved in the glycolytic pathway, and creatine phosphokinase (CPK), which is located in close proximity to the SR (Xu & Becker, 1998; Korge & Campbell, 1994). It is currently believed that the depletion of glycogen from this complex reduces SR Ca²⁺-cycling rates as a result of disturbances in energy homeostasis in close proximity to SERCA (Cuenda *et al.*, 1995) and the CRC (Han *et al.*, 1992) or as a result of structural alterations within the SR-glycogenolytic complex (Lees *et al.*, 2001).

A limitation of our previous study that investigated the relationship between muscle glycogen concentration and SR Ca²⁺-handling properties during exercise (Duhamel *et al.*, 2006c) was the fact that plasma glucose concentrations were not controlled. With our protocol,

a progressive reduction in plasma glucose was observed during the late stages of exercise (i.e. > 30 min) during Lo CHO, but not the Hi CHO condition. The greater reductions in plasma glucose during Lo CHO were also associated with greater increases in plasma EPI and NE when compared to Hi CHO. We did not assess serum insulin levels in our previous study; however, given that serum insulin concentrations mirror plasma glucose concentrations (Coggan & Coyle, 1991; Coyle, 1992b), it is likely that differences in serum insulin existed as well. Differences in blood glucose availability could alter SR Ca²⁺-cycling function via improved energy homeostasis and/or protection of muscle glycogen reserves (Xu *et al.*, 1995; Lees & Williams, 2004) while differences in the hormonal responses could affect intrinsic behaviour through second messenger regulation (MacLennan *et al.*, 2003; Wuytack *et al.*, 2002). Interestingly, as with experiments designed to manipulate muscle glycogen levels by exercise and diet (Bergstrom *et al.*, 1967), oral glucose supplementation during exercise also has an ergogenic effect (Coyle, 1992b; Hargreaves, 1999).

The use of oral glucose supplementation to delay the onset of fatigue during prolonged exercise has been well documented in humans (Coggan & Coyle, 1991; Coyle, 1992b) and animals (Bagby *et al.*, 1978; Karelis *et al.*, 2002; Marcil *et al.*, 2005). However, the mechanisms explaining how glucose supplements extend time to fatigue remain unclear. There is evidence suggesting that central (i.e. neural) processes (Nybo, 2003) may contribute to fatigue mechanisms; however, the literature generally supports a failure at the level of the working muscle as the primary site of fatigue during voluntary activity (Fitts, 1994). It is possible that reductions in plasma glucose concentrations and/or changes in the regulatory hormones during the late stages of exercise may adversely affect skeletal muscle function by

reducing SR Ca^{2+} -handling properties, thereby altering the Ca^{2+}_f , and reducing contractile activation.

To hypothesize that maintenance of blood glucose homeostasis during prolonged exercise can affect SR Ca^{2+} -cycling responses, it must be demonstrated that glucose supplementation results in changes in one or more of the factors involved in its regulation. In this regard, the literature is contradictory with regards to the effects of glucose supplementation on muscle metabolism (Christ-Roberts & Mandarino, 2004; Spencer *et al.*, 1991; Tsintzas *et al.*, 1996) and glycogen depletion patterns (Coyle, 1992a; McConell *et al.*, 1999; Tsintzas *et al.*, 1996) and blood hormonal responses (Coyle, 1992a; Galbo, 1999; Hargreaves, 1999).

The purpose of this study was to investigate the effects of oral glucose supplementation on SR Ca^{2+} -handling properties during prolonged, moderate intensity exercise in human skeletal muscle. We have hypothesized that prolonged exercise would progressively reduce V_{\max} , Ca^{2+} -uptake, and Ca^{2+} -release kinetics. We have also hypothesized that the reductions in SR Ca^{2+} -handling properties would occur in the absence of changes in Ca^{2+} -sensitivity (i.e. n_H and Ca_{50}), Ca^{2+} -transport efficiency (i.e. apparent coupling ratio) and membrane permeability for Ca^{2+} (i.e. ionophore ratio). Moreover, we have also hypothesized that, when the same absolute exercise protocol is performed with glucose supplementation, the disturbances in the V_{\max} , Ca^{2+} -uptake, and Ca^{2+} -release kinetics will be attenuated. The improvement in these properties will be associated with improved glucose homeostasis and will occur in the absence of differences in energy metabolism and glycogen content. Based on data from our laboratory (Duhamel *et al.*, 2006c) indicating that Ca_{50} and n_H are not different when plasma glucose concentrations are decreased and catecholamine concentrations are increased during exercise in Lo CHO states,

we have hypothesized that glucose supplementation will not alter n_H , Ca_{50} or PLN phosphorylation during exercise.

Research Design & Methods

Participants

Fifteen volunteers (14 male and 1 female) were recruited from the general student population at the University of Waterloo to participate in the study. Volunteers were healthy but not involved in exercise utilizing large muscle groups on a regular basis (i.e. not more than once per week; assessed by a questionnaire). The physical characteristics of the participants included age, 19.3 ± 0.4 yrs; height, 179 ± 4 cm; body mass, 78.5 ± 3.7 kg; body mass index (BMI, mass/height^2), 24.5 ± 0.8 kg/m^2 . Peak aerobic power ($VO_{2\text{peak}}$) was 3.45 ± 0.17 L/min. Volunteers were excluded from the study if their $VO_{2\text{peak}}$ was out of the normal range for this participant population ($35\text{-}55$ mL $O_2 \cdot \text{kg}^{-1}$ body wt $\cdot \text{min}^{-1}$) or if they had a BMI greater than 30. Participants were also excluded from this study if they had a history of exercise training, smoking, previous knee injuries, heart problems, diabetes, or exercise-induced respiratory problems. Laboratory visits were scheduled during the midfollicular phase of the menstrual cycle for the female participant in this study. This participant was not taking triphasic-type oral contraceptives. This study received approval from the Office of Research Ethics at the University of Waterloo. Volunteers were required to read detailed descriptions of the protocols employed in the study including the risks associated with each protocol prior to agreeing to participate in the study.

Experimental design

To investigate the effects of oral glucose supplementation on muscle SR Ca^{2+} -transport properties, two sessions of prolonged, moderate-intensity exercise ($\sim 60\%$ $\text{VO}_{2\text{peak}}$) were employed (Figure 4.1). One session served as the control condition (i.e. placebo, PLAC) and was used to investigate the effects of exercise in isolation without oral glucose supplementation. The other session served as the glucose supplementation condition (GLUC) and was identical to PLAC with the only difference being the administration of glucose supplements, designed to maintain blood glucose levels during the late stages (i.e. > 30 min) of exercise. The order of the two experimental conditions was randomized for 9 of 15 participants. The remaining 6 participants completed the PLAC condition prior to the GLUC condition. The latter sequence allowed for muscle tissue to be sampled at a matched time point in both conditions within this subgroup. The matched time point was selected to correspond to fatigue in the placebo condition and was unique to each individual.

Prior to the initial prolonged exercise test session, participants were asked to complete a 7-day diet journal to allow for the assessment of average daily nutritional and macronutrient intake. Based on the analysis of these 7-day diet journals (ESHA – Diet Analysis Plus, Version 7.0, Salem, OR), the average daily caloric intake for participants was 2824 ± 142 kcal, with approximately $49 \pm 2\%$, $30 \pm 2\%$, and $18 \pm 2\%$ of total energy coming from CHO, lipid and protein sources, respectively. These 7-day diet journals were returned to the participants prior to the second prolonged exercise test session. Participants were asked to strictly follow the diet journals and were instructed to contact the investigator if any alteration to the dietary plan was required. Participants were required to refrain from exercise and from ingesting alcohol and

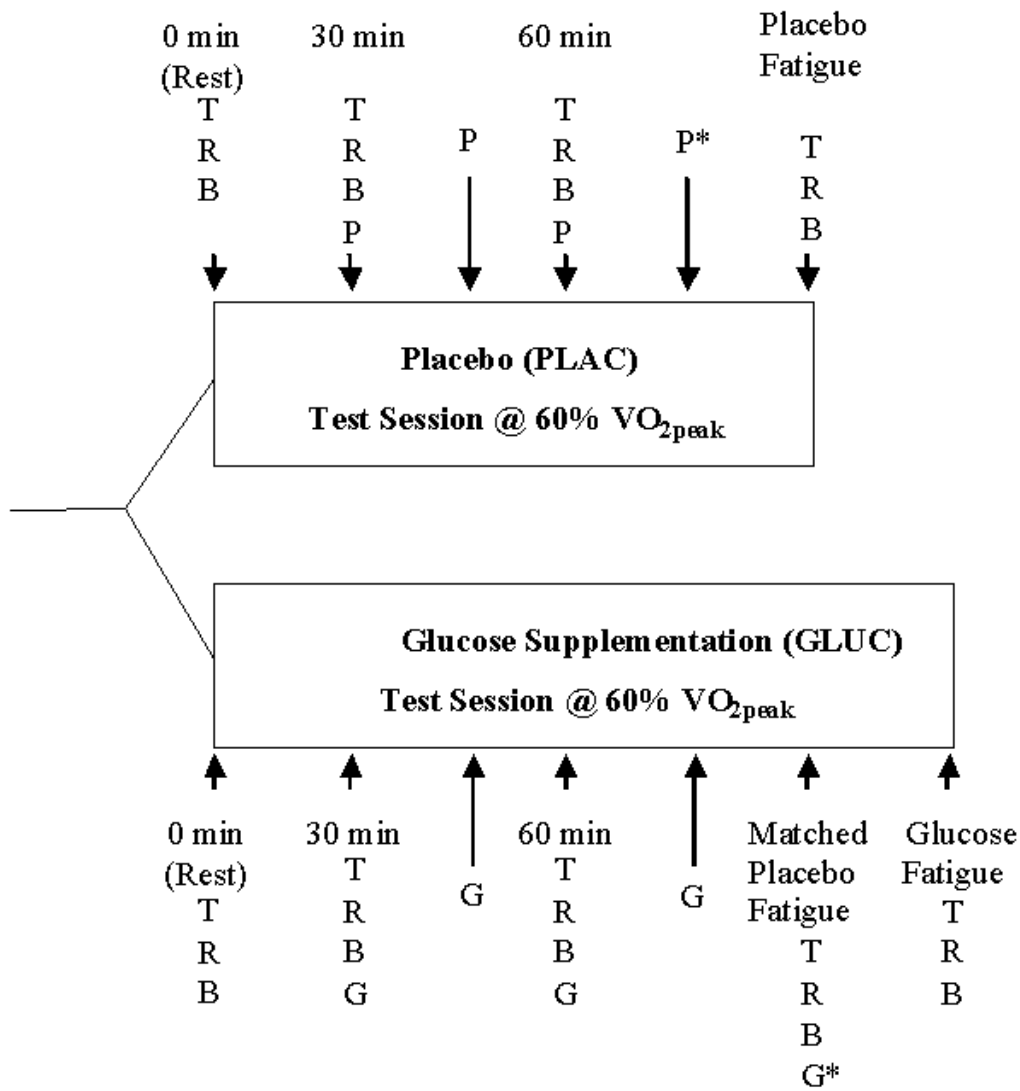


Figure 4.1: Experimental design used to characterize the effects of exercise and oral glucose supplementation on sarcoplasmic reticulum Ca²⁺-cycling properties in human skeletal muscle. T, tissue sampling using the needle biopsy technique. R, respiratory gas sampling; B, blood sampling ; G, glucose supplementation. P, placebo beverage. * placebo or glucose beverages were administered every 15 min until fatigue in each condition.

caffeine for the 4 day period preceding the exercise protocol. The prolonged cycle task was performed following an over night fast (~12 h) in a neutral environment (~20°C; ~50% relative humidity) at an intensity that was approximately 60% $\text{VO}_{2\text{peak}}$. Exercise was continued until volitional fatigue or when the participant could not maintain a cadence of at least 50 revolutions per min, even with verbal encouragement.

Glucose Supplements

The glucose supplement was a 6% solution of glucose, without the addition of any electrolytes. Participants were provided with a drink (volume dependent on body mass; ~1.00 g CHO per kg body mass in a 6% solution) starting after 30 min of exercise and continuing every 15 min thereafter. The average total volume ingested at each time point ranged between 100-300 mL. A placebo (Sugar Twin; Alberto-Culver Canada Inc; Toronto, ON, Canada) consisting of a 7.5 % Sugar Twin (water, sodium cyclamate (10%) benzoic acid, methyl paraben) solution was provided according to the same schedule using a similar volume as received during GLUC. Beverages were served at room temperature (~20°C). For participants who completed the PLAC condition prior to GLUC, beverage volumes were matched to the volume that was to be consumed during the GLUC condition at each time point. Test sessions were separated by at least 4-weeks and were conducted in the morning, following an overnight fast (~12 h).

Peak aerobic power determination and respiratory gas collection

A progressive exercise test was performed on an electrically braked cycle (Quinton 870) as previously described (Hughson *et al.*, 1995) to measure $\text{VO}_{2\text{peak}}$. Participants were required to

pedal at approximately 60 revolutions per min. After cycling at 25 W for a period of 4 min to establish baseline measurements, the work rate on the cycle ergometer was progressively ramped at 15 W per min until volitional fatigue. Inability to maintain at least 50 revolutions per min was used as the fatigue criterion. The exercise time during the progressive test ranged between 10-20 min for all participants. Verbal encouragement was given to the participants throughout the test.

An open-circuit gas collection system using continuous measurements was used to determine $VO_{2\text{peak}}$, as described previously (Hughson *et al.*, 1995). The $VO_{2\text{peak}}$, defined as the peak VO_2 observed during the progressive test, was obtained by averaging the data collected over a 25 s collection period. Heart rate was also monitored during the progressive test using standard electrocardiographic techniques (data not shown).

The gas collection system was calibrated daily, 30 min prior to all test sessions using standardized gas samples of known concentrations. All exercise sessions were performed on the same cycle ergometer and using the same respiratory gas collection system. Respiratory gas properties measured during the exercise tests include VO_2 , carbon dioxide ventilation (VCO_2) and expiratory ventilation (V_E). From these data, respiratory exchange ratios ($RER = VCO_2/VO_2$) were calculated. Stoichiometric equations and appropriate caloric equivalents (Woelfe, 1992; Frayn, 1983) were used to calculate carbohydrate (CHO) and lipid oxidation rates during the exercise according to *Equation 4.1* and *Equation 4.2*, respectively.

$$\text{CHO oxidation rate (mmol} \bullet \text{min}^{-1}\text{)} = \text{Equation 4.1}$$

$$25.196 \times VCO_2 - 17.499 \times VO_2 - 0.21349 \times 0.7155$$

$$\text{Lipid oxidation rate (mmol} \cdot \text{min}^{-1}\text{)} = \text{Equation 4.2}$$

$$1.9357 \times \text{VO}_2 - 1.9357 \times \text{VCO}_2 - 0.031978 \times 0.7155$$

Nitrogen excretion was assumed to be $135 \mu\text{g} \cdot \text{kg}^{-1} \cdot \text{min}^{-1}$ (Woelfe, 1992; Frayn, 1983). Although indirect calorimetry technically provides for an estimation of total glucose oxidation, we have followed the general practice of labeling it as CHO oxidation.

Blood sampling

Blood samples during the PLAC condition were collected at rest, during exercise (15, 30, 45, 60, and 90 min) and at fatigue ($\sim 115 \pm 6$ min) from a catheter inserted in the pre-warmed dorsal region of the hand. During GLUC, blood samples were collected at rest, during exercise (15, 30, 45, 60, and 90 min), at a time corresponding to fatigue during the PLAC condition ($\sim 115 \pm 6$ min) and at fatigue ($\sim 137 \pm 7$ min).

Resting hemoglobin (Hb) and hematocrit (Hct) values were determined in triplicate from whole blood using standardized differential centrifugation and spectrophotometric techniques. Changes in plasma volume content during exercise were calculated using corrections for whole body Hct (0.91) and trapped red cell volume (0.96) according to *Equation 4.3* and *Equation 4.4* (Chaplin *et al.*, 1953; Chaplin & Mollison, 1952).

$$\text{Hct}_{\text{corrected}} = \text{measured Hct} * 0.91 * 0.96 \quad \text{Equation 4.3}$$

$$\text{Plasma volume change} = \quad \text{Equation 4.4}$$

$$[100 / (100 - \text{Hct}_{\text{Time1}})] * [100 * (\text{Hct}_{\text{Time1}} - \text{Hct}_{\text{Time2}}) / \text{Hct}_{\text{Time2}}]$$

Where Hct_{Time1} and Hct_{Time2} represent the Hct content for a blood sample collected at two different times (e.g. rest compared to 15 min).

The remaining aliquots of whole blood, serum, and plasma samples were processed and frozen at -20°C until analyses. Blood glucose and lactate were determined fluorometrically, in triplicate, from the plasma aliquots that were deproteinized using perchloric acid (PCA) and centrifuged (Green *et al.*, 1991a). Plasma catecholamines (i.e. EPI and NE) were measured using high performance liquid chromatography (HPLC) techniques, previously published from our laboratory (Green *et al.*, 1991b). To obtain serum, whole blood was centrifuged and the supernatant removed. Serum FFA concentrations were analyzed as previously described using fluorometric techniques (Green *et al.*, 1991a). Serum was also used to analyze serum insulin concentrations using radioimmunoassay techniques (Coat-A-Count, Diagnostic Products, Intermedico, Toronto, ON). On a given day, all samples from three individuals for a given property were analyzed in triplicate.

Tissue sampling

Tissue samples were collected from 4 separate biopsy sites within the vastus lateralis under local anesthesia (2% xylocaine) in each condition (Figure 4.1). For PLAC, tissue samples were collected at rest, after 30 min and 90 min of exercise and at fatigue. During the GLUC condition, tissue samples were collected at rest, after 30 min and 90 min of exercise, and at fatigue during the GLUC condition in 9 of 15 participants. In the remaining 6 participants, the resting tissue sample was omitted and replaced with a tissue sample taken at a time corresponding to fatigue during the PLAC condition (i.e. matched placebo fatigue). This

approach was required based on restrictions for the number of biopsies (n=8) approved for this study by the Office of Research Ethics at the University of Waterloo. The decision to replace the resting tissue sample with a matched placebo fatigue tissue sample during GLUC was based on observations made in this study (data not shown), in addition to numerous experiments from our laboratory (Duhamel *et al.*, 2005; Duhamel *et al.*, 2004a; Duhamel *et al.*, 2004b) that have shown no differences in resting SR Ca²⁺-handling or metabolic properties between conditions when the experimental treatment was preceded by a normal CHO (~50% total kcal) diet. This approach allowed for direct comparison of tissue samples collected at a time corresponding to the placebo fatigue time point in PLAC and GLUC; thereby increasing the number of comparisons made between PLAC and GLUC at matched time points during exercise. Statistical analyses of all data were adjusted to account for this subgroup of participants, as described in the statistical analyses section of this paper.

Two tissue samples were taken from each site at each sampling time. The first sample was immediately placed into liquid N₂ and stored at -80°C until metabolite analyses were performed. The second tissue sample was used for determination of SR Ca²⁺-handling properties.

Assessment of muscle metabolites

Muscle metabolite analyses were performed as previously reported (Green *et al.*, 1992a), using fluorometric procedures (Lowry & Passonneau, 1972) and HPLC techniques (Ingebretsen *et al.*, 1982). The specific metabolites analyzed include ATP, PCr, inorganic phosphate (Pi), creatine (Cr), lactate (Lac) and selected glycolytic intermediates such as glucose, glucose-1-

phosphate (G-1-P), glucose-6-phosphate (G-6-P), fructose-6-phosphate (F-6-P), fructose-1,6-diphosphate (F-1,6-P), and pyruvate (Pyr).

Free ADP (ADP_f) and free AMP (AMP_f) concentrations were calculated according to *Equation 4.5*, as has been done previously in our laboratory (Green *et al.*, 1992b) and others (Dudley & Terjung, 1985) on the basis of the near-equilibrium properties of creatine phosphokinase (CPK) and adenylate kinase (AK) reactions. For ADP_f , the calculation involved use of the measured concentrations of ATP, PCr, and Cr in conjunction with calculated H^+ (Lawson & Veech, 1979).

$$ADP_f = (ATP \times Cr) / [(K_{CPK}) \times CP \times (-\log pH)] \quad \text{Equation 4.5}$$

Calculation of AMP_f , involved using the measured calculation of ATP and the calculated level of ADP according to *Equation 4.6*.

$$AMP_f = (ADP_f)^2 / (K_{AK} \times ATP) \quad \text{Equation 4.6}$$

Muscle pH was determined by the regression formula established by Sahlin *et al.* (Sahlin *et al.*, 1976). Measured values for lactate and pyruvate were utilized to calculate muscle pH according to *Equation 4.7*, using the dynamic work constant of 0.00413.

$$pH = 7.06 - [(0.00413) \times (Lac + Pyr)] \quad \text{Equation 4.7}$$

The equilibrium constants used for the CPK and AK reactions (K_{CPK} and K_{AdK}) at 38°C were $1.66 \times 10^9 \text{ M}^{-1}$ and 1.05, respectively (Lawson & Veech, 1979).

Muscle tissue samples were analyzed for total adenine nucleotide (ATP, ADP, and AMP) and inosine monophosphate (IMP) using HPLC techniques (Green *et al.*, 1989). These properties were measured in the same extract from which the other metabolite data were obtained. Quantification of proglycogen and macroglycogen was accomplished using the fluorometric technique described by Marchand *et al.* (Marchand *et al.*, 2002). Total glycogen content was calculated as the sum of the proglycogen and macroglycogen subfractions. All measurements, with the exception of muscle glycogen content, were performed using an extract from the same piece of freeze-dried tissue and were corrected to the average total creatine content (TCr) is calculated as the sum of PCr and Cr) of all tissue samples collected for each individual. During a given analytical session, all tissue samples from three individuals were analyzed in duplicate for a selected metabolite.

Assessment of sarcoplasmic reticulum Ca^{2+} -handling properties

To assess changes in Ca^{2+} -transport across the SR membrane, a variety of functional properties of SERCA, the CRC and the SR membrane were performed using crude muscle homogenates. Muscle samples (40-60 μg) were diluted 1:11 (w/v) in ice cold homogenizing buffer (pH 7.5) containing (in mM) 250 sucrose, 5 N-2-hydroxyethylpiperazine-N'-2-ethanesulfonic acid (HEPES), 0.2 phenylmethylsulfonyl fluoride (PMSF), 0.2% sodium azide (NaN_3). Dithiothreitol (DTT) was not used in the preparation of crude muscle homogenates since DTT could potentially reverse exercise-induced sulfhydryl oxidation during sample preparation. The muscles were homogenized with a Duall glass on glass hand homogenizer

(Kontes Glass Co.). Tissue samples were stored on ice from the time of extraction until homogenized. The total time between tissue extraction and homogenization was typically less than 10 min. Muscle homogenate aliquots (approximately 115 μL per aliquot; ~ 4 aliquots) were rapidly frozen in liquid N_2 and stored at $-80\text{ }^\circ\text{C}$ for future analysis of SR function. Assessments of the kinetics parameters of SERCA were made to characterize changes in V_{max} , n_{H} , and Ca_{50} . Additionally, we determined the relative amounts of passive Ca^{2+} leak across the SR membrane by comparing the ratio between V_{max} in the presence and absence ($V_{\text{max}(-)}$) of 1 μM Ca^{2+} -ionophore A23187 (ionophore ratio). We have also assessed the apparent coupling ratio, which provides an indication of the efficiency of SERCA to transport Ca^{2+} from the cytosol into the lumen of the SR per ATP hydrolyzed, by calculating the ratio between Ca^{2+} -uptake at 2000 nM and V_{max} . It should be emphasized that the properties used to determine the ratio were measured under different assay conditions that were optimized for each assay. In particular, V_{max} was assessed in the presence of the Ca^{2+} -ionophore A23187 and at $\text{Ca}^{2+}_{\text{f}} \sim 12.5\text{ }\mu\text{M}$; whereas, Ca^{2+} -uptake rates were determined in the absence of Ca^{2+} -ionophore A23187. Additionally, our measurements of Ca^{2+} -uptake are were completed at 2000 nM since the Ca^{2+} -sensitivity of Indo-1 is limited at high $\text{Ca}^{2+}_{\text{f}}$. We have used the term “apparent coupling ratio” to indicate that the parameters used to calculate this ratio were measured under different assay conditions.

SERCA activity

Measurement of SERCA kinetic properties were measured using a spectrophotometric assay (Simonides & van Hardeveld, 1990) modified by TA Duhamel (unpublished) for use on a plate reader (SPECTRAMax Plus; Molecular Devices) as previously described (Chapter 2,

Methods), with only minor alteration to the assay protocol. In this study, 3 different muscle samples were analyzed simultaneously on a single plate. Each sample was treated as an independent sample and was prepared by adding 40 μL of crude muscle homogenate to 5 mL cocktail buffer. Each sample was then aliquoted (300 μL) into 16 Eppendorf tubes and mixed with Ca^{2+} to generate 14 different Ca^{2+} concentrations ranging between 7.6 and 4.7 pCa units. Assay conditions were identical for each sample as described earlier (Chapter 2, Methods) with one exception. The difference in assay conditions was limited to one Eppendorf tube, in which Ca^{2+} ionophore A23187 was not included in the reaction cocktail. In all other Eppendorf tubes and for all 14 Ca^{2+} -concentrations used to generate the substrate-SERCA activity curve, Ca^{2+} ionophore A23187 (1 μM Sigma C-7522) was included. The Ca^{2+} ionophore A23187 was used to prevent the formation of a large Ca^{2+} gradient across the SR membrane. By measuring maximal SERCA activity in the presence (V_{max}) and in the absence ($V_{\text{max}(-)}$) of Ca^{2+} ionophore A23187, passive Ca^{2+} leak through the SR membrane was assessed. The inclusion of Ca^{2+} -ionophore A23187 allowed for the assessment of V_{max} ; whereas the exclusion of Ca^{2+} -ionophore A23187 from one aliquot of the homogenate cocktail allowed for the assessment of $V_{\text{max}(-)}$. For all samples, the assessment of V_{max} , $V_{\text{max}(-)}$ and calculation of ionophore ratios ($V_{\text{max}} / V_{\text{max}(-)}$), were completed at a pCa of 4.9. On a given analytical day, complete sets of samples from 6 individuals were analyzed for SERCA kinetics in duplicate. Kinetic data obtained using this plate reader technique are similar to results previously published from our group (Duhamel *et al.*, 2005; Duhamel *et al.*, 2004a; Schertzer *et al.*, 2002; Tupling *et al.*, 2001a). The coefficient of variation for V_{max} during this assay is 8.6% when the same sample was analyzed on different days and was 7.4% when analysis was repeated on the same day.

SR Ca^{2+} -uptake

Oxalate-supported Ca^{2+} -uptake rates were measured using the Ca^{2+} fluorescent dye Indo-1 according to the methods of O'Brien *et al.* (O'Brien, 1990; O'Brien *et al.*, 1991), as modified by Ruell *et al.* (Ruell *et al.*, 1995) and our laboratory (Tupling & Green, 2002). Fluorescence measurements were made on a spectrofluorometer (RatiomasterTM system, Photon Technology International) equipped with dual emission monochromators. The measurement of Ca^{2+}_f using this procedure is based on the difference in maximal emission wavelengths between the Ca^{2+} -bound Indo-1 complex and the Ca^{2+} -free Indo-1 complex as described previously in this thesis (Chapter Three) and by O'Brien *et al.* (O'Brien, 1990; O'Brien *et al.*, 1991).

The reaction buffer (pH 7.0) for muscle homogenates contained 200 mM KCl, 20 mM HEPES, 15 mM MgCl_2 , 10 mM NaN_3 , 10 mM PEP, 5 mM oxalate, and 5 μM TPEN. Prior to each assay, 1.5 μM Indo-1, 18 U/mL LDH and 18 U/mL PK were added to the 2 mL of reaction buffer. Immediately before collection of emission spectra, a volume of muscle homogenate was added to the cuvette containing the reaction buffer. Following initiation of data collection, 2.5 μL of 10 mM CaCl_2 was added to the cuvette, which produced a consistent starting Ca^{2+}_f of approximately 3.5 μM . Shortly after the achievement of a constant Ca^{2+}_f , 5 mM ATP was added to the cuvette to initiate Ca^{2+} -uptake. The generated curve from *Equation 2.2*, Ca^{2+}_f versus time, was then smoothed over 21 points using the Savitsky-Golay algorithm. Linear regression was performed on values ranging ± 100 nM, at Ca^{2+}_f of 500, 1000, 1500 and 2000 nM. Differentiating the linear fit curve will allow determination of Ca^{2+} -uptake rates. On a given analytical day, complete sets of samples from 3 individuals were analyzed for Ca^{2+} -uptake kinetics in duplicate. The coefficient of variation for duplicate measurements for Ca^{2+} -

uptake was $7.6 \pm 0.9\%$ when the same sample was analyzed on different days and $7.9 \pm 0.9\%$ when analysis was repeated on the same day.

SR Ca²⁺ -release

Sarcoplasmic reticulum Ca²⁺-release rates were measured according to the methods of Ruell *et al.* (Ruell *et al.*, 1995) as modified by our group (Tupling & Green, 2002). Sarcoplasmic reticulum Ca²⁺-release assays were conducted similar to the Ca²⁺-uptake assay procedures, where a dual emission spectrofluorometer (Ratiomaster™ system, Photon Technology International) records simultaneous photon counts per s for Indo-1 emission wavelengths previously defined. To assess Ca²⁺-release kinetics, homogenate samples were actively loaded with Ca²⁺ until a characteristic plateau in Ca²⁺_f was achieved. At this point, 20 mM 4-chloro-*m*-cresol (4-CMC) was added to the assay mixture to chemically stimulate Ca²⁺-release *in vitro*. The assay protocol results in 2 different Ca²⁺-release rates (Tupling & Green, 2002). Phase 1 Ca²⁺-release has been characterized as the peak rate of the initial fast phase of Ca²⁺-release that lasts ~1-3 s in duration; while Phase 2 Ca²⁺-release has been characterized as the more prolonged, slower rate of Ca²⁺-release lasting from ~4-10 s. Both phases of Ca²⁺-release have been calculated using the same methods as described for Ca²⁺-uptake, where the ionized Ca²⁺ concentration is calculated using *Equation 2.2* (Gryniewicz *et al.*, 1985). Subsequently, differentiating the linear fit curves allows determination of Ca²⁺-release rates. On a given analytical day, Ca²⁺-release kinetics were assessed from complete sets of samples from 3 individuals using the same assay sample as that used to assess Ca²⁺-uptake. The coefficients of variation for duplicate measurements for Ca²⁺-release was not calculated since only single measurements were used for Ca²⁺-release determinations due to tissue limitations.

Protein determination of homogenates was made by the method of Lowry (Lowry & Passonneau, 1972) as modified by Schacterle and Pollock (Schacterle & Pollack, 1973). Samples were analyzed in triplicate to determine protein concentration.

Western blot analysis

To assess PLN phosphorylation, site-specific polyclonal antibodies for anti-serine 16 (Ser16) PLN (sc-12963) and anti-threonine 17 (Thr17) PLN (sc-17024) phosphorylated forms of PLN were purchased from Santa Cruz Biotechnology (Santa Cruz, CA, USA). Crude muscle homogenates were loaded on 12.5% polyacrylamide gels. Proteins were separated using standard SDS-PAGE protocols and transferred to nitrocellulose membranes. After blocking with a 5% skim milk suspension, the membranes were treated with site-specific polyclonal antibodies raised against the Ser16 and Thr17 phosphorylated forms of PLN, washed in Tris-HCl, pH 7.5, 150 mM NaCl, 0.1% Tween 20 (Tris-buffered saline/0.1% Tween), and treated with horseradish peroxidase-conjugated secondary antibody (Santa Cruz Biotechnology). Membranes were washed in Tris-buffered saline, 0.1% Tween, and the signals were detected with an enhanced chemiluminescence kit (Amersham Biosciences) using a bio-imaging system and the GeneSnap software (Syngene) obtained from Fisher. Relative phosphorylation levels were determined by quantifying the optical density of bands at ~ 5-10 kDa and ~25 kDa, as indicated on the material data sheet for the PLN antibodies. For each antibody, the linearity of progressive increases in protein content was established before experiments were conducted (data not shown). Relative protein levels were determined by scanning densitometry and values were expressed as a % of Std. When direct comparisons were made between sampling times,

values were normalized to tissue samples collected at rest (0 min) and expressed as % of rest. All samples were analyzed in duplicate and on different gels.

Statistical analyses

Data are presented as means \pm S.E. A one-way analysis of variance (ANOVA) was utilized to compare differences between the sampling times within each condition. A two-way ANOVA (2 repeated measures) was utilized to discriminate between differences resulting from experimental condition and sampling time for matched samples. The data collected in the subgroup of participants (i.e. 6 of 15 volunteers) who had a tissue sample collected at a matched time corresponding to fatigue in PLAC (i.e. 115 ± 6 min) during both conditions were analyzed using a two-way ANOVA for the subgroup data. Where significant differences were found, Neuman-Kuels post hoc procedures were used to compare specific means. Significance was accepted at $P < 0.05$.

Results

Ride time to fatigue

Average cycle time to fatigue was longer during GLUC (137 ± 7 min), compared to PLAC (115 ± 6 min).

Glucose Supplementation

The total amount of CHO ingested during GLUC was 1.23 ± 0.11 g CHO per kg body mass, compared to 0.00 g CHO per kg body mass ingested during PLAC. The average volume ingested at each time point was 243 ± 17 mL per beverage; while individual volume per

beverage ranged between 100 to 313 mL per drink. Since cycle time to fatigue was significantly longer during GLUC compared to PLAC, participants ingested a greater number of beverages during GLUC (6.7 ± 0.5 beverages) compared to PLAC (5.3 ± 0.5 beverages). Consequently, the total volume of beverage ingested by participants was greater during the GLUC (1564 ± 142 mL) condition compared to PLAC (1262 ± 137 mL).

Respiratory gas measures

The relative exercise intensities were 57.2 ± 1.9 and 57.8 ± 1.2 % $\text{VO}_{2\text{peak}}$ at 15 min of exercise and 59.3 ± 0.7 and 60.3 ± 1.4 % $\text{VO}_{2\text{peak}}$ at 30 min of exercise during the PLAC and GLUC conditions, respectively. No differences in VO_2 , VCO_2 , or RER were observed between conditions at rest or during exercise (Table 4.1). However, main effects of exercise were found for VO_2 , VCO_2 and RER. For VO_2 , Rest < 15 min, 30 min < 60 min, 90 min, 115 \pm 6 min and 137 \pm 7 min. For VCO_2 , Rest < 15 min, 30 min, 60 min, 90 min, 115 \pm 6 min and 137 \pm 7 min. For RER, Rest < 15 min, 30 min > 60 min, 90 min, 115 \pm 6 min and 137 \pm 7 min.

Substrate oxidation

Respiratory exchange ratios were used to calculate substrate oxidation rates through the use of indirect calorimetry (Table 4.2). A main effect of exercise was found for CHO oxidation rates. For CHO oxidation, Rest < 15 min, 30 min, 60 min, 90 min, 120 min, fatigue. Lipid oxidation rates also increased above resting levels during exercise (main effect of exercise; Rest, 15 min, 30 min < 60 min, 90 min, 120 min, fatigue) regardless of condition. No differences between PLAC and GLUC conditions were observed for CHO or lipid oxidation rates.

Blood Hb, Hct and plasma volume changes

Resting Hb and Hct concentrations did not differ between PLAC (15.6 ± 0.7 g%; $45.7 \pm 0.8\%$) and GLUC (15.5 ± 0.6 g%; $45.7 \pm 0.9\%$), respectively. Exercise did increase Hct concentrations by $\sim 5\%$ during exercise in both PLAC and GLUC. However, no differences in Hct concentrations were observed between conditions at any sampling point.

As expected, 30 min of exercise reduced plasma volumes by 7.8 and 8.2% during PLAC and GLUC, respectively. No further changes in plasma volume occurred with exercise. Glucose supplementation did not alter this response.

Blood metabolites

During PLAC, blood glucose concentrations (Figure 4.2, Panel A) displayed the expected response, namely no change from rest for the initial 30 min of exercise, followed by a reduction at 90 min and 115 ± 6 min of exercise. During GLUC, the normal exercise-induced reductions in blood glucose were prevented. Comparisons across conditions indicated that plasma glucose concentrations during GLUC were 15, 19, 23 and 24% higher than those observed during PLAC at 60 min, 90 min, and 115 ± 6 min of exercise, and at fatigue in GLUC (137 ± 7 min) compared to fatigue during PLAC (115 ± 6 min), respectively.

Blood lactate concentrations (Figure 4.2, Panel B) measured during PLAC increased above resting levels with the onset of exercise and peaked at 30 min of exercise. Similar changes in plasma lactate concentrations were observed during GLUC at 15 and 30 min of exercise. No differences in plasma lactate concentrations were observed during the initial 60 min of exercise between PLAC and GLUC. However, differences between conditions were observed during the late stages of exercise. Plasma lactate concentrations were lower during GLUC, compared to

Table 4.1: Respiratory gas exchange measurements measured at rest and during prolonged exercise in the Placebo and Glucose conditions.

	Rest	15 min	30 min	60 min	90 min	115 ± 6 min	137 ± 7 min
VO₂							
PLAC	376 ± 39	1970 ± 105	2047 ± 103	2083 ± 114	2130 ± 77	2234 ± 123	
GLUC	369 ± 26	1987 ± 86	2060 ± 92	2140 ± 85	2194 ± 97	2094 ± 98	2255 ± 90
VCO₂							
PLAC	290 ± 31	1872 ± 106	1959 ± 99	1923 ± 101	1932 ± 71	2059 ± 113	
GLUC	284 ± 22	1881 ± 88	1935 ± 92	1971 ± 86	2010 ± 93	1910 ± 86	2089 ± 95
RER							
PLAC	0.77 ± 0.01	0.95 ± 0.01	0.96 ± 0.01	0.93 ± 0.01	0.91 ± 0.01	0.92 ± 0.01	
GLUC	0.77 ± 0.01	0.95 ± 0.01	0.94 ± 0.01	0.92 ± 0.01	0.92 ± 0.01	0.91 ± 0.01	0.92 ± 0.01

Values are means ± SE (n=15). PLAC, placebo condition. GLUC, glucose condition. Rest, represents 0 min. RER, respiratory exchange ratio, is calculated as the ratio between VCO₂ and VO₂. Units are ml · min⁻¹ for VO₂ and VCO₂. Main effects of exercise (P<0.05) were found for VO₂, VCO₂ and RER. For VO₂, Rest < 15 min, 30 min < 60 min, 90 min, 115 ± 6 min and 137 ± 7 min. For VCO₂, Rest < 15 min, 30 min, 60 min, 90 min, 115 ± 6 min and 137 ± 7 min. For RER, Rest < 15 min, 30 min > 60 min, 90 min, 115 ± 6 min and 137 ± 7 min.

Table 4.2: Calculated substrate oxidation rates at rest and during prolonged exercise in the Placebo and Glucose conditions.

	Rest	15 min	30 min	60 min	90 min	115 ± 6 min	137 ± 7 min
CHO Oxidation							
PLAC	0.48 ± 0.14	12.1 ± 0.85	12.9 ± 0.72	11.3 ± 0.68	11.0 ± 0.70	12.1 ± 0.79	
GLUC	0.45 ± 0.14	12.0 ± 0.78	12.1 ± 0.75	11.5 ± 0.75	11.5 ± 0.71	11.3 ± 0.62	12.0 ± 0.86
Lipid Oxidation							
PLAC	0.14 ± 0.02	0.17 ± 0.03	0.15 ± 0.03	0.29 ± 0.05	0.34 ± 0.04	0.33 ± 0.04	
GLUC	0.14 ± 0.01	0.18 ± 0.03	0.22 ± 0.03	0.31 ± 0.03	0.35 ± 0.04	0.34 ± 0.04	0.34 ± 0.04

Values are means ± SE (n=15). PLAC, placebo condition. GLUC, glucose condition. Rest, represents 0 min. CHO, carbohydrate. Units are mmol · min⁻¹. Main effects of exercise (P<0.05) were found for both CHO and Lipid oxidation. For CHO oxidation, Rest < 15 min, 30 min, 60 min, 90 min and 137 ± 7 min. For lipid oxidation, Rest, 15 min, 30 min < 60 min, 90 min, 115 ± 6 min and 137 ± 7 min.

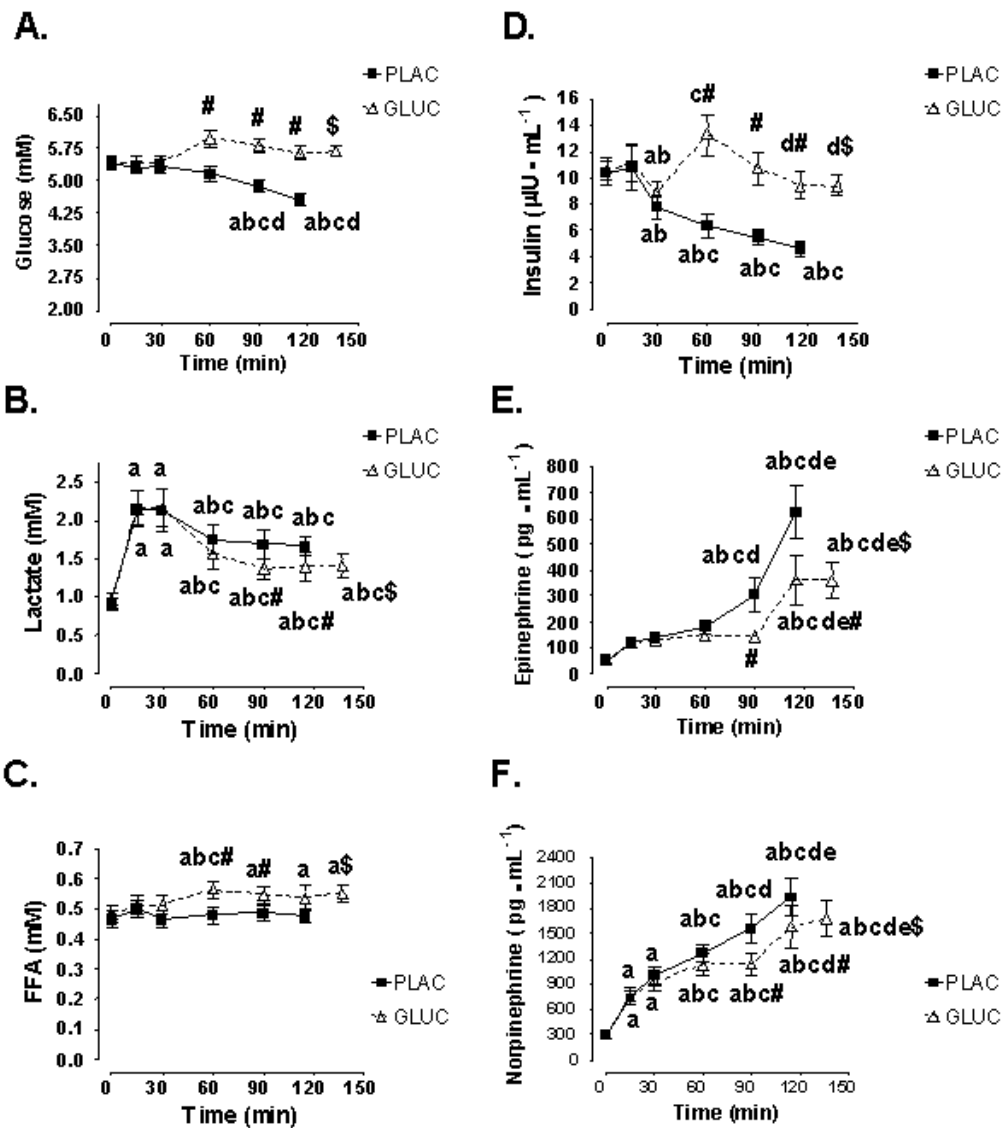


Figure 4.2: Blood metabolite and hormone concentrations measured at rest (0 min) and during prolonged exercise in the placebo (PLAC) and glucose (GLUC) conditions. Values are means \pm SE (n=15). Panel A, glucose. Panel B, lactate. Panel C, free fatty acids (FFA). Panel D: Insulin. Panel E: Epinephrine. Panel F, Norepinephrine. * Significantly different from rest ($P < 0.05$). ^a Significantly different from 15 min ($P < 0.05$). ^c Significantly different from 30 min ($P < 0.05$). ^d Significantly different from 60 min ($P < 0.05$). ^e Significantly different from 90 min ($P < 0.05$). # Significantly different from matched time point in PLAC ($P < 0.05$). \$ Significantly different from PLAC fatigue time point (i.e., 115 ± 6 min) ($P < 0.05$).

PLAC, at 90 min and 115 ± 6 min of exercise and at fatigue in GLUC (137 ± 7 min) compared to fatigue during PLAC (115 ± 6 min).

Serum FFA concentrations (Figure 4.2, Panel C) did not change in response to exercise during PLAC. During GLUC, a rise in serum FFA was observed following 60 min of exercise. As a result, serum FFA concentrations were higher during GLUC compared to PLAC following 60 min and 90 min of exercise, and at fatigue in GLUC (137 ± 7 min) compared to fatigue during PLAC (115 ± 6 min).

Blood hormone concentrations

Resting serum insulin concentrations were 10.4 ± 0.90 and 10.7 ± 0.79 $\mu\text{IU}\cdot\text{mL}^{-1}$ during PLAC and GLUC, respectively. Serum insulin concentrations (Figure 4.2, Panel D) were unchanged by the onset of exercise (i.e. 15 min) but were reduced below resting levels following 30 min of exercise during both PLAC and GLUC. During PLAC, plasma insulin concentrations continued to decrease reaching a minimum value of 4.65 ± 0.63 $\mu\text{IU}\cdot\text{mL}^{-1}$ following 115 ± 6 min of exercise. During GLUC, the normal exercise-induced reductions in plasma insulin concentrations were prevented. In fact, plasma insulin concentrations during GLUC were higher than those observed during PLAC at 60 min, 90 min, 115 ± 6 min and at fatigue in GLUC (137 ± 7 min) compared to fatigue during PLAC (115 ± 6 min).

Resting plasma EPI concentrations were 52 ± 8 and 50 ± 9 $\text{pg}\cdot\text{mL}^{-1}$ during PLAC and GLUC, respectively. Exercise increased EPI (Figure 4.2, Panel E) above resting levels at 90 min of exercise during the PLAC condition, with an even greater increase in EPI being observed following 115 ± 6 min of exercise. Exercise also increased plasma EPI concentrations during GLUC. However, increases in EPI were observed only after 115 ± 6 min of exercise. No

further changes in EPI concentrations beyond this time were observed during GLUC. When comparisons were made between conditions, larger increases in EPI concentrations were observed during PLAC following 90 min and 115 ± 6 min of exercise, and at fatigue in GLUC (137 ± 7 min) compared to fatigue during PLAC (115 ± 6 min).

Exercise also progressively increased NE (Figure 4.2, Panel F) above resting levels during both experimental conditions. However, the increase in NE was much more pronounced during PLAC compared to GLUC following 90 min and 115 ± 6 min of exercise, and at fatigue in GLUC (137 ± 7 min) compared to fatigue during PLAC (115 ± 6 min).

Muscle Metabolites

Muscle ATP concentrations were not altered by exercise or by glucose supplementation (Table 4.3). Additionally, PCr, Pi, Cr, pH, ADP_f, and AMP_f concentrations measured at rest were not different between PLAC and GLUC. However, main effects of exercise were found for PCr, Pi, Cr, pH, ADP_f, and AMP_f concentrations. For PCr, Rest > 30 min, 90 min, 115 ± 6 min and 137 ± 7 min. For Pi and Cr, Rest < 30 min, 90 min, 115 ± 6 min and 137 ± 7 min. For pH, Rest > 30 min and 90 min; 30 min < 90 min. For ADP_f and AMP_f, Rest < 30 min, 90 min, 115 ± 6 min and 137 ± 7 min. Glucose supplementation did not alter this exercise effect since no differences were found between condition regardless of metabolite.

No effect of exercise or glucose supplementation was found for total ATP, ADP or AMP concentrations (Table 4.4). However, a main effect of exercise (Rest < 30 min, 90 min, 115 ± 6 min and 137 ± 7 min) was found for IMP. Glucose supplementation did not alter this exercise effect.

Table 4.3: Selected muscle metabolite concentrations at rest and during prolonged exercise in the Placebo and Glucose conditions.

	Rest	30 min	90 min	115 ± 6 min	137 ± 7 min
ATP					
PLAC	24.0 ± 0.6	23.6 ± 0.7	23.8 ± 0.5	22.5 ± 0.7	
GLUC	23.8 ± 1.0	23.2 ± 0.7	23.8 ± 0.5	23.3 ± 0.8	22.9 ± 0.8
PCr					
PLAC	73.7 ± 3.3	34.7 ± 4.5	38.0 ± 3.6	35.2 ± 4.4	
GLUC	75.2 ± 3.1	40.5 ± 3.6	37.3 ± 4.0	34.6 ± 3.7	37.9 ± 4.5
Pi					
PLAC	43.8 ± 4.4	86.6 ± 9.4	87.7 ± 7.8	97.6 ± 7.9	
GLUC	38.5 ± 4.4	80.0 ± 9.0	87.9 ± 10.0	96.4 ± 12.5	84.1 ± 6.8
Cr					
PLAC	51.3 ± 3.4	90.3 ± 5.8	86.9 ± 5.1	89.8 ± 5.6	
GLUC	46.3 ± 5.0	84.5 ± 4.8	87.7 ± 6.3	95.5 ± 6.5	87.1 ± 5.6
pH					
PLAC	7.04 ± 0.00	6.95 ± 0.02	7.00 ± 0.01	7.02 ± 0.01	
GLUC	7.04 ± 0.00	6.97 ± 0.02	7.01 ± 0.01	7.01 ± 0.01	7.02 ± 0.01
ADP_i					
PLAC	119 ± 13	469 ± 100	382 ± 48	451 ± 68	
GLUC	107 ± 9	367 ± 92	427 ± 67	403 ± 52	404 ± 58
AMP_i					
PLAC	0.7 ± 0.2	14.4 ± 6.6	7.1 ± 1.6	9.1 ± 3.4	
GLUC	0.5 ± 0.1	10.1 ± 6.5	9.5 ± 2.6	9.0 ± 2.2	9.5 ± 3.3

Values are means ± SE (n=15). PLAC, placebo condition. GLUC, glucose condition. Rest, represents 0 min. Units are mM units · kg⁻¹ dry wt. ATP, Adenosine triphosphate; PCr, phosphocreatine; Pi, inorganic phosphate; Cr, creatine; pH, calculated hydrogen concentration (negative logarithm of hydrogen concentration); ADP_i, calculated free adenosine diphosphate concentration; AMP_i, calculated free adenosine monophosphate concentration. Main effects of exercise (P<0.05) were found for PCr, Pi, Cr, pH, ADP_i and AMP_i. For PCr, Rest > 30 min, 90 min, 115 ± 6 min and 137 ± 7 min. For Pi and Cr, Rest < 30 min, 90 min, 115 ± 6 min and 137 ± 7 min. For pH, Rest > 30 min and 90 min; 30 min < 90 min. For ADP_i and AMP_i, Rest < 30 min, 90 min, 115 ± 6 min and 137 ± 7 min.

Table 4.4: Muscle nucleotide concentrations measured at rest and during prolonged exercise in the Placebo and Glucose conditions.

		Rest	30 min	90 min	115 ± 6 min	137 ± 7 min
ATP	PLAC	24.3 ± 0.7	23.6 ± 0.6	23.5 ± 0.5	23.5 ± 1.3	
	GLUC	24.1 ± 0.8	23.1 ± 0.7	23.7 ± 0.5	23.1 ± 0.6	22.4 ± 0.9
ADP	PLAC	4.83 ± 0.23	5.18 ± 0.21	4.83 ± 0.20	4.86 ± 0.23	
	GLUC	4.65 ± 0.19	4.73 ± 0.15	4.94 ± 0.15	4.66 ± 0.19	4.64 ± 0.24
AMP	PLAC	0.146 ± 0.01	0.191 ± 0.03	0.140 ± 0.01	0.175 ± 0.02	
	GLUC	0.149 ± 0.01	0.166 ± 0.02	0.164 ± 0.01	0.150 ± 0.01	0.170 ± 0.01
IMP	PLAC	0.133 ± 0.02	0.354 ± 0.08	0.492 ± 0.12	0.617 ± 0.13	
	GLUC	0.132 ± 0.16	0.321 ± 0.09	0.400 ± 0.10	0.475 ± 0.12	0.487 ± 0.15

Values are means ± SE (n=15). PLAC, placebo condition. GLUC, glucose condition. Rest, represents 0 min. Units are mM units · kg⁻¹ dry wt. ATP, adenosine triphosphate; ADP, adenosine diphosphate; AMP, adenosine monophosphate. IMP, inosine monophosphate. A main effect of exercise (Rest < 30 min, 90 min, 115 ± 6 min and 137 ± 7 min; P<0.05) was found for IMP.

Table 4.5: Selected muscle glycolytic intermediate concentrations measured at rest and during prolonged exercise in the Placebo and Glucose conditions.

	Rest	30 min	90 min	115 ± 6 min	137 ± 7 min
Glucose					
PLAC	1.75 ± 0.17	4.23 ± 0.82	2.50 ± 0.35	1.79 ± 0.30	
GLUC	2.11 ± 0.26	4.57 ± 0.98	2.32 ± 0.21	2.04 ± 0.40	2.57 ± 0.25
G-1-P					
PLAC	0.07 ± 0.01	0.13 ± 0.02	0.08 ± 0.01	0.05 ± 0.01	
GLUC	0.03 ± 0.01	0.11 ± 0.03	0.07 ± 0.01	0.09 ± 0.03	0.06 ± 0.01
G-6-P					
PLAC	0.27 ± 0.08	0.57 ± 0.18	0.59 ± 0.15	0.31 ± 0.12	
GLUC	0.17 ± 0.06	0.61 ± 0.23	0.28 ± 0.08	0.40 ± 0.17	0.23 ± 0.08
F-6-P					
PLAC	0.06 ± 0.02	0.12 ± 0.03	0.12 ± 0.03	0.08 ± 0.02	
GLUC	0.04 ± 0.01	0.13 ± 0.04	0.07 ± 0.02	0.09 ± 0.03	0.07 ± 0.02
Pyr					
PLAC	0.22 ± 0.05	0.24 ± 0.05	0.23 ± 0.04	0.18 ± 0.03	
GLUC	0.23 ± 0.06	0.25 ± 0.06	0.20 ± 0.04	0.16 ± 0.04	0.19 ± 0.02
Lac					
PLAC	5.29 ± 0.62	25.7 ± 4.4	14.9 ± 3.2	9.87 ± 2.2	
GLUC	5.80 ± 1.2	21.1 ± 4.1	13.1 ± 2.6	11.0 ± 3.5	9.67 ± 1.5

Values are means ± SE (n=15). PLAC, placebo condition. GLUC, glucose condition. Rest, represents 0 min. Units are mM units · kg⁻¹ dry wt. G-1-P, glucose-1-phosphate; G-6-P, glucose-6-phosphate; F-6-P, fructose-6-phosphate; Pyr, pyruvate. Lac, lactate. A main effect of exercise (P<0.05) was found for glucose, G-1-P, G-6-P, F-6-P, and Lac. For glucose and G-1-P, Rest < 30 min, 90 min, 30 min > 90 min, 115 ± 6 min and 137 ± 7 min. For G-6-P and F-6-P, Rest < 30 min; 30 min > 115 ± 6 min and 137 ± 7 min. For Lac, Rest < 30 min, 90 min, 115 ± 6 min and 137 ± 7 min; 30 min > 90 min, 115 ± 6 min and 137 ± 7 min.

The effects of exercise on glycolytic intermediates (Table 4.5) depended on the specific intermediate examined. Pyruvate concentrations were not altered by exercise during either condition. In contrast, muscle glucose, G-1-P, G-6-P, F-6-P, and lactate concentrations were all elevated by exercise (main effect), typically peaking at 30 min. For glucose and G-1-P, Rest < 30 min, 90 min; 30 min > 90 min, 115 ± 6 min and 137 ± 7 min. For G-6-P and F-6-P, Rest < 30 min; 30 min > 115 ± 6 min and 137 ± 7 min. For Lac, Rest < 30 min, 90 min, 115 ± 6 min and 137 ± 7 min ; 30 min > 90 min, 115 ± 6 min and 137 ± 7 min. Glucose supplementation during exercise did not alter the response for any of the intermediates at any time point.

Pre-exercise total glycogen, proglycogen and macroglycogen concentrations were not different between experimental conditions (Figure 4.3). During exercise in PLAC, total muscle glycogen content was reduced by 42, 66, and 76% after 30 min, 90 min and at fatigue, respectively. During GLUC, total muscle glycogen content was reduced by 40, 62, 68 and 72% after 30 min, 90 min, 115 ± 6 min and 137 ± 7 min of exercise. Similar percent changes were also observed during exercise for proglycogen and macroglycogen data. Glucose supplementation did not alter total glycogen, proglycogen or macroglycogen content at any time point during exercise.

Sarcoplasmic reticulum properties

Resting V_{\max} were not different between PLAC and GLUC conditions. Exercise reduced SERCA V_{\max} (main effect of exercise) during both PLAC and GLUC conditions (Table 4.6; Figure 4.4, Panel A). During PLAC, V_{\max} were depressed by 10.9 and 18.2% after 90 min and 115 ± 6 min of exercise, respectively. During GLUC, V_{\max} were depressed by 7.4, 12.4 and

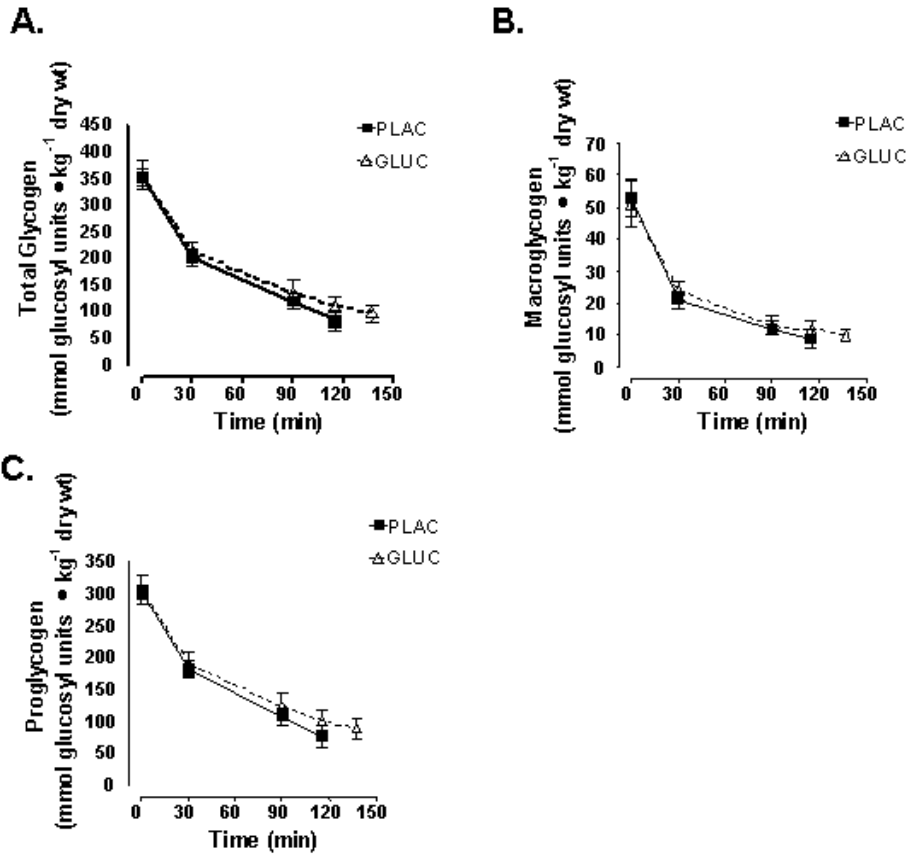


Figure 4.3: Muscle glycogen concentrations measured at rest (0 min) and during prolonged exercise in the placebo (PLAC) and glucose (GLUC) conditions. Values are means \pm SE (n=15). Panel A, total glycogen content. Panel B, macroglycogen content. Panel C, proglycogen content. A main effect of exercise (Rest > 30 min > 90 min > 115 \pm 6 min > 137 \pm 7 min; $P < 0.05$) was found for total, pro and macro glycogen content.

Table 4.6: Sarcoplasmic reticulum Ca^{2+} -ATPase kinetic parameters measured in muscle homogenates collected at rest and during exercise in the placebo and glucose conditions.

	Rest	30 min	90 min	115 ± 6 min	137 ± 7 min	
V_{\max}	PLAC	174 ± 7	162 ± 7	155 ± 6	142 ± 5	
	GLUC	177 ± 10	164 ± 7	161 ± 8	152 ± 6	143 ± 5
n_H	PLAC	1.60 ± 0.05	1.57 ± 0.04	1.56 ± 0.05	1.53 ± 0.05	
	GLUC	1.53 ± 0.04	1.58 ± 0.06	1.63 ± 0.07	1.59 ± 0.04	1.59 ± 0.06
Ca_{50}	PLAC	711 ± 58	694 ± 64	644 ± 50	730 ± 34	
	GLUC	713 ± 46	711 ± 67	625 ± 50	641 ± 49	637 ± 56
$V_{\max(-)}$	PLAC	35 ± 2	34 ± 2	33 ± 2	31 ± 2	
	GLUC	37 ± 2	34 ± 2	33 ± 2	31 ± 1	32 ± 2
Ionophore Ratio	PLAC	5.06 ± 0.20	4.86 ± 0.22	4.87 ± 0.27	4.67 ± 0.18	
	GLUC	4.81 ± 0.15	5.17 ± 0.29	4.99 ± 0.24	5.01 ± 0.18	4.71 ± 0.24
Basal ATPase	PLAC	11.6 ± 1.8	13.6 ± 2.5	12.0 ± 1.8	9.9 ± 1.8	
	GLUC	9.8 ± 1.6	11.4 ± 1.4	13.3 ± 1.9	10.2 ± 1.5	11.3 ± 2.2

Values are means ± SE (n=15). PLAC, placebo condition. GLUC, glucose condition. Rest, represents 0 min. V_{\max} maximal SERCA activity. n_H Hill slope defined as the relationship between SERCA activity and $[\text{Ca}^{2+}]_i$ for 10 to 90% V_{\max} . Ca_{50} the Ca^{2+} -concentration at $\frac{1}{2} V_{\max}$. Assessment of V_{\max} and calculation of ionophore ratios ($V_{\max} / V_{\max(-)}$), were completed at a pCa of 4.9 for all samples. V_{\max} was assessed in the presence of Ca^{2+} -ionophore A23187; while $V_{\max(-)}$ was assessed in the absence of Ca^{2+} -ionophore A23187. Ionophore ratios were calculated as the ratio between V_{\max} and $V_{\max(-)}$. pCa, is the negative logarithm of the Ca^{2+} concentration. Basal ATPase rates were measured in the presence of 1 μL cyclopiazonic acid (CPA), which is a specific inhibitor of SERCA. Units are nmol · mg protein⁻¹ · min⁻¹ for V_{\max} and basal ATPase. Units are nM for Ca_{50} . Ionophore ratio and n_H are relative units. A main effect of exercise ($P < 0.05$, Rest and 30 min > 90 min > 115 ± 6 min and 137 ± 7 min) was found for V_{\max} .

17.5% after 90 min, 115 ± 6 min and 137 ± 7 min of exercise, respectively. Glucose supplementation did not alter the exercise-induced reductions in V_{\max} .

Analysis of Ca^{2+} -dependent SERCA activities allowed for the assessment of additional kinetic parameters, including n_{H} and Ca_{50} (Table 4.6). During PLAC, n_{H} and Ca_{50} values measured in tissue collected at rest were 1.60 ± 0.05 and 711 ± 58 nM, respectively. During GLUC, n_{H} and Ca_{50} values were 1.53 ± 0.04 and 713 ± 46 nM, respectively. Neither exercise nor condition altered n_{H} or Ca_{50} .

To assess passive leak of Ca^{2+} through the SR membrane, we assessed SERCA activity in the absence (i.e. $V_{\max(-)}$) of Ca^{2+} ionophore A23187 (Table 4.6). No differences $V_{\max(-)}$ were observed at rest or at matched time points during exercise between conditions. Ionophore ratios, defined as $V_{\max} / V_{\max(-)}$, were not affected by exercise or by the glucose supplementation protocol (Table 4.6). Similarly, no differences were observed for Basal ATPase activities during exercise or between conditions at matched time points in PLAC and GLUC (Table 4.6).

To examine differences in SR Ca^{2+} -uptake rates ($\text{nmol} \cdot \text{mg protein}^{-1} \cdot \text{min}^{-1}$) between PLAC and GLUC conditions, we assessed Ca^{2+} -transport activity at 2000 nM in crude muscle homogenates using the fluorescent dye Indo-1 (Figure 4.4, Panel B). No differences in resting Ca^{2+} -uptake rates were observed between PLAC (6.4 ± 0.3) and GLUC (6.3 ± 0.4). Exercise reduced (main effect; Rest > 30 min and 90 min > Fatigue) Ca^{2+} -uptake rates during both PLAC and GLUC conditions. During PLAC, Ca^{2+} -uptake rates were reduced by 10.8, 15.8 and 26.9% after 30 min, 90 min, and 115 ± 6 min of exercise, respectively. During the GLUC condition, Ca^{2+} -uptake rates were depressed by 9, 9, 17 and 25% after 30 min, 90 min, 115 ± 6 min and 137 ± 7 min of exercise, respectively. No differences were observed between

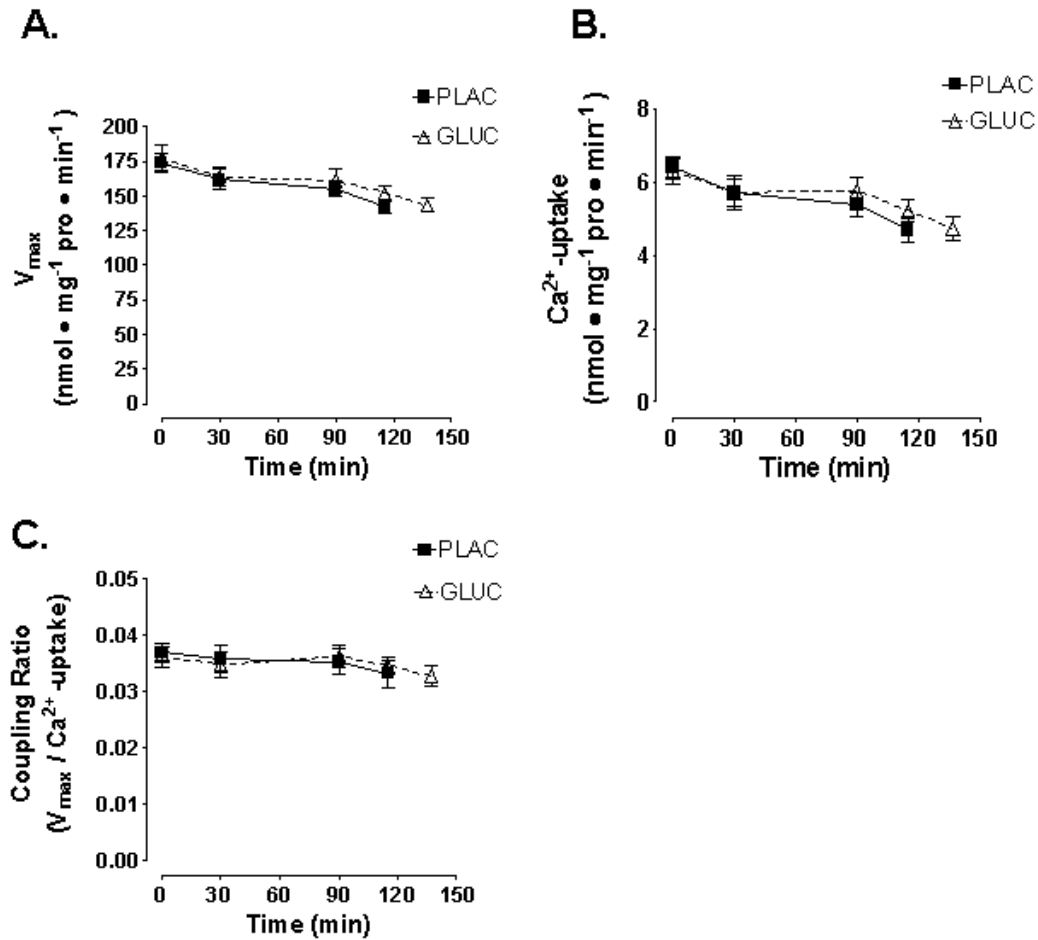


Figure 4.4: Sarcoplasmic reticulum Ca^{2+} -transport parameters measured at rest (0 min) and during prolonged exercise in the placebo (PLAC) and glucose (GLUC) conditions. Values are means \pm SE (n=15). Panel A, maximal SERCA activity (V_{max}). Panel B, calcium dependent Ca^{2+} -uptake rates assessed at 2000 nM Ca^{2+} . Panel C, Apparent coupling ratio. Apparent coupling ratios are relative units and are calculated as the ratio between Ca^{2+} uptake, assessed at 2000 nM Ca^{2+} and V_{max} . A main effect of exercise (Rest and 30 min > 90 min > 115 \pm 6 min and 137 \pm 7 min; $P < 0.05$) was found for V_{max} and Ca^{2+} -uptake.

conditions at any time point. In addition to Ca^{2+} -uptake measurements made at 2000 nM, we also assessed Ca^{2+} -uptake rates at 1500, 1000, and 500 nM (data not shown). The changes with exercise at these Ca^{2+} -concentrations were not different from those observed at 2000 nM. Glucose supplementation did not alter the response observed during exercise at any of these Ca^{2+} -concentrations.

To assess the effects of exercise and glucose supplementation on the efficiency of Ca^{2+} -transport across the SR membrane, we have calculated apparent coupling ratios (Ca^{2+} uptake rate at 2000 nM / V_{max}) (Figure 4.4, Panel C). No effect of exercise or glucose supplementation was found for apparent coupling ratios during either PLAC or GLUC.

No differences in resting Ca^{2+} -release rates ($\text{nmol}\cdot\text{mg protein}^{-1}\cdot\text{min}^{-1}$; Figure 4.5) were observed between PLAC (Phase 1, 23.4 ± 1.3 ; Phase 2, 7.3 ± 0.4) and GLUC (Phase 1, 23.0 ± 1.1 ; Phase 2, 7.3 ± 0.5), respectively. Exercise reduced (main effect of exercise) both Phase 1 and Phase 2 Ca^{2+} -release rates in both PLAC and GLUC conditions. For Phase 1 Ca^{2+} -release, Rest > 30 min, 90 min, 115 ± 6 min and 137 ± 7 min; 30 min > 115 ± 6 min and 137 ± 7 min). For Phase 2 Ca^{2+} -release, Rest > 30 min, 90 min, 115 ± 6 min and 137 ± 7 min; 90 min > 115 ± 6 min and 137 ± 7 min. Glucose supplementation did not alter the exercise-induced reductions in Ca^{2+} -release kinetics.

Phospholamban phosphorylation status

No effect of exercise or glucose supplementation was found for the 25 kDa and 10 kDa bands representing Ser16 PLN phosphorylation (Table 4.7). Similarly, the 25 kDa Thr17 phosphorylation band was unaltered by exercise or by glucose supplementation. In contrast, a

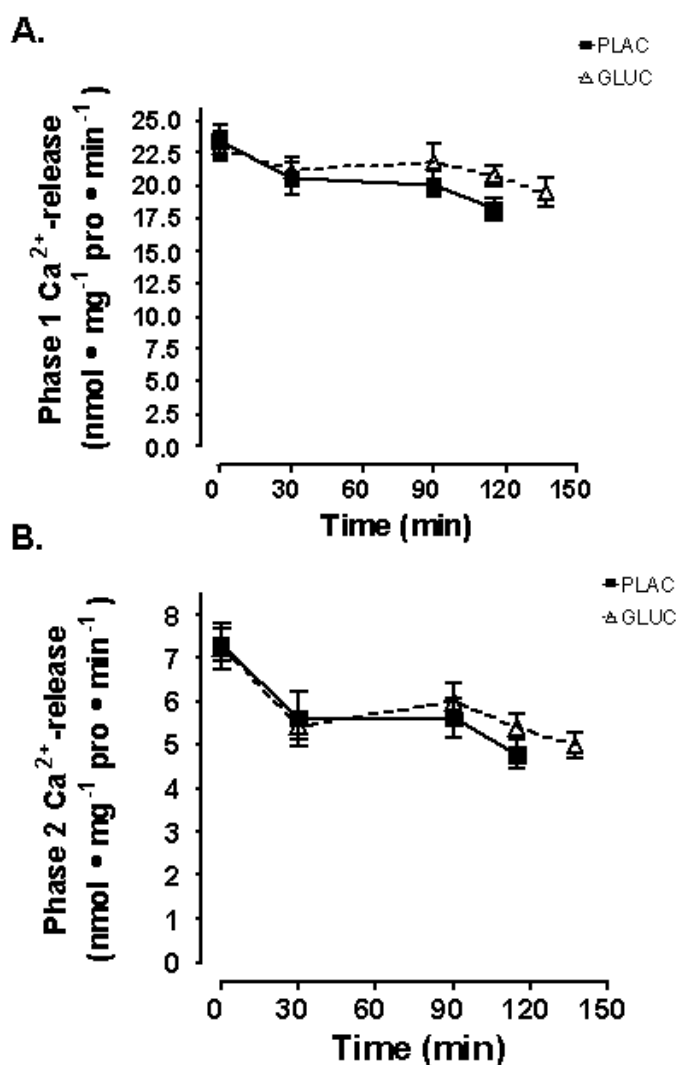


Figure 4.5: Sarcoplasmic reticulum Ca²⁺-release parameters measured at rest (0 min) and during prolonged exercise in the placebo (PLAC) and glucose (GLUC) conditions. Values are means \pm SE (n=15). Panel A, Phase 1 Ca²⁺-release, the initial, rapid rate of release. Panel B, Phase 2 Ca²⁺-release, the more prolonged, slower rate of release which follows Phase 1. A main effect of exercise (Rest > 30 min, 90 min, 115 \pm 6 min and 137 \pm 7 min; 30 min > 115 \pm 6 min and 137 \pm 7 min P<0.05) was found for Phase 1 Ca²⁺-release. A main effect of exercise (Rest > 30 min, 90 min, 115 \pm 6 min and 137 \pm 7 min; 90 min > 115 \pm 6 min and 137 \pm 7 min P<0.05) was found for Phase 2 Ca²⁺-release.

Table 4. 7: Phospholamban phosphorylation status measured at rest and during prolonged exercise in the Placebo and Glucose conditions.

	Rest	30 min	90 min	115 ± 6 min	137 ± 7 min
Ser16 ~ 25 kDa band					
PLAC	100.0	107.4 ± 7.7	106.2 ± 8.0	110.2 ± 8.9	
GLUC	100.0	99.3 ± 7.4	100.5 ± 7.8	99.3 ± 7.7	102.2 ± 8.2
Ser16 ~ 10 kDa band					
PLAC	100.0	98.4 ± 4.3	104.6 ± 8.0	104.0 ± 8.1	
GLUC	100.0	103.1 ± 6.3	101.6 ± 6.7	104.4 ± 9.9	103.6 ± 8.6
Thr17 ~25 kDa band					
PLAC	100.0	110.8 ± 7.7	99.6 ± 6.1	102.2 ± 8.9	
GLUC	100.0	101.0 ± 5.9	96.9 ± 4.4	96.1 ± 7.6	105.6 ± 10.6
Thr17 ~ 10 kDa band					
PLAC	100.0	122.5 ± 6.3	104.6 ± 8.5	105.5 ± 7.9	
GLUC	100.0	108.4 ± 5.4	96.4 ± 5.2	98.1 ± 6.1	104.1 ± 8.5

Values are means ± SE (n=15). PLAC, placebo condition. GLUC, glucose condition. Rest, represents 0 min. Units are arbitrary units expressed relative to the rest value for each condition (% rest). Ser16, the phosphorylated form of phospholamban on Serine16. Thr17, the phosphorylated form of phospholamban on Threonine17. A main effect of exercise (Rest < 30 min > 90 min, 115 ± 6 min and 137 ± 7 min; P<0.05) was found for the 10 kDa band of Thr17.

main effect of exercise was found for the 10 kDa Thr17 phosphorylation band. For the 10 kDa Thr17 phosphorylation band, Rest < 30 min > 90 min, 115 ± 6 min and 137 ± 7 min.

Discussion

This study investigated the hypothesis that oral glucose supplementation attenuates the onset of exercise-induced reductions in SR Ca^{2+} -handling properties in human skeletal muscle. As a consequence, glucose supplementation would associate with the increased cycle time to fatigue. Based on previous data (Duhamel *et al.*, 2006c), we also hypothesized that n_{H} , Ca_{50} and PLN phosphorylation would not differ between conditions as a result of the exercise-induced changes in regulatory hormones even though glucose supplementation is expected to create increased insulin and decreased EPI and NE concentrations. Our data confirms that prolonged exercise without glucose supplementation reduced V_{max} , Ca^{2+} -uptake and Ca^{2+} -release properties in a time-dependent fashion (Duhamel *et al.*, 2005; Duhamel *et al.*, 2006c; Duhamel *et al.*, 2004a; Duhamel *et al.*, 2004b). Moreover, exercise does not alter the Ca^{2+} -sensitivity (i.e. n_{H} or Ca_{50}) of SERCA, the efficiency of Ca^{2+} -transport (i.e. apparent coupling ratio) or permeability of the SR membrane for Ca^{2+} (i.e. ionophore ratio) (Duhamel *et al.*, 2005; Duhamel *et al.*, 2006c; Duhamel *et al.*, 2004a; Duhamel *et al.*, 2004b). As expected, exercise performance was improved with glucose supplementation, as indicated by the ~22 min longer time to fatigue. However, this ergogenic effect cannot be explained by differences in skeletal muscle SR Ca^{2+} -handling properties since, contrary to our hypothesis, glucose supplementation was without additional effect in modifying the exercise response. Nonetheless, our data does support our hypothesis that glucose supplementation during exercise did not alter SERCA Ca^{2+} -sensitivity (i.e. n_{H} or Ca_{50}) or PLN phosphorylation.

This study is the first to examine the effects of alterations in plasma glucose and the associated changes in the glucoregulatory hormone (i.e. catecholamines and insulin) concentrations on SR function in human skeletal muscle by directly manipulating these properties during exercise through the administration of oral glucose supplements. The oral glucose supplementation protocol used in this study caused plasma glucose, EPI, and NE concentrations to be elevated by 16-19, 73-138 and 15-30%, respectively, while insulin concentrations were reduced by 49-61% at matched exercise time points in GLUC, compared to PLAC. Additionally, our data also support previous literature (McConnell *et al.*, 1999; Coyle *et al.*, 1986; Lee-Young *et al.*, 2006) indicating that glucose supplementation does not alter endogenous glycogen utilization during exercise in humans. Collectively, these observations are important to our hypothesis since we have successfully altered plasma glucose, catecholamine and insulin concentrations without altering muscle glycogen utilization during exercise.

The observations made in this paper contribute to the growing body of evidence demonstrating that prolonged, moderate intensity exercise causes a progressive reduction in SR Ca^{2+} -handling properties in human skeletal muscle when assessed *in vitro* (Booth *et al.*, 1997; Duhamel *et al.*, 2004a; Duhamel *et al.*, 2006c; Duhamel *et al.*, 2005; Favero *et al.*, 1993; Tupling *et al.*, 2003). Our results also confirm that the exercise-induced reductions in V_{\max} occurred in the absence of changes in Ca^{2+} -sensitivity of the enzyme, as indicated by a lack of change in n_H and Ca_{50} , the apparent coupling ratio and the ionophore ratio (Duhamel *et al.*, 2005; Duhamel *et al.*, 2006c; Duhamel *et al.*, 2004a; Duhamel *et al.*, 2004b). Based on previous studies employing prolonged exercise in rats (Luckin *et al.*, 1991) and chronic low-frequency stimulation in rats and rabbits (Dux *et al.*, 1990), the reductions in Ca^{2+} -uptake can

most probably be explained by reductions in V_{\max} observed during exercise in this study. The reduction in V_{\max} can most likely be attributed to a reduction in the number of functional SERCA proteins (Favero, 1999). Such a reduction in SERCA function has been associated with structural alterations in the region of the nucleotide-binding site of the enzyme and occurs as a result of protein oxidation (Klebl *et al.*, 1998; Matsushita & Pette, 1992) and nitration induced by the accumulation of ROS (Klebl *et al.*, 1998) during repetitive activity.

Accompanying the exercise-induced reductions in V_{\max} and Ca^{2+} -uptake rates were reductions in SR Ca^{2+} -release kinetics. We have utilized a two-phase kinetic model to characterize distinct phases of Ca^{2+} release that occur following the addition of the Ca^{2+} -release agent 4-CMC. Phase 1 Ca^{2+} -release has been characterized as the initial fast phase of Ca^{2+} -release that lasts for ~1-3 s in duration; while Phase 2 Ca^{2+} -release has been characterized as the more prolonged, slower rate of Ca^{2+} -release occurring from ~4-10 s after the addition of 4-CMC (Tupling & Green, 2002). In this study, exercise-induced reductions occurred for both Phase 1 and Phase 2 Ca^{2+} -release rates with the reductions similar in both time and magnitude. Although the physiological significance of each Ca^{2+} -release phase remains unclear, it is likely that a similar mechanism was acting to reduce both phases of Ca^{2+} -release. Based on previous studies employing prolonged exercise in rats (Favero *et al.*, 1993), it would appear the disturbances in Ca^{2+} -release can be attributed to a reduction in the number of functional CRC, possibly as a result of protein oxidation associated with the accumulation of ROS (Favero, 1999).

Contrary to our hypothesis, we found no effect of oral glucose supplementation in modifying the SR Ca^{2+} -cycling responses to prolonged exercise. This was unexpected, given the beneficial effects of glucose on the regulation of cytosolic Ca^{2+}_f and the restoration of

contractile function (Chin & Allen, 1997). In our experimental design, oral glucose supplementation began at 30 min of exercise, providing a lead in period to allow for the exercise response to become established. Differences between PLAC and GLUC in the SR properties examined were expected at 90 min of exercise, the first tissue sampling point after the beginning of glucose supplementation and at the matched time point beyond 90 min of exercise, representing the point of fatigue in NG. Since our hypothesis was based on several previous studies using repetitive contractions which demonstrated a protective effect on a SR Ca^{2+} -function during increased CHO availability, at least with regard to muscle glycogen (Chin & Allen, 1997; Cuenda *et al.*, 1995; Duhamel *et al.*, 2006c; Lees *et al.*, 2001), the failure to find a glycemic effect invites further examination. However, it should be noted that our SR Ca^{2+} -cycling measurements were made *in vitro*, and therefore do not rule out the possibility that glucose supplementation may influence SR Ca^{2+} -cycling properties *in vivo*.

Oral glucose supplementation could promote a variety of responses, many of which could potentially affect SR function during the exercise state. To examine these possibilities, it was first necessary to determine that our glucose supplement schedule could abolish the reduction in blood glucose observed at 90 min of exercise and beyond. As expected, based on previous studies (Coggan & Coyle, 1991; Coyle, 1992a; McConnell *et al.*, 1999), blood glucose remained stable throughout exercise in GLUC. Accordingly, maintenance of blood glucose concentration could affect SR responses during exercise by altering muscle substrate utilization and metabolism and/or by altering the blood concentrations of selected hormones, known to alter cellular signaling mechanisms involved with short-term regulation of the SR. The role of glucose feedings on the response of these properties represented the second objective of this study.

To examine the possibility that glucose supplementation could have affected phosphorylation potential and/or metabolite accumulation and consequently SR Ca^{2+} -cycling in working muscle, we have measured the concentration of the high-energy phosphates (i.e. ATP, PCr, ADP_f , AMP_f), selected metabolites (i.e. Pi and Cr), and selected glycolytic intermediates (i.e. G-1-P, G-6-P, F-6-P, Pyr and Lac). We also measured IMP concentrations since this property is regarded as a more sensitive indicator of changes in ATP concentration during exercise (Hochachka & Matheson, 1992). Although we found the expected changes in these compounds with exercise, we did not observe any additional changes in these compounds during exercise with glucose supplementation. Generally, these data support previous studies that have examined the influence that glucose supplementation has on metabolic parameters (Coyle *et al.*, 1986; Lee-Young *et al.*, 2006; McConell *et al.*, 1999). However, our IMP data does not support the observations made by Spencer *et al.* (Spencer *et al.*, 1991) indicating that glucose supplementation attenuates the exercise-induced accumulation of IMP. The most likely explanation for this difference is the higher work rate ($\sim 70\% \text{VO}_{2\text{peak}}$) employed in their study compared to ours. This observation was important to the interpretation of our data since several papers in the literature have indicated that high-energy phosphate transfer (Rossi *et al.*, 1990) and glycolytic-derived ATP (Xu *et al.*, 1995) may preferentially fuel membrane functions such as ion transport (Rossi *et al.*, 1990; Xu *et al.*, 1995; Han *et al.*, 1992). The fact that we have not found an effect of glucose supplementation on energy metabolism during exercise may explain, at least in part, our failure to find an effect of glucose supplementation on SR Ca^{2+} -cycling since accumulation of one or more of these compounds have been shown to alter both Ca^{2+} -uptake (Tupling, 2004) and Ca^{2+} -release (Favero, 1999) *in vitro*.

Our hypothesis regarding the role of glucose supplementation on SR Ca^{2+} -cycling was also based on a potential difference in glycogen content during exercise with or without glucose supplementation. To investigate this possibility, we have assessed the metabolically distinct glycogen subfractions, namely proglycogen and macroglycogen, to determine if glucose supplementation during exercise could influence the utilization of particular subfraction (Derave *et al.*, 2000; Marchand *et al.*, 2002). As expected, proglycogen represented the predominant glycogen subfraction prior to exercise (Marchand *et al.*, 2002). During PLAC, exercise progressively reduced both proglycogen and macro glycogen contents in a manner similar to the changes in total glycogen content. Glucose supplementation did not alter this response. Since it appears that glucose supplementation did not alter the utilization pattern of glycogen subfractions in human skeletal muscle, it would follow that SR Ca^{2+} -cycling behaviour would not be affected. Since muscle glycogen levels appear to be directly involved in modifying the contractile-induced effect on SR Ca^{2+} -cycling (Chin & Allen, 1997; Duhamel *et al.*, 2006c; Lees *et al.*, 2001), the failure of our intervention to modify glycogen contents may be important in our inability to realize an experimental effect on SR responses. Unfortunately, tissue limitations associated with the human muscle biopsy technique did not allow us to assess the amount of glycogen bound to the SR. As a result, the possibility that glucose supplementation may alter the utilization pattern of glycogen in close proximity to the SR during exercise still exists.

A particularly inviting possibility for glucose supplementation to effect changes in SR function during exercise is via differences in selected blood hormonal responses. Blood glucose levels have a potent effect in regulating the secretion of both insulin from the pancreas and the catecholamines from the adrenal medulla (Cryer, 1993; Wasserman & Cherrington,

1996). Our results demonstrate marked differences between conditions in the response of these hormones to exercise. With GLUC, the normal reduction in serum insulin to prolonged exercise was blunted while both the EPI and NE time-dependent increases with exercise were substantially reduced. Our findings indicate that by preventing declines in blood glucose during prolonged exercise, the concentration of these hormones can be substantially altered. Our observations are similar to other studies that have reported similar effects on these hormones with glucose supplementation administered during sustained submaximal exercise (Galbo, 1999)

The blunting of the catecholamine response with GLUC would be expected to modify the intrinsic regulation of both SERCA and the CRC. It is generally accepted that EPI can affect increases in PLN phosphorylation through cAMP-dependent mechanisms, resulting in an increase in Ca^{2+} -sensitivity in the absence of changes in V_{max} of the enzyme (Gramolini *et al.*, 2006; MacLennan *et al.*, 2003). Since we failed to observe changes in SERCA kinetic properties, an increase in plasma EPI concentration by itself is not effective in modifying the Ca^{2+} -sensitivity of the enzyme. The lack of change in Ca^{2+} -sensitivity is also supported by our measurements of site-specific phosphorylation of PLN at Ser16 and Thr17, where expected increases (Rose *et al.*, 2006) were not observed. Specifically, our data indicate that exercise did not alter the PLN Ser16 phosphorylation during either PLAC or GLUC. Moreover, exercise did not alter PLN Thr17 phosphorylation assessed at 25 kDa, but did increase PLN Thr17 phosphorylation assessed at 10 kDa during both PLAC and GLUC at 30 min of exercise, before returning to pre-exercise levels as exercise progressed. Glucose supplementation did not modify PLN Ser16 or Thr17 phosphorylation during exercise. It is not clear why our results do not support the observations made by Rose *et al.* (Rose *et al.*, 2006); however it is possible that

differences in analytical techniques may have contributed to the observed differences. For example, protein kinase or phosphatase inhibitors were not added to the homogenizing medium used to characterize PLN phosphorylation in our study; whereas it was unclear if Rose *et al.* (Rose *et al.*, 2006) used protein kinase or phosphatase inhibitors. Another possibility to explain the apparent insignificant effect of glucose supplementation on SERCA Ca²⁺-sensitivity and PLN phosphorylation may be related to the exercise effect per se. For example, it is possible that the exercise-induced activation of protein kinase and phosphatase pathways creates contrasting effects that do not result in changes in net phosphorylation of PLN, which may, in part, contribute to the lack of change in Ca₅₀ and n_H during exercise with or without glucose supplementation.

Our experimental design also enables us to gain further insight into the regulation of CRC function during conditions where plasma catecholamine and insulin concentrations have been manipulated by oral glucose supplementation. Epinephrine and insulin signaling can activate various protein kinase and phosphatase pathways to alter CRC phosphorylation (MacLennan *et al.*, 2002; Reiken *et al.*, 2003; Liu & Brautigan, 2000), thereby regulating the open probability of the CRC. However, since we did not observe any changes in SR Ca²⁺-release kinetics between conditions, it is unlikely that CRC phosphorylation was differentially altered by glucose supplementation. Since plasma EPI decreased and serum insulin increased with GLUC during prolonged exercise, it is possible that contrasting effects of the two hormones did not result in a net change in phosphorylation of the CRC. Nonetheless, it should be emphasized that these measurements were made *in vitro*; therefore, the possibility that glucose supplementation may influence SR Ca²⁺-release kinetics *in vivo* cannot be ruled out.

Another possibility to explain the apparent insignificant effect of glucose supplementation on SR behaviour during exercise relates to the analytical approach to measuring the SR Ca^{2+} -cycling properties. Our measurements are based on *in vitro* techniques performed on crude homogenates under supposedly optimal conditions. As such, the increases in Ca^{2+} -release and SR Ca^{2+} -uptake that undoubtedly occurs “in vivo” in the transition from rest to exercise remain undetected. It is possible that changes “in vivo” mediated by our experimental conditions remain obscure because of analytical limitations. However, in recent work (Duhamel and Green, unpublished), we have been able to demonstrate that under supposedly optimal assay conditions, the effect of changes in selected hormones and selected protein kinase and phosphatase signaling pathways on the kinetic behaviour of SERCA can be detected. These results suggest that at least some of the potential mechanisms whereby glucose can alter SR Ca^{2+} -handling can be assessed *in vitro* under our assay conditions.

The results of this paper need to be put into perspective given limitations of our analytical techniques. It should be emphasized that the conditions under which the SR measurements were performed were optimized depending on which property was being assessed. For SERCA activity, the assay medium contained the Ca^{2+} ionophore A23187, which makes the membrane permeable to Ca^{2+} and allows the catalytic activity of the enzyme to be measured at submaximal and maximal Ca^{2+}_f (Berchtold *et al.*, 2000). Ca^{2+} ionophore A23187 is used to prevent the formation of a large Ca^{2+} gradient across the SR membrane that would cause back-inhibition of the enzyme (Berchtold *et al.*, 2000) and prevent determination of V_{\max} . For Ca^{2+} -uptake, the assay conditions required the SR membrane to be left intact since our analytical techniques uses the Ca^{2+} -sensitive dye Indo-1 to calculate the ratio between the Ca^{2+} bound and the Ca^{2+} free Indo-1 complex. Therefore, oxalate was used in the Ca^{2+} -uptake assay buffer to

prevent back inhibition of the enzyme since this compound is used to bind Ca^{2+} (Berchtold *et al.*, 2000). Although it would have been preferable to determine Ca^{2+} -uptake rates at maximal Ca^{2+}_f , assessment of Ca^{2+} -uptake rates were completed at submaximal Ca^{2+}_f due to the limited sensitivity of the fluorescent dye Indo-1. Based on these analytical differences, the conditions under which the measurements were performed should be considered when interpreting the apparent coupling ratios. Measurements of Ca^{2+} -release rates were assessed using an assay coupled with Ca^{2+} -uptake and therefore were completed in the presence of oxalate. Therefore, oxalate may have biased our Ca^{2+} -release measurements since Ca^{2+} must dissociate from oxalate prior to being exposed to Indo-1 in our assay medium. It would have been preferable to determine Ca^{2+} -release rates in the absence of oxalate. However, we have found that the active loading of muscle homogenates without oxalate takes ~60 min (unpublished). This duration is problematic when determining Ca^{2+} -uptake and Ca^{2+} -release kinetics since we have found that the homogenate is not stable during this time (Tupling *et al.*, 2004). Limitations

associated with the experimental model and sample size used in this study should also be considered when interpreting the results in this study. Although it would have been preferable to collect tissue samples at rest and also at the time corresponding to fatigue in PLAC (115 ± 6 min) during both PLAC and GLUC for all participants, ethical and tissue sampling limitations did not permit for 9 tissue biopsy samples to be collected. For this reason, resting tissue samples during the GLUC trial were replaced by a tissue sample that was collected at the time corresponding to fatigue in PLAC (115 ± 6 min) during GLUC for a subgroup of participants. This tissue-sampling schedule allowed us to make an additional comparison during exercise when plasma glucose, catecholamine and insulin concentrations were different between

conditions. The data collected in this subgroup were not different from the changes observed at 30 and 90 min of exercise and at fatigue observed in the main group of participants this study.

Since there appeared to be a small, but insignificant divergence between PLAC and GLUC during the late stages of exercise for Ca^{2+} -uptake ($P=0.24$) and Phase 1 Ca^{2+} -release ($P=0.35$), power calculations were performed to estimate the number of participants needed for an 80% power level. Power calculations were completed by comparing means for independent samples for matched time points using statistical software offered through the University of British Columbia website (Brant, 2006) based on the calculations detailed by Rosner (Rosner, 2006). For Ca^{2+} -uptake, 166, 53 and 652 volunteers would have to participate in this study to get an 80% power level at 90 min of exercise during both PLAC and GLUC, at a time corresponding to fatigue during the PLAC condition during both PLAC and GLUC (115 ± 6 min), and at the time corresponding to fatigue in PLAC (115 ± 6 min) compared to the time corresponding to fatigue in GLUC (137 ± 7 min), respectively. For Phase 1 Ca^{2+} -release, 120, 652, and 128 volunteers would have to participate in this study to get an 80% power level when the same comparisons were made. Based on these power calculations, we feel confident that we are able to conclude that glucose supplementation does not alter SR Ca^{2+} -handling properties in this study. Moreover, our conclusions are based on data collected from fifteen participants, which is larger than the typical sample size used in many exercise physiology studies (Booth *et al.*, 1997; Coyle *et al.*, 1986; Duhamel *et al.*, 2005; Duhamel *et al.*, 2004a; Duhamel *et al.*, 2004b; Green *et al.*, 1989; Green *et al.*, 1991a; Green *et al.*, 1991b; Lee-Young *et al.*, 2006; Marchand *et al.*, 2002; McConell *et al.*, 1999; Sahlin *et al.*, 1976; Tupling *et al.*, 2003; Tupling *et al.*, 2004).

The results of this paper also need to be interpreted in the context of the mixed fibre type composition of the human vastus lateralis. Since Type I and Type IIa fibres (Green *et al.*, 1990; Vollestad & Blom, 1985) represent ~90% of the fibre population in the human vastus lateralis (Saltin & Gollnick, 1983), the exercise-induced reductions in SR Ca²⁺-handling properties observed in this study represent the net change in SR function for all fibre types present in each muscle sample and do not represent a fibre type-specific response. However, we can not discount the possibility that our data were influenced by greater reductions in one fibre type compared to another since differences in fibre type activation during prolonged exercise are known to exist (Green *et al.*, 1990; Vollestad & Blom, 1985). Moreover, differences in SERCA protein isoform expression (Wu & Lytton, 1993) or the expression of other SR-associated proteins known to influence the intrinsic regulation of SR properties (Tupling, 2004) may have also caused SR properties to be affected to a greater extent in one fibre type compared to another. It would have been beneficial to determine the fibre type-specific changes in SR properties during exercise for Type I versus Type II fibres; however, this was not possible for the vastus lateralis given tissue limitations and technical limitations associated with the analytical techniques used in this study.

Summary

Our findings demonstrate that prolonged exercise leads to a progressive loss of SR Ca²⁺-handling properties in human skeletal muscle, assessed *in vitro*. Furthermore, it appears that the provision of glucose supplements during the late stages of exercise does not delay the onset of exercise-induced reductions to SR Ca²⁺-handling properties, assessed *in vitro*, in human skeletal muscle. Although glucose supplementation did increase exercise cycle time to fatigue

in this study, our data does not reveal an association with SR Ca²⁺-cycling. However, these data do not rule out the possibility that glucose supplementation may influence E-C coupling processes or SR Ca²⁺-cycling properties *in vivo*. Additionally, by combining these observations with the results from our previous study (Duhamel *et al.*, 2006c), the justification for classifying the depletion of muscle glycogen as a factor that contributes, in part, to the reduction of SR Ca²⁺-handling properties during prolonged exercise is strengthened since changes in plasma glucose, catecholamines and insulin do not alter SR properties during exercise in human skeletal muscle.

CHAPTER FIVE

SUMMARY, CONCLUSIONS AND FUTURE DIRECTIONS

Summary and Conclusions

The purpose of this thesis was to investigate the role that intracellular signaling pathways have on the regulation of SR Ca^{2+} -handling proteins, namely SERCA and CRC, in cardiac and skeletal muscle of different fiber type composition. To accomplish this aim, two basic strategies were employed. The studies described in Chapter Two and Chapter Three utilized a non-physiologic model to characterize second messenger effects using pharmacological interventions. The first study (i.e. Chapter Two) was designed to characterize the influence that β -adrenergic, CaMKII, and PKC signaling pathways have on SERCA kinetic properties in the LV and skeletal muscles of different fibre type in rats. The second study (i.e. Chapter Three) sought to characterize the influence that insulin signaling has on SERCA kinetic properties using the same tissues employed in the previous study. The final study (Chapter Four) was designed to use a physiologic model to investigate the collective effects that alterations in plasma glucose concentrations and the associated changes in plasma glucoregulatory hormone (i.e. catecholamines and insulin) concentrations have on SR Ca^{2+} -handling (e.g. V_{\max} , Ca^{2+} -uptake and Ca^{2+} -release kinetics) in human skeletal muscle by directly manipulating these properties through the administration of oral glucose supplements during exercise.

In general, the results described in Chapter Two and Three indicate that β -adrenergic, CaMKII and insulin signaling pathways increased SERCA Ca^{2+} -sensitivity in a tissue specific manner (Figure 5.1); whereas, PKC signaling reduced SERCA Ca^{2+} -sensitivity in all tissues. Moreover, PKC signaling also reduced SERCA V_{\max} in fast-twitch skeletal muscles, but not in the LV or SOL. The results described in Chapter Four indicate that changes in plasma glucose, epinephrine and insulin concentrations do not influence SR Ca^{2+} -handling properties in human skeletal muscle during exercise. However, since exercise did reduce SR Ca^{2+} -handling

Treatment	LV	SOL	EDL	RG	WG
β-adrenergic					
EPI	↑	↑	-	-	-
cAMP	↑	↑	-	-	-
PKA	↑	-	-	-	-
Regulator Protein	PLN	SLN	-	-	-
CaMKII					
CaM	↑	-	-	-	-
Regulator Protein	PLN	-	-	-	-
PKC					
PMA	↓	↓	↓	↓	↓
Regulator Protein	?	?	?	?	?
Insulin					
Insulin	↑	↑	↑	↑	↑
A-INS-R	↑	↑	↑	↑	↑
Regulator Protein	IRS	IRS	IRS	IRS	IRS

Figure 5.1: Summary of changes in sarco(endo)plasmic reticulum Ca^{2+} -ATPase (SERCA) Ca^{2+} -sensitivity obtained from the treatments utilized to characterize β -adrenergic signaling, Ca^{2+} -dependent calmodulin kinase II (CaMKII), Protein Kinase C (PKC) and insulin signaling in muscle homogenates in Chapter Two and Chapter Three. Muscle homogenates were prepared from left ventricle (LV), soleus (SOL), extensor digitorum longus (EDL), the red portion of gastrocnemius (RG), and the white portion of gastrocnemius (WG). EPI, epinephrine. cAMP, adenosine 3',5'-cyclic monophosphate. PKA, protein kinase A. CaM, calmodulin. PMA, is a PKC activator. A-INS-R, an activated form of the insulin receptor. Regulator Protein, represents the protein that is suggested to be acutely influencing SERCA kinetic properties in response to a given treatment. PLN, phospholamban. SLN, sarcolipin. IRS, insulin receptor substrate. ↑ indicates that SERCA Ca^{2+} -sensitivity is increased. ↓ indicates that SERCA Ca^{2+} -sensitivity is decreased.

properties during exercise with and without exercise, it is possible that the strength of the exercise signal overrode the hormonal influences observed to occur in resting muscles.

The results presented in Chapter Two supported our hypothesis, namely that β -adrenergic signaling increased the Ca^{2+} -sensitivity of SERCA, as reflected by reductions in Ca_{50} , without increasing V_{max} in the LV and SOL. Our data also support our hypothesis that β -adrenergic signaling reduces Ca_{50} in the LV via a cAMP-dependent PKA-dependent mechanism, whereas, an alternative cAMP-dependent mechanism that is not PKA-dependent influences Ca_{50} in the SOL. Based on the known expression of SLN protein and the lack of PLN in the SOL of rat (Vangheluwe *et al.*, 2005), we propose that SLN may be contributing to the observed β -adrenergic signaling effect in this tissue. However, our results do not rule out the possibility that another cAMP-dependent mechanism that is not PKA-dependent may be responsible for the changes in Ca_{50} in the SOL.

The CaMKII signaling experiments support the hypothesis that CaMKII activation would increase the Ca^{2+} -sensitivity of SERCA2a, which most likely occurs as a result of CaMKII-mediated PLN phosphorylation in the LV (Hawkins *et al.*, 1994; Hawkins *et al.*, 1995; Odermatt *et al.*, 1996; Xu & Narayanan, 2000). Our data also support the hypothesis that CaMKII would not alter SERCA kinetic properties in any of the skeletal muscles studied. This observation was not unexpected since PLN protein is not expressed in rat slow-twitch or fast-twitch skeletal muscle, but is expressed in the LV (Vangheluwe *et al.*, 2005). Our results do not support the hypothesis that CaMKII-activation would increase the V_{max} of SERCA2a in the LV and SOL (Hawkins *et al.*, 1994; Hawkins *et al.*, 1995; Xu & Narayanan, 2000). This finding contradicts previous literature (Hawkins *et al.*, 1994; Hawkins *et al.*, 1995; Xu & Narayanan, 2000) that has demonstrated that CaMKII increases the V_{max} of SERCA2a by directly

phosphorylating Ser38 within the enzyme (Hawkins *et al.*, 1994; Odermatt *et al.*, 1996; Xu & Narayanan, 2000) but supports the findings of Odermatt *et al.* (Odermatt *et al.*, 1996) showing no effect of CaM on the V_{\max} of SERCA2a.

Our PKC signaling data also support our hypothesis that PMA depresses SERCA Ca^{2+} -sensitivity (i.e. n_H and Ca_{50}) in the LV, SOL and fast-twitch skeletal muscles of the rat. However, in contrast to our hypothesis, PMA does not alter V_{\max} in the LV or SOL but does reduce V_{\max} in the EDL, WG, and RG. It is possible that differences in SERCA isoform expression may have contributed to the tissue specific responses. This possibility is supported by our observations indicating that PMA does not alter the V_{\max} of enriched SR vesicles containing SERCA2a prepared from LV, but that it does reduce the V_{\max} of enriched SR vesicles containing SERCA1a prepared from WG. However, our data does not rule out the possibility that proteins other than SERCA may have contributed to the tissue-specific response observed. Although our data clearly indicated that PMA negatively influenced V_{\max} in fast-twitch skeletal muscle and n_H and Ca_{50} in all tissues examined, it is not yet clear what mechanism(s) are mediating these effects. Accordingly, further research is needed to identify the PKC-dependent mechanisms that regulate SERCA kinetic properties in the LV and skeletal muscles.

The results presented in Chapter Three support our hypothesis that insulin signaling can acutely regulate SERCA kinetic properties. These experiments indicate that insulin increases SERCA Ca^{2+} -sensitivity in crude muscle homogenates and enriched SR vesicles prepared from rat LV and skeletal muscles. Moreover, our data demonstrate that insulin signaling promotes the interaction of IRS proteins (i.e. IRS-1 and IRS-2) with SERCA1a and SERCA2a in an insulin-dependent manner in all tissues examined. However, in conflict to our hypothesis, we

found that the insulin-induced changes in SERCA2a Ca^{2+} -sensitivity in the LV were not associated with changes in the PLN pentamer: monomer ratio or to changes in the PLN Ser16 or Thr17 phosphorylation. Our findings indicate that the IRS proteins bind directly with SERCA proteins regardless of muscle type. This mechanism may be analogous to the phosphorylation-mediated regulation of SERCA Ca^{2+} -sensitivity by PLN (James *et al.*, 1989) and SLN (Gramolini *et al.*, 2006) and represents a novel insulin-sensitive pathway capable of influencing SERCA kinetic properties. These data, in combination with the observations made by others (Algenstaedt *et al.*, 1997; Borge & Wolf, 2003; Xu *et al.*, 2000), demonstrate that IRS-1 and IRS-2 proteins should be added to the list of endogenous modulator proteins capable of acutely regulating SERCA kinetic properties in cardiac and skeletal muscle at submaximal Ca^{2+}_f .

The results presented in Chapter Four support our hypothesis that prolonged exercise progressively reduces V_{\max} , Ca^{2+} -uptake, and Ca^{2+} -release kinetics and that the reductions in SR Ca^{2+} -handling properties occur in the absence of changes in Ca^{2+} -sensitivity (i.e. n_H and Ca_{50}), Ca^{2+} -transport efficiency (i.e. apparent coupling ratio) and membrane permeability for Ca^{2+} (i.e. ionophore ratio). Consistent with our hypothesis, we have found that glucose supplementation did not influence energy metabolism and muscle glycogen content. Moreover, these data also support our hypothesis that glucose supplementation during exercise did not alter SERCA Ca^{2+} -sensitivity (i.e. n_H or Ca_{50}) or PLN phosphorylation. In contrast, our data did not support our hypothesis that the exercise-induced reductions to SR Ca^{2+} -handling properties would be attenuated by the provision of glucose supplements during the late stages of exercise. This was unexpected, given the beneficial effects of glucose on the regulation of cytosolic Ca^{2+}_f and the restoration of contractile function in mammalian single fibres (Chin & Allen, 1997).

Although glucose supplementation did increase exercise cycle time to fatigue in this study, our data did not reveal an association with SR Ca^{2+} -cycling, at least as assessed *in vitro*. It is possible that the strength of exercise signal overrides the hormonal influences observed in resting muscles. Additionally, these data do not rule out the possibility that glucose supplementation may influence E-C coupling processes or SR Ca^{2+} -cycling properties *in vivo*.

Future Directions

This research raises several issues for future investigation. From a clinical perspective, it appears that impaired SR Ca^{2+} -cycling is associated with many forms of cardiomyopathy. Interestingly, β -adrenergic, CaMKII, PKC, and insulin signaling pathways have all been implicated in the development of cardiomyopathy. Given the role of the SR in regulating Ca^{2+}_f and contractility, it is not yet clear if reductions in SR function contribute to the development of cardiomyopathy or is an adaptive response to another element of the pathophysiology of cardiomyopathy. Therefore, it would be beneficial to explore the possibility of using these signaling pathways to improve cardiac SERCA Ca^{2+} -cycling properties and to improve contractility in patients diagnosed with various cardiomyopathies.

Our insulin signaling observations introduce a novel finding to link insulin signaling with the regulation of SERCA kinetic properties. In fact, the proposed mechanism for IRS binding to SERCA appears to be regulated by a phosphorylation-mediated mechanism, which is analogous to the phosphorylation-mediated regulation of SERCA Ca^{2+} -sensitivity by PLN (James *et al.*, 1989) and SLN (Gramolini *et al.*, 2006). Therefore, it would be helpful to determine if this pathway regulates SERCA Ca^{2+} -sensitivity in cardiac and skeletal muscle of different species. Moreover, given that Ca^{2+}_f -regulation is adversely affected by diabetes, it would be valuable to

determine how this disease state affects the regulation of SERCA kinetic properties in heart and skeletal muscle. Clinical research has demonstrated that the most common complication of diabetes is an increased incidence of cardiovascular disease with heart failure being the leading cause of death in diabetic populations (Grundy *et al.*, 1999). In addition to an increased incidence of diabetes-induced hypertension and coronary artery disease, empirical evidence has also demonstrated that a diabetic cardiomyopathy contributes to the pathophysiology of the diabetic heart. Generally, the literature has demonstrated that remodeling of metabolic pathways (Belke *et al.*, 2000), contractile proteins (Malhotra *et al.*, 1995), sarcoplasmic reticulum Ca^{2+} -handling proteins (Netticadan *et al.*, 2001) and membrane phospholipid composition (Kuwahara *et al.*, 1997) contribute to the pathophysiology of diabetic cardiomyopathy. Therefore, it would be of value to determine if diabetes adversely affects SR Ca^{2+} -handling properties in cardiac and skeletal muscles. In addition, it would be of value to develop a stronger understanding of the affects that diabetes exerts on intracellular regulatory pathways that influence cardiac Ca^{2+} -handling protein function and expression.

Limitations

From a biochemical perspective, several limitations in these studies should be addressed. For example, our inability to directly demonstrate that the effect of insulin was mediated through an INS-TK dependent mechanism (i.e. experiments that used 80 μM AGL 2263 in Chapter Three) should be revisited. Another limitation to the current study was the inability to determine if the PMA-dependent changes in n_{H} and Ca_{50} were mediated through a PKC dependent mechanism. We attempted to establish that the PMA-induced changes in SERCA kinetic properties occurred as a result of PKC-dependent signaling by incubating samples in the

presence of the PKC inhibitor GFX. However, GFX did not prevent the PMA-dependent effects. In hindsight, we should have assessed SERCA kinetic properties in the presence of the biologically inactivated form of PMA. Therefore, it is recommended that strategies be developed to utilize INS-TK and PKC activators and inhibitors to demonstrate that these pathways were indeed directly responsible for the observed effects.

It is notable that the combined alterations in plasma glucose, catecholamine and insulin concentrations did not influence SR Ca^{2+} -handling during exercise. This observation may appear to directly contradict the notion that β -adrenergic and insulin signaling influence SERCA Ca^{2+} -sensitivity. However, this human study was designed to manipulate plasma glucose and consequently the glucoregulatory hormone (i.e. catecholamine and insulin) concentrations during the late stages of exercise. In fact, when the glucose supplementation protocol was started (i.e. 30 min of exercise) plasma catecholamine concentrations were already elevated above resting levels during both the PLAC and GLUC conditions. Therefore, it is possible that the effects of the catecholamines were already manifested. Additionally, since this study used an exercise stimulus, it is possible that the changes in plasma catecholamine and insulin during the late stages of exercise had no additional effect since several intracellular signaling pathways associated with exercise were already acting to ensure an appropriate response was completed. Therefore, it would be of value to characterize the influence that alterations in plasma glucose, catecholamine and insulin concentrations have on non-exercising human skeletal muscle. This information would establish if epinephrine and insulin could alter SERCA kinetic properties in human skeletal muscle.

The interpretation of our results is also limited since we did not characterize SERCA kinetic properties in the presence of combined treatments. For example, a combined β -

adrenergic and insulin treatment would have been beneficial since it would establish if these pathways interact to influence SERCA Ca^{2+} -sensitivity in the LV and skeletal muscles. Based on our observations, which indicate that β -adrenergic signaling influences Ca_{50} via a PLN- or SLN-mediated pathway in the LV and SOL, respectively, and on the observation that insulin signaling appears to influence Ca_{50} by promoting the interaction of IRS proteins with SERCA, it is possible that the effects of each pathway are additive. In the physiologic study, it is noteworthy that plasma EPI and NE were higher, while INS was lower, during PLAC compared to GLUC. Since our data indicated that both β -adrenergic and insulin signaling is capable of increasing SERCA Ca^{2+} -sensitivity, it is possible that the divergent changes in EPI and INS may have exerted different effects on Ca_{50} in this model. Accordingly, further research is warranted to examine the possibility that β -adrenergic and insulin signaling influence SERCA Ca^{2+} -sensitivity when both pathways are activated in combination.

REFERENCE LIST

- Algenstaedt, P., Antonetti, D. A., Yaffe, M. B., & Kahn, C. R. (1997). Insulin receptor substrate proteins create a link between the tyrosine phosphorylation cascade and the Ca²⁺-ATPases in muscle and heart. *J.Biol.Chem.* **272**, 23696-23702.
- Asahi, M., Kurzydowski, K., Tada, M., & MacLennan, D. H. (2002). Sarcolipin inhibits polymerization of phospholamban to induce superinhibition of sarco(endo)plasmic reticulum Ca²⁺-ATPases (SERCAs). *J.Biol.Chem.* **277**, 26725-26728.
- Asahi, M., Nakayama, H., Tada, M., & Otsu, K. (2003). Regulation of sarco(endo)plasmic reticulum Ca²⁺ adenosine triphosphatase by phospholamban and sarcolipin: implication for cardiac hypertrophy and failure. *Trends Cardiovasc.Med.* **13**, 152-157.
- Bagby, G. J., Green, H. J., Katsuta, S., & Gollnick, P. D. (1978). Glycogen depletion in exercising rats infused with glucose, lactate, or pyruvate. *J.Appl.Physiol* **45**, 425-429.
- Barnes, M., Gibson, L. M., & Stephenson, D. G. (2001). Increased muscle glycogen content is associated with increased capacity to respond to T-system depolarisation in mechanically skinned skeletal muscle fibres from the rat. *Pflugers Arch.* **442**, 101-106.
- Baron, A. D. (1994). Hemodynamic actions of insulin. *Am.J.Physiol* **267**, E187-E202.
- Belke, D. D., Larsen, T. S., Gibbs, E. M., & Severson, D. L. (2000). Altered metabolism causes cardiac dysfunction in perfused hearts from diabetic (db/db) mice. *Am.J.Physiol Endocrinol.Metab* **279**, E1104-E1113.
- Berchtold, M. W., Brinkmeier, H., & Muntener, M. (2000). Calcium ion in skeletal muscle: its crucial role for muscle function, plasticity, and disease. *Physiol Rev.* **80**, 1215-1265.
- Bergstrom, J., Hermansen, L., Hultman, E., & Saltin, B. (1967). Diet, muscle glycogen and physical performance. *Acta Physiol Scand.* **71**, 140-150.
- Bers, D. M. (2004). Macromolecular complexes regulating cardiac ryanodine receptor function. *J.Mol.Cell Cardiol.* **37**, 417-429.
- Bonen, A., Tan, M. H., & Watson-Wright, W. M. (1981). Insulin binding and glucose uptake differences in rodent skeletal muscles. *Diabetes* **30**, 702-704.

Booth, J., McKenna, M. J., Ruell, P. A., Gwinn, T. H., Davis, G. M., Thompson, M. W., Harmer, A. R., Hunter, S. K., & Sutton, J. R. (1997). Impaired calcium pump function does not slow relaxation in human skeletal muscle after prolonged exercise. *J.Appl.Physiol* **83**, 511-521.

Borge, P. D. Jr. & Wolf, B. A. (2003). Insulin receptor substrate 1 regulation of sarco-endoplasmic reticulum calcium ATPase 3 in insulin-secreting beta-cells. *J.Biol.Chem.* **278**, 11359-11368.

Bottinelli, R., Canepari, M., Reggiani, C., & Stienen, G. J. (1994). Myofibrillar ATPase activity during isometric contraction and isomyosin composition in rat single skinned muscle fibres. *J.Physiol* **481 (Pt 3)**, 663-675.

Brandl, C. J., Green, N. M., Korczak, B., & MacLennan, D. H. (1986). Two Ca²⁺ ATPase genes: homologies and mechanistic implications of deduced amino acid sequences. *Cell* **44**, 597-607.

Brant, R. Web-based sample size/power calculations. <http://stat.ubc.ca/~rollin/stats/ssize/> . 2006.

Braz, J. C., Gregory, K., Pathak, A., Zhao, W., Sahin, B., Klevitsky, R., Kimball, T. F., Lorenz, J. N., Nairn, A. C., Liggett, S. B., Bodi, I., Wang, S., Schwartz, A., Lakatta, E. G., DePaoli-Roach, A. A., Robbins, J., Hewett, T. E., Bibb, J. A., Westfall, M. V., Kranias, E. G., & Molkentin, J. D. (2004). PKC-alpha regulates cardiac contractility and propensity toward heart failure. *Nat.Med.* **10**, 248-254.

Brozinick, J. T., Jr., Reynolds, T. H., Dean, D., Cartee, G., & Cushman, S. W. (1999). 1-[N, O-bis-(5-isoquinolinesulphonyl)-N-methyl-L-tyrosyl]-4- phenylpiperazine (KN-62), an inhibitor of calcium-dependent camodulin protein kinase II, inhibits both insulin- and hypoxia-stimulated glucose transport in skeletal muscle. *Biochem.J.* **339 (Pt 3)**, 533-540.

Capogrossi, M. C., Kaku, T., Filburn, C. R., Pelto, D. J., Hansford, R. G., Spurgeon, H. A., & Lakatta, E. G. (1990). Phorbol ester and dioctanoylglycerol stimulate membrane association of protein kinase C and have a negative inotropic effect mediated by changes in cytosolic Ca²⁺ in adult rat cardiac myocytes. *Circ.Res.* **66**, 1143-1155.

Champeil, P., Riollet, S., Orłowski, S., Guillain, F., Seebregts, C. J., & McIntosh, D. B. (1988). ATP regulation of sarcoplasmic reticulum Ca²⁺-ATPase. Metal-free ATP and 8-bromo-ATP bind with high affinity to the catalytic site of phosphorylated ATPase and accelerate dephosphorylation. *J.Biol.Chem.* **263**, 12288-12294.

Chaplin, H. Jr. & Mollison, P. L. (1952). Correction for plasma trapped in the red cell column of the hematocrit. *Blood* **7**, 1227-1238.

Chaplin, H. Jr., Mollison, P. L., & Vetter, H. (1953). The body/venous hematocrit ratio: its constancy over a wide hematocrit range. *J.Clin.Invest* **32**, 1309-1316.

Cheatham, B. & Kahn, C. R. (1995). Insulin action and the insulin signaling network. *Endocr.Rev.* **16**, 117-142.

Chin, E. R. (2005). Role of Ca²⁺/calmodulin-dependent kinases in skeletal muscle plasticity. *J.Appl.Physiol* **99**, 414-423.

Chin, E. R. & Allen, D. G. (1997). Effects of reduced muscle glycogen concentration on force, Ca²⁺ release and contractile protein function in intact mouse skeletal muscle. *J.Physiol* **498** (Pt 1), 17-29.

Chin, E. R. & Green, H. J. (1996). Effects of tissue fractionation on exercise-induced alterations in SR function in rat gastrocnemius muscle. *J.Appl.Physiol* **80**, 940-948.

Christ-Roberts, C. Y. & Mandarino, L. J. (2004). Glycogen synthase: key effect of exercise on insulin action. *Exerc.Sport Sci.Rev.* **32**, 90-94.

Clarke, D. M., Loo, T. W., Inesi, G., & MacLennan, D. H. (1989a). Location of high affinity Ca²⁺-binding sites within the predicted transmembrane domain of the sarcoplasmic reticulum Ca²⁺-ATPase. *Nature* **339**, 476-478.

Clarke, D. M., Loo, T. W., & MacLennan, D. H. (1990). The epitope for monoclonal antibody A20 (amino acids 870-890) is located on the luminal surface of the Ca²⁺(+)-ATPase of sarcoplasmic reticulum. *J.Biol.Chem.* **265**, 17405-17408.

Clarke, D. M., Maruyama, K., Loo, T. W., Leberer, E., Inesi, G., & MacLennan, D. H. (1989b). Functional consequences of glutamate, aspartate, glutamine, and asparagine mutations in the stalk sector of the Ca²⁺-ATPase of sarcoplasmic reticulum. *J.Biol.Chem.* **264**, 11246-11251.

Coggan, A. R. & Coyle, E. F. (1991). Carbohydrate ingestion during prolonged exercise: effects on metabolism and performance. *Exerc.Sport Sci.Rev.* **19**, 1-40.

- Conlee, R. K., Rennie, M. J., & Winder, W. W. (1976). Skeletal muscle glycogen content: diurnal variation and effects of fasting. *Am.J.Physiol* **231**, 614-618.
- Coyle, E. F. (1992a). Carbohydrate feeding during exercise. *Int.J.Sports Med.* **13 Suppl 1**, S126-S128.
- Coyle, E. F. (1992b). Carbohydrate supplementation during exercise. *J.Nutr.* **122**, 788-795.
- Coyle, E. F., Coggan, A. R., Hemmert, M. K., & Ivy, J. L. (1986). Muscle glycogen utilization during prolonged strenuous exercise when fed carbohydrate. *J.Appl.Physiol* **61**, 165-172.
- Cryer, P. E. (1993). Glucose counterregulation: prevention and correction of hypoglycemia in humans. *Am.J.Physiol* **264**, E149-E155.
- Cuenda, A., Centeno, F., & Gutierrez-Merino, C. (1991). Modulation by phosphorylation of glycogen phosphorylase-sarcoplasmic reticulum interaction. *FEBS Lett.* **283**, 273-276.
- Cuenda, A., Nogues, M., Henao, F., & Gutierrez-Merino, C. (1995). Interaction between glycogen phosphorylase and sarcoplasmic reticulum membranes and its functional implications. *J.Biol.Chem.* **270**, 11998-12004.
- Damiani, E., Sacchetto, R., & Margreth, A. (2000). Variation of phospholamban in slow-twitch muscle sarcoplasmic reticulum between mammalian species and a link to the substrate specificity of endogenous Ca(2+)-calmodulin-dependent protein kinase. *Biochim.Biophys.Acta* **1464**, 231-241.
- Delp, M. D. & Duan, C. (1996). Composition and size of type I, IIA, IID/X, and IIB fibers and citrate synthase activity of rat muscle. *J.Appl.Physiol* **80**, 261-270.
- Derave, W., Gao, S., & Richter, E. A. (2000). Pro- and macroglycogenolysis in contracting rat skeletal muscle. *Acta Physiol Scand.* **169**, 291-296.
- Dode, L., De Greef, C., Mountian, I., Attard, M., Town, M. M., Casteels, R., & Wuytack, F. (1998). Structure of the human sarco/endoplasmic reticulum Ca²⁺-ATPase 3 gene. Promoter analysis and alternative splicing of the SERCA3 pre-mRNA. *J.Biol.Chem.* **273**, 13982-13994.
- Dudley, G. A. & Terjung, R. L. (1985). Influence of acidosis on AMP deaminase activity in contracting fast-twitch muscle. *Am.J.Physiol* **248**, C43-C50.

Duhamel, T. A., Green, H. J., Perco, J. G., & Ouyang, J. (2005). Metabolic and sarcoplasmic reticulum Ca²⁺ cycling responses in human muscle 4 days following prolonged exercise. *Can.J.Physiol Pharmacol.* **83**, 643-655.

Duhamel, T. A., Green, H. J., Perco, J. G., & Ouyang, J. (2006a). Comparative effects of a low-carbohydrate diet and exercise plus a low-carbohydrate diet on muscle sarcoplasmic reticulum responses in males. *Am.J.Physiol Cell Physiol* **291**, C607-C617.

Duhamel, T. A., Green, H. J., Perco, J. G., & Ouyang, J. (2006b). Effects of prior exercise and a low-carbohydrate diet on muscle sarcoplasmic reticulum function during cycling in women. *J.Appl.Physiol* **101**, 695-706.

Duhamel, T. A., Green, H. J., Perco, J. G., Sandiford, S. D., & Ouyang, J. (2004a). Human muscle sarcoplasmic reticulum function during submaximal exercise in normoxia and hypoxia. *J.Appl.Physiol* **97**, 180-187.

Duhamel, T. A., Green, H. J., Sandiford, S. D., Perco, J. G., & Ouyang, J. (2004b). Effects of progressive exercise and hypoxia on human muscle sarcoplasmic reticulum function. *J.Appl.Physiol* **97**, 188-196.

Duhamel, T. A., Perco, J. G., & Green, H. J. (2006c). Manipulation of Dietary Carbohydrates Following Prolonged Effort Modifies Muscle Sarcoplasmic Responses In Exercising Males. *Am.J.Physiol Regul.Integr.Comp Physiol.*

Dux, L., Green, H. J., & Pette, D. (1990). Chronic low-frequency stimulation of rabbit fast-twitch muscle induces partial inactivation of the sarcoplasmic reticulum Ca²⁺(+)-ATPase and changes in its tryptic cleavage. *Eur.J.Biochem.* **192**, 95-100.

Entman, M. L., Bornet, E. P., Barber, A. J., Schwartz, A., Levey, G. S., Lehotay, D. C., & Bricker, L. A. (1977a). The cardiac sarcoplasmic reticulum-glycogenolytic complex. A possible effector site for cyclic AMP. *Biochim.Biophys.Acta* **499**, 228-237.

Entman, M. L., Bornet, E. P., Van Winkle, W. B., Goldstein, M. A., & Schwartz, A. (1977b). Association of glycogenolysis with cardiac sarcoplasmic reticulum: II. Effect of glycogen depletion, deoxycholate solubilization and cardiac ischemia: evidence for a phosphorylase kinase membrane complex. *J.Mol.Cell Cardiol.* **9**, 515-528.

Entman, M. L., Keslensky, S. S., Chu, A., & Van Winkle, W. B. (1980). The sarcoplasmic reticulum-glycogenolytic complex in mammalian fast twitch skeletal muscle. Proposed in vitro counterpart of the contraction-activated glycogenolytic pool. *J.Biol.Chem.* **255**, 6245-6252.

- Favero, T. G. (1999). Sarcoplasmic reticulum Ca(2+) release and muscle fatigue. *J.Appl.Physiol* **87**, 471-483.
- Favero, T. G., Pessah, I. N., & Klug, G. A. (1993). Prolonged exercise reduces Ca²⁺ release in rat skeletal muscle sarcoplasmic reticulum. *Pflugers Arch.* **422**, 472-475.
- Ferrington, D. A., Reijneveld, J. C., Bar, P. R., & Bigelow, D. J. (1996). Activation of the sarcoplasmic reticulum Ca²⁺-ATPase induced by exercise. *Biochim.Biophys.Acta* **1279**, 203-213.
- Fitts, R. H. (1994). Cellular mechanisms of muscle fatigue. *Physiol Rev.* **74**, 49-94.
- Franzini-Armstrong, C. & Protasi, F. (1997). Ryanodine receptors of striated muscles: a complex channel capable of multiple interactions. *Physiol Rev* **77**, 699-729.
- Frayn, K. N. (1983). Calculation of substrate oxidation rates in vivo from gaseous exchange. *J.Appl.Physiol* **55**, 628-634.
- Galbo, H. (1999). Exercise physiology: Humoral function. *Sport Sci.Rev* **1**, 65-93.
- Gramolini, A. O., Trivieri, M. G., Oudit, G. Y., Kislinger, T., Li, W., Patel, M. M., Emili, A., Kranias, E. G., Backx, P. H., & MacLennan, D. H. (2006). Cardiac-specific overexpression of sarcolipin in phospholamban null mice impairs myocyte function that is restored by phosphorylation. *Proc.Natl.Acad.Sci.U.S.A* **103**, 2446-2451.
- Green, H. J., Grange, F., Chin, C., Goreham, C., & Ranney, D. (1998). Exercise-induced decreases in sarcoplasmic reticulum Ca(2+)-ATPase activity attenuated by high-resistance training. *Acta Physiol Scand.* **164**, 141-146.
- Green, H. J., Helyar, R., Ball-Burnett, M., Kowalchuk, N., Symon, S., & Farrance, B. (1992a). Metabolic adaptations to training precede changes in muscle mitochondrial capacity. *J.Appl.Physiol* **72**, 484-491.
- Green, H. J., Jones, L. L., Houston, M. E., Ball-Burnett, M. E., & Farrance, B. W. (1989). Muscle energetics during prolonged cycling after exercise hypervolemia. *J.Appl.Physiol* **66**, 622-631.

- Green, H. J., Jones, S., Ball-Burnett, M., & Fraser, I. (1991a). Early adaptations in blood substrates, metabolites, and hormones to prolonged exercise training in man. *Can.J.Physiol Pharmacol.* **69**, 1222-1229.
- Green, H. J., Jones, S., Ball-Burnett, M. E., Smith, D., Livesey, J., & Farrance, B. W. (1991b). Early muscular and metabolic adaptations to prolonged exercise training in humans. *J.Appl.Physiol* **70**, 2032-2038.
- Green, H. J., Smith, D., Murphy, P., & Fraser, I. (1990). Training-induced alterations in muscle glycogen utilization in fibre-specific types during prolonged exercise. *Can.J.Physiol Pharmacol.* **68**, 1372-1376.
- Green, H. J., Sutton, J. R., Wolfel, E. E., Reeves, J. T., Butterfield, G. E., & Brooks, G. A. (1992b). Altitude acclimatization and energy metabolic adaptations in skeletal muscle during exercise. *J.Appl.Physiol* **73**, 2701-2708.
- Grundy, S. M., Benjamin, I. J., Burke, G. L., Chait, A., Eckel, R. H., Howard, B. V., Mitch, W., Smith, S. C., Jr., & Sowers, J. R. (1999). Diabetes and cardiovascular disease: a statement for healthcare professionals from the American Heart Association. *Circulation* **100**, 1134-1146.
- Grynkiewicz, G., Poenie, M., & Tsien, R. Y. (1985). A new generation of Ca²⁺ indicators with greatly improved fluorescence properties. *J.Biol.Chem.* **260**, 3440-3450.
- Han, J. W., Thieleczek, R., Varsanyi, M., & Heilmeyer, L. M., Jr. (1992). Compartmentalized ATP synthesis in skeletal muscle triads. *Biochemistry* **31**, 377-384.
- Hargreaves, M. (1999). Metabolic responses to carbohydrate ingestion: effects on exercise performance. In *Perspectives in Sports Medicine and Exercise Science*, eds. Comb, D. & Moury, R., pp. 94-124. Cooper Publishing Company, Carmel, IN.
- Hargreaves, M. & Richter, E. A. (1988). Regulation of skeletal muscle glycogenolysis during exercise. *Can.J.Sport Sci.* **13**, 197-203.
- Hartell, N. A., Archer, H. E., & Bailey, C. J. (2005). Insulin-stimulated endothelial nitric oxide release is calcium independent and mediated via protein kinase B. *Biochem.Pharmacol.* **69**, 781-790.
- Hawkins, C., Xu, A., & Narayanan, N. (1994). Sarcoplasmic reticulum calcium pump in cardiac and slow twitch skeletal muscle but not fast twitch skeletal muscle undergoes

phosphorylation by endogenous and exogenous Ca²⁺/calmodulin-dependent protein kinase. Characterization of optimal conditions for calcium pump phosphorylation. *J.Biol.Chem.* **269**, 31198-31206.

Hawkins, C., Xu, A., & Narayanan, N. (1995). Comparison of the effects of the membrane-associated Ca²⁺/calmodulin-dependent protein kinase on Ca(2+)-ATPase function in cardiac and slow-twitch skeletal muscle sarcoplasmic reticulum. *Mol.Cell Biochem.* **142**, 131-138.

Helander, I., Westerblad, H., & Katz, A. (2002). Effects of glucose on contractile function, [Ca²⁺]_i, and glycogen in isolated mouse skeletal muscle. *Am.J.Physiol Cell Physiol* **282**, C1306-C1312.

Henriksson, J., Chi, M. M., Hintz, C. S., Young, D. A., Kaiser, K. K., Salmons, S., & Lowry, O. H. (1986). Chronic stimulation of mammalian muscle: changes in enzymes of six metabolic pathways. *Am.J.Physiol* **251**, C614-C632.

Hochachka, P. W. & Matheson, G. O. (1992). Regulating ATP turnover rates over broad dynamic work ranges in skeletal muscles. *J.Appl.Physiol* **73**, 1697-1703.

Holloway, G. P., Green, H. J., & Tupling, A. R. (2006). Differential effects of repetitive activity on sarcoplasmic reticulum responses in rat muscles of different oxidative potential. *Am.J.Physiol Regul.Integr.Comp Physiol* **290**, R393-R404.

Hughson, R. L., Green, H. J., & Sharratt, M. T. (1995). Gas exchange, blood lactate, and plasma catecholamines during incremental exercise in hypoxia and normoxia. *J.Appl.Physiol* **79**, 1134-1141.

Ingebretsen, O. C., Bakken, A. M., Segadal, L., & Farstad, M. (1982). Determination of adenine nucleotides and inosine in human myocard by ion-pair reversed-phase high-performance liquid chromatography. *J.Chromatogr.* **242**, 119-126.

Iwasa, Y. & Hosey, M. M. (1984). Phosphorylation of cardiac sarcolemma proteins by the calcium-activated phospholipid-dependent protein kinase. *J.Biol.Chem.* **259**, 534-540.

James, D. E., Jenkins, A. B., & Kraegen, E. W. (1985). Heterogeneity of insulin action in individual muscles in vivo: euglycemic clamp studies in rats. *Am.J.Physiol* **248**, E567-E574.

James, D. E., Zorzano, A., Boni-Schnetzler, M., Nemenoff, R. A., Powers, A., Pilch, P. F., & Ruderman, N. B. (1986). Intrinsic differences of insulin receptor kinase activity in red and white muscle. *J.Biol.Chem.* **261**, 14939-14944.

James, P., Inui, M., Tada, M., Chiesi, M., & Carafoli, E. (1989). Nature and site of phospholamban regulation of the Ca²⁺ pump of sarcoplasmic reticulum. *Nature* **342**, 90-92.

Jansson, E., Hjemdahl, P., & Kaijser, L. (1982). Diet induced changes in sympatho-adrenal activity during submaximal exercise in relation to substrate utilization in man. *Acta Physiol Scand.* **114**, 171-178.

Kadambi, V. J., Ponniah, S., Harrer, J. M., Hoit, B. D., Dorn, G. W., Walsh, R. A., & Kranias, E. G. (1996). Cardiac-specific overexpression of phospholamban alters calcium kinetics and resultant cardiomyocyte mechanics in transgenic mice. *J.Clin.Invest* **97**, 533-539.

Karelis, A. D., Peronnet, F., & Gardiner, P. F. (2002). Glucose infusion attenuates muscle fatigue in rat plantaris muscle during prolonged indirect stimulation in situ. *Exp.Physiol* **87**, 585-592.

Kimura, Y., Asahi, M., Kurzydowski, K., Tada, M., & MacLennan, D. H. (1998). Phospholamban domain Ib mutations influence functional interactions with the Ca²⁺-ATPase isoform of cardiac sarcoplasmic reticulum. *J.Biol.Chem.* **273**, 14238-14241.

Klebl, B. M., Ayoub, A. T., & Pette, D. (1998). Protein oxidation, tyrosine nitration, and inactivation of sarcoplasmic reticulum Ca²⁺-ATPase in low-frequency stimulated rabbit muscle. *FEBS Lett.* **422**, 381-384.

Korge, P., Byrd, S. K., & Campbell, K. B. (1993). Functional coupling between sarcoplasmic-reticulum-bound creatine kinase and Ca(2+)-ATPase. *Eur.J.Biochem.* **213**, 973-980.

Korge, P. & Campbell, K. B. (1994). Local ATP regeneration is important for sarcoplasmic reticulum Ca²⁺ pump function. *Am.J.Physiol* **267**, C357-C366.

Korn, L. J., Siebel, C. W., McCormick, F., & Roth, R. A. (1987). Ras p21 as a potential mediator of insulin action in *Xenopus* oocytes. *Science* **236**, 840-843.

Kranias, E. G. (1985). Regulation of Ca²⁺ transport by cyclic 3',5'-AMP-dependent and calcium-calmodulin-dependent phosphorylation of cardiac sarcoplasmic reticulum. *Biochim.Biophys.Acta* **844**, 193-199.

Kuwahara, Y., Yanagishita, T., Konno, N., & Katagiri, T. (1997). Changes in microsomal membrane phospholipids and fatty acids and in activities of membrane-bound enzyme in diabetic rat heart. *Basic Res. Cardiol.* **92**, 214-222.

Lalonde, R. J., Lepock, J. R., & Kruuv, J. (1991). Site of freeze-thaw damage and cryoprotection by amino acids of the calcium ATPase of sarcoplasmic reticulum. *Biochim. Biophys. Acta* **1079**, 128-138.

Lawson, J. W. & Veech, R. L. (1979). Effects of pH and free Mg²⁺ on the K_{eq} of the creatine kinase reaction and other phosphate hydrolyses and phosphate transfer reactions. *J. Biol. Chem.* **254**, 6528-6537.

Lee-Young, R., Palmer, M., Linden, K. C., Leplastrier, K., Canny, B. J., Hargreaves, M., Wadley, G. D., Kemp, B. E., & McConell, G. K. (2006). Carbohydrate ingestion does not alter skeletal muscle AMPK signalling during exercise in humans. *Am. J. Physiol. Endocrinol. Metab.*

Lees, S. J., Chen, Y. T., & Williams, J. H. (2004). Glycogen debranching enzyme is associated with rat skeletal muscle sarcoplasmic reticulum. *Acta Physiol Scand.* **181**, 239-245.

Lees, S. J., Franks, P. D., Spangenburg, E. E., & Williams, J. H. (2001). Glycogen and glycogen phosphorylase associated with sarcoplasmic reticulum: effects of fatiguing activity. *J. Appl. Physiol* **91**, 1638-1644.

Lees, S. J. & Williams, J. H. (2004). Skeletal muscle sarcoplasmic reticulum glycogen status influences Ca²⁺ uptake supported by endogenously synthesized ATP. *Am. J. Physiol Cell Physiol* **286**, C97-104.

Ligos, J. M., Gerwin, N., Fernandez, P., Gutierrez-Ramos, J. C., & Bernad, A. (1998). Cloning, expression analysis, and functional characterization of PKL12, a member of a new subfamily of ser/thr kinases. *Biochem. Biophys. Res. Commun.* **249**, 380-384.

Liu, J. & Brautigan, D. L. (2000). Insulin-stimulated phosphorylation of the protein phosphatase-1 striated muscle glycogen-targeting subunit and activation of glycogen synthase. *J. Biol. Chem.* **275**, 15940-15947.

Loukianov, E., Ji, Y., Baker, D. L., Reed, T., Babu, J., Loukianova, T., Greene, A., Shull, G., & Periasamy, M. (1998). Sarco(end)plasmic reticulum Ca²⁺ ATPase isoforms and their role in muscle physiology and pathology. *Ann. N. Y. Acad. Sci.* **853**, 251-259.

Lowry, O. H. & Passonneau, J. V. (1972). *A flexible system of enzymatic analysis*. Academic Press, New York.

Luckin, K. A., Favero, T. G., & Klug, G. A. (1991). Prolonged exercise induces structural changes in SR Ca(2+)-ATPase of rat muscle. *Biochem.Med.Metab Biol.* **46**, 391-405.

Lunde, P. K., Dahlstedt, A. J., Bruton, J. D., Lannergren, J., Thoren, P., Sejersted, O. M., & Westerblad, H. (2001). Contraction and intracellular Ca(2+) handling in isolated skeletal muscle of rats with congestive heart failure. *Circ.Res.* **88**, 1299-1305.

Lytton, J., Westlin, M., Burk, S. E., Shull, G. E., & MacLennan, D. H. (1992). Functional comparisons between isoforms of the sarcoplasmic or endoplasmic reticulum family of calcium pumps. *J.Biol.Chem.* **267**, 14483-14489.

MacLennan, D. H. (1990). Molecular tools to elucidate problems in excitation-contraction coupling. *Biophys.J.* **58**, 1355-1365.

MacLennan, D. H., Abu-Abed, M., & Kang, C. (2002). Structure-function relationships in Ca(2+) cycling proteins. *J.Mol.Cell Cardiol.* **34**, 897-918.

MacLennan, D. H., Asahi, M., & Tupling, A. R. (2003). The regulation of SERCA-type pumps by phospholamban and sarcolipin. *Ann.N.Y.Acad.Sci.* **986**, 472-480.

MacLennan, D. H., Brandl, C. J., Korczak, B., & Green, N. M. (1985). Amino-acid sequence of a Ca²⁺ + Mg²⁺-dependent ATPase from rabbit muscle sarcoplasmic reticulum, deduced from its complementary DNA sequence. *Nature* **316**, 696-700.

MacLennan, D. H. & Kranias, E. G. (2003). Phospholamban: a crucial regulator of cardiac contractility. *Nat.Rev Mol.Cell Biol.* **4**, 566-577.

MacLennan, D. H. & Lytton, J. (1992). Sarcoplasmic Reticulum. In *The Heart and Cardiovascular System*, ed. Fozzard et al., pp. 1203-1217. Raven Press Ltd, New York.

MacLennan, D. H., Rice, W. J., & Green, N. M. (1997). The mechanism of Ca²⁺ transport by sarco(endo)plasmic reticulum Ca²⁺-ATPases. *J.Biol.Chem.* **272**, 28815-28818.

Malhotra, A., Lopez, M. C., & Nakouzi, A. (1995). Troponin subunits contribute to altered myosin ATPase activity in diabetic cardiomyopathy. *Mol.Cell Biochem.* **151**, 165-172.

Marchand, I., Chorneyko, K., Tarnopolsky, M., Hamilton, S., Shearer, J., Potvin, J., & Graham, T. E. (2002). Quantification of subcellular glycogen in resting human muscle: granule size, number, and location. *J.Appl.Physiol* **93**, 1598-1607.

Marcil, M., Karelis, A. D., Peronnet, F., & Gardiner, P. F. (2005). Glucose infusion attenuates fatigue without sparing glycogen in rat soleus muscle during prolonged electrical stimulation in situ. *Eur.J.Appl.Physiol* **93**, 569-574.

Marx, S. O., Reiken, S., Hisamatsu, Y., Gaburjakova, M., Gaburjakova, J., Yang, Y. M., Rosemblyt, N., & Marks, A. R. (2001). Phosphorylation-dependent regulation of ryanodine receptors: a novel role for leucine/isoleucine zippers. *J.Cell Biol.* **153**, 699-708.

Marx, S. O., Reiken, S., Hisamatsu, Y., Jayaraman, T., Burkhoff, D., Rosemblyt, N., & Marks, A. R. (2000). PKA phosphorylation dissociates FKBP12.6 from the calcium release channel (ryanodine receptor): defective regulation in failing hearts. *Cell* **101**, 365-376.

Matsushita, S. & Pette, D. (1992). Inactivation of sarcoplasmic-reticulum Ca(2+)-ATPase in low-frequency-stimulated muscle results from a modification of the active site. *Biochem.J.* **285** (Pt 1), 303-309.

McConnell, G., Snow, R. J., Proietto, J., & Hargreaves, M. (1999). Muscle metabolism during prolonged exercise in humans: influence of carbohydrate availability. *J.Appl.Physiol* **87**, 1083-1086.

Meyer, R. A. & Terjung, R. L. (1980). AMP deamination and IMP reamination in working skeletal muscle. *Am.J.Physiol* **239**, C32-C38.

Morris, T. E. & Sulakhe, P. V. (1997). Sarcoplasmic reticulum Ca(2+)-pump dysfunction in rat cardiomyocytes briefly exposed to hydroxyl radicals. *Free Radic.Biol.Med.* **22**, 37-47.

Movsesian, M. A., Nishikawa, M., & Adelstein, R. S. (1984). Phosphorylation of phospholamban by calcium-activated, phospholipid-dependent protein kinase. Stimulation of cardiac sarcoplasmic reticulum calcium uptake. *J.Biol.Chem.* **259**, 8029-8032.

Netticadan, T., Temsah, R. M., Kent, A., Elimban, V., & Dhalla, N. S. (2001). Depressed levels of Ca²⁺-cycling proteins may underlie sarcoplasmic reticulum dysfunction in the diabetic heart. *Diabetes* **50**, 2133-2138.

Nicolas, J. M., Renard-Rooney, D. C., & Thomas, A. P. (1998). Tonic regulation of excitation-contraction coupling by basal protein kinase C activity in isolated cardiac myocytes. *J.Mol.Cell Cardiol.* **30**, 2591-2604.

Nishizuka, Y. (1986). Studies and perspectives of protein kinase C. *Science* **233**, 305-312.

Nybo, L. (2003). CNS fatigue and prolonged exercise: effect of glucose supplementation. *Med.Sci.Sports Exerc.* **35**, 589-594.

O'Brien, P. J. (1990). Calcium sequestration by isolated sarcoplasmic reticulum: real-time monitoring using ratiometric dual-emission spectrofluorometry and the fluorescent calcium-binding dye indo-1. *Mol.Cell Biochem.* **94**, 113-119.

O'Brien, P. J., Shen, H., Weiler, J., Mirsalimi, M., & Julian, R. (1991). Myocardial Ca-sequestration failure and compensatory increase in Ca-ATPase with congestive cardiomyopathy: kinetic characterization by a homogenate microassay using real-time ratiometric indo-1 spectrofluorometry. *Mol.Cell Biochem.* **102**, 1-12.

Odermatt, A., Becker, S., Khanna, V. K., Kurzydowski, K., Leisner, E., Pette, D., & MacLennan, D. H. (1998). Sarcolipin regulates the activity of SERCA1, the fast-twitch skeletal muscle sarcoplasmic reticulum Ca²⁺-ATPase. *J.Biol.Chem.* **273**, 12360-12369.

Odermatt, A., Kurzydowski, K., & MacLennan, D. H. (1996). The v_{max} of the Ca²⁺-ATPase of cardiac sarcoplasmic reticulum (SERCA2a) is not altered by Ca²⁺/calmodulin-dependent phosphorylation or by interaction with phospholamban. *J.Biol.Chem.* **271**, 14206-14213.

Ohta, S., Takeuchi, M., Deguchi, M., Tsuji, T., Gahara, Y., & Nagata, K. (2000). A novel transcriptional factor with Ser/Thr kinase activity involved in the transforming growth factor (TGF)-beta signalling pathway. *Biochem.J.* **350 Pt 2**, 395-404.

Ragolia, L. & Begum, N. (1997). The effect of modulating the glycogen-associated regulatory subunit of protein phosphatase-1 on insulin action in rat skeletal muscle cells. *Endocrinology* **138**, 2398-2404.

Reading, S. A., Murrant, C. L., & Barclay, J. K. (2003). Increased cAMP as a positive inotropic factor for mammalian skeletal muscle in vitro. *Can.J.Physiol Pharmacol.* **81**, 986-996.

Reiken, S., Lacampagne, A., Zhou, H., Kherani, A., Lehnart, S. E., Ward, C., Huang, F., Gaburjakova, M., Gaburjakova, J., Rosemblyt, N., Warren, M. S., He, K. L., Yi, G. H., Wang,

J., Burkhoff, D., Vassort, G., & Marks, A. R. (2003). PKA phosphorylation activates the calcium release channel (ryanodine receptor) in skeletal muscle: defective regulation in heart failure. *J.Cell Biol.* **160**, 919-928.

Rogers, T. B., Gaa, S. T., Massey, C., & Dosemeci, A. (1990). Protein kinase C inhibits Ca²⁺ accumulation in cardiac sarcoplasmic reticulum. *J.Biol.Chem.* **265**, 4302-4308.

Rose, A. J., Kiens, B., & Richter, E. A. (2006). Ca²⁺-calmodulin-dependent protein kinase expression and signalling in skeletal muscle during exercise. *J.Physiol* **574**, 889-903.

Rosner, B. (2006). *Fundamentals of Biostatistics*, 6 ed. Thomson Brooks/Cole, Scarborough, ON, Canada.

Rossi, A. M., Eppenberger, H. M., Volpe, P., Cotrufo, R., & Wallimann, T. (1990). Muscle-type MM creatine kinase is specifically bound to sarcoplasmic reticulum and can support Ca²⁺ uptake and regulate local ATP/ADP ratios. *J.Biol.Chem.* **265**, 5258-5266.

Rubin, B. B., Romaschin, A., Walker, P. M., Gute, D. C., & Korthuis, R. J. (1996). Mechanisms of postischemic injury in skeletal muscle: intervention strategies. *J.Appl.Physiol* **80**, 369-387.

Ruell, P. A., Booth, J., McKenna, M. J., & Sutton, J. R. (1995). Measurement of sarcoplasmic reticulum function in mammalian skeletal muscle: technical aspects. *Anal.Biochem.* **228**, 194-201.

Sacchetto, R., Damiani, E., Pallanca, A., & Margreth, A. (2000). Coordinate expression of Ca²⁺-ATPase slow-twitch isoform and of beta calmodulin-dependent protein kinase in phospholamban-deficient sarcoplasmic reticulum of rabbit masseter muscle. *FEBS Lett.* **481**, 255-260.

Sahlin, K., Harris, R. C., Nylind, B., & Hultman, E. (1976). Lactate content and pH in muscle obtained after dynamic exercise. *Pflugers Arch.* **367**, 143-149.

Sakuntabhai, A., Ruiz-Perez, V., Carter, S., Jacobsen, N., Burge, S., Monk, S., Smith, M., Munro, C. S., O'Donovan, M., Craddock, N., Kucherlapati, R., Rees, J. L., Owen, M., Lathrop, G. M., Monaco, A. P., Strachan, T., & Hovnanian, A. (1999). Mutations in ATP2A2, encoding a Ca²⁺ pump, cause Darier disease. *Nat.Genet.* **21**, 271-277.

Saltin, B. & Gollnick, P. D. (1983). Skeletal muscle adaptability: significance for metabolism and performance. In *Handbook of Physiology. Skeletal Muscle* pp. 551-631. Am. Physiol. Soc, Bethesda, MD.

Saucerman, J. J. & McCulloch, A. D. (2004). Mechanistic systems models of cell signaling networks: a case study of myocyte adrenergic regulation. *Prog.Biophys.Mol.Biol.* **85**, 261-278.

Schacterle, G. R. & Pollack, R. L. (1973). A simplified method for the quantitative assay of small amounts of protein in biologic material. *Anal.Biochem.* **51**, 654-655.

Schertzer, J. D., Green, H. J., Duhamel, T. A., & Tupling, A. R. (2003). Mechanisms underlying increases in SR Ca²⁺-ATPase activity after exercise in rat skeletal muscle. *Am.J.Physiol Endocrinol.Metab* **284**, E597-E610.

Schertzer, J. D., Green, H. J., Fowles, J. R., Duhamel, T. A., & Tupling, A. R. (2004). Effects of prolonged exercise and recovery on sarcoplasmic reticulum Ca²⁺ cycling properties in rat muscle homogenates. *Acta Physiol Scand.* **180**, 195-208.

Schertzer, J. D., Green, H. J., & Tupling, A. R. (2002). Thermal instability of rat muscle sarcoplasmic reticulum Ca(2+)-ATPase function. *Am.J.Physiol Endocrinol.Metab* **283**, E722-E728.

Seidler, N. W., Jona, I., Vegh, M., & Martonosi, A. (1989). Cyclopiazonic acid is a specific inhibitor of the Ca²⁺-ATPase of sarcoplasmic reticulum. *J.Biol.Chem.* **264**, 17816-17823.

Simmerman, H. K., Kobayashi, Y. M., Autry, J. M., & Jones, L. R. (1996). A leucine zipper stabilizes the pentameric membrane domain of phospholamban and forms a coiled-coil pore structure. *J.Biol.Chem.* **271**, 5941-5946.

Simonides, W. S. & van Hardeveld, C. (1990). An assay for sarcoplasmic reticulum Ca²⁺-ATPase activity in muscle homogenates. *Anal.Biochem.* **191**, 321-331.

Slack, J. P., Grupp, I. L., Ferguson, D. G., Rosenthal, N., & Kranias, E. G. (1997). Ectopic expression of phospholamban in fast-twitch skeletal muscle alters sarcoplasmic reticulum Ca²⁺ transport and muscle relaxation. *J.Biol.Chem.* **272**, 18862-18868.

Song, X. M., Ryder, J. W., Kawano, Y., Chibalin, A. V., Krook, A., & Zierath, J. R. (1999). Muscle fiber type specificity in insulin signal transduction. *Am.J.Physiol* **277**, R1690-R1696.

Spencer, M. K., Yan, Z., & Katz, A. (1991). Carbohydrate supplementation attenuates IMP accumulation in human muscle during prolonged exercise. *Am.J.Physiol* **261**, C71-C76.

Stephenson, D. G., Nguyen, L. T., & Stephenson, G. M. (1999). Glycogen content and excitation-contraction coupling in mechanically skinned muscle fibres of the cane toad. *J.Physiol* **519 Pt 1**, 177-187.

Sun, X. J., Rothenberg, P., Kahn, C. R., Backer, J. M., Araki, E., Wilden, P. A., Cahill, D. A., Goldstein, B. J., & White, M. F. (1991). Structure of the insulin receptor substrate IRS-1 defines a unique signal transduction protein. *Nature* **352**, 73-77.

Sun, X. J., Wang, L. M., Zhang, Y., Yenush, L., Myers, M. G., Jr., Glasheen, E., Lane, W. S., Pierce, J. H., & White, M. F. (1995). Role of IRS-2 in insulin and cytokine signalling. *Nature* **377**, 173-177.

Tada, M. & Inui, M. (1983). Regulation of calcium transport by the ATPase-phospholamban system. *J.Mol.Cell Cardiol.* **15**, 565-575.

Tada, M., Inui, M., Yamada, M., Kadoma, M., Kuzuya, T., Abe, H., & Kakiuchi, S. (1983). Effects of phospholamban phosphorylation catalyzed by adenosine 3':5'-monophosphate- and calmodulin-dependent protein kinases on calcium transport ATPase of cardiac sarcoplasmic reticulum. *J.Mol.Cell Cardiol.* **15**, 335-346.

Takeshima, H., Nishimura, S., Matsumoto, T., Ishida, H., Kangawa, K., Minamino, N., Matsuo, H., Ueda, M., Hanaoka, M., Hirose, T., & . (1989). Primary structure and expression from complementary DNA of skeletal muscle ryanodine receptor. *Nature* **339**, 439-445.

Taylor, W. R. & Green, N. M. (1989). The predicted secondary structures of the nucleotide-binding sites of six cation-transporting ATPases lead to a probable tertiary fold. *Eur.J.Biochem.* **179**, 241-248.

Toyofuku, T., Kurzydowski, K., Lytton, J., & MacLennan, D. H. (1992). The nucleotide binding/hinge domain plays a crucial role in determining isoform-specific Ca²⁺ dependence of organellar Ca(2+)-ATPases. *J.Biol.Chem.* **267**, 14490-14496.

Toyoshima, C., Nakasako, M., Nomura, H., & Ogawa, H. (2000). Crystal structure of the calcium pump of sarcoplasmic reticulum at 2.6 Å resolution. *Nature* **405**, 647-655.

Tsintzas, O. K., Williams, C., Boobis, L., & Greenhaff, P. (1996). Carbohydrate ingestion and single muscle fiber glycogen metabolism during prolonged running in men. *J.Appl.Physiol* **81**, 801-809.

Tupling, A. R. (2004). The sarcoplasmic reticulum in muscle fatigue and disease: role of the sarco(endo)plasmic reticulum Ca²⁺-ATPase. *Can.J.Appl.Physiol* **29**, 308-329.

Tupling, A. R., Asahi, M., & MacLennan, D. H. (2002). Sarcolipin overexpression in rat slow twitch muscle inhibits sarcoplasmic reticulum Ca²⁺ uptake and impairs contractile function. *J.Biol.Chem.* **277**, 44740-44746.

Tupling, A. R., Gramolini, A. O., Duhamel, T. A., Kondo, H., Asahi, M., Tsuchiya, S. C., Borrelli, M. J., Lepock, J. R., Otsu, K., Hori, M., MacLennan, D. H., & Green, H. J. (2004). HSP70 binds to the fast-twitch skeletal muscle sarco(endo)plasmic reticulum Ca²⁺ -ATPase (SERCA1a) and prevents thermal inactivation. *J.Biol.Chem.* **279**, 52382-52389.

Tupling, A. R., Green, H. J., Roy, B. D., Grant, S., & Ouyang, J. (2003). Paradoxical effects of prior activity on human sarcoplasmic reticulum Ca²⁺-ATPase response to exercise. *J.Appl.Physiol* **95**, 138-144.

Tupling, R. & Green, H. (2002). Silver ions induce Ca²⁺ release from the SR in vitro by acting on the Ca²⁺ release channel and the Ca²⁺ pump. *J.Appl.Physiol* **92**, 1603-1610.

Tupling, R., Green, H., Senisterra, G., Lepock, J., & McKee, N. (2001a). Effects of 4-h ischemia and 1-h reperfusion on rat muscle sarcoplasmic reticulum function. *Am.J.Physiol Endocrinol.Metab* **281**, E867-E877.

Tupling, R., Green, H., Senisterra, G., Lepock, J., & McKee, N. (2001b). Ischemia-induced structural change in SR Ca²⁺-ATPase is associated with reduced enzyme activity in rat muscle. *Am.J.Physiol Regul.Integr.Comp Physiol* **281**, R1681-R1688.

Tupling, R., Green, H., & Tupling, S. (2001c). Partial ischemia reduces the efficiency of sarcoplasmic reticulum Ca²⁺ transport in rat EDL. *Mol.Cell Biochem.* **224**, 91-102.

Vangheluwe, P., Schuermans, M., Zador, E., Waelkens, E., Raeymaekers, L., & Wuytack, F. (2005). Sarcolipin and phospholamban mRNA and protein expression in cardiac and skeletal muscle of different species. *Biochem.J.* **389**, 151-159.

- Viner, R. I., Williams, T. D., & Schoneich, C. (2000). Nitric oxide-dependent modification of the sarcoplasmic reticulum Ca-ATPase: localization of cysteine target sites. *Free Radic.Biol.Med.* **29**, 489-496.
- Vollestad, N. K. & Blom, P. C. (1985). Effect of varying exercise intensity on glycogen depletion in human muscle fibres. *Acta Physiol Scand.* **125**, 395-405.
- Wasserman, D. H. & Cherrington, A. D. (1996). Regulation of extramuscular fuel sources during exercise. In *Handbook of Physiology, Section 12: Exercise, Regulation and Integration of Multiple Systems*, ed. Rowell, L. B. & S. R. J., pp. 1036-1074. Oxford University Press, New York.
- Wegener, A. D. & Jones, L. R. (1984). Phosphorylation-induced mobility shift in phospholamban in sodium dodecyl sulfate-polyacrylamide gels. Evidence for a protein structure consisting of multiple identical phosphorylatable subunits. *J.Biol.Chem.* **259**, 1834-1841.
- Wegener, A. D., Simmerman, H. K., Lindemann, J. P., & Jones, L. R. (1989). Phospholamban phosphorylation in intact ventricles. Phosphorylation of serine 16 and threonine 17 in response to beta-adrenergic stimulation. *J.Biol.Chem.* **264**, 11468-11474.
- White, M. F. & Kahn, C. R. (1994). The insulin signaling system. *J.Biol.Chem.* **269**, 1-4.
- Winegrad, S. (1965). Role of intracellular calcium movements in excitation-contraction coupling in skeletal muscle. *Fed.Proc.* **24**, 1146-1152.
- Woelfe, R. R. (1992). *Radioactive and stable isotope tracers in biomedicine.*, pp. 119-164. Wiley-Liss, New York.
- Wright, D. C., Geiger, P. C., Rheinheimer, M. J., Han, D. H., & Holloszy, J. O. (2004). Phorbol esters affect skeletal muscle glucose transport in a fiber type-specific manner. *Am.J.Physiol Endocrinol.Metab* **287**, E305-E309.
- Wu, K. D. & Lytton, J. (1993). Molecular cloning and quantification of sarcoplasmic reticulum Ca(2+)-ATPase isoforms in rat muscles. *Am.J.Physiol* **264**, C333-C341.
- Wuytack, F., Raeymaekers, L., & Missiaen, L. (2002). Molecular physiology of the SERCA and SPCA pumps. *Cell Calcium* **32**, 279-305.

Xu, A. & Narayanan, N. (2000). Reversible inhibition of the calcium-pumping ATPase in native cardiac sarcoplasmic reticulum by a calmodulin-binding peptide. Evidence for calmodulin-dependent regulation of the V(max) of calcium transport. *J.Biol.Chem.* **275**, 4407-4416.

Xu, G. G., Gao, Z. Y., Borge, P. D., Jr., Jegier, P. A., Young, R. A., & Wolf, B. A. (2000). Insulin regulation of beta-cell function involves a feedback loop on SERCA gene expression, Ca(2+) homeostasis, and insulin expression and secretion. *Biochemistry* **39**, 14912-14919.

Xu, K. Y. & Becker, L. C. (1998). Ultrastructural localization of glycolytic enzymes on sarcoplasmic reticulum vesicles. *J.Histochem.Cytochem.* **46**, 419-427.

Xu, K. Y., Zweier, J. L., & Becker, L. C. (1995). Functional coupling between glycolysis and sarcoplasmic reticulum Ca²⁺ transport. *Circ.Res.* **77**, 88-97.

Yamauchi, K., Milarski, K. L., Saltiel, A. R., & Pessin, J. E. (1995). Protein-tyrosine-phosphatase SHPTP2 is a required positive effector for insulin downstream signaling. *Proc.Natl.Acad.Sci.U.S.A* **92**, 664-668.

Yu, J., Zhang, H. F., Wu, F., Li, Q. X., Ma, H., Guo, W. Y., Wang, H. C., & Gao, F. (2006). Insulin improves cardiomyocyte contractile function through enhancement of SERCA2a activity in simulated ischemia/reperfusion. *Acta Pharmacol.Sin.* **27**, 919-926.

Zhang, X. M., Kimura, Y., & Inui, M. (2005). Effects of phospholipids on the oligomeric state of phospholamban of the cardiac sarcoplasmic reticulum. *Circ.J.* **69**, 1116-1123.

Zierath, J. R. (2002). Invited review: Exercise training-induced changes in insulin signaling in skeletal muscle. *J.Appl.Physiol* **93**, 773-781.

APPENDIX ONE

Thesis Presentation Slides

1.

ROLE OF SECOND MESSENGER SIGNALING PATHWAYS IN THE REGULATION OF SARCOPLASMIC RETICULUM Ca^{2+} -HANDLING PROPERTIES IN THE LEFT VENTRICLE AND SKELETAL MUSCLES OF DIFFERENT FIBRE TYPE COMPOSITION

University of Waterloo
Dept. of Kinesiology,
Waterloo, ON, Canada
N2L 3G1

Todd A. Duhamel
NSERC
CRSNG

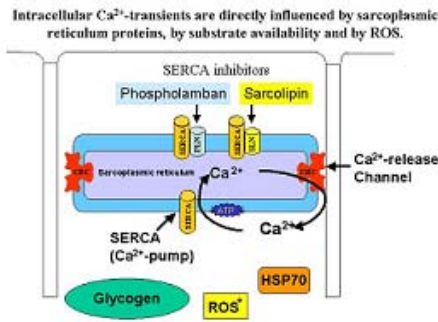
Differences in protein isoform expression contribute to the functional differences that exist between cardiac and skeletal muscles

Muscle	MLCK1	MLCK2	GS	SERCA1a	SERCA2a	PLN	SLN
LV	100%	-	10.4	-	100	100	?
SOL	84%	11%	4.5	40	60	-	100
EDL	4%	96%	3.5	100	-	-	?
RG	51%	48%	5.7	100	-	-	?
WG	-	100%	1.7	100	-	-	?

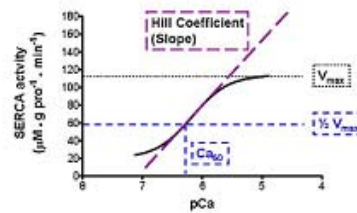
These differences suggest that specific signaling pathways may influence SERCA kinetic properties to a greater extent in tissues that express specific cellular or molecular characteristics unique to one tissue compared to another

5.

2.



SERCA substrate-activity curve and kinetic properties

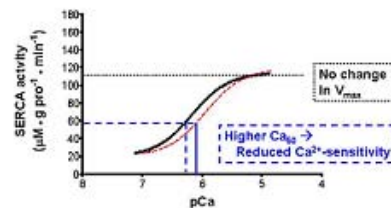


6.

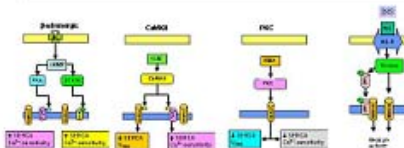
3.

Statement of the Problem
The overall objective of this thesis was to examine mechanisms involved in the acute regulation of sarcoplasmic reticulum Ca^{2+} -handling properties by second messenger signaling pathways in skeletal and cardiac muscle.

Ca^{2+} -sensitivity can be reduced by inhibition of SERCA activity at sub-maximal Ca^{2+} -concentrations



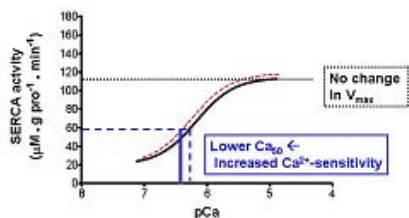
4.



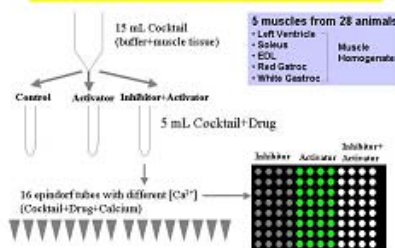
7.

8.

1. **Ca²⁺-sensitivity can be increased by removal of the inhibitory proteins on SERCA at sub-maximal [Ca²⁺]_i**



Modified Spectrophotometric Assay

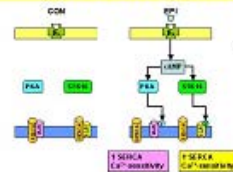


5.

2. **ACUTE REGULATION OF SERCA KINETIC PROPERTIES BY β -ADRENERGIC, Ca²⁺-DEPENDENT CALMODULIN KINASE II AND PROTEIN KINASE C SIGNALING IN CARDIAC AND SKELETAL MUSCLE**

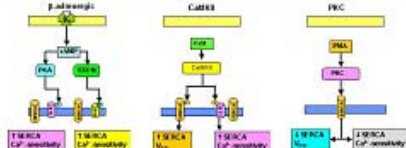
University of Waterloo
 Dept. of Kinesiology, Waterloo, ON, Canada. N2L 2G1
 Todd A. Duhamel, HJ Green, AR Tupling and J Onyiah
 NSERC CRNG

Method used to determine Epinephrine-dependent changes in SERCA activity



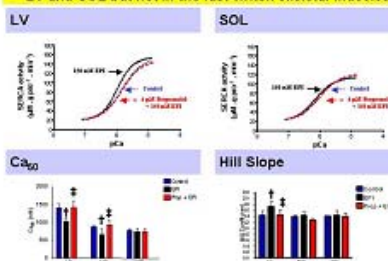
6.

3. **Three signaling pathways are known to regulate SERCA kinetic properties in cardiac tissue**



However, few studies have characterized the influence that β -adrenergic, CaMKII, and PKC signaling pathways have on the regulation of SERCA kinetic properties in skeletal muscle.

Epinephrine increased SERCA Ca²⁺-sensitivity in LV and SOL but not in the fast-twitch skeletal muscles



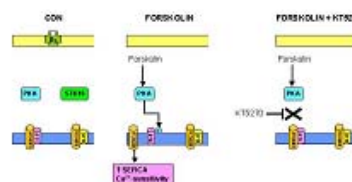
7.

4. **Purpose**
 To characterize the role of β -adrenergic, CaMKII and PKC signaling in the acute regulation of SERCA kinetic properties in the LV and skeletal muscles of a rat

Hypotheses:

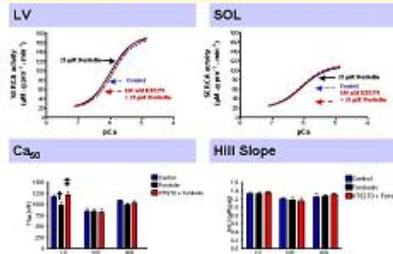
- β -adrenergic signaling will increase SERCA Ca²⁺-sensitivity, without reducing V_{max}, in the LV, SOL and fast-twitch skeletal muscle.
- CaMKII signaling will increase V_{max} and will also increase SERCA Ca²⁺-sensitivity in the LV and SOL but not fast-twitch skeletal muscle.
- PKC signaling will reduce V_{max} and SERCA Ca²⁺-sensitivity in all tissues examined.

Method used to determine PKA-dependent changes in SERCA activity

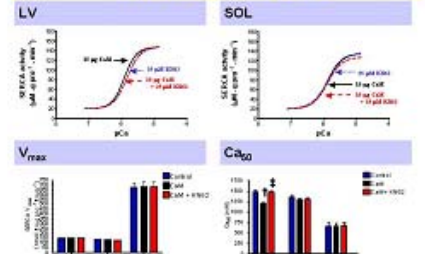


8.

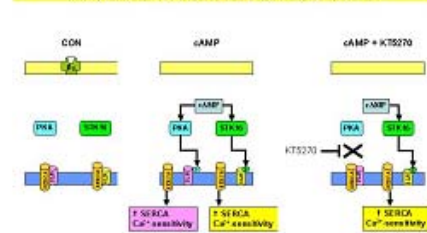
1. SERCA Ca²⁺-sensitivity is increased via a PKA-dependent mechanism in the LV but not in skeletal muscle



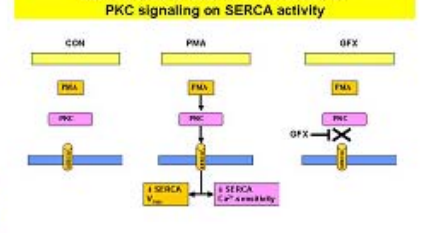
5. CaMKII signaling increases SERCA Ca²⁺-sensitivity in LV but not SOL, without altering V_{max}



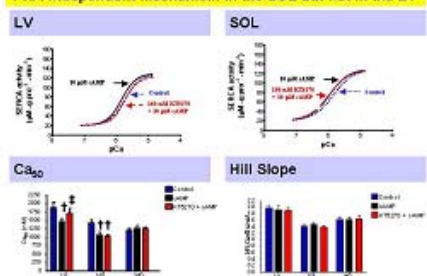
2. Method used to determine changes in SERCA activity that are cAMP-dependent but PKA-independent



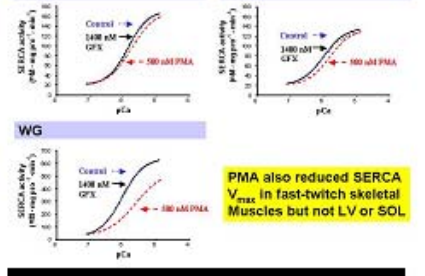
6. Method used to determine the effects of PKC signaling on SERCA activity



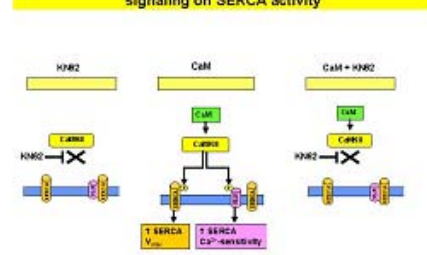
3. SERCA Ca²⁺-sensitivity is increased through a PKA-independent mechanism in the SOL but not in the LV



7. PKC signaling reduces SERCA Ca²⁺-sensitivity in all tissues



4. Method used to determine the effects of CaMKII signaling on SERCA activity



Conclusions

β₁-adrenergic signaling:
 LV – ↑ Ca²⁺-sensitivity via a cAMP and PKA-dependent mechanism → PLN
 SOL – ↑ Ca²⁺-sensitivity via an alternative cAMP-dependent but PKA-independent mechanism → SLN
 EDL, RG, WG – No effect

CaMKII activation
 LV – ↑ Ca²⁺-sensitivity → PLN; no effect on V_{max}
 SOL – No effect; no effect on V_{max}
 EDL, RG, WG – No effect

PKC activation
 LV, SOL – ↓ Ca²⁺-sensitivity
 EDL, RG, WG – ↓ Ca²⁺-sensitivity; ↓ V_{max}

1.

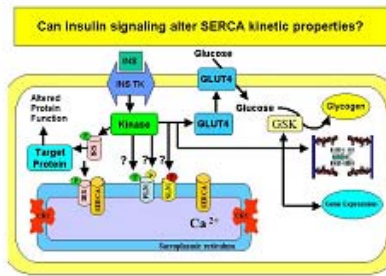
Chapter Three

INSULIN SIGNALING INCREASES THE Ca²⁺-SENSITIVITY OF SERCA PROTEINS IN CARDIAC AND SKELETAL MUSCLE

University of Waterloo
 Dept. of Kinesiology, Waterloo, ON, Canada, N2L 3G1

Todd A. Duhamel, HJ Green, and J Ouyang
 NSERC GRANT

2.



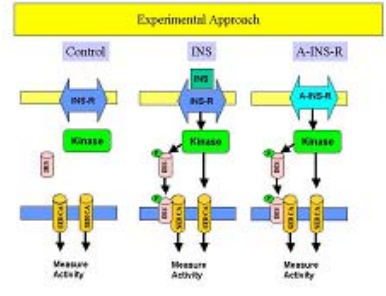
3.

Purpose
 To determine if insulin can acutely regulate SERCA kinetic properties in the LV and skeletal muscles.

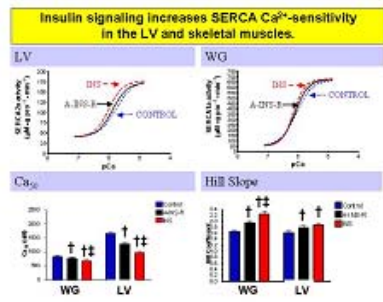
Hypotheses:

1. Insulin will acutely alter SERCA kinetic properties in LV and skeletal muscles.
2. Insulin will promote the interaction of IRS proteins with SERCA
3. Insulin signaling will alter PLN phosphorylation, leading to changes in SERCA2a Ca²⁺-sensitivity in LV.

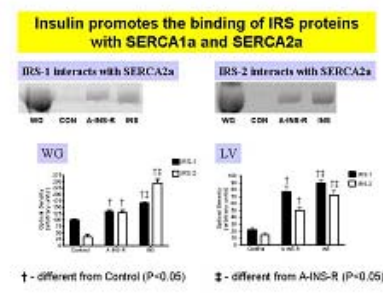
4.



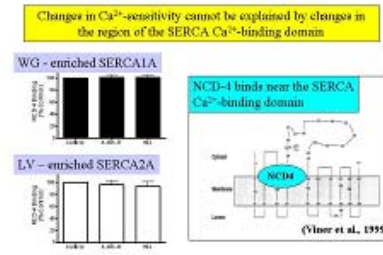
5.



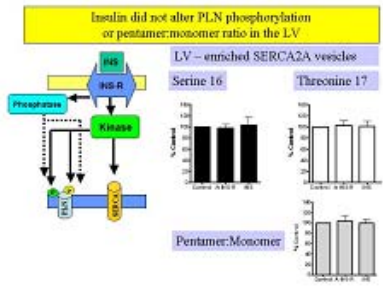
6.



7.



8.



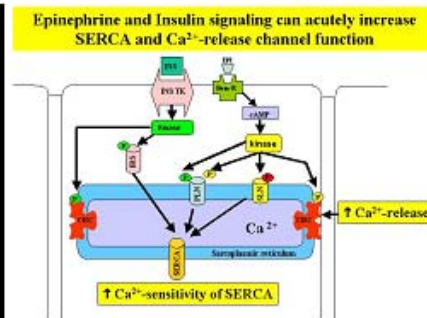
1. **Conclusions**

Insulin signaling acutely increases SERCA Ca^{2+} -sensitivity in LV and skeletal muscles.

Insulin signaling promotes the physical interaction of IRS proteins with SERCA1a and SERCA2a *in vitro*.

Changes in SERCA Ca^{2+} -sensitivity cannot be explained by alterations near the SERCA nucleotide or Ca^{2+} -binding domains or to changes in PLN status.

These data suggest that IRS proteins should be added to the list of endogenous modulator proteins capable of acutely regulating SERCA kinetic properties in cardiac and skeletal muscle.



2. **Chapter Four**

EFFECTS OF EXERCISE AND ORAL GLUCOSE SUPPLEMENTATION ON SARCOPLASMIC RETICULUM Ca^{2+} -CYCLING PROPERTIES IN HUMAN SKELETAL MUSCLE

University of Waterloo

Todd A. Duhamel, R.D. Stewart, K.P. Foley, L.C. Smith, J. Ouyang, and H.J. Green.

Dept. of Kinesiology, Waterloo, ON, Canada, N2L 3G1

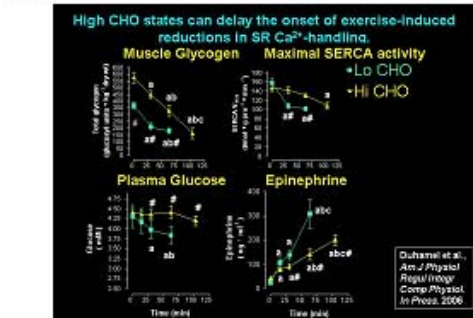
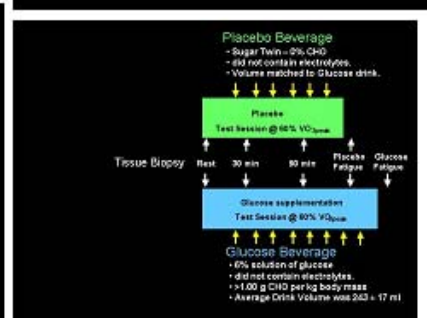
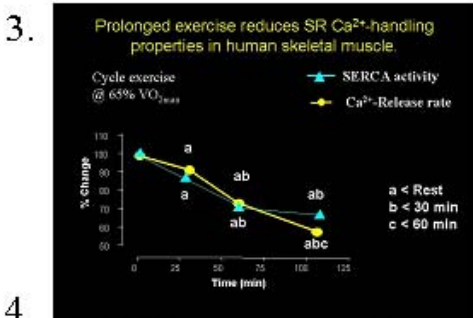
6. **Model**

Glucose supplementation during exercise directly influences plasma glucose, insulin and catecholamine concentrations but does not alter muscle glycogen utilization in humans.

Coyte et al., J Appl Physiol 81(1): 165-72, 1996.
 Margreus and Briggs, J Appl Physiol 85(4): 1553-5, 1998.
 McCormick et al., J Appl Physiol 87(2): 1003-6, 1999.

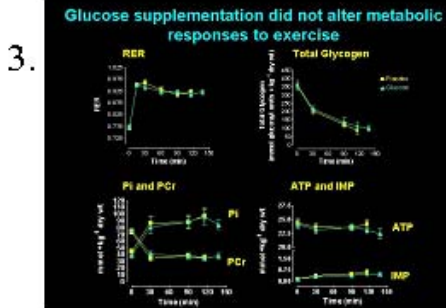
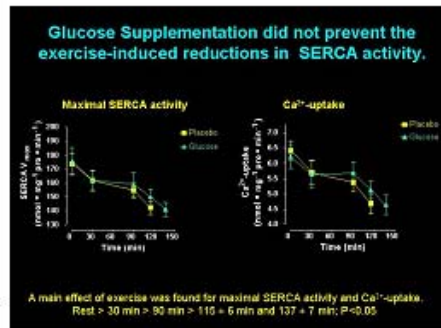
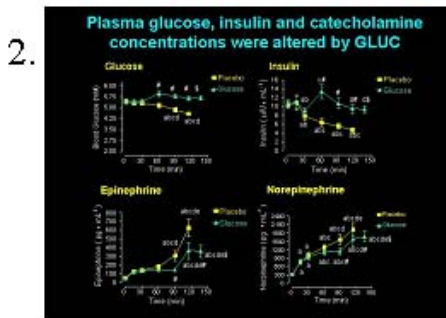
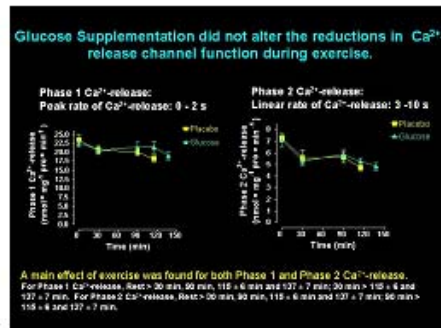
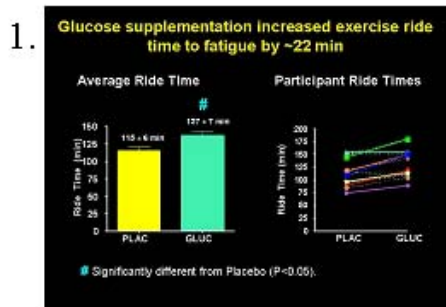
Purpose

To determine if glucose supplementation during exercise can delay or prevent exercise-induced reductions in SR Ca^{2+} -handling properties in human skeletal muscle.



8. **Hypotheses:**

1. Prolonged exercise to fatigue will reduce SR Ca^{2+} -handling properties in human skeletal muscle.
2. Exercise ride times will be prolonged with glucose supplementation.
3. Glucose supplementation will delay the onset of exercise-induced reductions in SR Ca^{2+} -handling properties as a result of elevated plasma glucose, insulin and catecholamine concentrations.



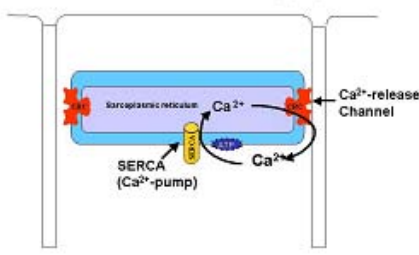
6. **Conclusions**

Glucose supplementation does not alter magnitude or the time-course of exercise induced reductions in SR Ca²⁺-handling properties in human skeletal muscle.

The increase in exercise ride time with glucose supplementation cannot be explained by differences in skeletal muscle SR Ca²⁺-handling properties, measured *in vitro*.

These data indirectly support the possibility that muscle glycogen content may influence SR Ca²⁺-handling properties in skeletal muscle since muscle glycogen utilization was not altered in this study.

What affect will glucose supplementation exert on SR Ca²⁺-handling properties?



Thesis Summary and Conclusions

Todd A. Duhamel

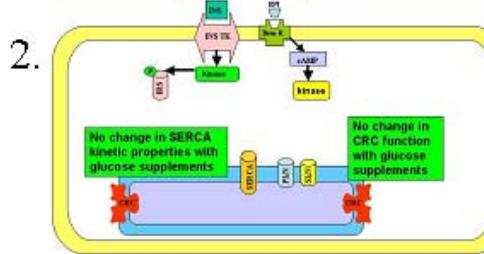
University of Waterloo

Dept. of Kinesiology, Waterloo, ON, Canada, N2L 3G1

1.

Treatment	LV	SOL	EDL	RG	WG
β -adrenergic					
EPI	↑	↑	-	-	-
cAMP	↑	↑	-	-	-
PKA	↑	-	-	-	-
Regulator Protein	PLN	SLN	-	-	-
CaMKII					
CaM	↑	-	-	-	-
Regulator Protein	PLN	-	-	-	-
PKC					
PMA	↓	↓	↓	↓	↓
Regulator Protein	?	?	?	?	?
Insulin					
Insulin	↑	↑	↑	↑	↑
A-INS-R	↑	↑	↑	↑	↑
Regulator Protein	IRS	IRS	IRS	IRS	IRS

Glucose supplementation did not alter SR Ca²⁺-handling properties during exercise



3.

UNIVERSITY OF MANITOBA

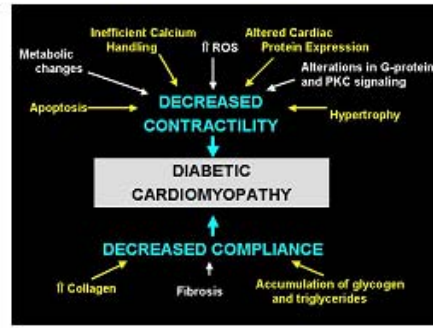
St-Boniface General Hospital Research Centre

Future Directions...

HEART & STROKE Foundation

IMPACT
Integrated and Mentored
Pulmonary and Cardiovascular Training

CHR IRSC



5.

Acknowledgements

Supervisor

- Howie Green

Mentors

- Russ Tupling
- Rich Hughson
- Jay Thomson
- Mike Sharratt

Expert Technical Leadership

- Marg Burnett
- Jing Ouyang

Medical Doctors

- Dr. John Moll
- Dr. Trevor Hill
- Dr. Don Ranney

The Green Lab

- Riley Stewart
- Kevin Foley
- Jenn Perco
- Melissa Thomas
- Justine Yau
- Sharon Rich

The Tupling Lab

- Eric Bombardier
- Chris Vigna

6.

APPENDIX TWO

Data that were not included in Chapter Two

Appendix Table 2.1: Effects of Propranolol, Epinephrine or Propranolol+ Epinephrine on SERCA kinetic properties in homogenates from left ventricle and skeletal muscle of different fibre type composition.

	4 μ M Propranolol	150 nM Epinephrine	4 μ M Propranolol + 150 nM Epinephrine
LV			
V_{\max}	135 \pm 5	132 \pm 6	135 \pm 7
n_H	1.99 \pm 0.07	2.36 \pm 0.07 †	2.03 \pm 0.07 ‡
Ca_{50}	1504 \pm 79	1240 \pm 26 †	1425 \pm 75 ‡
SOL			
V_{\max}	131 \pm 9	132 \pm 9	134 \pm 9
n_H	1.27 \pm 0.04	1.71 \pm 0.12 †	1.31 \pm 0.08 ‡
Ca_{50}	941 \pm 82	755 \pm 63 †	981 \pm 133 ‡
EDL			
V_{\max}	712 \pm 31	704 \pm 29	700 \pm 31
n_H	1.91 \pm 0.08	1.92 \pm 0.06	1.91 \pm 0.09
Ca_{50}	794 \pm 16	771 \pm 15	787 \pm 27
WG			
V_{\max}	712 \pm 37	716 \pm 39	707 \pm 41
n_H	1.73 \pm 0.07	1.70 \pm 0.08	1.72 \pm 0.07
Ca_{50}	883 \pm 51	881 \pm 56	872 \pm 58
RG			
V_{\max}	476 \pm 8	474 \pm 7	478 \pm 7
n_H	1.76 \pm 0.10	1.78 \pm 0.08	1.81 \pm 0.06
Ca_{50}	795 \pm 30	762 \pm 25	764 \pm 17

Values are Means \pm S.E. n=7. LV, left ventricle. SOL, soleus. EDL, extensor digitorum longus. WG, the white portion of the gastrocnemius. RG, the red portion of the gastrocnemius. Epinephrine is a β -adrenergic activator. Propranolol is a β -adrenergic inhibitor. V_{\max} , maximal SERCA activity. n_H , hill slope defined as the relationship between SERCA activity and $[Ca^{2+}]_f$ for 10 to 90% V_{\max} . Ca_{50} , the Ca^{2+} -concentration at $\frac{1}{2} V_{\max}$. Units for V_{\max} are $nmol.mg^{-1}.min^{-1}$. Units for n_H are arbitrary units. Units for Ca_{50} are nM. † - Significantly different from 4 μ M propranolol ($P < 0.05$). ‡ - Significantly different from 150 nM epinephrine ($P < 0.05$).

Appendix Table 2.2: Effects of KT5720, Forskolin or KT5720 + Forskolin on SERCA kinetic properties in homogenates from left ventricle and skeletal muscle of different fibre type composition.

	100 nM KT5720	25 μ M Forskolin	100 nM KT5720 + 25 μ M Forskolin
LV			
V_{\max}	141 \pm 7	143 \pm 6	146 \pm 6
n_H	2.22 \pm 0.10	2.29 \pm 0.07	2.20 \pm 0.07
Ca_{50}	1627 \pm 57	1295 \pm 30	1441 \pm 61 †‡
SOL			
V_{\max}	117 \pm 6	121 \pm 5	120 \pm 7
n_H	1.63 \pm 0.06	1.67 \pm 0.09	1.61 \pm 0.07
Ca_{50}	793 \pm 86	754 \pm 23	767 \pm 53
EDL			
V_{\max}	778 \pm 42	790 \pm 44	791 \pm 45
n_H	1.69 \pm 0.05	1.66 \pm 0.04	1.64 \pm 0.07
Ca_{50}	875 \pm 13	928 \pm 34	916 \pm 32
WG			
V_{\max}	625 \pm 38	639 \pm 33	632 \pm 37
n_H	2.04 \pm 0.07	2.03 \pm 0.12	2.00 \pm 0.09
Ca_{50}	685 \pm 28	697 \pm 17	677 \pm 11
RG			
V_{\max}	433 \pm 10	437 \pm 8	424 \pm 10
n_H	1.98 \pm 0.08	2.00 \pm 0.09	1.94 \pm 0.06
Ca_{50}	692 \pm 39	706 \pm 42	689 \pm 38

Values are Means \pm S.E. n=7. LV, left ventricle. SOL, soleus. EDL, extensor digitorum longus. WG, the white portion of the gastrocnemius. RG, the red portion of the gastrocnemius. Forskolin is a protein kinase A (PKA) activator. KT5720 is a PKA inhibitor. V_{\max} , maximal SERCA activity. n_H , hill slope defined as the relationship between SERCA activity and $[Ca^{2+}]_f$ for 10 to 90% V_{\max} . Ca_{50} , the Ca^{2+} -concentration at $\frac{1}{2} V_{\max}$. Units for V_{\max} are $nmol.mg^{-1}.min^{-1}$. Units for n_H are arbitrary units. Units for Ca_{50} are nM. † - Significantly different from 100 nM KT5720 (P<0.05). ‡ - Significantly different from 25 μ M forskolin (P<0.05).

APPENDIX THREE

Data that were presented in Figures in Chapter Three

Appendix Table 3.1: Co-immunoprecipitation of insulin receptor substrate (IRS)-1 and IRS-2 with SERCA1a using white gastrocnemius homogenates or SERCA2a using left ventricular homogenates.

	Control	30 ng A-INS-R	100 nM Insulin
WG			
IRS-1	100 ± 6	134 ± 5 †	168 ± 2 †‡
IRS-2	34 ± 11	129 ± # †	245 ± 15 †‡
LV			
IRS-1	22 ± 3	77 ± 9 †	90 ± 5 †‡
IRS-2	14 ± 4	50 ± 5 †	72 ± 7 †‡

Values are Means ± S.E; n=4. Optical density of IRS-1 and IRS-2 proteins assessed by Western blot techniques using the 1st elution of sample from the co-immunoprecipitation antibody MA3-919. † Significantly different from Control (P<0.05). ‡ Significantly different from A-INS-R (P<0.05).

Appendix Table 3.2: Fluorescein isothiocyanate (FITC) and N-cyclohexyl-N'-(dimethylamino-alpha-naphthyl) carbodiimide (NCD-4) binding capacity of SR vesicles enriched in SERCA1a prepared from the white gastrocnemius or SR vesicles enriched in SERCA2a prepared from the left ventricle in response to 30 ng active insulin receptor or 100 nM insulin

	Control	30 ng A-INS-R	100 nM Insulin
FITC			
SERCA1a	100	97 ± 3	102 ± 4
SERCA2a	100	103 ± 7	102 ± 9
NCD4			
SERCA1a	100	101 ± 5	101 ± 4
SERCA2a	100	96 ± 7	94 ± 7

Values are Means ± S.E; n=8. Control, a control sample. A-INS-R, 30 ng of an activated form of the insulin receptor. INS, 100 nM insulin.

Appendix Table 3.3: Assessments of phospholamban status in response to activation of insulin signaling in SR vesicles enriched in SERCA2a and prepared from the left ventricle. Panel A, phospholamban pentamer:monomer ratio.

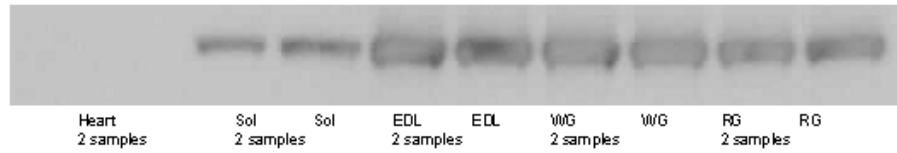
	Control	A-INS-R	Insulin	A-PKA	CaM
PLN Ratio (Pentamer:Monomer)	100	104 ± 10	100 ± 7	104 ± 4	100 ± 3
Ser16-PLN	100	98 ± 6	103 ± 14	127 ± 6 \$	95 ± 10
Thr17-PLN	100	103 ± 8	101 ± 9	98 ± 4	118 ± 4 \$

Values are Means ± S.E; n=8. PLN ratio, phospholamban pentamer:monomer ratio. Ser16-PLN, the Ser16 phosphorylated form of phospholamban. Thr17-PLN, the Thr17 phosphorylated form of phospholamban. Control, a control sample. A-INS-R, 30 ng of an activated form of the insulin receptor. INS, 100 nM insulin. A-PKA, an activated form of PKA. CaM, bovine brain calmodulin. A 1 way-ANOVA indicated no differences between control, A-INS-R or INS. Therefore, A-PKA and CaM samples were tested to confirm the validity of the Ser16 and Thr17 antibodies. Student T-tests were utilized to make comparisons between control samples with A-PKA and control samples with CaM since these conditions were assessed on independent gels and not concurrently with A-INS-R or 100 nM INS. \$ Significantly different from control.

APPENDIX FOUR

Example Western Blot Figures

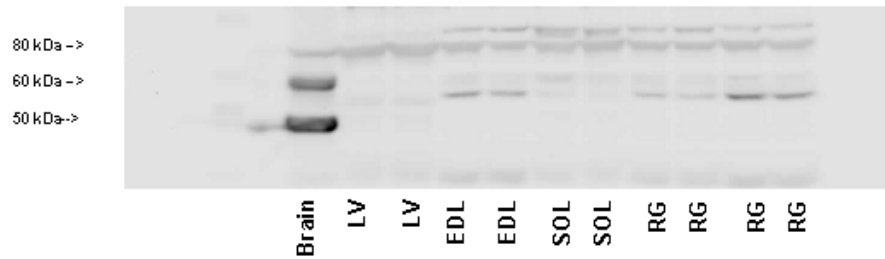
SERCA1a – Tissue scan



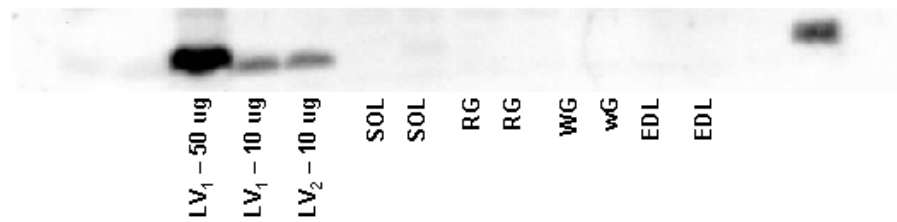
SERCA2a – Tissue scan



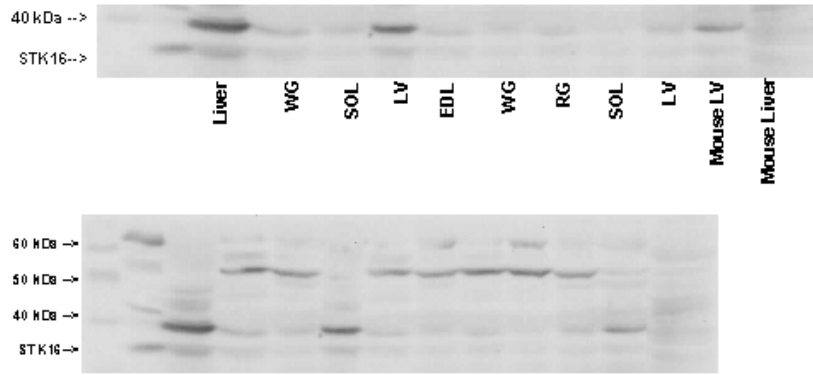
CaMKII – Tissue scan



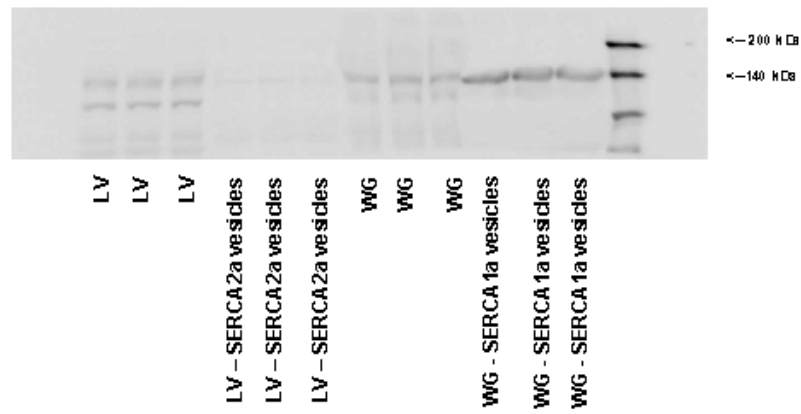
PLN – Tissue scan



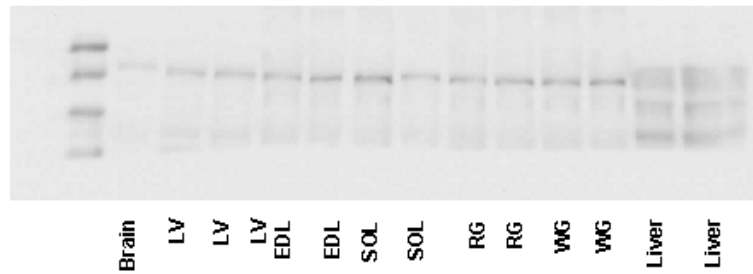
STK16 – Tissue Scan



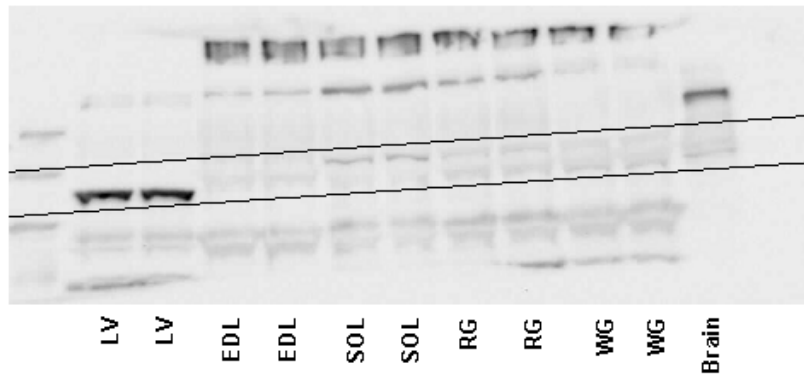
IRS-1 – Vesicles versus homogenates



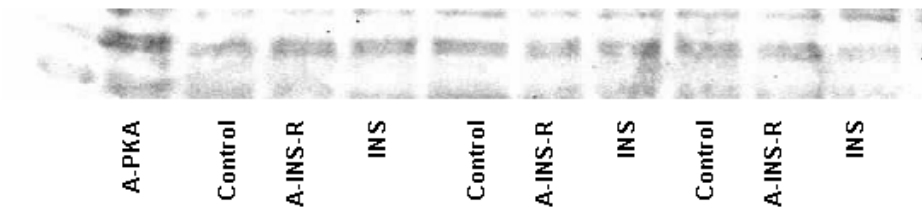
IRS-1 – Tissue scan



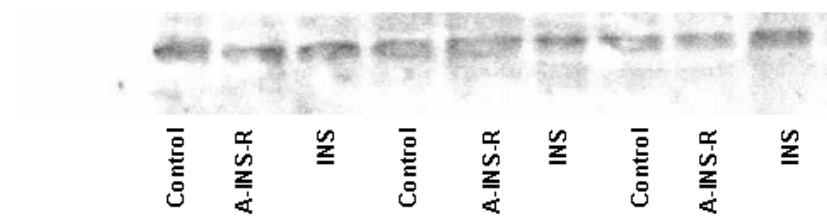
IRS-2 - Tissue Scan



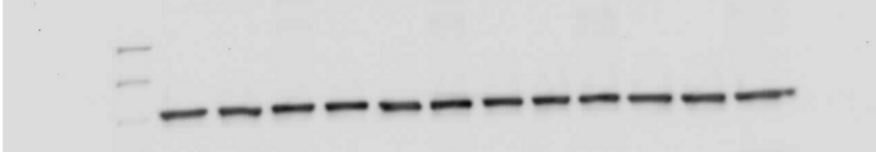
PLN – Ser16 Phosphorylation



PLN – Thr17 Phosphorylation

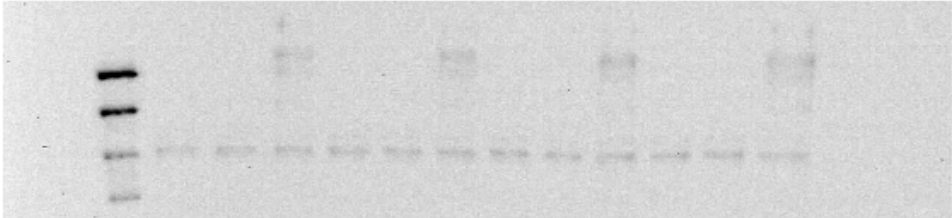


FITC Binding – SERCA1a



Control
A-INS-R
INS
Control
A-INS-R
INS
Control
A-INS-R
INS
Control
A-INS-R
INS

FITC Binding – SERCA2a



Control
A-INS-R
INS
Control
A-INS-R
INS
Control
A-INS-R
INS
Control
A-INS-R
INS

APPENDIX FIVE

Data that were presented in Figures in Chapter Four

Appendix Table 4.1 : Individual participant ride time to fatigue data during the prolonged exercise tests in the Placebo and Glucose conditions.

Participant Code	PLAC	GLUC
TP	110	150
KC	115	112
AM	95	110
DC	150	180
AD	118	150
LK	145	180
AP	150	150
DS	110	151
IC	75	90
MR	90	120
DF	150	150
RS	110	150
MC	120	142
EH	97	115
MK	85	105
Mean ± SE	115 ± 6	137 ± 7 #

Values are individual data (n=15). PLAC, placebo condition. GLUC, glucose condition. Units are minutes. # significantly different from PLAC (P<0.05).

Appendix Table 4.2. Hematocrit concentration and plasma volume changes sampled at rest and during prolonged exercise in the Placebo and Glucose conditions.

	Rest	30 min	115 ± 6 min	137 ± 7 min
Hematocrit				
PLAC	45.7 ± 0.8	48.0 ± 0.8	47.7 ± 0.8	
GLUC	45.7 ± 0.9	48.1 ± 0.7	47.7 ± 0.7	47.1 ± 0.7
Plasma volume				
PLAC	100.0	92.2 ± 1.3	93.3 ± 1.2	
GLUC	100.0	91.8 ± 1.5	95.3 ± 1.4	95.3 ± 1.4

Values are means ± SE (n=15). PLAC, placebo condition. GLUC, glucose condition. Rest represents 0 min. Units are % whole blood for hematocrit and are % of rest for plasma volume. A main effect of exercise was found for hematocrit (Rest < 30 min, 90 min, 115 ± 6 min and 137 ± 7 min; P<0.05) and plasma volume (Rest > 30 min, 90 min, 115 ± 6 min and 137 ± 7 min; P<0.05).

Appendix Table 4.3: Blood metabolite and hormone concentrations during prolonged exercise in the Placebo and Glucose conditions.

	Rest	15 min	30 min	60 min	90 min	115 ± 6 min	137 ± 7 min
Plasma Glucose (mM)							
PLAC	5.40 ± 0.14	5.30 ± 0.14	5.32 ± 0.15	5.15 ± 0.17	4.86 ± 0.15 abcd	4.55 ± 0.12 abode	5.68 ± 0.14 \$
GLUC	5.43 ± 0.14	5.39 ± 0.16	5.42 ± 0.16	5.98 ± 0.20 #	5.80 ± 0.13 #	5.93 ± 0.16 #	
Plasma Lactate (mM)							
PLAC	0.91 ± 0.08	2.15 ± 0.21 a	2.12 ± 0.28 a	1.75 ± 0.18 abc	1.69 ± 0.18 abc	1.67 ± 0.13 abc	1.40 ± 0.16 \$
GLUC	0.96 ± 0.10	2.14 ± 0.23 a	2.16 ± 0.26 a	1.56 ± 0.19 abc	1.36 ± 0.14 # abc	1.39 ± 0.19 # abc	
Plasma FFAs (mM)							
PLAC	0.47 ± 0.03	0.50 ± 0.03	0.47 ± 0.03	0.48 ± 0.03	0.49 ± 0.03	0.48 ± 0.02	0.55 ± 0.03 \$
GLUC	0.48 ± 0.03	0.51 ± 0.03	0.51 ± 0.03	0.66 ± 0.03 # abc	0.55 ± 0.03 # a	0.54 ± 0.04 # a	
Insulin (uIU·ml⁻¹)							
PLAC	10.36 ± 0.90	10.82 ± 1.77	7.78 ± 0.91 ab	6.36 ± 0.92 ab	5.50 ± 0.58 abc	4.65 ± 0.63 abc	9.40 ± 0.80 \$
GLUC	10.67 ± 0.79	11.03 ± 1.37	8.96 ± 0.76	13.30 ± 1.55 # c	10.73 ± 1.24 #	9.46 ± 1.04 # d	
Epinephrine (pg·ml⁻¹)							
PLAC	52 ± 8	123 ± 18	137 ± 16	180 ± 28	307 ± 63 abcd	627 ± 101 abode	361 ± 71 \$
GLUC	50 ± 9	117 ± 18	132 ± 16	150 ± 20	142 ± 19 #	363 ± 96 # abodef	
Norepinephrine (pg·ml⁻¹)							
PLAC	305 ± 26	734 ± 86 a	1004 ± 98 ab	1276 ± 110 abc	1659 ± 180 abcd	1936 ± 220 abode	1882 ± 206 \$
GLUC	307 ± 35	757 ± 95 a	937 ± 112 a	1131 ± 130 abc	1141 ± 127 # abc	1588 ± 261 # abode	

Values are means ± SE (n=15). PLAC, placebo condition. GLUC, glucose condition. Rest, represents 0 min. Units are mM for glucose, lactate and free fatty acids, uIU · ml⁻¹ for insulin and pg · ml⁻¹ for epinephrine and norepinephrine. a significantly different from rest (P<0.05). b significantly different from 15 min (P<0.05). c significantly different from 30 min (P<0.05). d significantly different from 60 min (P<0.05). e significantly different from 90 min (P<0.05). # significantly different from matched time point in PLAC (P<0.05). \$ significantly different from PLAC fatigue time point (i.e.; 115 ± 6 min) (P<0.05).

Note: the insulin concentrations ranged between 194 and 554 pg·ml⁻¹.

Appendix Table 4.4: Muscle glycogen concentrations measured at rest and during prolonged exercise in the Placebo and Glucose conditions.

	Rest	30 min	90 min	115 ± 6 min	137 ± 7 min
Total Glycogen					
PLAC	354 ± 16	203 ± 16	120 ± 15	84 ± 20	
GLUC	357 ± 28	213 ± 20	136 ± 25	112 ± 18	98 ± 18
Pro Glycogen					
PLAC	302 ± 12	181 ± 14	107 ± 13	75 ± 18	
GLUC	306 ± 23	189 ± 18	122 ± 22	100 ± 16	88 ± 17
Macro Glycogen					
PLAC	53 ± 6	21 ± 3	12 ± 2	9 ± 3	
GLUC	51 ± 7	24 ± 3	13 ± 3	12 ± 2	10 ± 2

Values are means ± SE (n=15). PLAC, placebo condition. GLUC, glucose condition. Rest, represents 0 min. Units are mmol glucosyl units · kg⁻¹ dry wt. Total glycogen content is the sum of pro glycogen plus macro glycogen content. A main effect of exercise (Rest > 30 min > 90 min > 115 ± 6 min and 137 ± 7 min; P<0.05) was found for total, pro and macro glycogen content.

Appendix Table 4.5: Sarcoplasmic reticulum hydrolytic, Ca^{2+} -transport, and apparent coupling ratio parameters measured at rest and during prolonged exercise in the Placebo and Glucose conditions.

		Rest	30 min	90 min	115 ± 6 min	137 ± 7 min
V_{\max}	PLAC	174 ± 7	162 ± 7	155 ± 6	142 ± 5	
	GLUC	177 ± 10	164 ± 7	161 ± 8	152 ± 6	143 ± 5
Ca^{2+} -Uptake	PLAC	6.41 ± 0.31	5.71 ± 0.38	5.39 ± 0.31	4.68 ± 0.33	
	GLUC	6.30 ± 0.37	5.73 ± 0.47	5.77 ± 0.36	5.23 ± 0.30	4.73 ± 0.32
Coupling Ratio	PLAC	0.037 ± 0.001	0.036 ± 0.002	0.035 ± 0.002	0.033 ± 0.002	
	GLUC	0.036 ± 0.002	0.036 ± 0.002	0.036 ± 0.002	0.036 ± 0.002	0.033 ± 0.002

Values are means ± SE (n=15). PLAC, placebo condition. GLUC, glucose condition. Rest, represents 0 min. Units are nmol · mg protein⁻¹ · min⁻¹ for V_{\max} and Ca^{2+} -uptake. Calcium dependent Ca^{2+} -uptake rates were assessed at 2000 nM Ca^{2+} . Coupling ratio, defined as Ca^{2+} uptake assessed at 2000 nM / V_{\max} . A main effect of exercise (Rest and 30 min > 90 min > 115 ± 6 min and 137 ± 7 min; P<0.05) was found for V_{\max} and Ca^{2+} -uptake.

Appendix Table 4.6: Sarcoplasmic reticulum Ca^{2+} -release parameters measured at rest and during prolonged exercise in the Placebo and Glucose conditions.

	Rest	30 min	90 min	115 ± 6 min	137 ± 7 min
Phase 1					
PLAC	23.4 ± 1.3	20.6 ± 1.3	20.1 ± 0.98	18.2 ± 0.79	
GLUC	23.0 ± 1.1	21.1 ± 1.0	21.8 ± 1.4	20.7 ± 0.78	19.5 ± 1.08
Phase 2					
PLAC	7.31 ± 0.39	5.60 ± 0.64	5.61 ± 0.45	4.78 ± 0.35	
GLUC	7.27 ± 0.54	5.43 ± 0.33	6.01 ± 0.44	5.41 ± 0.31	4.98 ± 0.30

Values are means ± SE (n=15). PLAC, placebo condition. GLUC, glucose condition. Rest, represents 0 min. Units are nmol · mg protein⁻¹ · min⁻¹. Phase 1 Ca^{2+} -release, the initial, rapid rate of release. Phase 2 Ca^{2+} -release, the more prolonged, slower rate of release which follows Phase 1. Main effects of exercise ($P < 0.05$) were found for both Phase 1 and Phase 2 Ca^{2+} -release. For Phase 1 Ca^{2+} -release, Rest > 30 min, 90 min, 115 ± 6 min and 137 ± 7 min; 30 min > fatigue in each condition [i.e.; PLAC 115 ± 6 min and GLUC 137 ± 7 min]. For Phase 2 Ca^{2+} -release, Rest > 30 min, 90 min, 115 ± 6 min and 137 ± 7 min; 90 min > fatigue in each condition [i.e.; PLAC 115 ± 6 min and GLUC 137 ± 7 min].

Appendix Table 4.7: Sarcoplasmic reticulum Ca^{2+} -uptake rates measured in the presence and absence of ruthenium red.

	Rest	30 min	90 min	115 ± 6 min	137 ± 7 min
Ca²⁺-Uptake					
2000 nM					
PLAC	6.41 ± 0.31	5.71 ± 0.38	5.39 ± 0.31	4.68 ± 0.33	
GLUC	6.30 ± 0.37	5.73 ± 0.47	5.77 ± 0.36	5.23 ± 0.30	4.73 ± 0.32
1500 nM					
PLAC	4.86 ± 0.23	4.34 ± 0.29	4.09 ± 0.24	3.55 ± 0.25	
GLUC	4.80 ± 0.29	4.36 ± 0.36	4.38 ± 0.29	3.97 ± 0.22	3.60 ± 0.24
1000 nM					
PLAC	3.33 ± 0.17	2.95 ± 0.20	2.78 ± 0.16	2.40 ± 0.16	
GLUC	3.26 ± 0.19	2.98 ± 0.24	2.94 ± 0.19	2.69 ± 0.15	2.42 ± 0.16
500 nM					
PLAC	1.79 ± 0.08	1.58 ± 0.10	1.48 ± 0.08	1.27 ± 0.09	
GLUC	1.74 ± 0.10	1.57 ± 0.13	1.56 ± 0.11	1.41 ± 0.08	1.26 ± 0.09
Ca²⁺-Uptake with Ruthenium Red					
2000 nM					
PLAC	7.19 ± 0.50	6.64 ± 0.41	6.41 ± 0.26	5.44 ± 0.17	
GLUC	7.28 ± 0.51	6.60 ± 0.64	6.68 ± 0.80	6.34 ± 0.70	5.93 ± 0.77
1500 nM					
PLAC	5.36 ± 0.41	4.89 ± 0.31	4.76 ± 0.18	4.04 ± 0.11	
GLUC	5.44 ± 0.42	4.89 ± 0.48	4.94 ± 0.59	4.74 ± 0.51	4.39 ± 0.54
1000 nM					
PLAC	3.51 ± 0.25	3.22 ± 0.20	3.16 ± 0.11	2.65 ± 0.08	
GLUC	3.58 ± 0.26	3.18 ± 0.32	3.27 ± 0.40	3.11 ± 0.34	2.84 ± 0.36
500 nM					
PLAC	1.70 ± 0.13	1.56 ± 0.11	1.52 ± 0.06	1.27 ± 0.05	
GLUC	1.75 ± 0.14	1.56 ± 0.18	1.54 ± 0.20	1.50 ± 0.18	1.31 ± 0.17

Values are means ± SE (n=15). PLAC, placebo condition. GLUC, glucose condition. Rest, represents 0 min. Units are nmol · mg protein⁻¹ · min⁻¹. A main effect of exercise (Rest > 30 min and 90 min > 115 ± 6 min and 137 ± 7 min; P<0.05) was found for Ca²⁺-uptake rates assessed at 2000, 1500, 1000, and 500 nM in the absence of ruthenium red. A main effect of exercise (Rest > PLAC 115 ± 6 min and GLUC 137 ± 7 min; P<0.05) was found for Ca²⁺-uptake rates assessed at 2000, 1500, 1000, and 500 nM in the presence of ruthenium red.

Appendix Table 4.8: Sarcoplasmic reticulum Ca^{2+} -release channel leak rates measured at rest and during prolonged exercise in the Placebo and Glucose conditions.

		Rest	30 min	90 min	115 ± 6 min	137 ± 7 min
CRC Leak						
	2000 nM					
	PLAC	0.02 ± 0.39	0.01 ± 0.32	0.37 ± 0.35	0.19 ± 0.39	
	GLUC	-0.01 ± 0.45	-0.17 ± 0.55	0.05 ± 0.53	0.30 ± 0.58	0.43 ± 0.60
	1500 nM					
	PLAC	-0.10 ± 0.32	-0.14 ± 0.25	0.19 ± 0.26	0.09 ± 0.28	
	GLUC	-0.13 ± 0.35	-0.24 ± 0.43	-0.09 ± 0.37	0.17 ± 0.43	0.22 ± 0.42
	1000 nM					
	PLAC	-0.24 ± 0.20	-0.20 ± 0.15	0.07 ± 0.19	-0.03 ± 0.18	
	GLUC	-0.20 ± 0.22	-0.31 ± 0.29	-0.09 ± 0.25	0.02 ± 0.28	0.05 ± 0.28
	500 nM					
	PLAC	-0.28 ± 0.10	-0.24 ± 0.08	-0.09 ± 0.13	-0.12 ± 0.10	
	GLUC	-0.26 ± 0.11	-0.28 ± 0.17	-0.24 ± 0.12	-0.10 ± 0.15	-0.14 ± 0.12

Values are means ± SE (n=15). PLAC, placebo condition. GLUC, glucose condition. Rest, represents 0 min. Units are nmol · mg protein⁻¹ · min⁻¹.

APPENDIX SIX

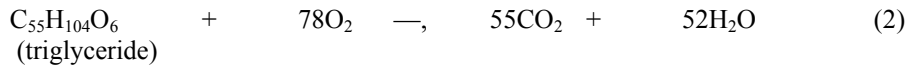
Calculation of Substrate Oxidation

Calculation of Substrate Oxidation

The measurement of oxygen consumption (O_2) and carbon dioxide production (CO_2) can be used to quantify the rate of carbohydrate (CHO) and fat oxidation using indirect calorimetry. The stoichiometry of oxidation of glucose is:



Therefore, each mole of glucose oxidized consumes six moles of oxygen and produces six moles of carbon dioxide. The respiratory quotient (RQ) is equal to 1.0. The stoichiometry of an average fat (triglyceride) is:



The above triglyceride is assumed to be palmitoyl-stearoyl-oleoyl-glyceride as a representative of the average composition of triglyceride (TG). Each mole (861 g) of TG utilizes 78 moles of oxygen and produces 55 moles of carbon dioxide to produce a respiratory quotient equal to 0.7. The precise stoichiometry for protein oxidation cannot be written due to the large variation in the structure of the various amino acids. On average 1g of protein consumes 0.966 litres of oxygen and produces 0.782 litres of carbon dioxide, to produce a respiratory quotient (RQ) of 0.81. These values are expressed as a function of total urinary nitrogen excreted. One gram of urinary nitrogen is assumed to represent the consumption of 6.04 litres of oxygen and the production of 4.89 litres of carbon dioxide.

Since one mole of gas (either O_2 or CO_2) occupies 22.4 litres, we can summarize the above information in the following table:

Substrate	O_2 L·mmole ⁻¹ fuel	CO_2 L·mmole ⁻¹ fuel	O_2 L·g ⁻¹ fuel	CO_2 L·g ⁻¹ fuel
Glucose	0.13428	0.13428	0.746	0.746
Fat (TG)	1.74783	1.23123	2.03	1.43
N	0.08456	0.06804	6.04	4.89

From these figures and from the relation between urinary nitrogen excretion and protein oxidation, total oxygen consumption and carbon dioxide production are expressed by the following equations:

$$O_2 (\text{L} \cdot \text{min}^{-1}) = 0.746c + 2.03f + 6.04n \quad (3)$$

$$CO_2 (\text{L} \cdot \text{min}^{-1}) = 0.746c + 1.43f + 4.89n \quad (4)$$

Where c, f and n refer to the grams oxidized per minute of carbohydrate and fat respectively and n is the rate of excretion of urinary nitrogen in $\text{g} \cdot \text{min}^{-1}$. Solving for the rate of carbohydrate and fat oxidation:

$$c (\text{g} \cdot \text{min}^{-1}) = 4.55 CO_2 - 3.21 O_2 - 2.87n \quad (5)$$

$$f (\text{g} \cdot \text{min}^{-1}) = 1.67 O_2 - 1.67 CO_2 - 1.92n \quad (6)$$

Where both CO_2 and O_2 are expressed in $\text{L} \cdot \text{min}^{-1}$.

To determine the rate of oxidation in $\text{mmole} \cdot \text{min}^{-1}$:

$$O_2 (\text{L} \cdot \text{min}^{-1}) = 0.13428c + 1.7478f + 0.078456n \quad (7)$$

$$CO_2 (\text{L} \cdot \text{min}^{-1}) = 0.13428c + 1.2312f + 0.0680n \quad (8)$$

Where c, f and n are in mmoles. Therefore:

$$c(\text{mmole}\cdot\text{min}^{-1}) = 25.196\text{CO}_2 - 17.749\text{O}_2 - 0.21349n \quad (9)$$

$$f(\text{mmole}\cdot\text{min}^{-1}) = 1.9357\text{O}_2 - 1.9357\text{CO}_2 - 0.031978n \quad (10)$$

Where both CO₂ and O₂ are expressed in L·min⁻¹.

Once CO₂ and O₂ are known, it is possible to calculate the total energy expenditure (TEE):

$$\text{TEE (kcal}\cdot\text{day}^{-1}) = \frac{3.9\text{CO}_2(\text{L}\cdot\text{day}^{-1})}{\text{RQ}} + 1.11\text{CO}_2(\text{L}\cdot\text{day}^{-1}) \quad (11)$$

In many studies it is not practical to obtain urinary nitrogen, so a value for N excretion is assumed. For participants that are on a normal mixed American diet consuming a diet of 1.0g protein per kg, then the N excretion is 150 mg N/kg day.

The above calculations of substrate utilization ignore gluconeogenesis and therefore in an exercise state may underestimate the glucose and fat oxidation rates. The rates of substrate utilization may also be confounded if glucose is infused and some of the glucose is converted to fat. The RQ can also be affected by the bicarbonate buffering system (in non-steady state exercise) and therefore led to errors in the estimation of the rate of substrate oxidation.

The above calculation of carbohydrate oxidation also assumes that all the glucose is derived from plasma. However, during exercise, muscle glycogen can become the major source of carbohydrate oxidation. Since one water molecule is lost in the linkage of the glucose molecules in the formation of glycogen therefore the stoichiometry of muscle glycogen oxidation differs slightly from that described above for glucose. Therefore, equations 5 and 6 apply to plasma glucose utilization, whereas, the following when muscle glycogen is the source of carbohydrates:

$$c_2(\text{g}\cdot\text{min}^{-1}) = 4.081\text{CO}_2 - 2.875\text{O}_2 - 2.593\text{N}(\text{g}\cdot\text{min}^{-1}) \quad (12)$$

$$f_2(\text{g}\cdot\text{min}^{-1}) = 1.503\text{O}_2 - 1.503\text{CO}_2 - 1.728\text{N}(\text{g}\cdot\text{min}^{-1}) \quad (13)$$

To calculate the true CHO oxidation rate (C_T), the relative contribution of glucose (k) and glycogen (m) would have to be known and then the following correction could be applied:

$$(C_T) = kc_1 + mc_2 \quad (14)$$

The above calculations will be performed using the **Substrate Calculator**.

Let's Simplify - Working Simply With Previously Learned Calorimetry Concepts

Although the above calculations do at first look complicated, they are no more difficult than any other calculations you have performed in other courses. You could estimate the substrate utilization using the relationships you learned in either kin 300 or kin 105. You will need to use the following two tables:

Metabolic Values for Carbohydrates, Fats and Proteins

	Carbohydrates	Fats	Proteins
Kilocalories per gram	4.1	9.3	4.3
Litres of CO ₂ per gram	0.75	1.43	0.78
Litres of O ₂ per gram	0.75	2.03	0.97
Respiratory Quotient	1.00	0.70	0.80
Kilocalories per Litre of O ₂	5.0	4.7	4.5
Moles ATP per Litre O ₂	6.5	5.6	--

Adapted from: Consolazio and Johnson (1971).

Caloric Value per Litre of Oxygen for Respiratory Quotient (RQ) Values

Non protein R Q	Kcal per Litre O₂	Kilocalories Derived CHO (%)	from Fats (%)
0.70	4.686	0.00	100.0
0.71	4.690	1.10	98.9
0.72	4.702	4.76	95.2
0.73	4.714	8.40	91.6
0.74	4.727	12.0	88.0
0.75	4.739	15.6	84.4
0.76	4.751	19.2	80.8
0.77	4.764	22.8	77.2
0.78	4.776	26.3	73.7
0.79	4.788	29.9	70.1
0.80	4.801	33.4	66.6
0.81	4.813	36.9	63.1
0.82	4.825	40.3	59.7
0.83	4.838	43.8	56.2
0.84	4.850	47.2	52.8
0.85	4.862	50.7	49.3
0.86	4.875	54.1	45.9
0.87	4.887	57.5	42.5
0.88	4.899	60.8	39.2
0.89	4.911	64.2	35.8
0.90	4.924	67.5	32.5
0.91	4.936	70.8	29.2
0.92	4.948	74.1	25.9
0.93	4.961	77.4	22.6
0.94	4.973	80.7	19.3
0.95	4.985	84.0	16.0
0.96	4.998	87.2	12.8
0.97	5.010	90.4	9.58
0.98	5.022	93.6	6.37
0.99	5.035	96.8	3.18
1.00	5.047	100.0	0.00

Adapted from Consolazio and Johnson (1971).

Assume: A normal resting O₂ = 0.3 L·min⁻¹

Normal RQ = 0.85 (approximately 50% CHO and 50% fat utilization)
 Caloric equivalent of oxygen (when RQ = 0.85) = 4.862 kcal·L⁻¹
 CHO provide 4.1 kcal·g⁻¹
 Fats provide 9.3 kcal·g⁻¹
 Molar mass CHO = 180g·mole⁻¹
 Molar mass fat = 861g·mole⁻¹

Therefore: To determine mmoles of CHO utilized:
 50% of O₂ = 0.3 L·min⁻¹ or 0.15 L·min⁻¹ is provided by CHO utilization.

$$\begin{aligned} \text{mmoles} \cdot \text{min}^{-1} &= \frac{0.15 \text{ L}}{\text{min}^{-1}} * \frac{4.862 \text{ kcal}}{\text{min}^{-1}} * \frac{\text{g}}{\text{L O}_2} * \frac{1 \text{ mole}}{4.1 \text{ kcal}} * \frac{1000 \text{ mmoles}}{180 \text{ g}} && \text{1 mole} \\ &= 0.99 \text{ mmoles} \cdot \text{min}^{-1} \end{aligned}$$

And for the determination of the mmoles of Fat utilized:
 50% of O₂ = 0.3 L·min⁻¹ or 0.15 L·min⁻¹ is provided by fat utilization.

$$\begin{aligned} \text{mmoles} \cdot \text{min}^{-1} &= \frac{0.15 \text{ L}}{\text{min}^{-1}} * \frac{4.862 \text{ kcal}}{\text{min}^{-1}} * \frac{\text{g}}{\text{L O}_2} * \frac{1 \text{ mole}}{9.3 \text{ kcal}} * \frac{1000 \text{ mmoles}}{861 \text{ g}} && \text{1 mole} \\ &= 0.09 \text{ mmoles} \cdot \text{min}^{-1} \end{aligned}$$

We will calculate the amount of substrate utilized in mmole·min⁻¹ for both carbohydrate (9) and fats (10) using the “**Substrate Calculator**”. This simplifies the calculation and also corrects for protein breakdown.

Reference

Consolazio and Johnson. Measurement of energy cost in humans. **Fed. Proc. 30(4): 1444 - 1453, 1971.**

Woelfe, Robert R. *Radioactive and stable isotope tracers in biomedicine: Principles and Practice of kinetic analysis.* New York. John Wiley & Sons, Inc., Pub. 1992. p. 235 - 241.

APPENDIX SEVEN

Detailed procedures for muscle homogenization and isolation of SR vesicles

DETAILED PROCEDURES FOR MUSCLE HOMOGENIZATION AND ISOLATION OF SR VESICLES

Muscle Homogenization

- 1) Clean the homogenizer head, and place on ice in ultra pure water (UPW). Place homogenization (PMSF) buffer and two cleaned centrifuge (10 ml) tubes for each condition (6 conditions-3 muscles for control and stimulation limbs) on ice. Only attach the head of the homogenizer immediately prior to the initiation of the homogenization procedure (ensuring head remains cold).

Note: It is important to remember which centrifuge tubes correspond to their respective condition and muscle.

- 2) Once the electrical stimulation and surgical procedures have been completed, place muscle in large weigh boats containing homogenizing buffer and keep on ice, clean all tissue of connective tissue, and cut into small pieces:
 - Make sure the plantaris muscle is removed and discarded
 - Make sure the soleus muscle and red gastrocnemius muscle are placed in separate weigh boats to ensure contamination is limited
- 3) Take approximately 1/6th of the muscle and blot/dry with a Kimwipe, and proceed to weigh.
- 4) Place in 16 x 100 mm tube with PMSF buffer to create a 10:1 volume to weight ratio.
- 5) Homogenize muscle at a speed of 16500 rpm (setting of 16.5) for two 30 s burst, separated by a 30 s break (30 s on – 30 s off – 30 s on).

Note: It is important to keep the tubes containing the muscle on ice at all times, especially during the homogenization, to minimize any temperature fluctuations.

- 6) Pipette the homogenized sample equally into the two centrifuge tubes corresponding to the appropriate condition (keep on ice).
- 7) Repeat steps 3-6 for the remaining muscle.
- 8) Vortex both centrifugation tubes containing muscle, and using a positive displacement pipette place 200 μ l (100 μ l from each tube) of the sample into 5 Ependorf tubes labeled appropriately and place in liquid nitrogen immediately.

Note: Important to label as homogenate. As well, clean the homogenization blade with UPW between each sample (making sure this is done with tube in ice). It is also very important to get homogenate samples frozen in liquid nitrogen as quickly as possible.

- 9) Repeat for all muscles and for all conditions.
- 10) Remove all samples from the liquid nitrogen, and place in a sample box (labeled and previously cooled in a -40^oC freezer), and immediately place in -80^oC freezer for storage.
- 11) Clean homogenizer with UPW, and wipe down with Kimwipes. Make sure all connective tissue is removed, and run with ethanol to dry.

Isolation of SR – Centrifugation

Turn the centrifuge on (with vacuum on and temperature set to 4^oC) prior to homogenizing. Place the rotor (stored at 4^oC) within the centrifuge. The rotor only holds 12 tubes, which means only 6 conditions can be isolated at a time (2 tubes per condition).

- 1) Hit the vacuum button to break the seal, making it possible to open the lid (to initiate a spin the vacuum must be on, and to open the lid the vacuum must be terminated)
- 2) Vortex and dry each tube prior to placing into the rotor. It is important to remain organized and to counterbalance the samples.
- 3) Lock the rotor lid on, making sure to check that the rubber washers are in place

- 4) 1st spin: speed = 6500 rpm; time = 10 min
- 5) Hit vacuum button – temperature should drop to 4^oC. Once vacuum reads 800 or less hit start to initiate spin
 - in order to start spin you must enter time and speed, then hit enter, followed by start.
- 6) During 1st spin place clean centrifuge tubes (2 per condition) on ice.
- 7) Following spin remove centrifuged tubes and immediately place on ice (stay organized).

Note: Rotor must remain cold, so when working with samples replace rotor lid in centrifuge and hit vacuum (dropping temperature to 4^oC).

- 8) Using a Pasteur pipette remove supernatant and place in clean tubes, make sure equal volume in each tube to ensure balance during spin. Discard pellet.
- 9) 2nd spin: speed = 10500 rpm; time = 18 min
- 10) During 2nd spin place clean tubes on ice, and clean used tubes. This entails using UPW and scrubbing with a pipe cleaner.
- 11) Following spin transfer supernatant to clean tubes using a Pasteur pipette (do this as quickly as possible, since the pellet will re-suspend).
- 12) 3rd spin: speed = 10500 rpm; time = 18 min
- 13) Following spin transfer supernatant to clean tubes using a Pasteur pipette (do this as quickly as possible, since the pellet will re-suspend).
- 14) 4th spin: speed = 23400 rpm; time = 60 min
- 15) During 4th spin make 600 mM KCl PMSF buffer
 - need approximately 10 ml per condition
 - place on ice
 - take out large hand homogenizer, and place on ice
- 16) Following 4th spin discard supernatant and KEEP PELLETT.
- 17) Immediately place 2.5 ml 600 mM KCl PMSF buffer into each tube.
- 18) Scrape (re-suspend) the pellet in each tube with the end of a small hand homogenizer.
- 19) Once the last pellet is re-suspended a 30 min incubation is started.
- 20) Add 5.0 ml of 600 mM KCl PMSF buffer to the large hand homogenizer.
- 21) Using a positive displacement pipette, transfer the re-suspended pellets (2 tubes per condition) to the large hand homogenizer (final volume 10 ml).
- 22) Gently hand homogenize a couple of times to completely ensure re-suspension, and place into a clean centrifugation tube.
- 23) Repeat for each condition, making sure to clean the hand homogenizer with UPW between conditions.

Note: There should now be only 1 tube per condition, again ensure that these tubes are always kept on ice.

- 24) Place the tubes in the centrifuge for the remainder of the 30 min incubation (hit the vacuum button to ensure incubation at 4^oC).
- 25) 5th spin: speed = 9000 rpm; time = 10 min
- 26) Following the 5th spin transfer supernatant to clean tubes (previously placed on

ice), discard pellet.

- 27) 6th spin: speed = 23400 rpm; time = 60 min
- 28) Discard supernatant using a Pasteur pipette, and re-suspend the pellet in 500 μ l PMSF buffer by using the reverse end of a small hand homogenizer.
- 29) Using a positive displacement pipette transfer sample into a small hand homogenizer – gently homogenize to completely re-suspension.
- 30) Using a positive displacement pipette transfer into Ependorf tubes, and quickly freeze in liquid nitrogen.
 - 8 tubes with 50 μ l
 - 4 tubes with 25 μ l
- 31) Clean hand homogenizer with UPW.
- 32) Repeat for all conditions.
- 33) Place samples in appropriate sample boxes, and place in -80^oC freezer.
- 34) Return rotor to storage rack located in fridge, and clean all remaining used centrifuge tubes with soap, UPW and a pipe cleaner. Invert to dry overnight.

APPENDIX EIGHT

Methods to assess sarcoplasmic reticulum properties.

Methods to assess sarcoplasmic reticulum properties.

SR Ca²⁺-ATPase reagent buffer

Reagent	Mass for 200 ml	Final Concentration
KCl	2.982 g	200 mM
HEPES	953.2 mg	20 mM
NaN ₃ (sodium azide)	130.02 mg	10 mM
EGTA	76.08 mg	1 mM
MgCl ₂	285.63 mg	15 mM
PEP (phosphoenol pyruvate)	930.6 mg	10 mM

Add reagents to 150 ml of ultra pure water (UPW)

pH to 7.0 at 37 °C with KOH

Bring volume to 200 ml

Store at -4 °C

Note: Calibrate the pH metre at 37 °C

Other reagents	Mass	Volume	Final Concentration
PK	-	-	18 U·ml ⁻¹
LDH	-	-	18 U·ml ⁻¹
Calcium ionophore (Sigma-C7522)	10 mg	10 ml ethanol	1 mg·ml ⁻¹
NADH (Make up fresh daily)	7.1 mg	400 µl UPW	0.3 mM
CPA (Sigma C1530)	50 mg	3.71 ml chloroform	40 mM
Indo-1	1.0 mg	1.257 glycine buffer	1 mM
"Low Ca ²⁺ " – dilute "Stock" CaCl ₂ by 10x to get a solution = 10 mM CaCl ₂			
"Stock" CaCl ₂ is 100 mM (ORION, 922006)			

Calculation of SERCA activity

Rate of NADH disappearance (Abs·min⁻¹) = slope (m) from Kinetics program

$M_{\text{corrected}} (\text{OD}^2 \text{ units} \cdot \text{min}^{-1}) = -1 \cdot m$

$\text{NADH}_{\text{rate of disappearance}} = m_{\text{corrected}} (\text{OD units} \cdot \text{min}^{-1}) / 6.271 \text{ units} \cdot \mu\text{M}^{-1}$

Make sure to correct slopes from plate reader from the volume that you loaded back to the assumed 1 cm path length that is required for the calculation. Note, to do this correction you must use the path length function on the plate reader and then apply it to your slope. Eg – if you load ~100 uL of volume, the path length correction is approximate 0.300 to 0.350. Take your slope, divide it by this correction factor to get the slope for a path length equal to 1 cm.

Total ATPase activity ($\mu\text{M} \cdot \text{mg}^{-1} \cdot \text{min}^{-1}$) = $\text{NADH}_{\text{rate of disappearance}} (\mu\text{M} \cdot \text{min}^{-1}) / \text{Protein content (mg)}$

The Ca²⁺-ATPase activity = total ATPase activity – basal ATPase activity

Basal ATPase activity is determined in a similar way to total ATPase activity except that the $\text{NADH}_{\text{rate of disappearance}}$ is collected after the addition of CPA, a specific inhibitor of the Ca²⁺-ATPase

SERCA activity assay adapted for Plate Reader

PLATE READER SERCA ASSAY		Todd Duhamel	September, 2005.
3 Drug Comparison			
Step 1	Pipette Calcium into epindorf to get 16 different Calcium concentrations. This needs to be done for each drug of interest. Therefore to analyze 3 drugs at once, you need to load 3 racks x 16 epindorfs each. Set epindorf racks aside for now, you will use these racks in Step 6.		
Step 2	15.3 mL ATPase Buffer 54 uL LDH 54 uL PK 31.5 uL Ionophore		
Step 3	Add SR vesicles 6 uL WG vesicles to 15 mL Buffer (25 ug protein) 40 uL Heart vesicles to 15 mL Buffer (100 ug protein)		
Step 4	Split cocktail into aliquots of 5 mL into 3 test tubes.		
Step 5	Add Drug of interest to each tube.		
Step 6	Transfer 300 uL from one test tube into each of the 16 epindorfs that contain the 16 different Calcium concentrations you loaded in Step 1. Note: Add CPA to one epindorf to get basal ATPase.		
Step 7	Vortex Epindorfs and Load wells on a clear plate with 100 uL from each epindorf. Load duplicate wells for each epindorf tube reads.		
Step 8	Add NADH to plate. I usually add 2 uL NADH with a repeater pipette to each well immediately prior to reading the plate. Note: Use is 4x dilute NADH since it is easier to pipette accurately. weigh NADH, then divide by 71, then multiply by 4, add this amount of water (in mL) to the NADH powder, mix and use.		
Step 8	Place loaded plate into Spec Plate reader and complete a Path Length correction read.		
Step 9.	Change templates and Read Plate on Spec Plate reader for a kinetic assay. Temp = 37 degrees Celsius Time = 30 min Wavelength = 340 nm		

Epindorfs	Low Ca ²⁺ to Add
1	12.0
2	15.0
3	18.0
4	21.0
5	22.5
6	24.0
7	24.8
8	25.5
9	26.3
10	27.0
11	27.8
12	28.5
13	29.3
14	30.0
15	31.5
16	31.5 + CPA

APPENDIX NINE

Measurement techniques to assess SR Ca²⁺-uptake and release

CA²⁺-UPTAKE AND RELEASE DETERMINATIONS

Table 3 - SR homogenate Ca²⁺-uptake and release buffer

Reagent	Mass for 200 ml	Final Concentration
KCl	2.982 g	200 mM
HEPES	953.2 mg	20 mM
NaN ₃	130.02 mg	10 mM
TPEN	0.425 mg	5 μM
MgCl ₂	285.63 mg	15 mM
Oxalate	184.2 mg	5 mM

(oxalic acid, MW = 184.2 g mol⁻¹)

Add reagents to 150 ml of UPW (with active stir bar)
 Heat to 37⁰C and then pH to 7.0 with 2N KOH
 Bring final volume to 200 ml with UPW, Recheck pH, store at -4⁰C

Table 4 - Ca²⁺-uptake and release assay

Reagent	Mass	Volume	Final Concentration
CaCl ₂	-	-	100 mM
“Low” CaCl ₂	-	900 μl UPW with 100 μl CaCl ₂	10 mM
Mg·ATP	4.538 g	30 ml UPW	250 mM
Glycine	0.37535 g	100 ml UPW	50 mM
Indo-1	0.1 mg	1.257 ml glycine	50 mM
“Stock” EGTA	475.5 mg	25 ml UPW	200 mM
EGTA	-	200 μl stock EGTA 800 μl UPW	50 mM

Note: dissolve MgATP in 15 ml UPW, pH to 7.0 using 2N KOH then bring to a final volume of 30 ml. Store at -20⁰C.

Note: dissolve glycine in 70 ml UPW, pH to 11.0 using 2N KOH and bring to a final volume of 100 ml using UPW. Store at 4⁰C.

Note: dissolve “stock” EGTA in 20 ml UPW, pH to 7.0 using 2N KOH and bring to a final volume of 25 ml using UPW. Store at room temperature in the dark.

Procedure

- 1) Heat frozen buffer to 37 °C in water bath
- 2) Turn on flourometer water bath, set temperature to 37 °C
- 3) Turn on flourometer power Arc lamp (LPS-220; PTI) ignite lamp
- 4) Turn on flourometer power source – motor driver (MD-5020; PTI)
- 5) Turn on stir bar motor
- 6) Add 1 ml of buffer, 1 ml Indo-1 and 10 ml “low” CaCl₂ to a four sided cuvette with stir bar
- 7) Open Felix software
- 8) Open ‘uptake’ acquisition folder
- 9) Under display function ensure that the correct background is entered
- 10) Click acquire
 - ensure monochromater is set to 355 nm, dial on back of motor driver
 - if not correctly set to 355 nm open hardware set up folder, click lightening bold and enter the new value on back of monochromater in pop up window. Close folder to save, and re-acquire (check again to make sure set to 355 nm)
- 11) Add 1806 ml buffer to a four sided cuvette with a stir bar
- 12) Add 1.0 µl Indo-1
- 13) Amount of tissue;
 - add 150 µl Sol Hom
 - add 100 µl RG Hom
 - add 50 µl WG Hom
- 14) Add ~3.0 µl “low” CaCl₂
- 15) Click start
- 16) Add 40 µl Mg ATP
- 17) Once free and bound lines plateau add 145 µl EGTA (this is R_{min})
- 18) Add 20 µl CaCl₂ (this is R_{max})

Note: Final volume should be, 2.0 ml, this means that RG homogenate trials should have 1856 µl of buffer, and WG homogenate trials should have 1906 µl of buffer.

For Ca²⁺-Release,

Follow uptake procedures with the exception of the last two points, once a plateau is reached add 10 µl of 4-CMC. Collect data for ~3 min following this addition to ensure phase 1 and phase 2 can be distinguished.

Analysis

For every uptake file calibrate the following way

- 1) Open concentration equation from drop down menu
- 2) Click equation box, and then click edit equation
- 3) Highlight R_{\min} (highest point on curve)
 - select the ratio curve and click 'capture value' corresponding to R_{\min}
 - select the B curve (yellow) and click 'capture value' corresponding to Sf2
- 4) Highlight R_{\max} (lowest part of yellow curve)
 - select the B curve (yellow) and click 'capture value' corresponding to Sb2
 - select the ratio curve and click 'capture value' corresponding to R_{\max}
- 5) In Kd window enter a value of 250
- 6) Save equation, and click okay
 - apply equation to ratio curve
- 7) Select newly generated curve, and under math menu select smooth function
 - smooth curve 21 times
 - delete raw curve
- 8) To view curve select fixed min. and max. from the axis menu
 - enter a value of 0 for minimum value, and 4000 for the maximum value
- 9) To analyze uptake at 2000 nM:
 - select the linear fit function from the math list
 - highlight the curve from 2100-900 on y-axis
 - ensure you have the correct curve selected, and execute
 - the open window should display the range you have selected, as well as the slope of the line (this is the rate of $[Ca^{2+}]_f$ disappearance)

Repeat this procedure for all desired $[Ca^{2+}]_f$ levels (1500, 1000 and 500 nM)

- 10) Open the previously collected release file for the same muscle sample, and apply the uptake calibration by selecting the ratio curve, and from the drop down menu located on the top tool bar highlight the displayed Grynkiewicz equation, and click apply.
- 11) Select newly generated curve, and under the math menu select smooth function
 - smooth curve 21 times
 - delete original curve
- 12) To analyze phase 1
 - from axis menu select fixed min. and max.
 - select 0 for min. value and 1000 for max. value
 - highlight the appropriate area of the curve and select linear fit function from math drop menu, click execute
 - the open window should display the range you have selected, as well as the slope of the line (this is the rate of release)
- 13) To analyze phase 2 repeat above steps only highlight appropriate area of curve

APPENDIX TEN

Co-immuno precipitation assay protocol

Co-IP Protocol
Pierce Seize X Protein G Immunoprecipitation Kit

Todd Duhamel

July 6, 2006

Get Chris, or another lucky, to go and buy a coffee for you while the Co-IP chemicals equilibrate to room temperature.

Binding of Antibody to Gel.

- Step 1** Take kit out of Fridge and let warm up to room temperature.
- Step 2**
- a** Add 500 mL Ultra Pure water to dry blend buffer (PBS package).
 - b** Add 0.02% Sodium Azide and store at 4 degrees Celcius for long term if needed.
(in 500 mL this would be a mass of 0.100 grams Sodium Azide).
- Step 3** If you want to run 3 conditions you will need to set up 3 micro centrifuge tubes with 3 Spin Cup Columns inside.
- Step 4**
- a** Gently mix (by swirling) the bottle of 50% Slurry Immobilized Protein G until you get an even suspension
 - b** Add 100 uL of 50% Slurry to each Spin Column in the micro centrifuge tubes.
- Step 5** Centrifuge tubes in the Beckman centrifuge with the F2402H Rotor.
- Speed = 6419 RPM
 - RCF (g) = 3000 G
 - Time = 1 min
- Step 6**
- a** Throw away the flow through liquid in the bottom of the micro centrifuge tubes.
 - b** Replace spin cups by putting them back into the micro centrifuge tubes.
- Step 7**
- a** Wash the gell by adding 400 uL of Binding/wash buffer to each tube.
 - b** Cap the tube and gently mix the gel by inversion and gentle shaking.
 - c** **Tape the lids shut on the spin/rotating rack to make sure the lids don't open spilling the fluid/sample.**
 - d** Centrifuge tubes in the Beckman centrifuge with the F2402H Rotor.
- Speed = 6419 RPM
 - RCF (g) = 3000 G
 - Time = 1 min
- Step 8**
- a** Throw away the flow through liquid in the bottom of the micro centrifuge tubes. (Repetition of Steps 6 and 7)
 - b** Replace spin cups by putting them back into the micro centrifuge tubes.
- Step 9**
- a** Wash the gell by adding 400 uL of Binding/wash buffer to each tube.
 - b** Cap the tube and gently mix the gel by inversion and gentle shaking.
 - c** Centrifuge tubes in the Beckman centrifuge with the F2402H Rotor.
- Speed = 6419 RPM
 - RCF (g) = 3000 G
 - Time = 1 min
- Step 10** Throw away the flow through liquid in the bottom of the micro centrifuge tubes.
- Step 11** Place spin cups into 3 new micro centrifuge tubes.

- Step 12** Mix antibody with binding/wash buffer in a test tube and then aliquot into the spin cups in Step 11. Recommended total antibody protein is 50-500 ug of antibody. This is a lot of antibody. \$\$\$ Make enough for all spin cups (antibodies + 400 uL Binding/wash buffer for each spin cup).
- Step 13** Cap the tube and gently mix the gel by inversion using a rocker.
Time = 15 - 30 min
- Step 14** Centrifuge tubes in the Beckman centrifuge with the F2402H Rotor.
Speed = 6419 RPM
RCF (g) = 3000 G
Time = 1 min
- Step 15** Discard the flow through. - you can keep it assess antibody binding if you wish to use the 280 method described in the protocol.
- Step 16**
- Place spin cups into 3 new micro centrifuge tubes.
 - Add 500 uL Binding/wash buffer.
 - Cap the tubes.
 - Mix by inverting tube 5-10 times.
- Step 17** Centrifuge tubes in the Beckman centrifuge with the F2402H Rotor.
Speed = 6419 RPM
RCF (g) = 3000 G
Time = 1 min
- Step 18** Throw away the flow through liquid in the bottom of the micro centrifuge tubes.
- Step 19**
- Replace spin cups into micro centrifuge tubes.
 - Add 500 uL Binding/wash buffer.
 - Mix by inverting tube 5-10 times.
- Step 20** Centrifuge tubes in the Beckman centrifuge with the F2402H Rotor.
Speed = 6419 RPM
RCF (g) = 3000 G
Time = 1 min
- Step 21** Throw away the flow through liquid in the bottom of the micro centrifuge tubes.
- Step 22**
- (Another Repeat of Steps 16-18) Replace spin cups into micro centrifuge tubes.
 - Add 500 uL Binding/wash buffer.
 - Mix by inverting tube 5-10 times.
- Step 23** Centrifuge tubes in the Beckman centrifuge with the F2402H Rotor.
Speed = 6419 RPM
RCF (g) = 3000 G
Time = 1 min
- Step 24** Throw away the flow through liquid in the bottom of the micro centrifuge tubes.
- Step 25** Place spin cups into 3 new micro centrifuge tubes.
These tubes now contain the non-crosslinked antibody-gel complex.

- Step 26**
- a Puncture the foil covering one tube of DSS with a pippette tip.
 - b Add 80 uL of DMSO.
 - c Mix by drawing the volume up and down the pippette tip until the DSS is dissolved.
- Step 27** Add 6 uL of DSS to each micro centrifuge tube containing the Antibody-gel complex.
Discard the extra DSS since it is only good for a short period.
- Step 28** Cap the tube and gently mix the gel by inversion using a rocker.
Time = 30 - 60 min
- Step 29** Centrifuge tubes in the Beckman centrifuge with the F2402H Rotor.
Speed = 6419 RPM
RCF (g) = 3000 G
Time = 1 min
- Step 30** Throw away the flow through liquid in the bottom of the micro centrifuge tubes.
- Step 31**
- a **Add 500 uL of the Immuno Pure Elution Buffer to the spin cups.**
 - b Cap the tubes.
 - c Mix by inverting tube 5-10 times.
- Step 32** Centrifuge tubes in the Beckman centrifuge with the F2402H Rotor.
Speed = 6419 RPM
RCF (g) = 3000 G
Time = 1 min
- Step 33** Throw away the flow through liquid in the bottom of the micro centrifuge tubes.
Replace spin cups by putting them back into the micro centrifuge tubes.

- Step 34** - Repeat Steps 31 to 33 four additional times.
Time 1
- a **Add 500 uL of the Immuno Pure Elution Buffer to the spin cups.**
 - b Cap the tubes.
 - c Mix by inverting tube 5-10 times.
- Step 35** Centrifuge tubes in the Beckman centrifuge with the F2402H Rotor.
Speed = 6419
RCF (g) = 3000
Time = 1 min
- Step 36** Throw away the flow through liquid in the bottom of the micro centrifuge tubes.
Replace spin cups by putting them back into the micro centrifuge tubes.

The repeats are required to remove all excess DSS and uncoupled Antibody.

The repeats are required to remove all excess DSS and uncoupled Antibody.

- Step 37** - Repeat Steps 31 to 33 four additional times.
Time 2
- a **Add 500 uL of the Immuno Pure Elution Buffer to the spin cups.**
 - b Cap the tubes.
 - c Mix by inverting tube 5-10 times.

Step 38 Centrifuge tubes in the Beckman centrifuge with the F2402H Rotor.
Speed = 6419
RCF (g) = 3000
Time = 1 min

Step 39 Throw away the flow through liquid in the bottom of the micro centrifuge tubes.
Replace spin cups by putting them back into the micro centrifuge tubes.

Step 40 - Repeat Steps 31 to 33 four additional times.
Time 3
a Add 500 uL of the Immuno Pure Elution Buffer to the spin cups.
b Cap the tubes.
c Mix by inverting tube 5-10 times.

The repeats are required to remove all excess
DSS and uncoupled Antibody.

Step 41 Centrifuge tubes in the Beckman centrifuge with the F2402H Rotor.
Speed = 6419
RCF (g) = 3000
Time = 1 min

Step 42 Throw away the flow through liquid in the bottom of the micro centrifuge tubes.
Replace spin cups by putting them back into the micro centrifuge tubes.

Step 43 - Repeat Steps 31 to 33 four additional times.
Time 4 - Thank god.
a Add 500 uL of the Immuno Pure Elution Buffer to the spin cups.
b Cap the tubes.
c Mix by inverting tube 5-10 times.

The repeats are required to remove all excess
DSS and uncoupled Antibody.

Step 44 Centrifuge tubes in the Beckman centrifuge with the F2402H Rotor.
Speed = 6419
RCF (g) = 3000
Time = 1 min

Step 45 Throw away the flow through liquid in the bottom of the micro centrifuge tubes.
Replace spin cups by putting them back into the micro centrifuge tubes.

Step 46 **a** Place spin cups into 3 new micro centrifuge tubes.
b Wash by adding 500 uL Biding/Wah Buffer

Step 47 Centrifuge tubes in the Beckman centrifuge with the F2402H Rotor.
Speed = 6419
RCF (g) = 3000
Time = 1 min

Step 48 **a** Replace spin cups by putting them back into the micro centrifuge tubes.
b Wash by adding 500 uL Biding/Wah Buffer

Step 49 Centrifuge tubes in the Beckman centrifuge with the F2402H Rotor.
Speed = 6419
RCF (g) = 3000
Time = 1 min

Step 50 Discard flow through.
Keep the antibody-gel complex.

The antibody-gel complex is now ready. This is the CROSS-LINKED antibody-gel complex.

You can either go and use the gel with your samples...as described in Antigen Immunoprecipitation.
or proceed to Storage conditions if you want to save the crosslinked antibody-gel complex for later use.

- Step 51** **Prepare sample as described on separate sample preparation sheet.**
Make sure to solubilize the proteins using Tween-20 buffer. Do you know how to do this?
- Step 52** Now take the solubilized protein sample and dilute sample down with Co-IP binding/wash buffer in a 1:1 ratio
This will cut the concentration in half. You need a maximum total volume of 500 uL.
- Step 53** Load between 200 - 500 uL of diluted sample into 1 Co-IP spin cup with gel
Mix for 4 hours at room temperature (85% binding) or overnight (~12-16 hours) at 4 degrees celcius (100% binding).
Tape the lids shut on the spin/rotating rack to make sure the lids don't open spilling the fluid/sample.
- Step 54** Centrifuge tubes in the Beckman centrifuge with the F2402H Rotor.
Speed = 6419
RCF (g) = 3000
Time = 1 min
- Step 55** **a** Place spin cups into 3 new micro centrifuge tubes.
b Add 500 uL of the Binding/Wash buffer to the spin cups.
c Cap the tubes.
d Mix by inverting tube 5-10 times.
- Step 56** Centrifuge tubes in the Beckman centrifuge with the F2402H Rotor.
Speed = 6419
RCF (g) = 3000
Time = 1 min
- Step 57** **a** Throw away the flow through liquid in the bottom of the micro centrifuge tubes.
b Replace spin cups by putting them back into the micro centrifuge tubes.
- Step 58** **a** Add 500 uL of the Binding/Wash buffer to the spin cups.
b Cap the tubes.
c Mix by inverting tube 5-10 times.
- Step 59** Centrifuge tubes in the Beckman centrifuge with the F2402H Rotor.
Speed = 6419
RCF (g) = 3000
Time = 1 min
- Step 60** **a** Throw away the flow through liquid in the bottom of the micro centrifuge tubes.
b Replace spin cups by putting them back into the micro centrifuge tubes.
- Step 61** **a** Add 500 uL of the Binding/Wash buffer to the spin cups.
b Cap the tubes.
c Mix by inverting tube 5-10 times.
- Step 62** Centrifuge tubes in the Beckman centrifuge with the F2402H Rotor.
Speed = 6419
RCF (g) = 3000
Time = 1 min
- Step 63** Throw away the flow through liquid in the bottom of the micro centrifuge tubes.
- Step 64** Place spin cups into 3 new micro centrifuge tubes.
- Step 65** **The protein-antibody-gel complex is now ready.**

Note - we are going to use these samples for a Western blot - therefore there is no reason to neutralize the samples.
Note - the low pH may make the sample buffer change colour - don't worry about it.

Step 66 **Add 190 uL of Elution Buffer to spin cup.**

Step 67 Mix by inversion 10 times.

Step 68 Centrifuge tubes in the Beckman centrifuge with the F2402H Rotor.

Speed = 6419
RCF (g) = 3000
Time = 1 min

Step 69 **Keep the Liquid flow through since this is you sample- Label Fraction 1.**

Also keep the spin cup contents since you will repeat steps 66 to 69 since some sample is still left.

Step 70 **Add 190 uL of Elution Buffer to spin cup.**

Step 71 Mix by inversion 10 times.

Step 72 Centrifuge tubes in the Beckman centrifuge with the F2402H Rotor.

Speed = 6419
RCF (g) = 3000
Time = 1 min

Step 73 **Keep the Liquid flow through since this is you sample- Label Fraction 2.**

Also keep the spin cup contents since you will repeat steps 66 to 69 since some sample is still left.

Step 74 **Add 190 uL of Elution Buffer to spin cup.**

Step 75 Mix by inversion 10 times.

Step 76 Centrifuge tubes in the Beckman centrifuge with the F2402H Rotor.

Speed = 6419
RCF (g) = 3000
Time = 1 min

Step 77 **Keep the Liquid flow through since this is you sample- Label Fraction 3.**

Also keep the spin cup contents since you will repeat steps 66 to 69 since some sample is still left.

Step 78 **Add 190 uL of Elution Buffer to spin cup.**

Step 79 Mix by inversion 10 times.

Step 80 Centrifuge tubes in the Beckman centrifuge with the F2402H Rotor.

Speed = 6419
RCF (g) = 3000
Time = 1 min

Step 81 **Keep the Liquid flow through since this is you sample- Label Fraction 4.**

Also keep the spin cup contents since you will will reuse the spin cups for other trials.
Process immediately to the Gel regeneration step.

Step 82 Add 500 uL Binding/Wash Buffer to the spin cup.
Cap the tubes.
Mix by inversion ~ 10 times.

Step 83 Centrifuge tubes in the Beckman centrifuge with the F2402H Rotor.
Speed = 6419
RCF (g) = 3000
Time = 1 min

Step 84 Throw away the flow through liquid in the bottom of the micro centrifuge tubes.
Replace spin cups by putting them back into the micro centrifuge tubes.

Step 85 Add 500 uL of the Binding/Wash buffer to the spin cups.
Cap the tubes.

Step 84 Mix by inverting tube 5-10 times.

Pause here if you intend to reuse the gel for another sample in the next 1 hour period.

Step 85 Centrifuge tubes in the Beckman centrifuge with the F2402H Rotor.
Speed = 6419
RCF (g) = 3000
Time = 1 min

Step 86 Throw away the flow through liquid in the bottom of the micro centrifuge tubes.
Replace spin cups by putting them back into the micro centrifuge tubes.

Note the gel is ready to reuse again at this stage if you are going to use it right away.
Go to Step 51 - Antigen Immunoprecipitation if you want to use the gel now.

If you want to go home and want to reuse the gel another day, continue with steps 87 and 88.

Step 87 Add 500 uL Binding/wash buffer to spin cup.
Ensure the buffer has 0.02% Sodium Azide in it as a preservative for long term storage.
Cap the tubes.
Wrap in laboratory film to prevent gel from drying out.

Step 88 Store the wrapped microcentrifuged tubes in the fridge.

APPENDIX ELEVEN

NCD-4 assay protocol

NCD-4 assay protocol

NCD4 - Stock dilution

Store at -80 degrees.

INPUT--> Mass = 25 mg Volume wanted = 0.017 Liters

We have = 0.025 g

MW = 292.4 grams per mol

$n = \text{mass} / \text{MW}$
therefore we have = 0.000085 mols

We want 5 mM final concentration
which is 0.005 M final concentration

concentration = mols / Volume
Therefore, in 1.00 L the final concentration would be = 0.000085 M which = 0.085 mM
Therefore, in 0.017 L the final concentration would be = 0.005029 M which = 5.03 mM

$n = CV$
 $C = n/V$
 $C = ?$
 $n = 0.000085 \text{ mols}$
 $V = 0.019 \text{ L}$
 $C = 0.00449996 \text{ M}$
 $C = 4.499964 \text{ mM}$
ratio of 4.5 mM to 5 mM 0.89473684

Therefore add 17 mL Ethanol to 25 mg NCD4 powder to get 5.03 mM final Concentration.

Wash Buffer

Store at 4 degrees Celcius in Fridge.

500 mL Distilled H2O
0.595 g HEPES
1.000 g NaN3
0.0174 g PMSF

pH to 7.5

Diluted NCD4 Buffer (NCD4+Wash Buffer) - make fresh daily.

Input --> We need to add this much final volume to each sample 1.5 mL into each sample
of samples needed to run = 28 samples

Input --> This is the [Stock] = $c1V1 = c2V2$
 $c1 = 4.50 \text{ mM} = 0.004 \text{ M}$

Input --> we want a [final] = $c2 = 150 \text{ uM} = 0.00015 \text{ M}$
calc --> in this final volume = $V2 = 42.0 \text{ mL} = 0.04200 \text{ L}$

calc --> Solve for V1 in Liters $V1 = 0.001400 \text{ L}$

**Therefore we need to add this volume of [Stock] = 1400.0 uL of stock NCD4 to
40.600 mL of Wash Buffer. to make enough volume of NCD4 Buffer for 28 samples
pH to 6.2**

Make fresh on the day of your assay.
Keep in the dark
Final NCD4 concentration will be 150 uM.
Refer to protocol to see when you add NCD4.

Incubate samples with NCD4 buffer for 3 hours in the dark.

NCD4- Assay

Sample preparation	protein concentration : Load this much protein	volume to load	
sample name	ug/uL	ug total protein	uL
Input --> Heart vesicles	4.164	200 ug	48.0 uL
White Gastroc	4.120	200 ug	48.5 uL
schertzer sample	1.63	200 ug	122.7 uL

1. Load 200 ug of total protein for each sample into an ultra centrifuge tube.
2. Add 7.5 mL Wash Buffer to samples in each ultra centrifuge tube.
3. Centrifuge at 23,400 RPM for 15 min.
4. Discard supernatant. Note the pellet will be nearly invisible. Scrape everything as best you can.
5. Work in the dark from now on.
6. Resuspend pellet in 1.2 mL diluted-NCD4-Wash buffer using a hand homogenizer.
Note the pellet will be nearly invisible. Scrape everything as best you can.
Transfer the sample into an epindorf tube or keep in ultra centrifuge tubes.
7. Mix by inversion if epindorfs and incubate for 3 hours in the dark.
or slowly vortex for 3 hours in the ultra centrifuge tube using th emulti vortexer.
8. Transfer samples to clean ultra centrifuge tubes or keep in the ultracentrifuge tubes if this is where the sample is.
9. Add 5 mL Wash buffer.
10. Centrifuge at 23,400 RPM for 15 min.
11. Discard supernatant. Note the pellet will be nearly invisible. Scrape everything as best you can.
12. Resuspend pellet in 1.5 mL diluted-NCD4-Wash buffer using a hand homogenizer.
Note the pellet will be nearly invisible. Scrape everything as best you can.
Transfer the sample into an epindorf tube or keep in ultra centrifuge tubes.
13. Add 6 mL Wash buffer.
14. Centrifuge at 23,400 RPM for 15 min.
15. Discard supernatant. Note the pellet will be nearly invisible. Scrape everything as best you can.
16. Resuspend pellet in 1.000 mL Wash buffer using a hand homogenizer..
Transfer the sample into an epindorf tube.
17. Load 250 uL into wells on a black plate.
18. Read plate on the flourscent plate reader.
Use scan mode on the plate reader.
Excite at 340 nm.
Scan emission wavelengths between 400 to 430 nm.
Report the peak RFU value and if you are interested, the peak wavelength.

APPENDIX TWELVE

FITC binding assay protocol

FITC binding assay protocol

1) Add 5 μ g of total protein (SR vesicles) to Ca²⁺-ATPase buffer such that the final volume is 50 μ l. eg. 6 μ l of SR vesicles in 44 μ l Ca²⁺-ATPase buffer

2) IN THE DARK

add 250 μ l of FITC labeling buffer (50mM Tris-HCl pH 8.8, 250mM sucrose, 0.1mM CaCl₂, 5mM MgCl₂, 20 μ M FITC (FITC is made up separately in ethanol and added so that the final concentration is 20 μ M) and protease inhibitor cocktail tablets) to the 50 μ l of SR. Lightly vortex and let mix on the automatic mixer at room temperature of 1 hour.

3) IN THE DARK

Add 300 μ l of either reducing or non-reducing 2X Sample Buffer (125mM Tris-HCl pH 6.8, 5% SDS, 10% (v/v) glycerol, 0.01% bromophenol blue, 5% (v/v) mercaptoethanol) to each tube. The reaction is now ceased and you may continue working in the light.

*note: the initial concentration of protein was 0.1 μ g/ μ l (5 μ g/50 μ l). Taking into account the final volume of 600 μ l the protein concentration is now (0.0083333 μ g/ μ l)

4) On a 7.5% Acrylamide gel load 30 μ l of FITC labeled sample (30 μ l * 0.0083333 = 0.250 μ g total protein). Run and transfer gel to PVDF membrane as per usual.

5) *block for 1 hour in 10% milk

*primary antibody 1 hour 1:5000 dilution in 5% milk anti-fluorescein/Oregon Green monoclonal antibody 4-4-20

*secondary antibody anti-mouse 1:5000 dilution in mixture of 6ml TBS-T and 2mL 10% milk for 1 hour

6) detect using ECL reagents (Amersham) at 30second exposures

FITC BUFFER RECIPE

Measurements are for 100mL of H₂O

Chemical	Molecular Weight (g/mol)	Mass Used (g)	Concentration
Tris-HCl	157.6	0.788	50mM
CaCl ₂	110.98	0.00111	0.1mM
MgCl ₂	95.21	0.047605	5mM
Sucrose	342.3	8.5575	250mM
FITC	389.38	3.115uL Stock FITC	20μM
*note make up Stock FITC separate in 40mL EtOH			
FITC stock	389.38	100mg vial	6.42mM

*Combine first 4 ingredients in ~80mL of H₂O and pH to 8.8 using KOH bring up to final volume

*Freeze 1mL aliquots at -80°C

*To achieve 20uM FITC in the buffer add 3.115uL of Stock FITC just before incubating the sample in FITC Buffer